RAFT-HDA Chemistry

Conception, Development and Application of a Facile Tool for Precision Macromolecular Engineering

Zur Erlangung des akademischen Grades eines
DOKTORS DER NATURWISSENSCHAFTEN
(Dr. rer. nat.)

Fakultät für Chemie und Biowissenschaften
Karlsruher Institut für Technologie (KIT) - Universitätsbereich

genehmigte

DISSERTATION

von

Andrew John Inglis

aus

Sydney, Australien

Dekan: Prof. Dr. S. Bräse
Referent: Prof. Dr. C. Barner-Kowollik
Korreferent: Prof. Dr. M. Wilhelm
Tag der mündlichen Prüfung: 19.10.2010

Die vorliegende Arbeit wurde von Februar 2008 bis September 2010 unter Anleitung von Prof. Dr. Christopher Barner-Kowollik und Assoc. Prof. Dr. Martina H. Stenzel an der University of New South Wales, Sydney, Australien (Februar 2008-Juni 2008) und unter Anleitung von Prof. Dr. Christopher Barner-Kowollik am Karlsruher Institut für Technologie (KIT) - Universitätsbereich (Juli 2008-September 2010) angefertigt.

It may be that the gulfs will wash us down:
It may be we shall touch the Happy Isles,
And though we are not now that strength which in old days
Moved earth and heaven;
That which we are, we are
One equal temper of heroic hearts,
Made weak by time and fate, but strong in will
To strive, to seek, to find and not to yield.

-Adapted from *Ulysses*-

Alfred Lord Tennyson (1809-1892)

Abstract

The conceptualization, development and application of the herein named *RAFT-HDA Chemistry* is reported. This chemistry is presented as a facile conjugation method (falling within the field of *click* chemistry) whereby synthetic polymeric materials may be covalently linked to other species, including other polymers with high efficiency.

Electron-deficient dithioesters are effectively used as controlling agents in RAFT polymerizations to yield well-defined polymer chains that inherently carry a reactive heterodienophile end-group. Such polymers were subsequently reacted with open-chain diene functional compounds in hetero Diels-Alder (HDA) cycloadditions which resulted in the formation of well-defined block copolymers and star-shaped polymers in an efficent, modular fashion. The significance of these two results lies in the fact that the performance of RAFT-HDA chemistry was found to be comparable to that of the widely used copper (I) catalysed azide-alkyne cycloaddition (CuAAC), however requiring fewer synthetic steps and eschewing the use of a toxic copper catalyst.

Developing the chemistry to beyond a mere concept, ultra-fast macromolecular couplings were achieved by using more reactive cyclopentadienyl species. Extension of the technique of modular block copolymer construction to unprecedentedly high molecular weights ($> 100\,000$ g·mol^{-1}) is also achieved which not only serves to highlight the efficacy of this newly developed strategy, but stretches the boundaries of modular polymer synthesis. Further confirmation of the high purity of block copolymers that are directly accessible via RAFT-HDA chemistry was provided by an in-depth 2D LACCC-SEC analysis which, aside from being the only analysis of its kind within the realm of *click* chemistry, was also used to validate a relatively inexpensive and simple SEC deconvolution procedure to achieve comparably accurate compositional data of block copolymer mixtures.

Perhaps more long reaching, this work subsequently precipitated the design of a rather robust and more efficient technique to synthesize a variety of cyclopentadienyl functional materials, which were advantageously used in the generation of novel colour-switchable and reversibly cross-linking polymeric materials. Such cyclopentadienyl functional materials are therefore envisaged to be a highly valued commodity in the future application of Diels-Alder chemistry to the macromolecular sciences.

Contents

1

Introduction

The ubiquity of polymeric materials in modern society stands as testimony to the importance of the various technological developments that have led to their creation. Indeed, from the early days within the field where synthetic polymers were used mainly as bulk materials for the fabrication of a variety of products, the ability to control various aspects of macromolecular architecture, composition and chemical functionality have given rise to tailor-made functional materials that have enabled and enriched technological advancement in academic and industrial endeavours alike.

Being just as important as the ability to achieve specific goals is the ease with which they may be achieved. The concept of controlling macromolecular architecture and functionality is taken to exemplify this matter. Living anionic polymerization, in many respects, is held as the gold standard for precisely controlling the molecular weight and macromolecular architecture of synthetic polymers.[1] Nevertheless, from a practical perspective, achieving such outcomes can be rather difficult due to the highly stringent reaction conditions that are required. Furthermore, the diversity of monomers that may be polymerized by such a technique restricts the breadth and, hence, the applicability of materials that are thereby synthesized.

In contrast, free radical polymerization (FRP) is a comparatively simple technique to generate a wide variety of polymeric materials in terms of the ranges of molecular weights that may be reached and the diversity of polymerizable monomers, including those that contain functionality that would not be compatible with other methods.

While the process is comparatively non-demanding, the caveat lies in the very little control that is possible, given the highly reactive nature of the radical species that are involved.

Undoubtably being a milestone in synthetic polymer chemistry is the development of the various technologies that enable a considerable level of control over FRP, the so-called *controlled* radical polymerization (CRP) methods.* The three most widely adopted techniques, nitroxide mediated polymerization (NMP),[3] atom transfer radical polymerization (ATRP)[4, 5] and reversible addition-fragmentation chain transfer (RAFT) polymerization[6, 7] strive to combine the versatility and ease of free radical processes with the exquisite control over molecular weight and macromolecular architecture that is offered by such methods as living anionic polymerization. Although, on their own, a wealth of polymeric materials with precisely controlled molecular weights, architectures and chemical functionality can be readily generated, achieving a higher level of complexity and precision has been accomplished by combining these techniques with classical organic transformations in a modular approach.

Modularity in modern polymer chemistry has fast enabled the design and synthesis of functional materials with unprecedented precision and efficiency. Collectively labelled as *click* chemistry[8] are the various highly efficient chemical transformations that may be used to effectively *link* pre-prepared polymeric structures with small molecules or even other polymer chains.[9–11] The fundamental strategy simply involves the use of a CRP process to generate a well-defined polymeric building block bearing a reactive functionality either at an end-group or along the polymer backbone. A species bearing the complementary functionality can then be conjugated to the polymer chain to produce the targeted product.

To date, the most widely adopted *click* reaction is the copper (I) catalysed azide-alkyne cycloaddition (CuAAC).[12, 13] Whilst being, arguably, one of the most efficient transformations that may be used to achieve polymer conjugation, the requirement of catalysis with cytotoxic copper species and the subsequent necessity to remove this from the reaction mixture are significant limitations that have warranted the exploration of alternative chemistries to be used in its place. One such class of transformations is Diels-Alder chemistry.

Although Diels-Alder reactions have successfully been used as a conjugation method in polymer science,[14–16] the high temperatures required to drive the already slow reactions limit their applicability. However, Diels-Alder systems are increasingly becoming a highly valued commodity in the macromolecular sciences for their ability to be thermally reversible and robust. As such, unique materials may thereby be

*According to recent IUPAC recommendations, the term *controlled radical polymerization* should be replaced by the term *reversible-deactivation radical polymerization*[2]

synthesized that are able to reversibly change between different physical states when triggered by an external stimulus.[17]

As it stands, however, there is currently a synthetic gap in the literature in which a variety of reactive dienophiles and dienes are in need of being precisely incorporated into polymeric materials if Diels-Alder chemistry is really going to flourish as a conjugation technique. A survey of the existing literature shows that the vast majority of publications concerning this topic make use of commercially available (and chemically accessible) furan and maleimide derivatives, which constitutes but one system.[18]

Striving to provide a convenient and faster Diels-Alder system, the present investigation conceptualizes and develops *RAFT-HDA Chemistry* as a facile chemical tool for use in macromolecular conjugations. It will be shown that the use of electron-deficient dithioester compounds as controlling agents in RAFT polymerization provide direct access to highly reactive and well-defined dienophilic polymeric materials for use with Diels-Alder chemistry. Furthermore, the application of this newly developed chemistry in the synthesis of novel, reversibly thermoresponsive materials is investigated. For ease of navigation, the flowchart presented in Figure 1.1 provides an overview of all work presented herein and how each chapter relates to the others.

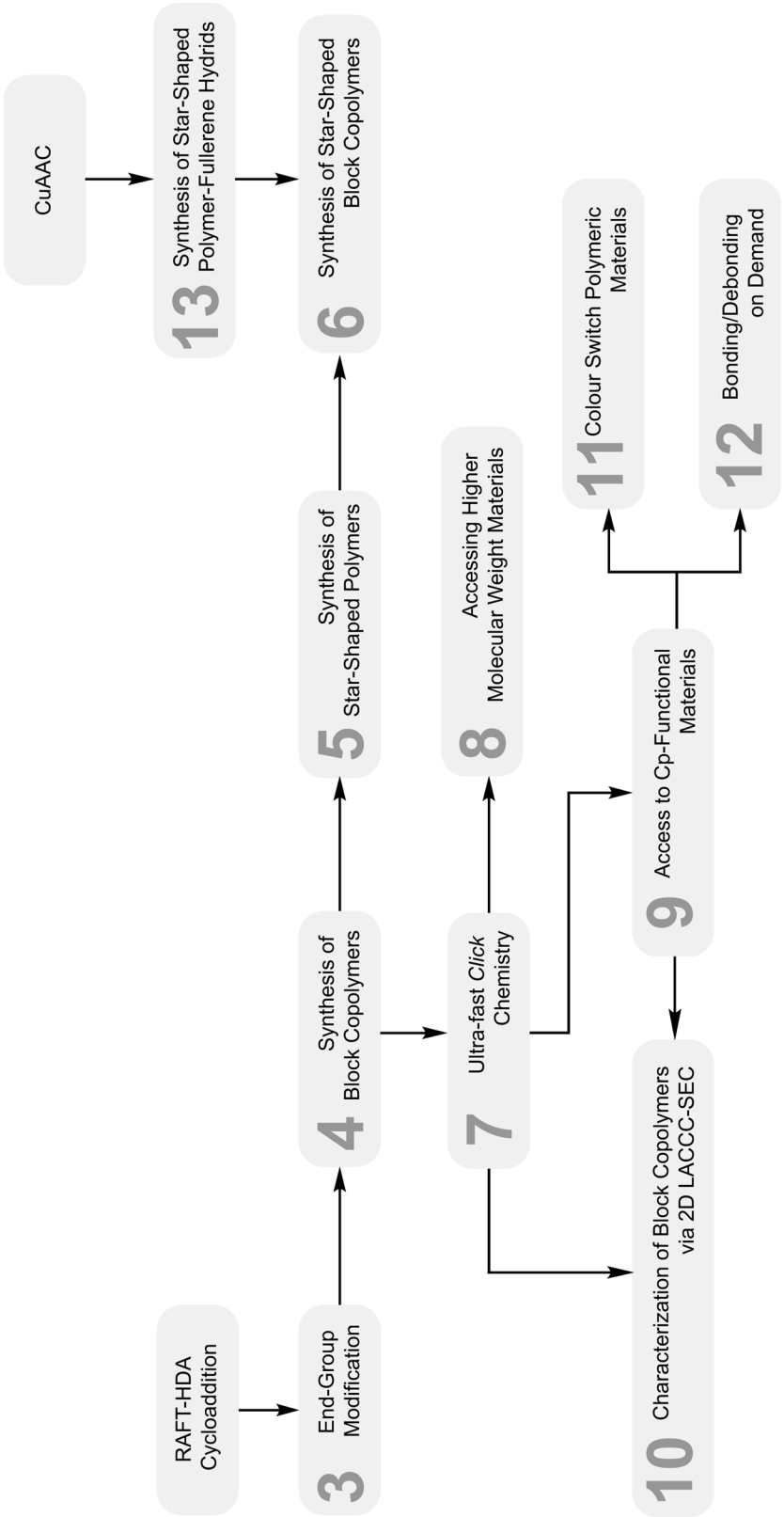

Figure 1.1 Flowchart outlining the content of this work.

References

[1] Hadjichristidis, N.; Pitsikalis, M.; Pispas, S.; Iatrou, H. *Chem. Rev.* **2001**, *101*, 3747–3792.

[2] Jenkins, A. D.; Jones, R. G.; Moad, G. *Pure Appl. Chem.* **2010**, *82*, 483–491.

[3] Hawker, C. J.; Bosman, A. W.; Harth, E. *Chem. Rev.* **2001**, *101*, 3661–3688.

[4] Matyjaszewski, K.; Xia, J. H. *Chem. Rev.* **2001**, *101*, 2921–2990.

[5] Ouchi, M.; Terashima, T.; Sawamoto, M. *Chem. Rev.* **2009**, *109*, 4963–5050.

[6] Moad, G.; Chong, Y. K.; Postma, A.; Rizzardo, E.; Thang, S. H. *Polymer* **2005**, *46*, 8458–8468.

[7] Barner, L.; Davis, T. P.; Stenzel, M. H.; Barner-Kowollik, C. *Macromol. Rapid Commun.* **2007**, *28*, 539–559.

[8] Kolb, H. C.; Finn, M. G.; Sharpless, K. B. *Angew. Chem. Int. Ed.* **2001**, *40*, 2004–2021.

[9] Hawker, C. J.; Wooley, K. L. *Science* **2005**, *309*, 1200–1205.

[10] Binder, W. H.; Sachsenhofer, R. *Macromol. Rapid Commun.* **2008**, *29*, 952–981.

[11] Sumerlin, B. S.; Vogt, A. P. *Macromolecules* **2010**, *43*, 1–13.

[12] Rostovtsev, V. V.; Green, L. G.; Fokin, V. V.; Sharpless, K. B. *Angew. Chem. Int. Ed.* **2002**, *41*, 2596–2599.

[13] Tornoe, C. W.; Christensen, C.; Meldal, M. *J. Org. Chem.* **2002**, *67*, 3057–3064.

[14] Durmaz, H.; Colakoclu, B.; Tunca, U.; Hizal, G. *J. Polym. Sci., Part A: Polym. Chem.* **2006**, *44*, 1667–1675.

[15] Durmaz, H.; Dag, A.; Altintas, O.; Erdogan, T.; Hizal, G.; Tunca, U. *Macromolecules* **2007**, *40*, 191–198.

[16] Dag, A.; Durmaz, H.; Hizal, G.; Tunca, U. *J. Polym. Sci., Part A: Polym. Chem.* **2008**, *46*, 302–313.

[17] Chen, X. X.; Dam, M. A.; Ono, K.; Mal, A.; Shen, H. B.; Nutt, S. R.; Sheran, K.; Wudl, F. *Science* **2002**, *295*, 1698–1702.

[18] Sanyal, A. *Macromol. Chem. Phys.* **2010**, *211*, 1417–1425.

2

Modularity in Modern Polymer Chemistry-A Literature Review

2.1 Free Radical Polymerization

Conventional free radical polymerization utilizes reactive radical species as the progenitors of high molecular weight polymers. The chain reaction process, by which such materials are formed, consists of four main elements: initiation, propagation, termination and chain transfer.

Initiation is the process by which free radicals are introduced into the system and allow for polymer chains to grow through the continuous addition of monomer. This occurs in two stages, the first of which involves the formation of primary radicals (Eq. 2.1). Most commonly, this is achieved through the thermally or photolytically induced homolysis of an initiator molecule, but may also be achieved via irradiation or redox chemistry. Typical initiator molecules are based upon azo- or peroxy compounds. The rate coefficient of such initiator dissociation (k_d) is typically of the order of 10^{-5} s^{-1}. The second stage involves the addition of the formed primary radicals to the vinyl bond of the monomer (Eq. 2.2). In this process, the radical species is transferred to the vinyl monomer ($k_i \approx 10^4$ $M^{-1} \cdot s^{-1}$), to which addition of another monomer unit may take place. Upon repetition, a macro-radical species is formed and continues to grow as more and more monomer units are added to the chain. This is called propagation (Eq.

2.3). Values for the rate coefficient of propagation (k_p) in free radical polymerization are typically $10^{3\pm1}$ $M^{-1}\cdot s^{-1}$.

$$I{-}I \xrightarrow{k_d} 2\,I^{\bullet} \tag{2.1}$$

$$I^{\bullet} + M \xrightarrow{k_i} P_1^{\bullet} \tag{2.2}$$

$$P_n^{\bullet} + M \xrightarrow{k_p} P_{n+1}^{\bullet} \tag{2.3}$$

Termination processes are those in which radical species are irreversibly removed from the polymerizing system, resulting in inactive or *dead* polymer chains. Termination may occur by two different mechanisms: combination (Eq. 2.4) or disproportionation (Eq. 2.5). The combination of two growing macro-radicals results in the formation of a *dead* polymer chain of length equal to the sum of the individual lengths of the two macro-radicals. Disproportionation, on the other hand, involves the abstraction of hydrogen from one macro-radical by another. This results in the formation of two *dead* polymer chains of length equal to that of the corresponding macro-radicals. Importantly, the abstraction process leaves one of the polymer chains bearing an unsaturated end-group which, depending upon its structure, may behave as a macromonomer and thus be re-initiated by the addition of another radical species. Radical termination reactions ($k_t \approx 10^8$ $M^{-1}\cdot s^{-1}$) are diffusion controlled. Consequently, increases in solution viscosity and chain entanglement with conversion effectively lead to a reduction in the rate of termination, resulting in *auto acceleration* behaviour.[1] The overall effect of termination processes, nevertheless, is a reduction in radical concentration, ultimately leading to a cessation of the chain reaction.

$$P_n^{\bullet} + P_m^{\bullet} \xrightarrow{k_{tc}} P_{n+m} \tag{2.4}$$

$$P_n^{\bullet} + P_m^{\bullet} \xrightarrow{k_{td}} P_n^{=} + P_m{}^{H} \tag{2.5}$$

Another process that leads to the formation of *dead* polymer chains is chain transfer. This process involves the termination of a propagating macro-radical by the transfer of hydrogen (or some other species) to it from another compound that is present in the polymerization system. This may be the monomer, initiator, formed polymer or the solvent, which are collectively referred to as 'T' in Eq. 2.6 and Eq. 2.7. Although being a *chain breaking* process, chain transfer reactions are radical displacement reactions which do not alter the radical concentration of the system. However, its effect on the polymerization is dependent upon the relative rate of re-initiation of the newly formed radical species in comparison to that of the original propagating radical.

Whilst the overall process is rather robust in that it allows for the polymerization of a wide variety of monomers using mild reaction conditions, is tolerant to water and

$$P_n^{\bullet} + T \xrightarrow{k_{tr}} P_n + T^{\bullet} \quad (2.6)$$

$$T^{\bullet} + M \xrightarrow{k_{ri}} P_i^{\bullet} \quad (2.7)$$

can lead to a broad range of materials when multiple monomers are copolymerized; a major limitation is the severe lack of control it offers for some of the most fundemental aspects of macromolecular structure. These include polydispersity (*PDI*), architecture and composition. By contrast, anionic polymerization is very well suited to controlling these properties, albeit under rather stringent reaction conditions and applicable to a relatively small number of monomers.[2]

Anionic polymerization, under the appropriate reaction specifications, may be labelled as a form of *living* polymerization. As introduced by Szwarc,[3] a *living* polymerization is a molecular chain growth process in which there are no chain breaking reactions (transfer and termination). As such, effective control over end-group functionality and molecular weight is achievable. Further characterized by a linear evolution of molecular weight with monomer conversion and following linear semilogarithmic kinetic profiles, achieving *living* properties in free radical polymerizations has been a principal focus of development in polymer science over the past 20 years.

2.2 Controlling Free Radical Polymerization

In the strictest sense, a truly *living* polymerization based upon radical chemistry is an impossibility as bimolecular termination reactions can never be completely suppressed. Nevertheless, many of the qualities of *living* processes can be largely emulated (in a radical polymerization) by a number of strategies. For this reason, the term *controlled* will be used to describe these systems.

Controlled radical polymerization (CRP) may be achieved by employing one of two generic mechanisms: reversible termination or reversible degenerative chain transfer. However, a feature that is common to both strategies is a rapid exchange between *dormant* and *active* radical species, which allows for the simultaneous growth of all polymer chains with a concomitant supression of radical termination reactions. Nitroxide Mediated Radical Polymerization (NMP)[4] and Atom Transfer Radical Polymerization (ATRP)[5, 6] provide the control in radical polymerizations by adopting the reversible termination approach whereas Reversible Addition-Fragmentation Chain Transfer (RAFT) polymerization[7–9] makes use of a degenerative chain transfer mechansim. The fundamental principles of each of these systems are briefly outlined in the following.

2.2.1 Nitroxide Mediated Radical Polymerization

NMP is a specific type of stable free radical polymerization (SFRP) in which stable nitroxide radicals are used to reversibly terminate propagating chains through the formation of an alkoxyamine. The polymerization may be brought about by one of two avenues. One method involves the use of a conventional radical initiator [such as 2,2'-azobis(isobutyrlnitrile) (AIBN) or benzoyl peroxide] and stable nitroxide radical [most conveniently 2,2,6,6-tetramethylpiperidine-1-oxyl (TEMPO)]. The other method requries the use of an appropriately designed alkoxyamine, the thermal decomposition of which produces a reactive radical and stable nitroxide radical fragments. In both cases, two different radical species are present- a reactive radical that adds onto the double bond of the monomer and propagates, and the stable *mediating* radical, which can reversibly terminate with the propagating species. The general mechanism of NMP is presented in Figure 2.1.

During the polymerization, only the reactive radical species can undergo radical-radical coupling. Thus, at the onset of polymerization, the reaction mixture will contain a slight excess of the *mediating* or persistant radical as some of the reactive radical species irreversibly (and unavoidably) terminate. This comparatively elevated concentration of the *mediating* radical enhances its ability to reversibly terminate with the remaining propagating species and, thus, decreases the amount of radical-radical coupling. This phenomenon - the persistant radical effect - provides the kinetic mechanism which controls the polymerization process.[10]

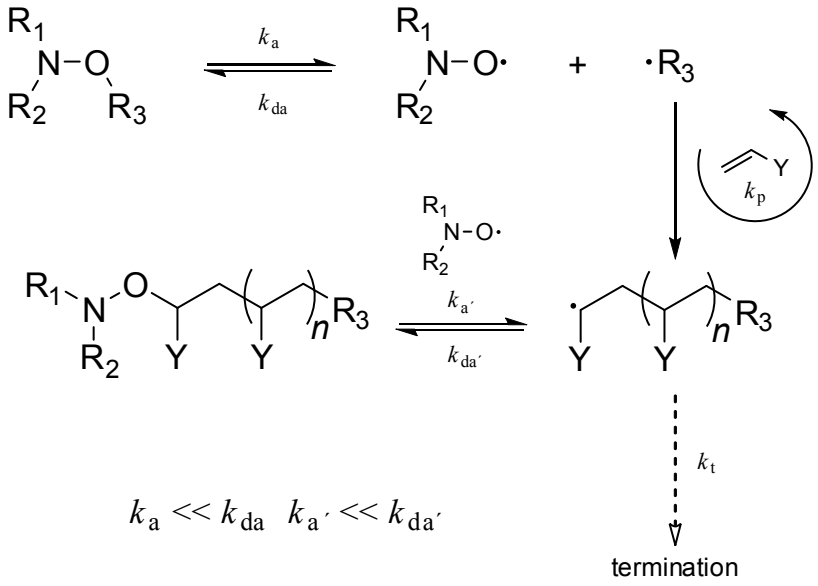

Figure 2.1 General mechanism of NMP.

2.2.2 Atom Transfer Radical Polymerization

ATRP is perhaps the most studied, both mechanistically and synthetically, CRP method to date.[5, 6] Operating under essentially the same reversible termination mechansim as NMP, radical generation in ATRP is achieved by a reversible redox process in which a solubilzed transition metal compound (most commonly CuBr) undergoes a simultaneous single electron transfer and halogen abstraction with an organic halide. The thus generated radical can subsequently initate polymerization and the now oxidized transition metal compound behaves as the stable radical (called the *deactivator* within this context).

A redox-goverened equilibrium is therefore established between the propagating *active* species and the non-propagating *dormant* species. Providing a well controlled system requires the equilibrium constant ($K_{ATRP} = k_a/k_{da}$) to be sufficiently small in order to ensure that the concentration of propagating species is low enough to significantly suppress bimolecular termination reactions, yet large enough to achieve a reasonable propagation rate. Typical values of K_{ATRP} lie within the range of 10^{-4} to 10^{-9}.[11] The controlling mechanism of ATRP is presented in Figure 2.2.

In an ideal ATRP, greater than 90 % of the polymer chains retain the halide chain terminus. Typically, for this to be achieved, the polymerization must be stopped at low monomer conversion (< 40 %). Loss of the chain-end functionality usually arises from the cumulative action of a number of different processes, which include bimolecular termination reactions, side reactions of the propagating radical with the copper catalyst (outer sphere electron transfer in which the radical is oxidized to a carbocation

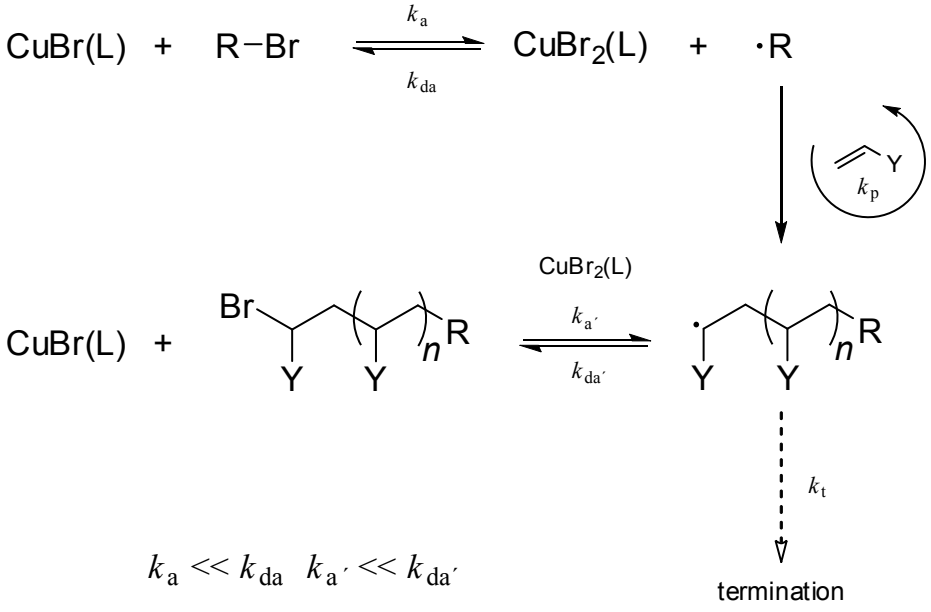

Figure 2.2 General mechanism of ATRP. L = Ligand.

or reduced to a carbanion in the presence Cu^{II} and Cu^{I} respectively), and a Cu^{II} catalysed β-H elimination (particularly in the case of styrene-type monomers). All in all, the retention of halide functionality in polymers prepared by ATRP is a highly advantageous characteristic of the technique in that it may be utilized as a synthetic handle (as will be shown later) to perform a variety of post-polymerization chemical transformations.

2.2.3 Reversible Addition-Fragmentation Chain Transfer Polymerization

The RAFT process operates under the principle of degenerative chain transfer to provide control over a radical polymerization. Propagating radicals in a polymerization (initiated by a conventional radical initiator) are reversibly captured by a thiocarbonyl thio compound and induced into a *dormant* state. The thiocarbonyl thio compound, or RAFT agent, is most commonly a dithioester in which the Z- and R- fragments (as depicted in Figure 2.3) are carefully chosen. The former is instrumental in dictating the stability/reactivity of the thiocarbonyl group toward radical addition and influencing the stability of the generated intermediate adduct radical, which is correlated to its ability to fragment and regenerate the thiocarbonyl bond. The latter, called the leaving group, is the moiety to which the labile end-group of the propagating radical is transferred. The choice of appropriate Z- and R- fragments is based upon the nature of the monomer that is to be polymerized.

After initiation, the growing polymer chain engages the RAFT agent and the radical is transferred to the R-group, which is designed to efficiently initiate further polymerization. A typical RAFT polymerization will have between a 5- and 10-fold excess of RAFT agent to radical initiator, which ensures that the vast majority of polymer chains are actually initiated by the R fragment of the RAFT agent and the resulting polymer chains bear the dithioester as an end-group. The fast interchange of propagating radicals that ensues sufficiently suppresses the occurance of bimolecular termination and other transfer reactions such that the polymerization displays *living* characterisitics.[7] The accepted mechanism of the RAFT process is presented in Figure 2.3.

It is important to note that in NMP and ATRP, the controlling mechanism ensures a low propagating radical concentration. While this suppressess the occurance of termination reactions, it also suppresses the rate of propagation. Bimolecular termination reactions proceed with second-order kinetics with respect to the radical concentration whereas propagation is only first-order. Thus, if the radical concentration is halved, the rate of propagation is also halved, but the rate of termination is reduced by a factor of four. In the case of RAFT polymerization, as one propagating radical is induced into a *dormant* state another propagating radical is released. Thus, at least in

theory, the radical concentration in a RAFT polymeriaztion is not reduced by the controlling mechanism as is the case for NMP and ATRP, so it should proceed with an unaffected propagation rate. In practice, however, retardation of the propagation rate is observed. Possible explainations for this phenomena include radical coupling between the intermediate dithioester radical and a propagating radical, and a slow or delayed fragmentation step in the transfer process.[12]

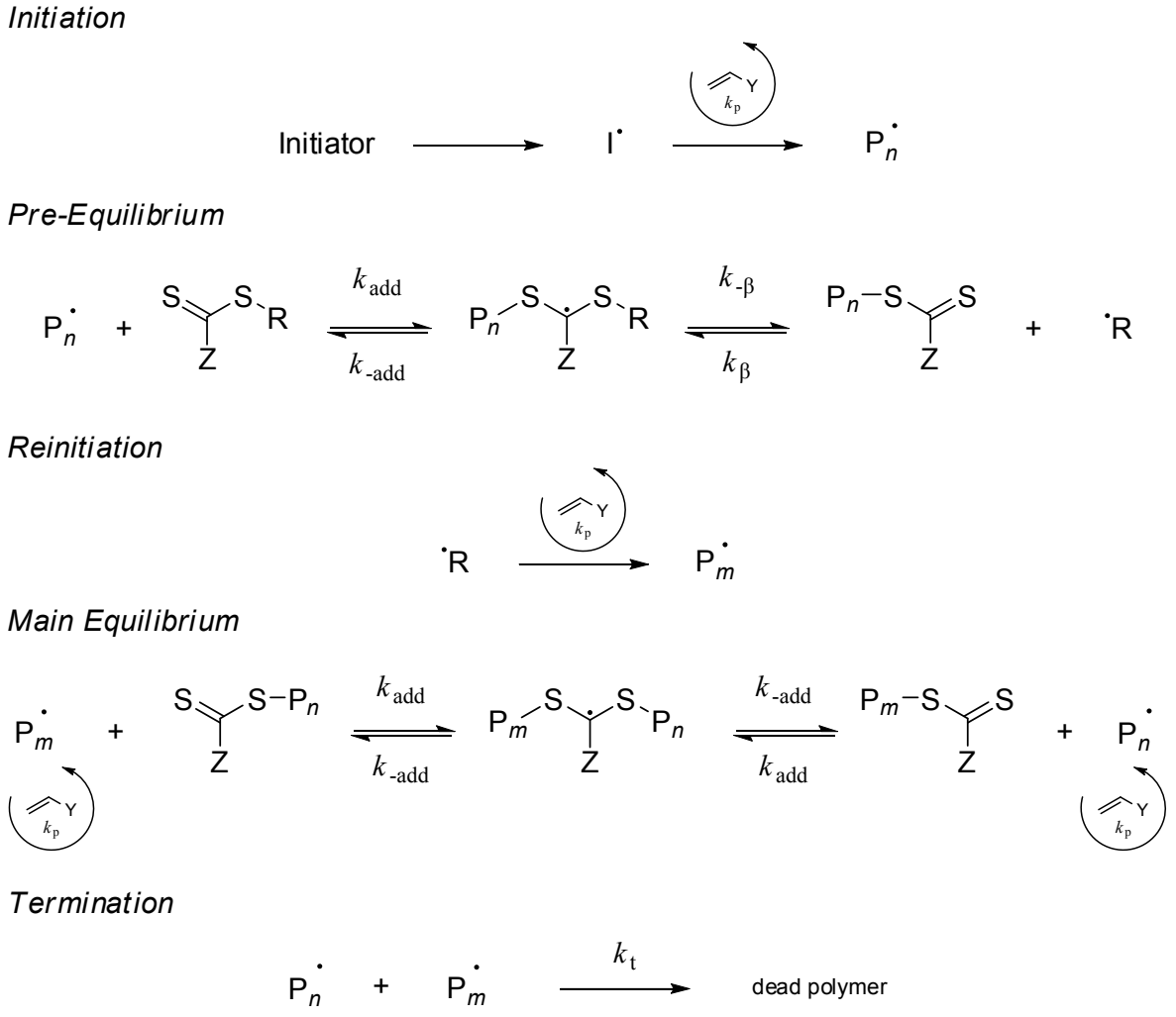

Figure 2.3 General mechanism of RAFT polymerization.

2.2.4 Controlling Macromolecular Architecture and Functionality

The ability to control a radical polymerization by the previously described techniques allows for the design of well-defined polymeric materials in terms of polymer composition, topology and chemical functionality. The feature common to the various CRP methods that enables this is the fact that the functionality integral to the controlling mechanism is incorporated into the final polymer structure. For example, polymers formed by NMP bear initiator functionality at one end of the chain and an alkoxyamine at the other. ATRP polymers have a similar α-ω-functionalization pattern, with the initator fragment at one end, and halide functionality at the other. Polymers formed by a RAFT process will likewise bear thiocarbonyl thio functionality.

It can therefore easily be imagined (and has been realized) that the design of initiators/controlling agents to include specific chemical functionality will impart that functionality to whatever polymer is thereafter synthesized. Most commonly, hydroxyl and carboxylic acid functionalitzed ATRP initiators and RAFT agents have been effectively used to produce the correspondingly chain-end functional polymers.[13–19] The retention of functionality in polymer chains responsible for the controlling mechanism effectively preserves the propagating species in a *dormant* state. Therefore, polymers prepared via CRP may be chain-extended by using them as a macroinitiator or macro-RAFT agent in a subsequent polymerization, leading to the formation of block copolymer structures.[20]

In more elaborate examples of macromolecular engineering, the design of multifunctional initiators/controlling agents lead to the synthesis of well-defined polymeric architectures. The strongest exemplification of this notion is this generation of star-shaped polymers. Here, a *core* molecule is synthesized which carries either a multitude of halide functionality or dithioester functionality. During polymerization, one linear chain is grown per controlling function, thus producing a star macromolecule with the number of arms corresponding to the number of controlling functionalities.[21, 22] A graphical overview of the structures that are achieveable through CRP is presented in Figure 2.4.

Despite the great versatility displayed by the above described technologies, there are some inherent limitations to what can be synthesized. For example, the production of block copolymer structures via chain extension is restricted to monomers of comparable radical reactivity. The consequences of vastly different monomer reactivities can be illustrated by the example of the preparation of a (hypothetical) block copolymer made from vinyl acetate and styrene. The combination of the highly reactive vinyl acetate derived radical and the relatively unreactive styrene derived radical

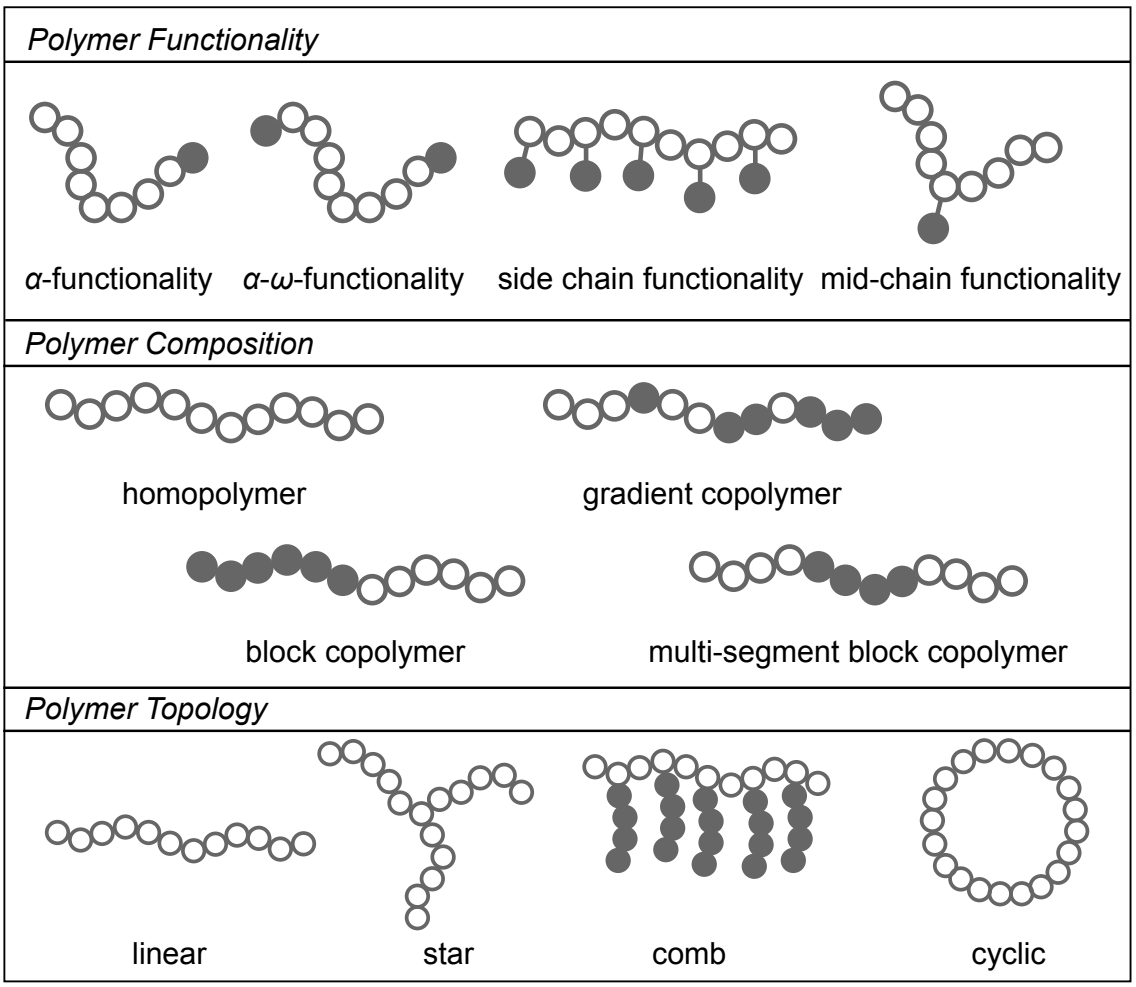

Figure 2.4 Macromolecular engineering by CRP.

precludes the use of a single controlling agent or initiating system to achieve a well-defined block structure. To date, the most convenient method to polymerize vinyl acetate in a controlled fashion is by the RAFT process, using a xanthate controlling agent.[23] However, this methodology is not appropriate for polymerizing most other monomers. It should be noted that rather recently a *switchable* RAFT agent was designed such that both highly reactive monomers (such as vinyl acetate) and relatively less reactive monomers (such as styrene and methyl methacrylate) could be polymerized in a controlled fashion.[24] The switching between protonated and deprotonated states of the Z-group, as depicted in Figure 2.5, changes the reactivity of the thiocarbonyl bond toward radical addition and the stability of the intermediate adduct radical. This allows for the generation of block copolymers, via a chain-extension approach, from monomers of disparate radical reactivity using a single controlling agent.

Additionally, in order to synthesize polymer conjugates from different classes of monomers (e.g. vinylic monomers and lactones), polymerization initiators/controlling agents must be specifically designed to perform different techniques

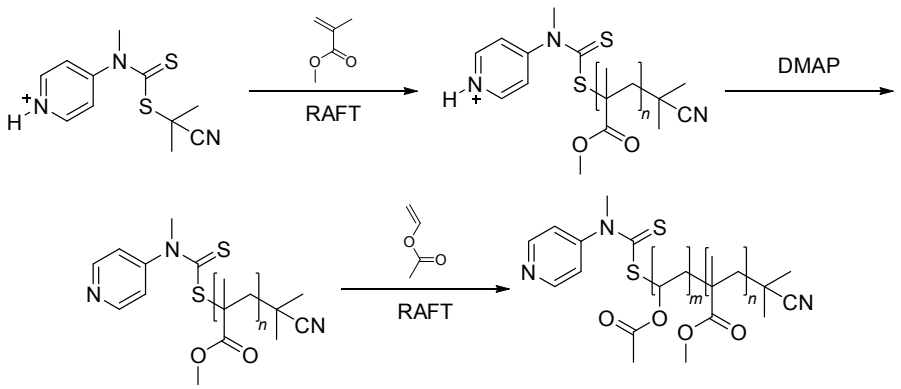

Figure 2.5 Use of switchable RAFT agents for the controlled polymerization of monomers with disparate radical reactivity. DMAP= 4-dimethylaminopyridine.

of polymerization. For example, an NMP initiator equipped with a hydroxyl moiety to perform Ring Opening Polymerization (ROP), as depicted in Figure 2.6.[25] It would therefore be highly advantageous to separately prepare polymeric building blocks with complete freedom of the synthetic route taken for their synthesis. The only requirement would be that the polymer chains bear complementary functionalities such that they may be coupled in a post-polymerization reaction. For this to be practically viable, highly efficient conjugation chemistry is required. Initial efforts into this modular approach to macromolecular design borrowed heavily from the, at the time, newly developed concept of *click* chemistry.

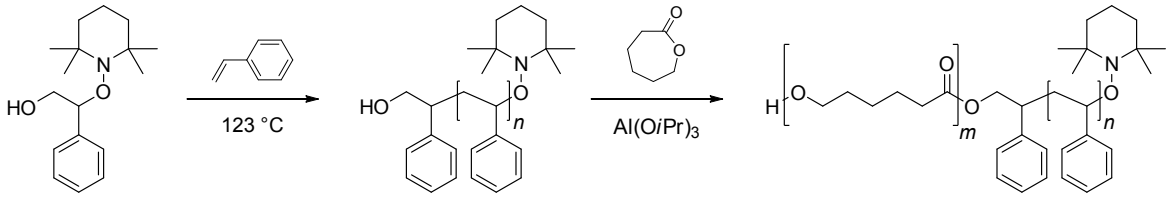

Figure 2.6 Successive NMP and ROP from a single multi-functional initiator.

2.3 Click Chemistry and Modular Synthesis

The concept, or rather the philosophy of *click* chemistry was conceived in 2001 by Sharpless and colleagues,[26] the fundamental premise of which is the use of highly efficient chemical transformations to generate new compounds in a modular approach. In order for a chemical process, inclusive of the specific reaction used, to be classified as a *click* process, it must adhere to the following rather stringent criteria:

- The process must be modular;
- Must be wide in scope;

- Produce very high yields and only inoffesive by-products;
- Purification must be achievable through non-chromatographic techniques;
- Be stereospecific;
- Require simple reaction conditions with simple product isolation;
- Be performed with readily available starting materials and reagents;
- Make use of either no solvent, a benign solvent or a solvent that can be easily removed; and
- The reaction product must be stable under physiological conditions.

The immediately recognized classes of reactions that were deemed to fulfill such criteria were listed as:

- Pericyclic reactions such as 1,3-dipolar and Diels-Alder cycloadditions;
- Nucelophilic substitution reactions such as ring opening additions to strained heterocycles (e.g. epoxides, aziridinium ions);
- Non-Aldol type carbonyl addition chemistry (e.g. urea, hydrazone, amide and aromatic heterocycle formation); and
- Addition reactions to carbon-carbon multiple bonds (e.g. Michael addition reactions, epoxidation and dihydroxylation).

The fundamental reason why these reactions earn the *click* status is their high thermodynamic driving force (> 80 kJ·mol^{-1}). This property facilitates the rapid procession of the reaction to completion and to be highly selective for a single product. This consequently simplifies compound synthesis and subsequent purification. Shortly after the publication of this concept, the groups of Sharpless[27] and Meldal[28] independently reported the copper (I) catalysed azide-alkyne cycloaddition (CuAAC) which

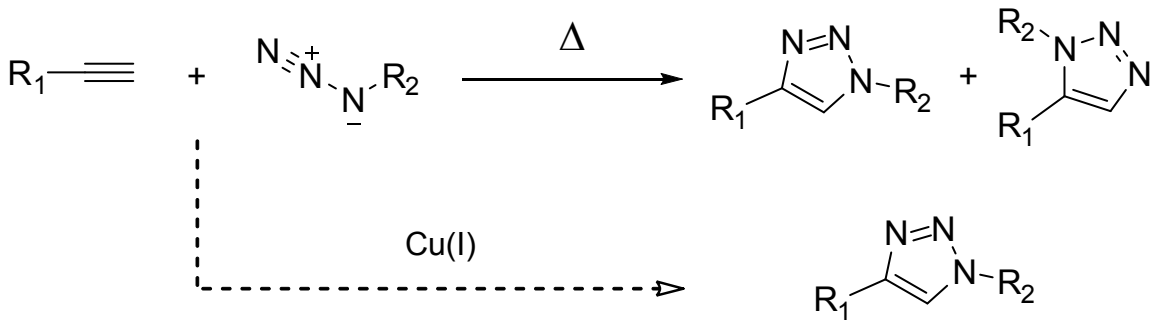

Figure 2.7 1,3-Dipolar cycloaddition between terminal azides and alkynes in comparison to the CuAAC.

very quickly came to be identified as the flagship reaction of *click* chemistry (Figure 2.7). Azides and alkynes are very energetic species and yet they are amongst the least reactive functionalities in organic chemistry, owing to their very high kinetic stability. 1,3-Dipolar cycloadditions between azides and alkynes are well known, with a mixture of 1,4- and 1,5- disubstituted triazoles being the reaction products.[29] The CuAAC, on the other hand, proceeds rapidly with complete regioselectivity towards the 1,4- substituted adduct at ambient temperature.

With such a highly efficient reaction that is well suited to conjugative chemistry, the CuAAC was quickly adopted in polymer and materials science, with the initial reports appearing in 2004.[30–32] Since then, many more examples have emerged to such a point that the generation of well-defined functional polymeric materials and complex macromolecular architectures is now dominated by modular synthetic pathways.[33]

To highlight two critical publications in this field, Opsteen and van Hest[34] were the first to put *click* chemistry into practice for the preparation of diblock copolymers. Various combinations of poly(styrene), poly(methylmethacylate) (prepared via ATRP) and poly(ethylene glycol) were coupled to form block structures using the CuAAC. Nicely complementing this ATRP route, Barner-Kowollik and Stenzel[35] reported the synthesis of novel poly(styrene)-*block*-poly(vinyl acetate) copolymers using a combination of the CuAAC and RAFT chemistry. After these important realizations, CRP processes are now primarily used to synthesize functional macromolecular building blocks, which are assembled into higher order structures through conjugation.[36] The CuAAC has certainly lead the way in this respect. The principle of modular conjugation in polymer chemistry is conceptualized in Figure 2.8.

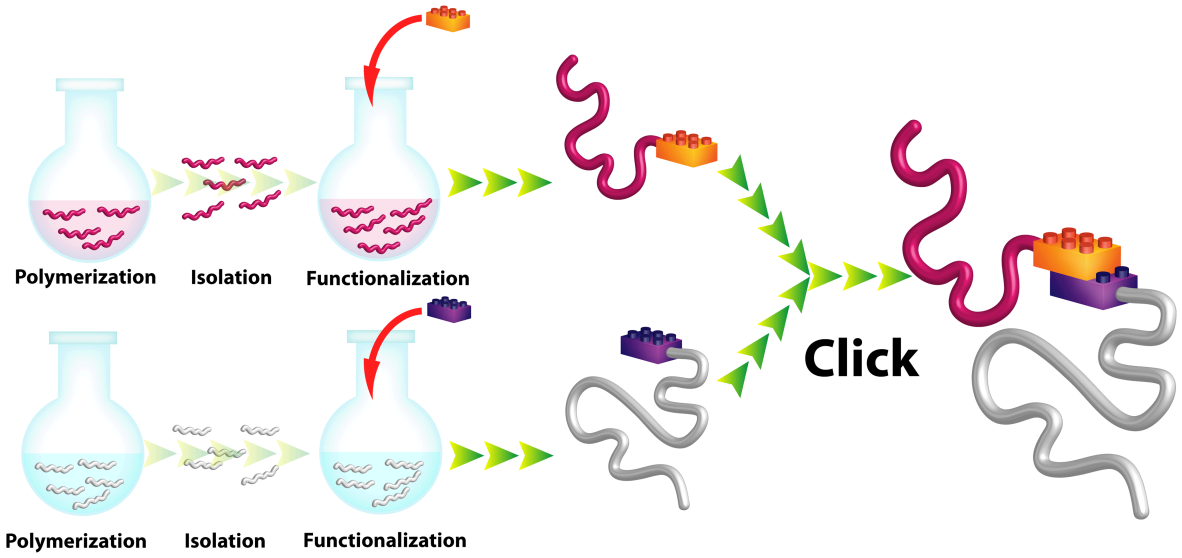

Figure 2.8 Modular conjugation of independently generated building blocks via *click* chemistry.

2.4 Ultra Rapid Approaches to Macromolecular Conjugation

The evolution of the synthetic macromolecular sciences has largely been driven by the increasing need for purposefully designed and precisely engineered materials for use in a wide variety of 'high demand' applications in fields ranging from biomedicine to the nanosciences. In pursuit of meeting such demands, the two major (and fundamental) issues that lie at the core of modern polymer research are controlling macromolecular architecture and chemical functionality. To this end, the relatively recent developments of CRP technologies and highly orthogonal and efficient conjugation chemistries (many of which have been described as *click* chemistry) that may be thereafter applied have given us, as chemists, the ability to control these properties with unprecedented precision.

Although the use of such processes as ATRP and RAFT polymerization have been exploited in and of themselves in producing well-defined architectures, it has only been with the introduction of the *click* chemistry philosophy[26, 33, 36–38] and the development of the tools with which it may be carried out that we have seen a tremendous burst of creativity in the design and synthesis of functional materials. As such, there has been no shortage of reviews dedicated to this very subject matter. To highlight just a few key examples, the use of highly efficient chemical transformations within the general context of macromolecular engineering has been discussed in the excellent review of Hawker and Wooley[39] and the perspective article of Sumerlin and Vogt.[40] Meanwhile, Klok and co-workers[41] have specifically focused upon the post-polymerization modification of polymers constituted from monomers bearing chemoselective handles.

The greatest utility that *click* chemistry has brought to macromolecular chemistry is allowing one the freedom to choose from virtually any synthetic technique to generate functional, polymeric intermediates. We now start to view our synthetic polymers as building blocks, as smaller parts of an ultimately larger structure achievable through conjugation. The concept of macromolecular conjugation may be defined by the following:

- The covalent addition of small molecules to form a larger structure, i.e. step growth polymerization in an arithmetic fashion;
- Dendrimer synthesis: covalent addition of small molecules in a geometric fashion;
- Functionalization of a polymer with a smaller molecule through a covalent linkage either to a polymer end-group or to multiple positions along the polymer backbone;

- Polymer-polymer conjugation: the direct coupling of two (or more) polymers or the indirect coupling via a small multifunctional linker; and
- Conjugation of a polymer to a surface.

It is readily observable upon inspection of the literature that there are a number of tools available that may be used to carry out all the above forms of macromolecular conjugation. However, now that there is an increasing interest in combining synthetic polymer chemistry with biology (and other chemically sensitive systems) within the context of conjugation, there is a concomitant increasing need for highly orthogonal, rapid and mild conjugation chemistries that can be efficiently applied under the conditions generally required for such systems: ambient temperature, absence of toxic catalysts and considerably dilute. Awareness of this burgeoning interest is especially reflected in two recent publications. Lutz recently highlighted various copper-free azide-alkyne cycloadditions within the context of macromolecular ligation chemistry.[42] In a much wider scope, Schubert and colleagues recently presented a collection of copper-free *click* technologies that extend beyond azide-alkyne chemistry.[43] Nevertheless, the focus of both of these publications is strictly upon the absence of copper from the discussed reactions and not necessarily upon other conditions.

2.4.1 Cycloadditions with Strained or Activated Alkynes

Typically, organic azides and terminal alkynes do not react together (within the context of a *click* reaction) at ambient temperature and in the absence of a transition metal catalyst. Atypically however, alkynes may be activated by alternative strategies that eschew the use of a catalyst altogether. The manners in which activation may be achieved have been either the application of ring-strain to an alkyne, the incorporation of an electron-withdrawing group (EWG) or a combination of both.

One of the earliest examples, if not the first, of a strained-ring promoted cycloaddition between an alkyne and azide was provided by Wittig and Krebs in 1961.[44] Neat cyclooctyne was reacted with phenylazide to yield the corresponding triazole as the only product. This has been appropriated by Bertozzi and colleagues for selective modifications of biomacromolecules and living cells.[45] With their now called 'first generation' cyclooctyne (Figure 2.9a), successful copper-free and ambient temperature cycloadditions with azides were achieved, although the reaction kinetics were comparable to those of the incumbent Staudinger ligation technology[46] and much slower than the CuAAC. Furthermore, the non-catalysed azide-alkyne cycloadditions (in general) do no show the same regioselectivity as the CuAAC. However, in the vast

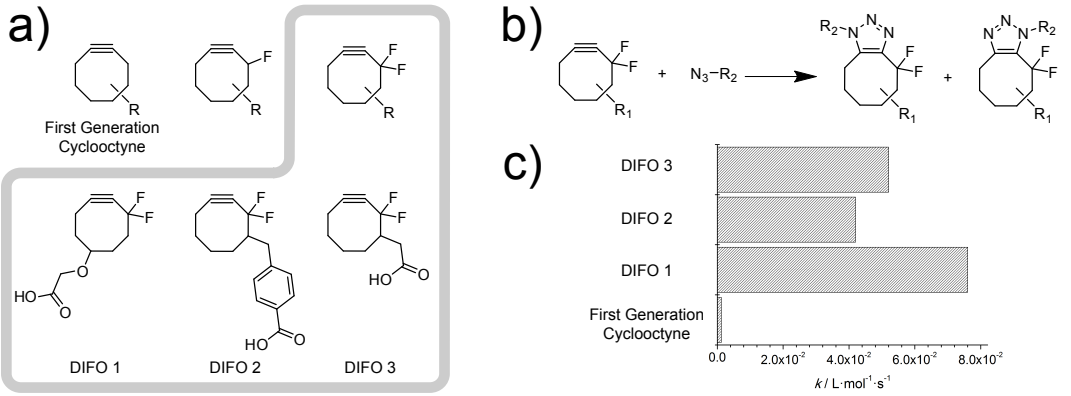

Figure 2.9 a) Structures of the various cyclooctyne derivatives used in copper-free azide-alkyne cycloadditions; b) Non regio-specific copper-free and rapid cycloaddition between azides and DIFO derivatives; c) Comparison of the second-order rate coefficients for the reactions of selected cyclooctyne derivatives and benzyl azide at ambient temperature.

majority of cases, regioselectivity is not a crucial criterion for coupling reactions, least of all in macromolecular chemistry.

A dramatic improvement in reactivity was subsequently achieved through the introduction of EWG (specifically propargylic fluorine atoms) to the cyclooctyne derivative. The monofluorinated variant only provided a roughly two-fold increase in reactivity;[47] however the difluorinated derivative [named difluorinated cyclooctyne (DIFO) 1] improved upon the reactivity by a further 20-fold increase (approximately).[48] As such, highly efficient labeling of azide-expressed cells was achieved within 1 hour of exposure to DIFO under ambient conditions.

Such fluorinated cyclooctynes have proven to be biocompatible and stable in aqueous media in addition to their remarkable reactivity. However, the synthesis of DIFO 1 is very inefficient, achieving under 2 % yield in twelve steps. Furthermore, its hydrophobicity was shown to also contribute to non-specific protein and cell binding. Substantially improving the efficiency of the synthesis of DIFO derivatives, Bertozzi and colleagues reported DIFO 2 and DIFO 3, which were formed in a 6-step, 36 % yield and a 7-step, 28 % yield strategy respectively.[49] It is noted that the reactivities of the discussed DIFO derivatives are comparable. The structures of these cyclooctyne derivatives, a general reaction schematic and a graphical comparison of their reactivities are presented in Figure 2.9.

The azide-DIFO cycloadditions therefore present a mild and fast conjugation methodology perfectly suited to biochemical applications such as *in vivo* dynamic imaging of cell-surface glycans in live cells. However, the laborious synthetic pathway of the precursor DIFO derivatives still stands in the way of such a system being more widely investigated and, as of yet, the technique has not been applied to the design and construction of synthetic materials.

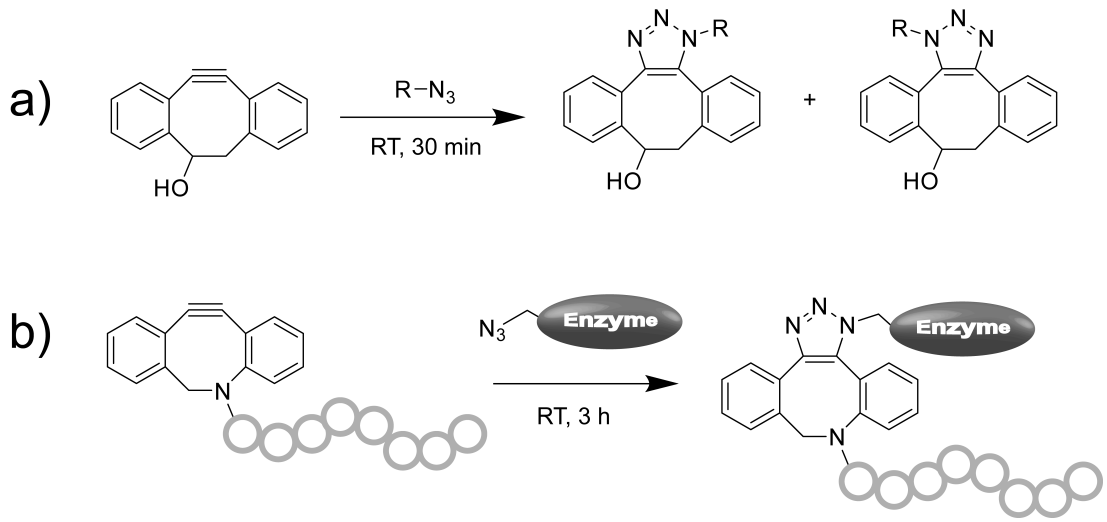

Figure 2.10 a) Strained cyclooctyne utilized by Boons *et al.*[50] for mild and rapid cycloadditions with azides; and b) PEGylation of enzymes via copper-free azide-alkyne cycloaddition.

An alternative strategy was reported by Boons and colleagues in which additional ring-strain was applied to a cyclooctyne by the introduction of aromatic rings to either side of the reactive centre (Figure 2.10a).[50] Such 4-dibenzocyclooctynols show similar reactivity to that of the DIFO derivatives of Bertozzi and are biocompatible. In model studies, various azides and cyclooctyne were mixed in an equimolar ratio and were found to undergo quantitative conversion into the corresponding 1,2,3-triazole within 30 minutes at ambient temperature. Such cyclooctynes are also claimed to have a long shelf life and there exists the potential to further enhance reaction performance by decorating the aromatic moieties with EWGs. Furthermore, a functional aza-dibenzocyclooctyne was made to great use in the recently reported PEGylation of an enzyme (Figure 2.10b).[51] Taking this into consideration, along with the simpler synthesis when compared to the DIFO derivatives, it is envisaged that such structures will be the ones to push forward the application of fast, copper-free azide-alkyne cycloaddition chemistry to include further synthetic polymer conjugations.

Yet another strategy to boost the reactivity of alkynes towards cycloadditions with azides is through the direct functionalization of the alkyne with an EWG. Ju and colleagues investigated a series of such alkynes (Figure 2.11).[52] All reactions with model compounds were performed in aqueous solution at ambient temperature and were performed with a 1:1 stoichiometry. Depending upon the structure of the alkyne, the reactions were completed within 6-12 hours. It is interesting to note that in one illustrated example, complete regioselectivity for the 1,4-regioisomer of the triazole was observed. Furthermore, and similar to the earlier examples from Bertozzi and Boons, electron-deficient internal alkynes may also undergo efficient cycloadditions with azides. This is noteworthy as the CuAAC may only be used for terminal alkynes.

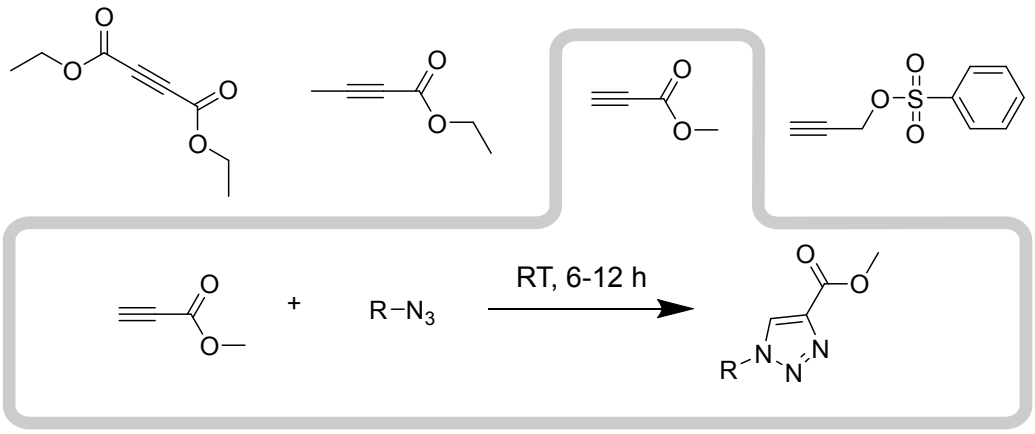

Figure 2.11 Use of electron-deficient alkynes in catalyst-free cycloadditions with azides.

Accelerating the rate of reaction such that it may be completed within 2 hours, Gouin and Kovensky reported a further electron-deficient alkyne (*p*-toluene sulfonyl alkyne) as shown in Figure 2.12a.[53] After initial trials with azido-diethylene glycol at 100 °C with and without microwave irradiation, it was discovered that by quickly removing the reaction solvent under reduced pressure at 16 °C (< 10 minutes), high conversions could be obtained within 2 hours. The explanation given for such an observation is the high concentrations of reactants that are obtained upon solvent removal. Interestingly, the rapid evaporating process produced the corresponding 1,4-regioisomer with high selectivity (> 90 %).

Upon extending the process to include a variety of azides, the high rate of reaction and high regioselectivity was further confirmed in the vast majority of cases. Although the alkyne investigated is far simpler than those already discussed, the requirement of rapid solvent removal can be rather inconvenient. Thus, the reaction would not be suitable for many biological applications where dilute conditions are necessary. In addition, a series of experiments in which the *p*-toluene sulfonyl alkyne was reacted with unprotected amine-bearing azides resulted in an ultra rapid, selective and quantitative Michael-type addition of the amino group to the alkyne (Figure 2.12b). Although the authors use these results to highlight the lack of orthogonalilty of the

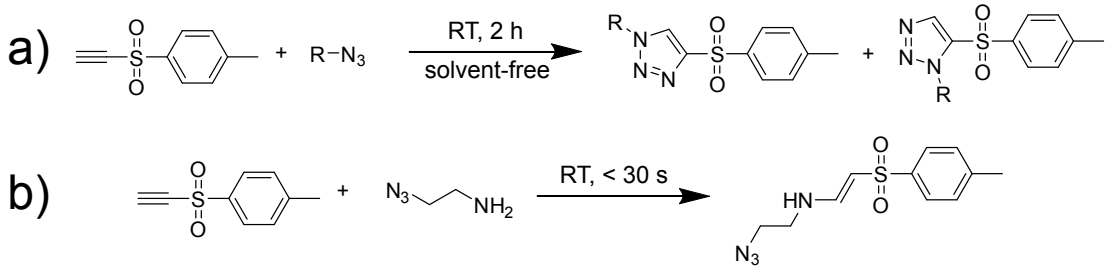

Figure 2.12 a) Solvent-free reaction between electron-deficient alkynes and azides; b) Ultra-rapid side reaction of electron-deficient alkynes with primary amines.

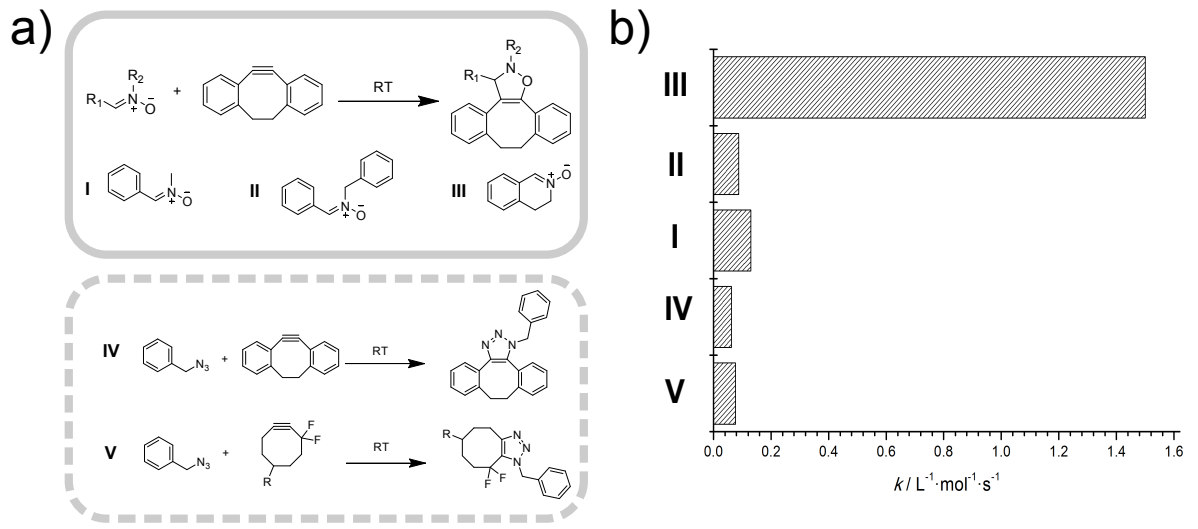

Figure 2.13 a) 1,3-Dipolar cycloadditions of nitrones with a benzannulated cyclooctyne alongside the selected reference reactions of benzyl azide with benzannulated cyclooctyne (IV) and of benzyl azide with a DIFO derivative (V); b) Comparison of the second-order rate coefficients of the reactions I-V presented in (a).

reaction when it comes to amino functionality, the use of this 'side reaction' should be further evaluated within the context of ultra fast and mild conjugations.

Thus far, the use of an azide as a dipole in such cycloadditions had been discussed. However, very recently Pezacki and colleagues demonstrated the use of a series of nitrones in 1,3-dipolar cycloadditions with benzannulated cyclooctyne, some of the structures of which are presented in Figure 2.13.[54] For all 14 nitrones studied, very high (if not quantitative) conversions were achieved within reaction times of 2-110 minutes at ambient temperature, using a 1:1 stoichiometry. Figure 2.13 compares measured second-order rate constants (k) for selected nitrones with those observed for the reactions of benzyl bromide with the benzannulated cyclooctyne and of benzyl bromide with a DIFO compound. Upon correlating I, II, IV and V (as labelled in Figure 2.13a) with the values of k in Figure 2.13b, one notices that the reactivity of the nitrones are comparable to those of the reference reactions (IV and V). However, and rather impressively, the rate of the reaction of III is about 25-fold faster than that of IV and 20-fold faster than that of V. The authors partially attribute this enhanced reactivity to the ring strain in the cyclic nitrone. Although purely a small-molecule model study, such chemistry certainly holds promise for the field of macromolecular chemistry as a mild, ultra-rapid conjugation technique.

Without a doubt, the CuAAC has led the way as far as *click* chemistry is concerned, but through its limitations it has also served as the inspiration of the development of the above discussed catalyst-free variants. Although these technologies have only been applied in relatively low molecular weight chemistry, they certainly hold great

potential to be brought to the same platform as the CuAAC. It is only the accessibility of the starting activated alkynes that prevents these methods from flourishing.

2.4.2 Thiol-ene/Thiol-yne Chemistry

Borne out of a rich history in the field of photopolymerization, the thiol-ene reaction has been widely investigated in recent years as a convenient conjugation technique in macromolecular science.[55, 56] However, it was the work of Schlaad and colleagues that made the initial efforts to extend such chemistry to the efficient modification of well-defined polymeric materials and surfaces.[57–59] Within this context, there are two main modes in which the thiol-ene reaction may be applied: the ionic mechanism or the radical mechanism. The ionic mechanism is taken to represent the various methods of performing Michael-type additions of the thiol moieties to an alkene whereas the radical mechanism is taken to encompass the ways in which thiyl radicals are generated and add across the double bond of the alkene. As will be highlighted below, there are important differences between the two (each offering their own advantages and disadvantages) which should be taken into consideration when formulating an experimental design. Figure 2.14 presents the general thiol-ene reaction pathway.

In perhaps the most elegant example to date of the use of thiol-ene chemistry for macromolecular synthesis, Hawker and colleagues prepared up to fourth generation dendrimers with unprecedented efficiency.[60] In a strategy involving sequential thiol-ene reactions and esterifications to build up the dendritic structure, the solvent-free thiol-ene reaction was performed under ambient conditions of atmosphere and temperature by simple irradiation with a hand-held UV-lamp (λ_{ex} = 365 nm). Trace amounts of the photoinitiator 2,2-dimethoxy-2-phenylacetophenone (DMPA) were required to kick-start the reaction, which took a total of 30 minutes.

Importantly, no perceptible reduction in efficiency was observed as the number of generations increased. However, when a 1:1 stoichiometry between thiol and alkene groups was utilized, incomplete conversion was observed. In order to drive the reactions to completion, 1.5 equiv. of thiol to alkene was required. In this case, the excess was in no means a cause for concern as the reaction products could be easily isolated through simple precipitation procedures. This would generally be the case

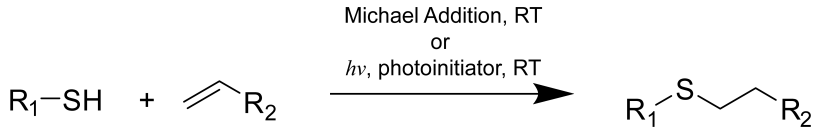

Figure 2.14 UV-promoted radical addition and Michael-type addition of thiols to alkenes in the thiol-ene reaction.

for all macromolecular thiol-ene reactions in which the species that must be used in excess is of small molecular weight, however problems begin to arise when an excess of a macromolecular species is required.

In a further, and more comprehensive investigation into radical based thiol-ene chemistry, Hawker and colleagues prepared a series of polymers with either single or multiple alkene functionality and *clicked* on a variety of commercially available mercaptans under both photoinitiation (with trace amounts of DMPA) and thermal initiation [in the presence of radical initiator 2,2'-azobis(2-methylpropionitrile)].In all cases studied, the photoinitiated thiol-ene reactions (all performed at ambient temperature) could be made to proceed to completion in times ranging from 30 minutes to 2 hours.

These examples already prove the efficiency of thiol-ene reactions, however they have only dealt with couplings between alkene-functional macromolecules and small molecular weight thiols. Examples in which fast thiol-ene reactions have been used for truly macromolecular couplings have made use of the ionic mechanistic pathway.

Arguably, the most convincing example of Michael-type thiol-ene chemistry for macromolecular-macromolecular conjugations comes from Dove and colleagues.[61] In the initial part of the investigation, maleimide-capped poly(lactic acid) (PLA) was prepared and the end-groups modified via a triethylamine (TEA) catalysed Michael addition with a variety of thiols. In the majority of cases, a 1.05 equiv. of thiol and 1 equiv. of TEA to alkene resulted in quantitative conversions in times ranging from < 5 minutes to 2 hours. Importantly, the structure of the thiol played an important role in the efficiency of the reactions. To point out just one example, the reaction with the sterically demanding *t*-BuSH required 1 week to achieve quantitative conversion using 5 equiv. thiol and 2 equiv. TEA.

Extending these results to include macromolecular-macromolecular couplings, bi- and tri- functional thiol compounds were used to generate homo-coupling between two PLA chains and 3-arm star-shaped PLA respectively. In both cases, an excess of thiol (1.1 equiv.) was required to ensure complete conversion of all maleimide functionality. In such systems (where an excess of a linker is used) a statistical mixture of products is formed. In the case of the block homocoupling, a mixture of the required block, the product resulting from a single PLA chain adding to the thiol linker and bis-functional thiol linker is produced. It may be observed that only the target product contains no thiol functionality. A similar product distribution can also be expected for star formation. The thiol containing side products are then cleverly (albeit relatively expensively) removed through the use of an iodoacetate resin. A subsequent precipitation produces very well-defined products, both of which were formed within 2 hours at room temperature.

An alternative and convenient approach that is also highly versatile is the use of polymers prepared via RAFT polymerization as precursors to thiol-capped polymers.

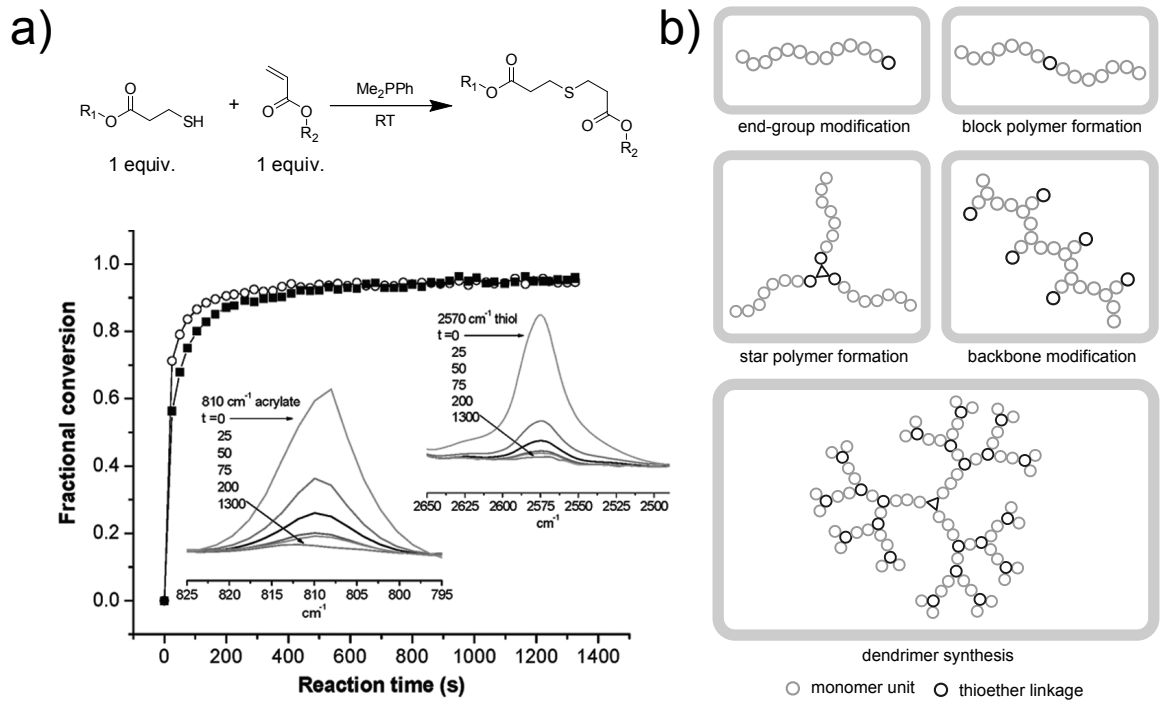

Figure 2.15 a) Kinetics of the thiol-ene reaction monitored via FT-IR spectroscopy;[62] b) Various polymeric architectures achieveable by thiol-ene chemistry.

RAFT polymerization is the most versatile controlled radical polymerization method in terms of the wide variety of monomers that may be used. As such, the combination of this technology with thiol-ene chemistry offers, arguably, the greatest accessibility to synthetic functional materials.

Lowe, Hoyle and co-workers recently presented a one-pot strategy in which dithioester-capped polymer, alkene and a hexylamine (HexAM)/dimethylphenylphosphine (DMPP) catalyst system were used to perform a sequential aminolysis and Michael addition.[63, 64] This was used to generate 3-arm star polymers quite rapidly at ambient temperature by employing a triacrylate as the star core. Although proceeding under ultra rapid and mild conditions, a considerable number of 2-arm and 1-arm star material * was also formed, which the authors claim arose from a number of factors, including the use of impure starting materials and the required excess of thiol-capped polymer (1.5 equiv. with respect to thiol functionality). Figure 2.15 shows examples of the kinetics of the phosphine catalysed thiol-ene reaction and the variety of macromolecular architectures that have been prepared (by either ionic or radical pathways) respectively. The above described pathways to star polymers via thiol-ene chemistry is graphically depicted in Figure 2.16.

*The terms '2-arm' and '1-arm' star material are taken to denote species arising from two polymer chains and a single polymer chain coupling to the tri-functional core respectively.

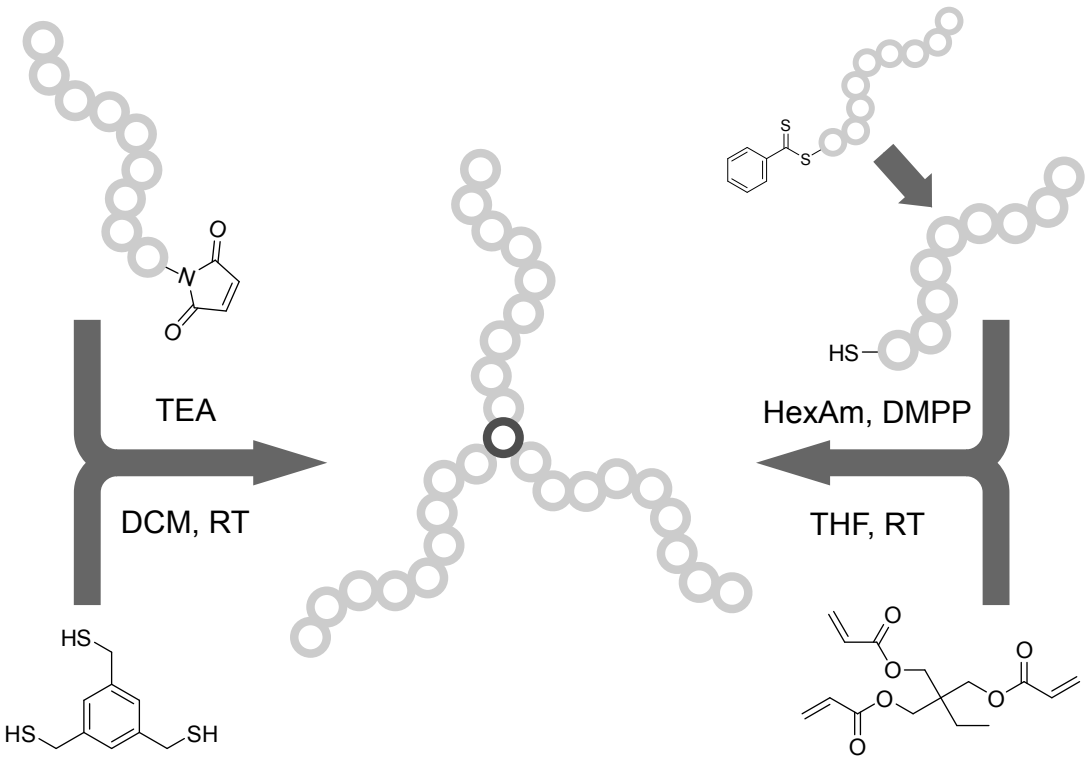

Figure 2.16 Strategies for polymeric star formation via the thiol-ene route as utilized by Dove (left) and by Hoyle and Lowe (right). TEA = triethylamine, DCM = dichloromethane, HexAM = hexylamine, DMPP = dimethylphenylphosphine.

Making further use of the phosphine catalysed thiol-ene reaction, Lowe and Hoyle showed that it is orthogonal to the radical based addition of thiols to alkynes, now referred to as thiol-yne chemistry.[62] Operating under essentially the same mechanism as the radical-based thiol-ene chemistry, two thiols may add across the alkyne triple bond (in two steps) in a manner illustrated in Figure 2.17a. In the small molecule investigation by Lowe and Hoyle, the thiol-ene reaction was observed to attain 90 % conversion in 2.5 minutes, with 17 minutes required to reach quantitative conversion (increasing the phosphine content could speed up the reaction to < 1 minute). The thiol-yne reaction (which was performed under UV-irradiation at ambient temperature and in the presence of DMPA) was observed to attain > 90 % conversion in about 1.5 min, with full conversion requiring 10 minutes. The results from a FT-IR kinetic experiment are presented in Figure 2.17b. One limitation in this specific technique is that the thiol-ene reaction must be performed first as thiol-yne chemistry is not orthogonal to radical-based thiol-ene chemistry.

Taking advantage of the 'two for one' mechansim of the thiol-yne reation, Stenzel and colleagues used this chemistry in the efficient construction of dendrimers in much the same way as Hawker reported using thiol-ene reactions.[65] In this case, however, the number of branching points that are generated in each generation of the synthesis are double that which can be obtained from the thiol-ene route. The thiol-yne reactions

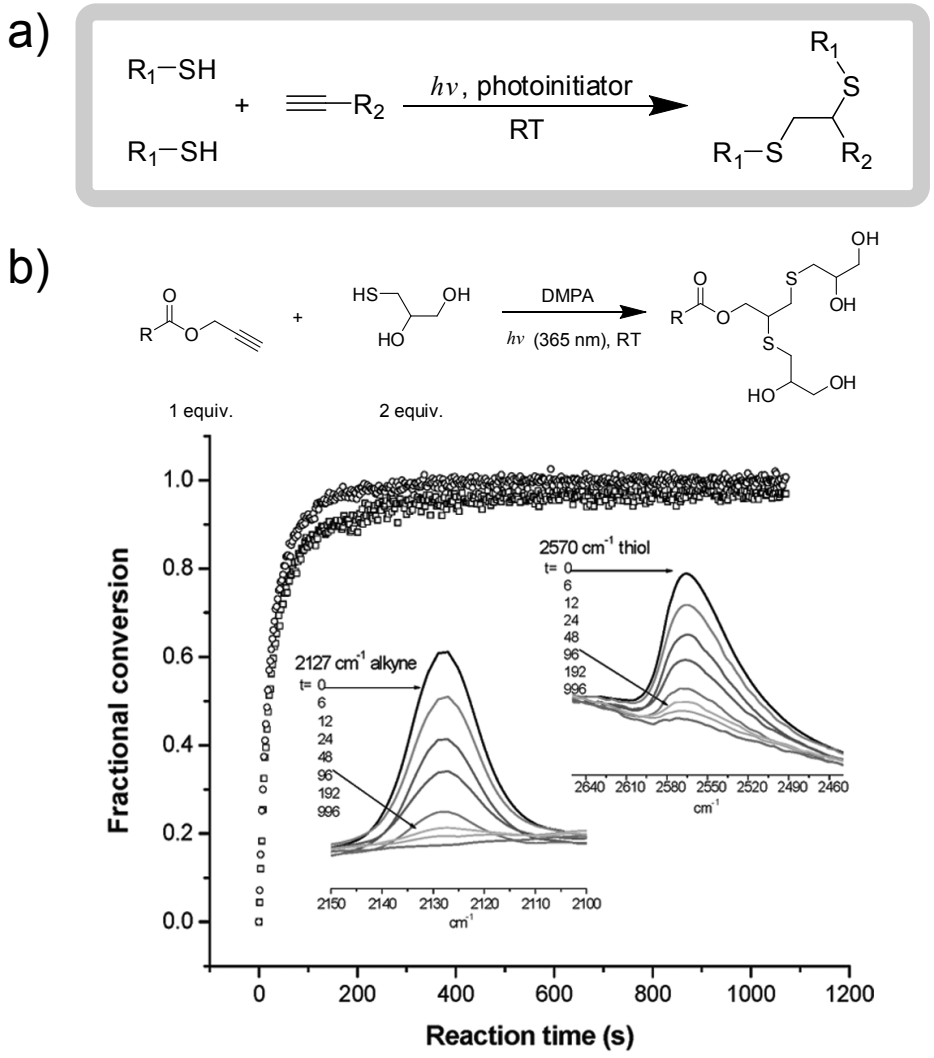

Figure 2.17 a) The UV-promoted radical addition of thiols to alkynes: the thiol-yne reaction; b) Kinetics of the thiol-yne reaction monitored via FT-IR spectroscopy.[62] DMPA = 2,2-dimethoxy 2-phenylacetophenone.

were carried out by UV-irradiation at ambient temperature in the presence of DMPA. As was similarly observed by Hawker, the efficiency of the reaction appeared to be 'generation-independent', requiring only 10 minutes to achieve quantitative conversions. Perrier and colleagues also recently made use of a similar approach to access functional, hyper-branched polymers starting from small molecules equipped with both thiol and alkyne functionality.[66] To give but one final example, the use of direct sunlight as the radiation source was used to demonstrate the great practicality of thiol-yne chemistry in the modification of alkyne-functional polymeric brushes tethered to a surface.[67]

It is therefore apparent that thiol-ene and thiol-yne chemistry can be utilized to great advantage in macromolecular conjugation owing to their high efficiency, rapid reaction kinetics and mild reaction conditions. However, it must be stressed that macromolecular-macromolecular conjugations have only been successfully reported through the use of the Michael-type variant of the reaction. Attempts to achieve efficient macromolecular-macromolecular couplings via the radical variant of thiol-ene chemistry has been met with profound difficulty and, although exceedingly long reaction times may allow for such a reaction to work as intended, it falls outside the realm of ultra-rapid conjugation.[68] Although most of the small molecule kinetic studies have used a 1:1 stoichiometry of thiol to alkene (or 2:1 thiol to alkyne in the case of thiol-yne chemistry); when multiple macromolecular species are involved, an excess of the thiol is typically required. For systems in which polymer chain-end modifications are performed, excesses of small molecules are not a problem as purification of the polymer is very straightforward. However, in macromolecular-macromolecular conjugations (such as block copolymer formation or convergent star synthesis), more elaborate purification methodologies are required, the most convenient (however relatively expensive) of which is the use of an iodoacetate resin to remove excesses of thiol.

2.4.3 Thiol-Isocyanate Chemistry

In yet another example of the chemical versatility of thiols, their base catalysed reaction with isocyanates is very fast and can be utilized with considerable ease. Such a reaction was used by Klemm and Stöckl in the convenient preparation of thiol- and isocyanate- terminated thiocarbamate prepolymers, as depicted in Figure 2.18.[69] By varying the stoichiometry, either di-thiol or di-isocynate functional poly(thiourethane)s could be assembled within 1 hour at ambient temperature.

Extrapolating from this work, Hoyle and colleagues combined this chemistry with thiol-ene reactions to achieve segmented polythiourethane elastomers.[70] A simple

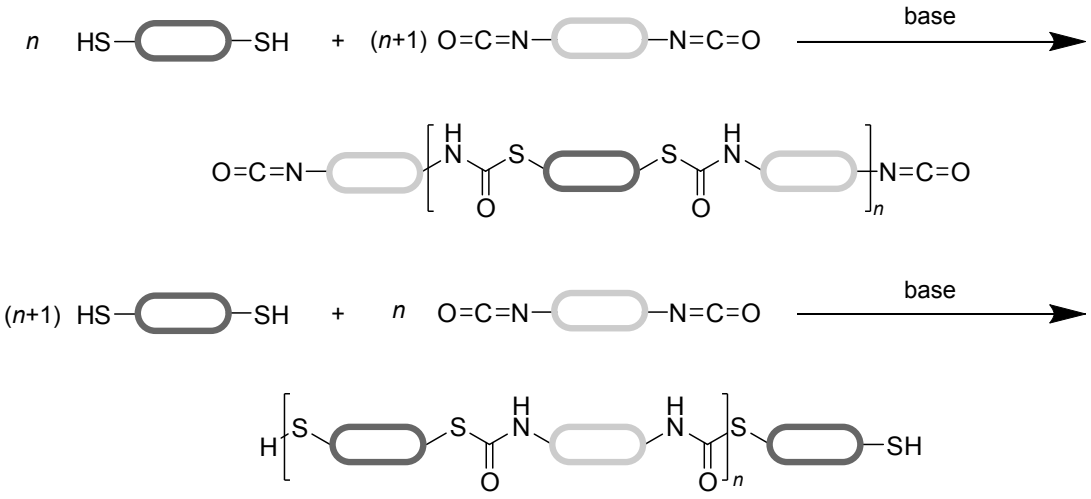

Figure 2.18 Step-growth polymerization via the thiol-isocyanate reaction, yielding poly(thiourethane)s.

mixing of di-thiol prepolymer, diisocyanate linker and a catalytic amount of TEA (0.03 - 0.1 wt%) resulted in 95 % conversion of the isocyanate within 10 minutes.

The use of the base catalysed thiol-isocyanate reaction in the quantitative preparation of ω-functional polymers was also recently reported.[71] Here, RAFT polymerization was used to prepare poly(*N*,*N*-diethylacrylamide), the dithioester end-group of which was transformed into a thiol moiety by aminolysis. Subsequent end-group modification of the resulting thiol-terminated polymer was achieved in an overnight, ambient temperature and oxygen-free reaction with one of a collection of commercially available isocyanates in the presence of TEA (Figure 2.19a).

Although a 2-fold excess of isocyanate was used and the reactions were allowed to proceed overnight, a real-time reaction kinetics experiment was performed. Hexyl isocyanate, thiol-terminated polymer and TEA were added in the ratio of 1:1:1.75 in THF and the reaction that followed was monitored at 20 °C. As can clearly be observed in Figure 2.19b, 94 % conversion of the isocyanate is achieved within 15 minutes. It is important to note that the thiol-isocyanate reaction is not orthogonal to the base catalysed Michael addition of thiols to alkenes, as was observed by Lowe when attempting to conjugate 2-isocyanoethyl methacrylate, although this system still showed significant selectivity towards the thiocarbamate adduct.[71] Furthermore, it should be noted that isocyanates are very reactive (and toxic) compounds which can react with hydroxyl functionality, amine functionality, water and even with themselves. This imposes obvious limitations to the applicability of such chemistry as a conjugation method in polymer science.

Therefore, the base catalysed thiol-isocyanate reaction qualifies as an ultra rapid and mild conjugation procedure that may be easily applied to the macromolecular sciences. As of yet, it has only been utilized as a mechanism for step-growth poly-

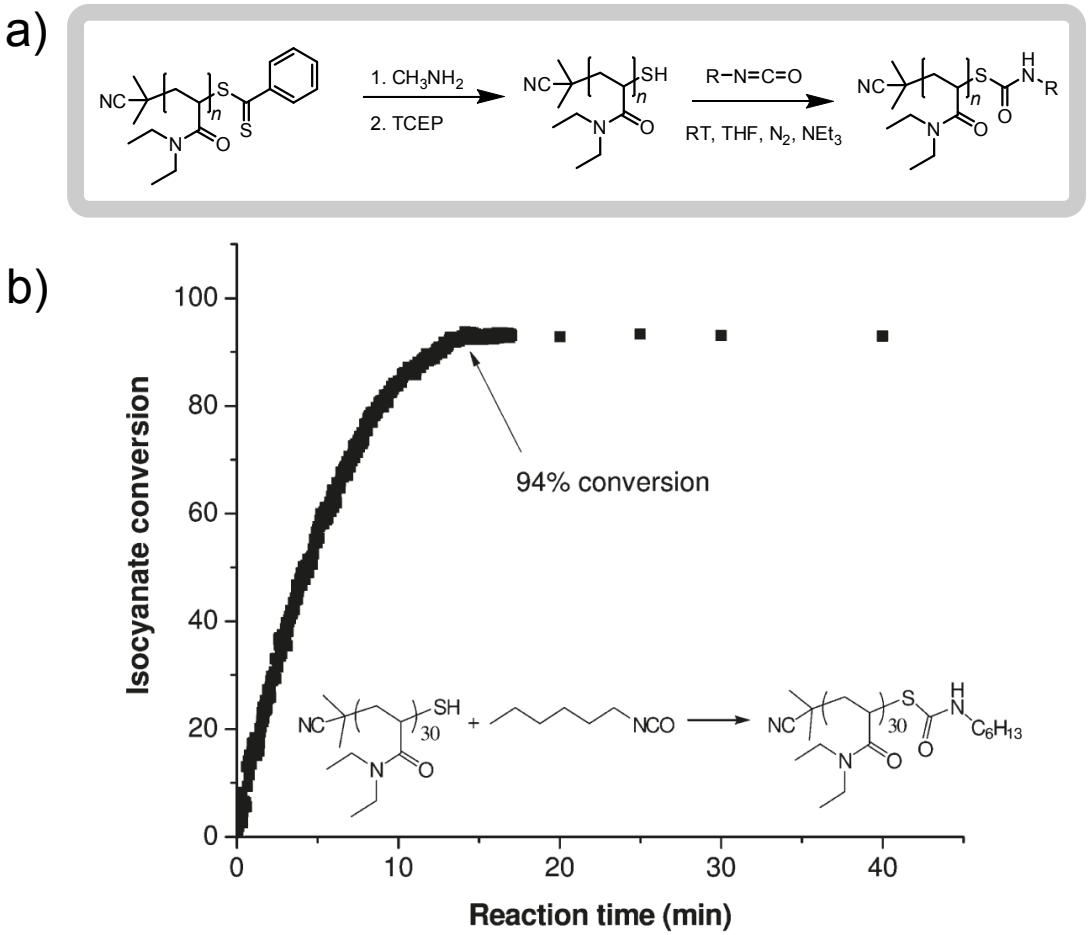

Figure 2.19 a) Aminolysis of a polymer chain formed via RAFT polymerization and reaction of the resulting thiol with an isocyanate; b) Real-time kinetics of the thiol-isocyanate reaction, monitored by FT-IR spectroscopy. TCEP = tris(2-carboxyethyl)phosphine.

merization and in the end-group modification of polymers with, by comparison, much smaller molecules. In order to be more widely adopted, macromolecular-macromolecular couplings must be attempted and in order for that to be achieved, a more universal strategy for equipping polymer chains with isocyanate groups is required. Unfortunately, the severe lack of orthogonality will surely prevent such chemistry from reaching the scope of other efficient conjugation technologies such as the CuAAC.

2.4.4 Thio-Bromo Chemistry

In this final example of the broad applicability the thiol moiety has within conjugative chemistry, the nucleophilic thio-bromo reaction is beginning to make an impact in macromolecular science. Typically, a base such as TEA is used to deprotonate the thiol, which can then efficiently react with α-bromoesters in a thio-etherification reaction.

The first noteworthy example comes from Percec and colleagues, in which the synthesis of up-to G4 dendrimers was achieved through sequential thio-bromo and acylation reactions.[72] The initial thio-bromo reaction of thioglycerol (1.2 equiv.) with a secondary α-bromoester in the presence of TEA (1.2 equiv.) in acetonitrile yielded the required G2 dendrimer in only 5 minutes at ambient temperature. However, unlike the observations of Hawker and colleagues (who made use of UV-initiated thiol-ene reactions),[60] longer reaction times were required with increasing generation (20 minutes and 45 minutes required for G3 and G4 dendrimers respectively). Furthermore, silica gel chromatography was required to isolate the various dendrimers at each generation, something which was not required in the case of the UV-initiated thiol-ene reaction earlier discussed. Additionally, a potentially important note from the authors regarded the large exotherm that occurs at the beginning of the reaction. Therefore even though no external heating source is used, the reaction temperature could increase substantially unless extra care is taken.

In a further example, dendritic macromolecules were synthesized via a combination of single-electron transfer living radical polymerization (SET-LRP) and thio-bromo *click* reactions in a novel 'branch and grow' strategy (Figure 2.20).[73] This involved SET-LRP of methyl acrylate from a multi-functional initiator, followed by conversion of the bromide end-groups with thioglycerol via the thio-bromo reaction. Acylation of the resulting hydroxyl chain termini with 2-bromopropionyl bromide then yielded another multi-functional initiator for SET-LRP that contained twice as many initiating sites as the previous generation. Again, in each case an excess of TEA and thioglycerol were required (1.2 equiv.) and longer reaction times were needed for higher generations.

More recently, Davis and Lowe extended this concept to include polymers prepared via RAFT polymerization as macromolecular thiol precursors.[74] Dithiobenzoate-based RAFT agents were synthesized bearing double α-bromoester functionality in the R-group fragment. Two were synthesized, one bearing secondary bromide functionality; the other with tertiary bromide functionality. Use of these compounds to mediate controlled polymerization of various monomers yielded low molecular weight polymer chains bearing ω-dithiobenzoate end-groups and α-bis bromoester end-groups. The simple addition of a HexAm/TEA (1:2) catalyst system resulted in the *in situ* aminolysis of the dithioester end-group and the subsequent reaction of the formed thiol with the bromide functionality of neighbouring polymer chains. In consequence, multiblock and hyperbranched polymers were readily formed (Figure 2.21).

As part of an initial model study, poly(methyl acrylate) (PMA) prepared via RAFT polymerization in the presence of a conventional RAFT agent (bearing no bromide functionality) was separately reacted with methyl 2-bromopropionate (MBP) and

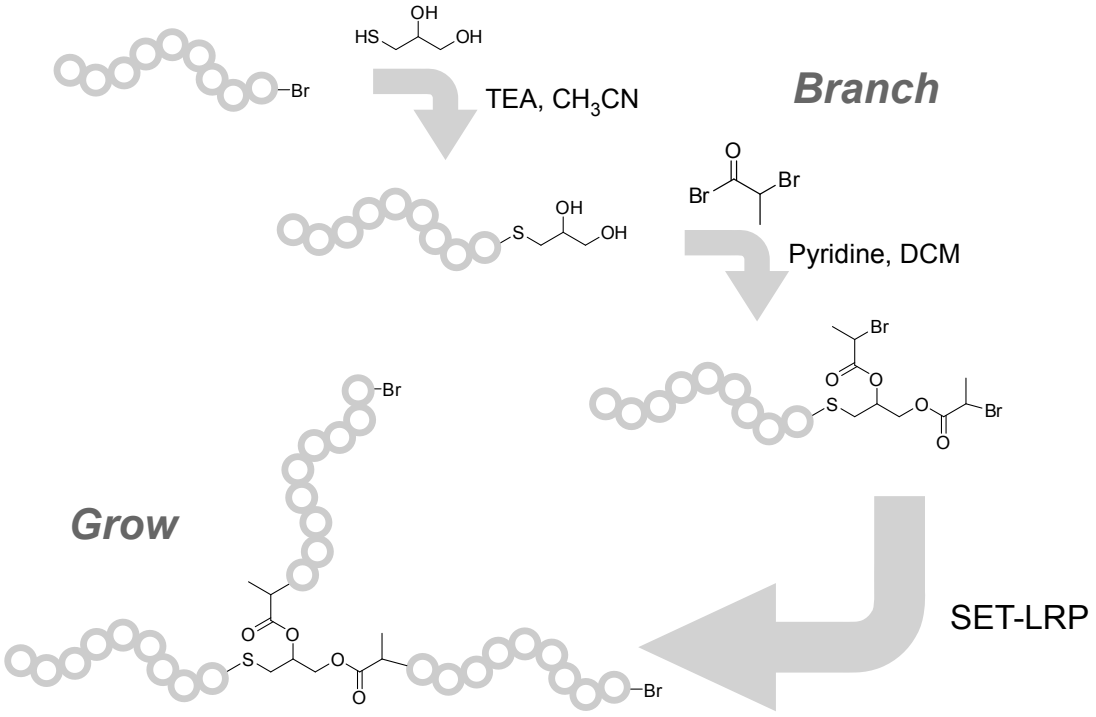

Figure 2.20 The 'Branch and Grow' strategy of polymer design as utilized by Percec and colleagues. TEA = triethylamine, DCM = dichloromethane.

ethyl 2-bromoisobutyrate (EBiB) (2-fold excess), using a mixture of HexAm and TEA (1:2). Based upon ESI-MS measurements, the reaction with MBP was completed within 30 minutes, however a significant quantity of side products (identified as cyclic thiolactone) were observed. The end-group functionality was subsequently estimated to be 73-80 %. Similar experiments involving poly(*N*-isopropylacrylamide) (PNIPAM) in place of PMA resulted in an estimated $\geq$ 95 % ω-functionality. When MBP was replaced by EBiB, an expectedly longer reaction time (3 hours) was required to obtain high yields of the corresponding thioether product. Translating these model studies to the generation of hyperbranched polymers, high yields were attained within 30 minutes when secondary bromides were utilized. Upon replacing secondary for tertiary bromides, a 20 hour reaction time was required to achieve comparable yields.

An additional interesting observation is that the thio-bromo reaction is kinetically favoured over the competing disulfide formation that must always be considered in such systems. The thio-bromo *click* reaction is obviously very convenient in that it makes use of not only readily available materials, but also some of the most common end-groups encountered in modern polymer chemistry. It therefore has the potential to become a valuable addition to the *click* chemistry toolbox.

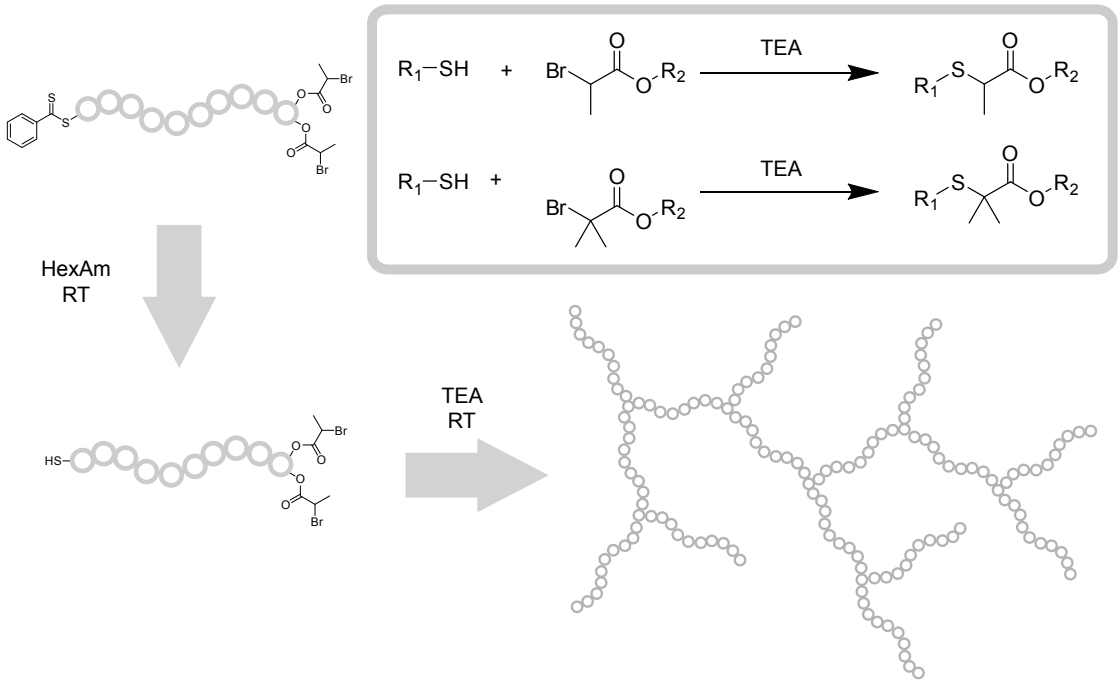

Figure 2.21 The use of the thio-bromo reaction to achieve highly branched polymers from narrow disperse polymer precursors.

2.4.5 Inverse Electron-Demand Diels-Alder Cycloaddition

The reversibility of the conventional Diels-Alder reaction makes it a prime candidate for the synthesis of 'smart materials' that exhibit a temperature dependent transition between two physical properties (such as viscosity or colour). However, many applications (such as biological labelling) require irreversible conjugation chemistry that also is very fast under mild and dilute reaction conditions. For such purposes, the inverse electron demand Diels-Alder (IVED-DA) reaction between electron-deficient tetrazine derivatives and various alkenes is incredibly efficient.

The overall transformation (Figure 2.22) occurs through an initial catalyst-free [4+2] cycloaddition after which N_2 is released through a subsequent retro-[4+2] cycloaddition. To date, the most effective alkene for such reactions is *trans*-cyclooctene.

After publishing the facile synthesis of *trans*-cyclooctene derivatives from the readily accessible *cis*-cyclooctene,[75] Fox and colleagues extended this work to develop a fast bioconjugation strategy based upon IVED-DA cycloadditions.[76] Maleimide functional *trans*-cyclooctene was coupled to thioredoxin (after reduction to produce the solvent exposed cysteine) via standard Michael addition chemistry. The now *trans*-cyclooctene functional thioredoxin (Trx-ene) could then be further modified extremely efficiently with an electron-deficient tetrazine (3,6-di-(2-pyridyl)-*s*-tetrazine) shown in the left side of Figure 2.23. The overall strategy is depicted in Figure 2.24.

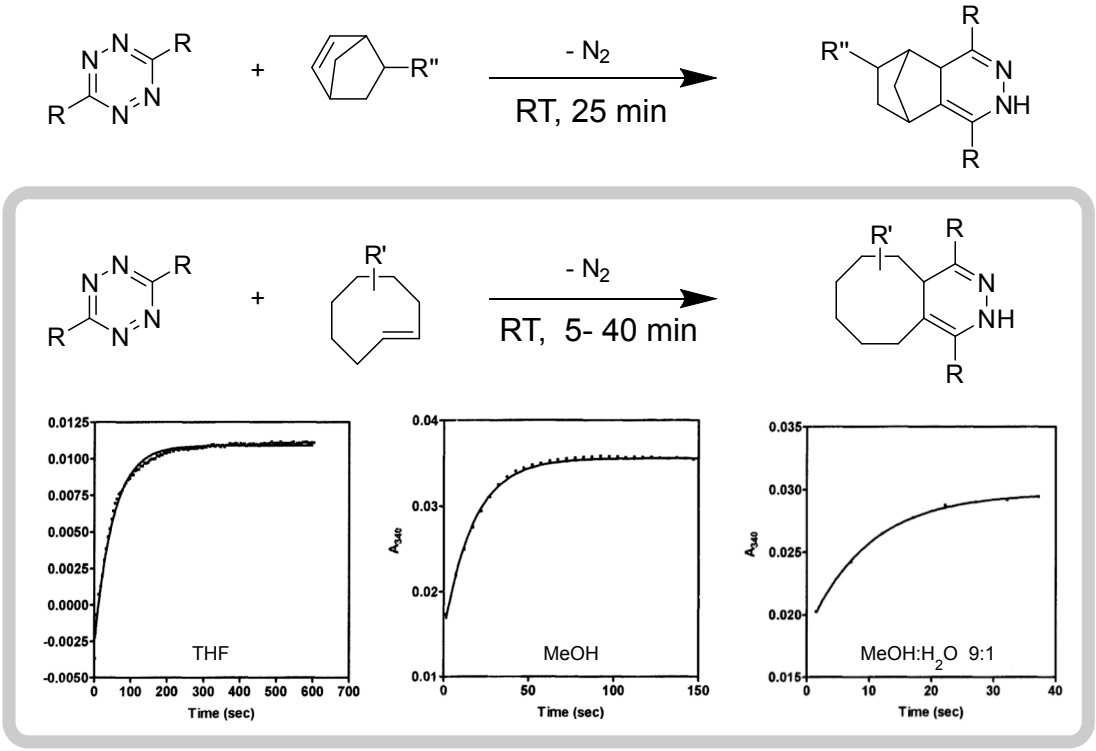

Figure 2.22 The inverse electron-demand Diels-Alder reaction between tetrazines and strained alkenes. The kinetics of the cycloaddition is greatly influenced by the solvent in which the reaction is performed.

The reaction of 2 equiv. of tetrazine (30 µM) with Trx-ene (15 µM) in aqueous media resulted in complete conversion into the expected Diels-Alder adduct within 5 minutes at ambient temperature. However, in a model reaction in which *trans*-cyclooctene and 3,6-di-(2-pyridyl)-*s*-tetrazine were reacted in a 1:1 ratio and in low micromolar concentrations (5 µM); 40 minutes was required to attain quantitative conversion, thus further illustrating the extremely efficient and rapid nature of the transformation. Curiously, tetrazines bearing additional functionality were also synthesized, however not utilized in conjugation studies. Furthermore, experiments in which model reactions were performed in cell media and in cell lysate produced $>$ 80 % yield of adduct (analysed by ESI-MS against an internal standard), indicating that the reaction is tolerant to a broad range of biological functionality. In spite of these encouraging results, 3,6-di-(2-pyridyl)-s-tetrazine was also observed to undergo significant reaction with nucleophiles (50 % conversion with $BuNH_2$ in 4 hours, and 50 % conversion with EtSH in 10 minutes) and also significant decomposition in pure water (50 % after 2 hours).

Hildebrand and colleagues used as similar strategy to achieve highly selective fluorescent labelling of live cells.[77] Unlike the various tetrazines described previously, the asymmetric, amine-functional tetrazine investigated here [3-(*p*-Benzylamino)-1,2,4,5-tetrazine, right side of Figure 2.23] had a significantly higher stability in aqueous

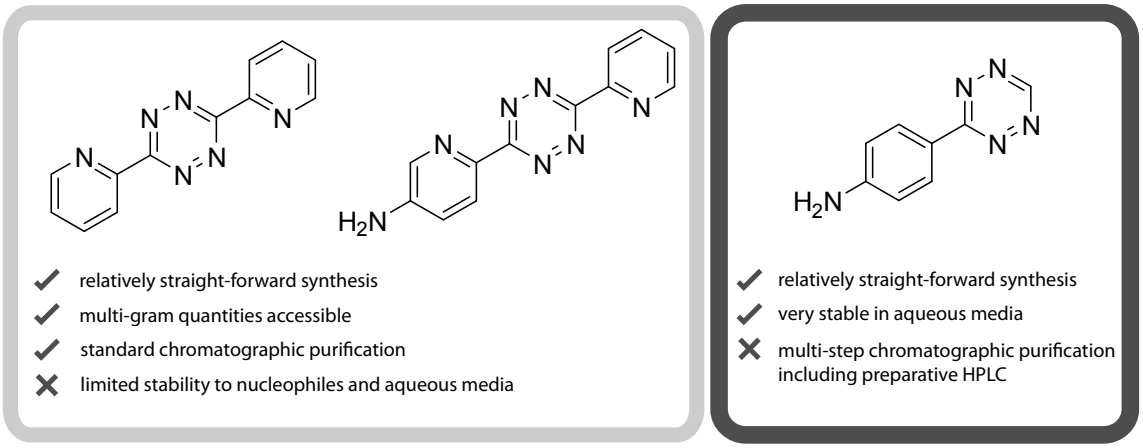

Figure 2.23 Comparison of the various tetrazines that have been successfully utilized in ultra-rapid and mild conjugations.

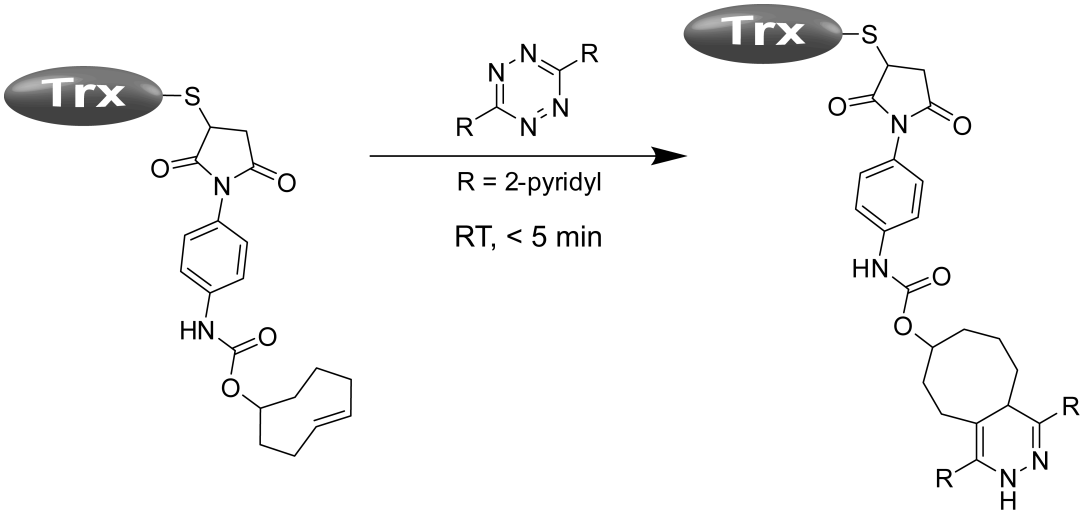

Figure 2.24 Modification of thioredoxin (Trx) via the IVED-DA cycloaddition.

and biological media. In addition, the tetrazine proved to also be highly reactive towards the IVED-DA reaction - initially with various norbornene derivatives (20 - 25 minutes required for quantitative conversion) and later with the highly active *trans*-cyclooctene (10 minutes required for quantitative conversion) - at ambient temperature.[78] Despite this highly desirable improvement, one caveat lies in the generation of the 3-(*p*-Benzylamino)-1,2,4,5-tetrazine. Although the synthesis is relatively straight forward, purification on the other hand required a multi-step chromatographic separation - including preparative HPLC. Thus increasing the scale of the synthesis, at this stage, may prove problematic.

The IVED-DA cycloaddition between electron-deficient tetrazines and various alkenes (in particular *trans*-cyclooctene) - although non-regioselective - is an extremely efficient, rapid and mild chemical transformation. With respect to macromolecular science, however, the modification of a protein via this strategy by Fox and colleagues stands as the only example to date.[76] Further extending this reaction to perform macromolecular conjugations on synthetic polymers is, arguably, limited to the relatively low accessibility of viable tetrazines. Although the tetrazines reported by Fox and colleagues proved to have limited compatibility with nucleophiles and aqueous environments, their ease of synthesis may be key in initial attempts at combining such a technology with CRP.

2.4.6 Cycloadditions Involving Nitrile Oxides

A reaction that is set to gain momentum within the field of macromolecular science over the next few years is the cycloaddition of nitrile oxides with alkynes and norbornenes to form isoxazoles and isoxazolines respectively (Figure 2.25). Whilst strictly a catalyst-free reaction, the *in situ* generation of the requisite nitrile oxide from the respective oxime precursor typically makes use of a mixture of a dipole generating agent (such as Chloramine-T) and a weak base (such as aqueous $NaHCO_3$).

Heaney, Lutz and co-workers introduced the nitrile oxide-alkyne reaction as a mild means of modifying the end-groups of alkyne-functional polymers formed by

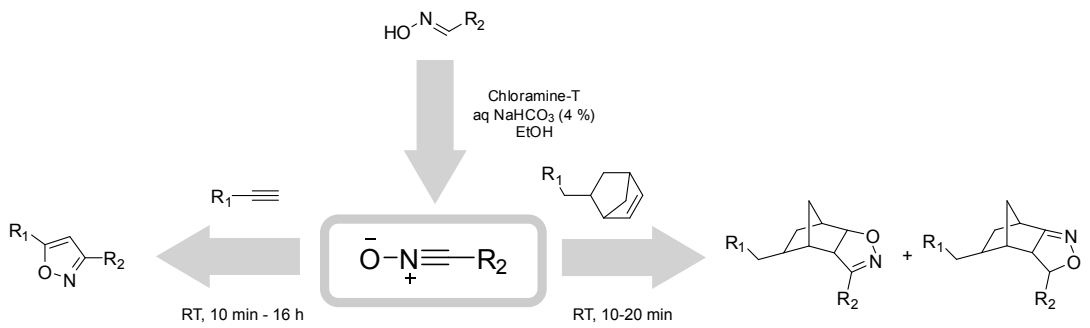

Figure 2.25 Cycloadditon of nitrile oxides with alkynes/alkenes.

ATRP.[79] Although proceeding to high yields and with great regioselectivity at room temperature, a 16 hour reaction was required, utilizing a 50 to 70-fold excess of the precursor oxime. Interestingly, extension of this methodology to solid-phase oligonucleotide conjugation resulted in good conversions in just 10-30 minutes, an observation that was not readily explained.[80]

Making use of norbornenes in place of alkynes, Carell and colleagues explored the modification of DNA with a variety of oximes via the *in situ* nitrile oxide-norbornene cycloaddition.[81] In this case, complete conversions were obtained at room temperature in 10-20 minutes, although a 10-fold excess of nitrile oxide with respect to the norbornene moieties was utilized.

Although the highly efficient copper (I) catalysed[82] and ruthenium (II) catalysed[83] variants of the reaction have been previously reported, a definitive kinetic investigation of transition metal-free reactions between nitrile oxides and alkynes (in macromolecular systems) is still lacking. Furthermore, such chemistry has also been effectively employed as a mechanism for step-growth polymerization, however not under ambient conditions.[84, 85] It is also worth noting that the isoxazoles that are formed after such a cycloaddition may be partially reduced to β-aminoenone groups or fully reduced to β-aminoalcohol groups. Such generation of new functional groups (with relative ease) has already been proven to be successful in the formation of cross-linked polymer networks.[85] As a further note, nitrile oxides may also react with a relatively wide range of nucleophiles (including thiols).[86] Thus the orthogonality of such chemistry must be carefully taken into consideration on a case by case basis in macromolecular science.

Therefore, as it stands, the nitrile oxide-alkyne cycloaddition holds promise as a mild conjugation strategy for macromolecular systems; however it still remains to be shown that efficient macromolecular-macromolecular conjugations are achievable through the use of equimolar stoichiometry of the respective reactive partners.

2.4.7 Oxime Formation

Amongst the list of highly efficient chemical transformations that were outlined in the definitive *click* chemistry paper by Sharpless and colleagues was carbonyl chemistry of the non-aldol type.[26] One such reaction is oxime formation, resulting from the catalyst-free/ambient temperature reaction of aldehydes/ketones with aminooxy functionalities (Figure 2.26).

The use of this strategy has rarely been encountered as a conjugation technique in macromolecular chemistry. Nevertheless, in a very nice example Maynard and coworkers prepared a variety of aminooxy functional polymers via ATRP and conju-

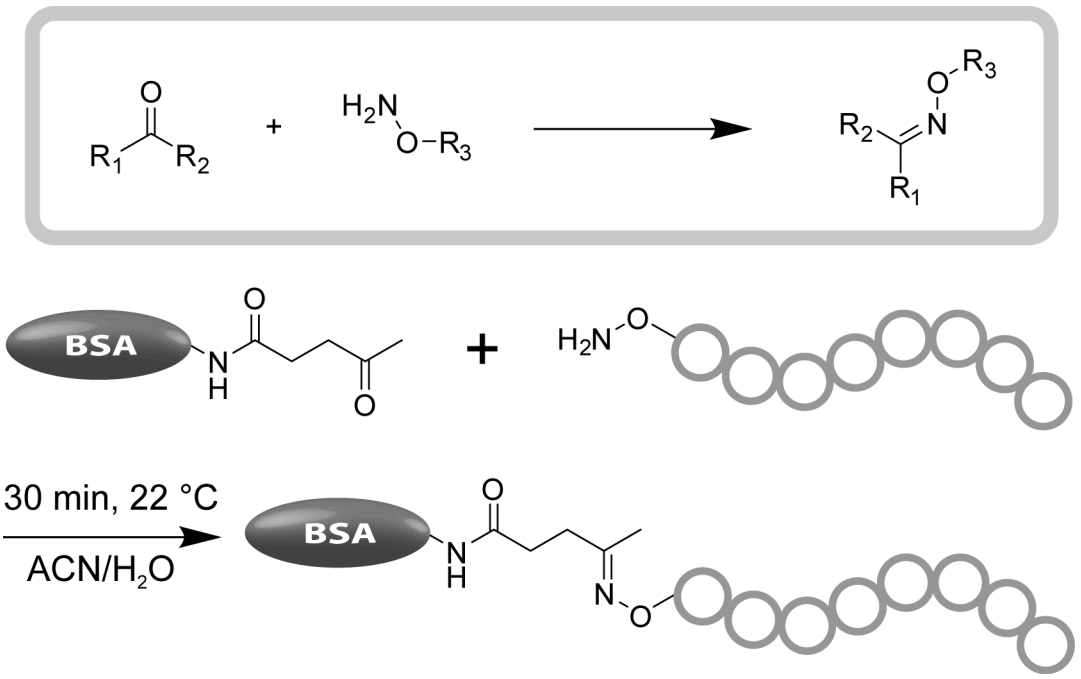

Figure 2.26 Oxime formation as a mild tool for bioconjugation.

gated them to *N*-leuvinyl lysine modified bovine serum albumin (BSA).[87] The reaction was completed in only 30 minutes, producing the well-defined bioconjugate (Figure 2.26).

In a further example, Kochendoefer and colleagues synthesized an aminooxy-functionalized CCL-5 protein for the site-specific attachment of a propionaldehyde-derivative of poly(ethylene glycol) monomethyl ether.[88] The oxime-forming reaction only required 1 hour at ambient temperature to achieve almost quantitative conversion, utilizing a 2-fold excess of the synthetic polymer. Importantly, the conjugation reaction (in addition to the various synthetic steps required to attach the *clickable* functionality) was proven to have no observable impact on the correct folding of the protein, its tertiary structure or its antiviral activity.

Therefore, the oxime-forming reaction presents a mild and rapid conjugation approach that is biocompatible. However, the stability of the linkage that is generated must be further evaluated in a variety of macromolecular systems in order to determine in which applications it is suited, given that oximes are susceptible to further transformations such as hydrolysis, and rearrangements (Beckmann) that would result in an effective reversion of the conjugation.

2.4.8 Tetrazole-Ene Reaction

Ultra rapid conjugation reactions that may be triggered by some external stimulus (such as the addition of a catalyst or exposure to UV light) are highly desirable as it

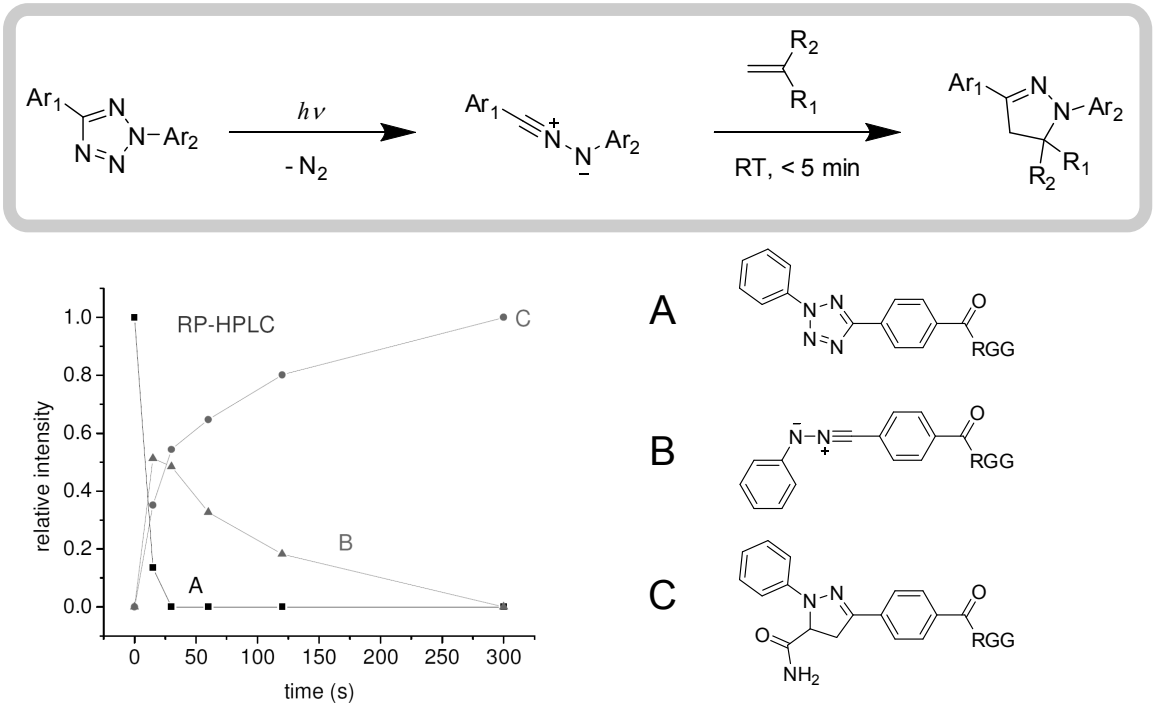

Figure 2.27 Kinetics of the photo-inducible cycloaddition between 2,5-diaryltetrazoles and alkenes.

allows for exquisite reaction control in complex, multi-component systems. One such reaction is the photo-inducible 1,3-dipolar cycloaddition between 2,5- diaryl tetrazoles and alkenes (Figure 2.27).

Upon photo irradiation, 2,5-diaryl tetrazoles undergo an extremely fast cycloreversion to release N_2 and produce the corresponding nitrile-imine, which is then available to undergo a cycloaddition with a suitable dipolarophile such as an alkene. Using a hand-held UV lamp operating at a wavelength of 302 nm, Lin and colleagues successfully modified tetrazole-functionalized proteins with acrylamide within a few minutes at ambient temperature.[89] It must be noted, however that a 50-fold excess of acrylamide was utilized and 90 % conversion was achieved after 2 minutes, as determined by LC-MS anaylsis (Figure 2.27). Aside from the fast rate of reaction, the *click* conjugates are also fluorescent, which is particularly advantageous for monitoring the labelling of non fluorescent proteins.

In a further example, a genetically encoded alkene-containing protein in *Escherichia coli* was modified with a library of 2,5-diaryl tetrazoles under similar conditions.[90] Although the photo-induced formation of the nitrile-imine was very fast (2 minutes), the subsequent cycloaddition with the allyl phenyl ether functional protein was considerably slower (the reaction was allowed to proceed overnight at 4 °C). By comparison, the second-order rate constant of the cycloaddition with allyl phenyl ether was determined to be $0.00202 \pm 0.00007\ M^{-1} \cdot s^{-1}$ whereas that for acrylamide (as was used in the previous example) was determined to be $0.15\ M^{-1} \cdot s^{-1}$. A reasonable explanation

for this observation is the lower LUMO energy of acrylamide than that of allyl phenyl ether, which offers better orbital overlap with the HOMO of the nitrile imine.

It is apparent from these studies that the photo-inducible 1,3-cycloaddition between 2,5-diaryl tetrazoles and alkenes is bio-orthogonal, very rapid, highly selective and may be performed in biological media. Many of the reactions that have been discussed have comparable reaction kinetics, many times at the expense of complicated synthetic strategies to arrive at the *clickable* functionality. In the present case, however, functional 2,5-diaryl tetrazoles are readily synthesized and may be purified by simple non-chromatographic techniques. The additional element of control that is offered by this reaction in terms of its UV-trigger makes it a highly attractive inclusion in the design of other conjugates that may be desired in macromolecular science. As such, its implementation in the construction of functional materials would be of significant value.

2.5 Diels-Alder Chemistry as a Conjugation Tool in Macromolecular Science

2.5.1 Step-Growth Polymerization

In 1926, Staudinger and Bruson described a high temperature polymerization of cyclopentadiene.[91] The mechanism of the reaction was postulated to involve succesive 1,2-additions of cyclopentadiene units, as depicted in Figure 2.28. Predating the seminal work of Diels and Alder, in which the mechanism of the eponymous reaction was described;[92] Staudinger was not to know that his proposed structures of poly(cyclopentadiene) were in fact incorrect. Alder and Stein later corrected Staudinger's structure for poly(cyclopentadiene) in 1931, making use of the now known [4+2] cycloaddition pathway.[93]

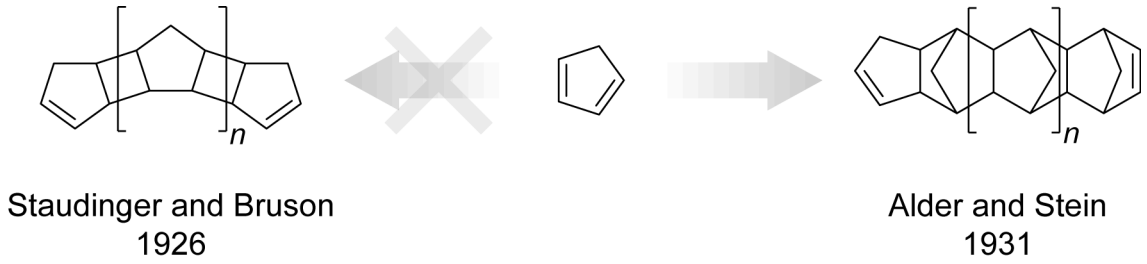

Figure 2.28 The structures of poly(cyclopentadiene) as initially proposed by Staudinger and Bruson; and as later corrected by Alder and Stein.

The Diels-Alder (DA) reaction was therefore investigated within the context of macromolecular science initially as a mechanism of step-growth polymerization. In comparison to other [4+2] cycloadditions, such as that between cyclopentadiene and *p*-benzoquinone, the self-condensation of cyclopentadiene is rather inefficient. Further diene-dienophile pairs were subsequently investigated for the formation of polymeric materials. In one notable publication, Bailey and colleagues reported a polymeric DA reaction between 2-vinyl-1,3-butadiene (diene) and *p*-benzoquinone, *m*-phenylenebismaleimide, ethylenediacrylate, and *N,N'*-methylenediacrylamide (bisdienophiles).[94] Rather ingeniously, the DA reaction of 2-vinyl-1,3-butadiene with the above bisdienophiles results in the formation of another diene which can further react and thus allowing for a step-growth process. The process is exemplified in Figure 2.29.

2.5.2 Precise Macromolecular Conjugation

The use of DA chemistry for much more precise macromolecular engineering has, only relatively recently, been achieved through the incorporation of diene/dienophile

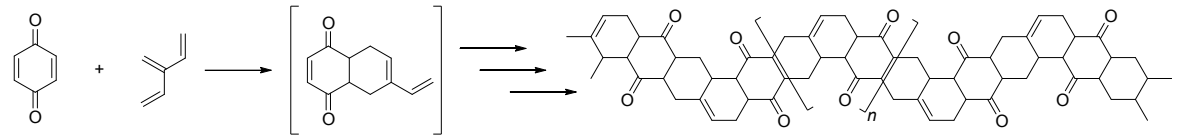

Figure 2.29 Step-growth polymerization via DA chemistry.

functionality at very well-defined positions within pre-formed polymer chains. Undoubtably, CRP has been the enabling technology for such a development. Shortly after the reported combination of CRP and the CuAAC for the modular construction of various complex macromolecular structures, Hizal and Tunca investigated the use of anthracene and maleimide functional polymeric building blocks to achieve similar outcomes (Figure 2.30).[95]

By synthesizing anthracene/maleimide functional ATRP initiators, or equipping commercially available poly(ethylene glycol) monomethylether with the appropriate complementary functionality, the DA cycloaddition as a means of polymeric conjugation has successfully been used to generate very precise structures ranging from block copolymers,[95, 96] star polymers,[97–99] graft polymers[100] and more complex architectures.[101, 102] Although making use of readily available starting materials and no catalyst, elevated temperatures ($>$ 110 °C) and extended reaction times (36-120 hours) are severe limitations.

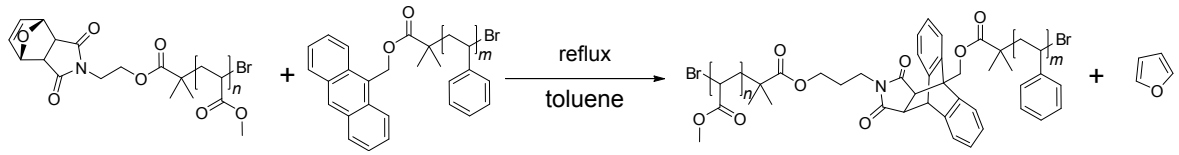

Figure 2.30 Modular block copolymer synthesis by DA chemistry.

2.5.3 Reversibly Linked and Cross-Linked Materials

In recent years, there has been somewhat of a surge of activity in exploiting the reversibility of DA chemistry in the construction of thermally-responsive and reversibly cross-linked polymeric materials. The most widely investigated diene/dienophile pair within this context is furan/maleimide, owing to their convenience in terms of commercial availability, chemical accessibility and also the manageable temperature range in which the forward (60 °C upper limit) and reverse reactions (90 °C lower limit) may be performed.

Wudl and colleagues reported, and subsequently patented, a process in which multifunctional furan and maleimide monomers are cross-linked via DA reactions to form a *self-healing* polymeric material.[103] Upon heating the material to above 120 °C, the

DA adducts underwent a retro-DA reaction, thus disconnecting some of the material's cross-links, which could subsequently be re-formed upon cooling. Using this reversible process, it was shown that heating a fractured material to over 120 °C enabled it to regain 83 % of its original strength.

Combining this technology with CRP, Haddleton and colleagues used appropriately functionalized ATRP initiators to generate polymer chains bearing maleimide and furan end-groups. The, in this case limited, ability of the polymers to link and de-link upon thermal cycling was demonstrated as depicted in Figure 2.31.[104]

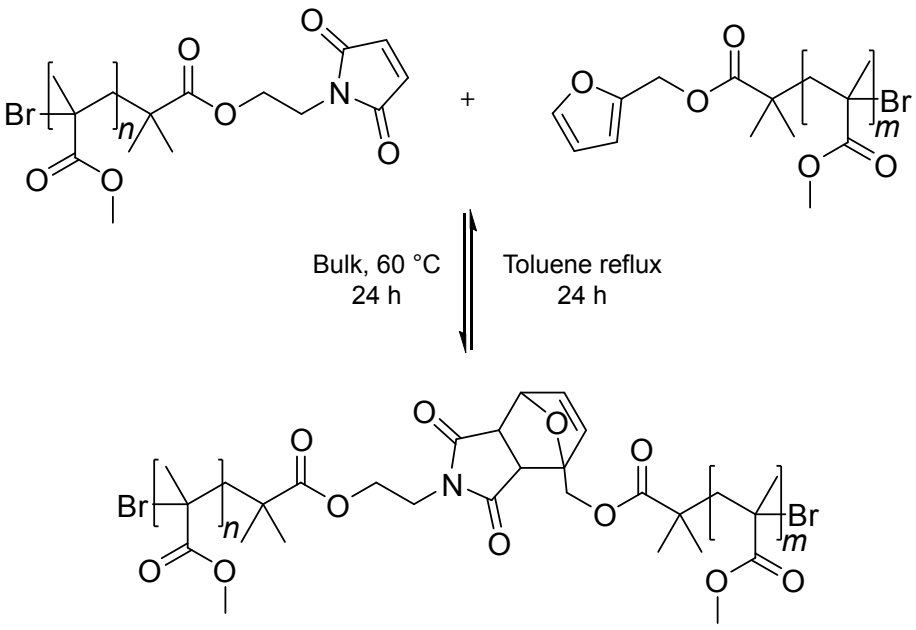

Figure 2.31 Reversible block copolymer formation via DA chemistry.

2.5.4 Diels-Alder Reactivity of Thiocarbonyl Compounds

Generally speaking, thiocarbonyl compounds tend to be more reactive as heterodienophiles in pericyclic reactions than their oxygenated counterparts. The reason for this is that there is relatively poor overlap of the C-2p and S-3p orbitals in the C=S π bond in comparison to the corresponding orbital overlaps in carbonyl compounds. This results in the C=S bond being weaker and longer than the C=O bond, which places less ring strain during the formation of the cyclic transition state of the DA adduct.[105]

Thiocarbonyl compounds as dienophiles have been the subject of extensive investigation.[105–108] Of particular importance is the fact that the reactivity of the thiocarbonyl group is significantly affected by the nature of its substituents; as such, the order of reactivity of these compounds is illustrated in Figure 2.32.

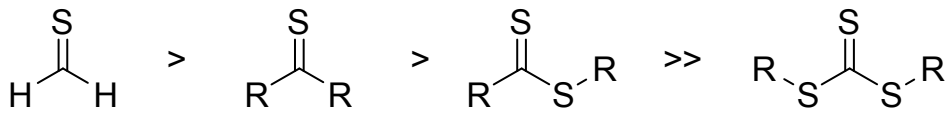

Figure 2.32 Dienophilicity of thiocarbonyl compounds.

RAFT agents are typically dithioester compounds which have lower reactivity in DA reactions than thioaldehydes and thioketones. However, it is the objective of the present investigation to evaluate the feasibilty of using dithioesters in hetero Diels-Alder (HDA) reactions as a conjugation strategy within the context of macromolecular chemistry since these compounds can successfully mediate CRP and be retained as an end-group functionality in the resulting polymer chain. Beslin and Metzner investigated the DA reactivity of a series of methyl dithioesters bearing alkyl or phenyl substituents.[109] Using either butadiene or 2,3-dimethylbutadiene as the diene, low to moderate yields (20-73 %) of the targeted cycloadducts were obtained after a standard period of 3 days at 160 °C. Clearly, such a system is not suitable in the guise of a quantitative and mild conjugation strategy. However, by reducing the electron density of the thiocarbonyl bond, the dienophilicity of dithioesters can be significantly increased. This may be achieved by appending an EWG to the thiocarbonyl carbon atom.

2.5.5 Electron-Deficient Dithioesters

The reduction in electron density of the thiocarbonyl bond through the action of an α-EWG lowers the energy of its LUMO. This makes provision for a much better orbital overlap with the HOMO of the diene during the DA reaction (Figure 2.33). As such, the DA activity of a variety of EWG bearing dithioesters has been investigated over the years,[110–119] the outcomes of which are summarized in Figure 2.34.

While these structures behave as efficient heterodienophiles (at least in comparison to other dithioesters), they may not necessarily be able to mediate CRP. Adopting RAFT terminology, the R-group of these dithioesters are not suitable for use in controlling a radical polymerization, however such a fragment does not influence the dienophilicity of the thiocarbonyl bond and can easily be modified during their synthesis. The main concern is the Z-group (the α-EWG) as this is responsible for governing the reactivity of the thiocarbonyl bond to radical addition and the stability of the intermediate adduct radical (cf. Figure 2.3). Of the dithioesters presented in Figure 2.34, only derivatives of the first two entries have been shown (thus far) to adequately control radical polymerization.[120–123]

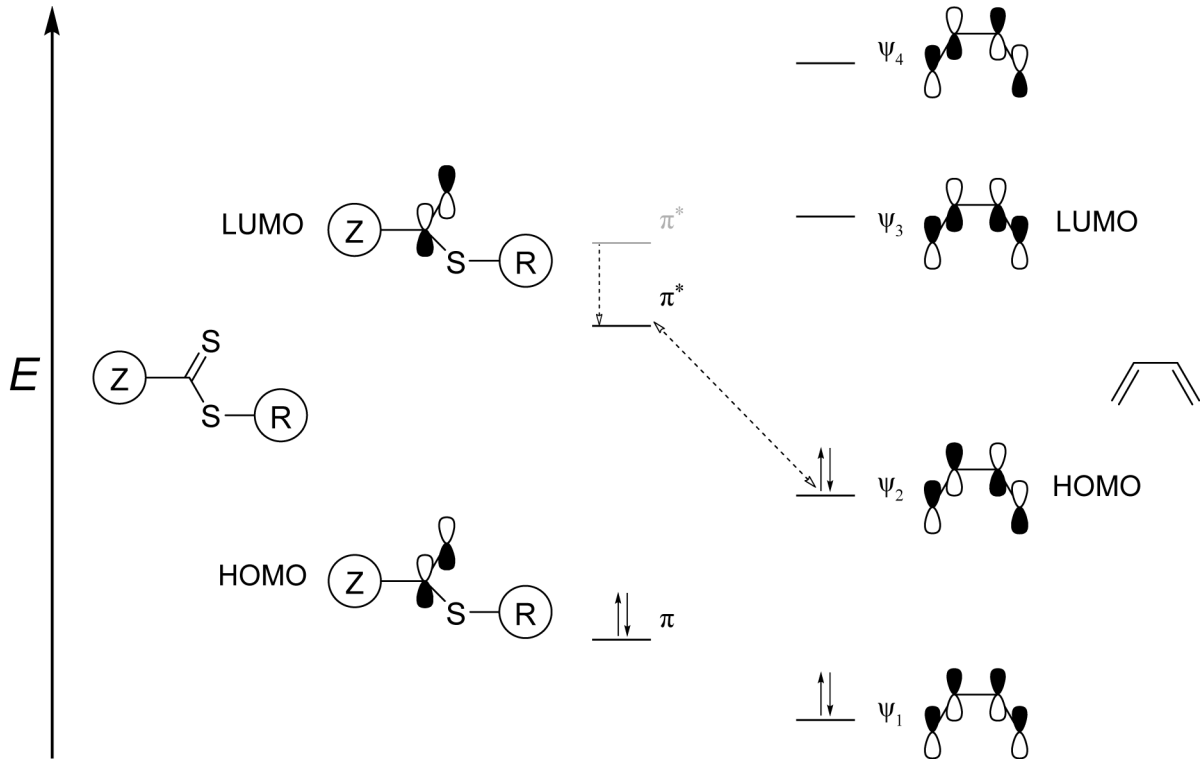

Figure 2.33 Molecular Orbital diagram of the Diels-Alder reaction between dithioesters and dienes. The provision of an electron-withdrawing *Z*-group lowers the energy of the LUMO of the dithioester, thus enabling better orbital overlap with the HOMO of the diene.

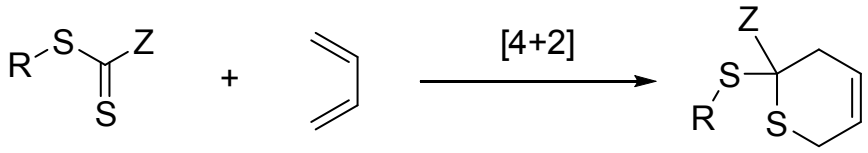

Diene / Dienophile	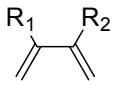		Ref.
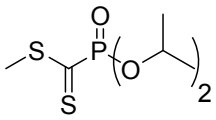	RT, 24 h (R_1=R_2=H) RT, 24 h (R_1=H, R_2=Me) 50 °C, 6h (R_1=R_2=Me) $ZnCl_2$, RT, 45 min BF_3, RT, 1 min	RT, 1h	[115,118]
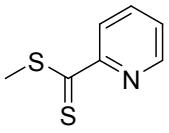	BF_3, 45 °C, 15 min (R_1=R_2=Me) BF_3, 35 °C, 1h (R_1=R_2=Me)	---	[119]
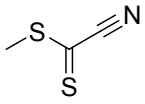	RT, 30 min (R_1=R_2=H)	0 °C, < 1min	[111,112]
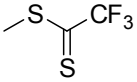	0 °C-RT, < 24 h	0 °C, < 2 min	[110]
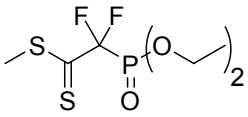	50 °C, 15 h (R_1=R_2=H) 66 °C, 6h (R_1=H, R_2=Me) 66 °C, 4h (R_1=R_2=Me)	RT, 2 h	[116]
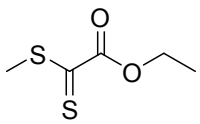	RT, 16h (R_1=R_2=Me)	---	[114]
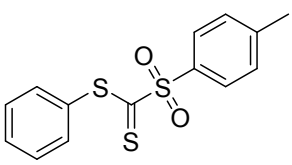	RT, 2 min (R_1=R_2=Me)	RT, < 1min	[113,117]

Figure 2.34 Overview of the existing *state-of-the-art* in DA reactions with dithioesters.

2.5.6 Electron-Deficient Dithioesters as Controlling Agents in RAFT Polymerization

The first instance of the use of phosphoryldithioformates as RAFT agents was reported in 2001 by Benaglia.[120] Initially using benzyl (diethoxyphosphoryl)dithioformate as a RAFT agent, the polymerization of styrene was investigated (Figure 2.35). At low to moderate monomer conversion (< 30 %), satisfactory control of the polymerization was obtained in terms of both the molecular weight and chain-end functionality. However, prolonging the polymerization to achieve higher monomer conversions lead to a loss of control and the resulting polymers had polydispersities comparable to those obtained from conventional free radical polymerization (typically > 2). Such inefficent control was attributed to a slow rate of addition/fragmentation compared to the rate of monomer propagation. Such a conclusion has since not been elaborated upon in the literature.

Prior to the present investigation, the use of such dithioesters in RAFT polymerizations has only been reported on one other occassion, by the same group.[121] Here, the synthesis of novel tertiary dithioesters bearing α-diethoxyphosphoryl moieties via a radical exchange reaction was the prinicpal focus of the study. Nevertheless, the formed dithioesters were shown to control the radical polymerization of both styrene and methyl methacrylate.

Another class of electron-deficient dithioesters that have experimentally been proven to behave as RAFT agents are those which bear a pyridinyl α-substituent. Alberti and colleagues evaluated the use of 2-, 3- and 4- pyridinyl dithioesters as RAFT agents in the radical polymerization of styrene (Figure 2.36).[122] The rather extensive investigation revealed that, although providing a poorer level of control than the highly common dithiobenzoates, the pyridinyl dithioesters performed significantly better than the above described phosphoryl analogues. A tertiary derivative of the 4-pyridinyl dithioester was also successfully used to mediate controlled polymerization of methyl methacrylate.[123] Again, preceding the present investigation, these stand as the only examples of the use of such compounds in radical polymerization.

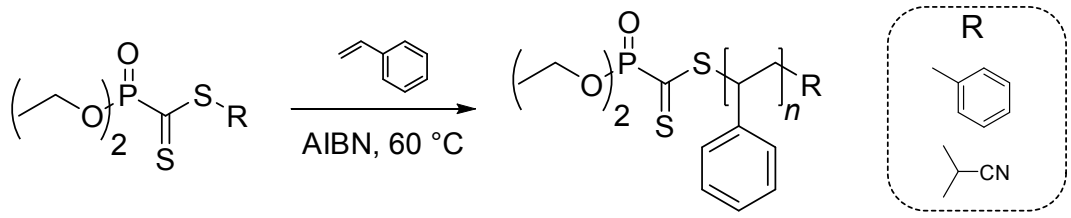

Figure 2.35 (Diethoxyphosphoryl)dithioformates as controlling agents in RAFT polymerization.

The RAFT process is a balance of stability. The intermediate adduct radical that is generated during the chain transfer reactions responsible for the controlling mechanism must be sufficiently stable as the addition of a propagating radical during its formation is competitive with propagation. However, if this adduct radical is too stable, its fragmentation to yield another propagating radical and regenerate the thiocarbonyl compound will be delayed, thus retarding the overall rate of polymerization. The crucial element in governing this stability is, as mentioned previously, the Z-group. In the case where the Z-group is also an EWG, the generated adduct radical is further stabilized, and thus longer lived, via the captodative effect.

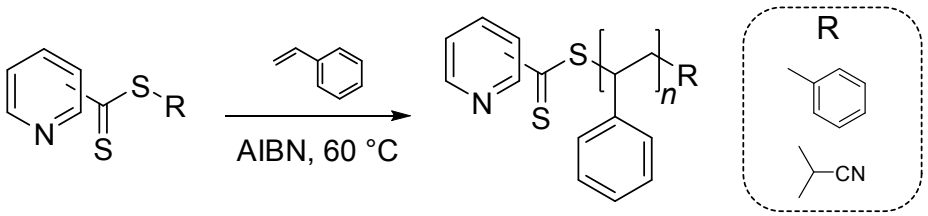

Figure 2.36 Pyridinyldithioformates as controlling agents in RAFT polymerization.

Concurrent with the present investigation, α-sulfonyl dithioesters similar in structure to the last entry of Figure 2.34 were evaluated in their ability to mediate RAFT polymerization. Being much more strongly electron-deficient than the above described examples, it would be expected that (within the context of a RAFT process) the rate of polymerization would be further retarded due to the stronger stability of the adduct radical that is formed. Interestingly, however, the electron-withdrawing effect of the sulfonyl dithioesters was observed to be sufficiently high to promote a DA reaction with styrene (Figure 2.37) and a (hypothesized) Michael-type addition with *n*-butyl acrylate (Figure 2.38). As such, these compounds are not at all suitable for general use as RAFT agents. However, isobornyl acrylate (being a comparatively more sterically hindered monomer) was successfully polymerized in a controlled fashion, without the occurence of the above described side-reactions.

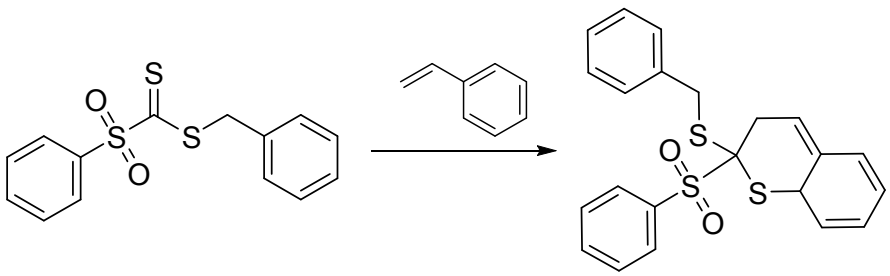

Figure 2.37 Proposed side-reaction of α-sulfonyl dithioesters with styrene.

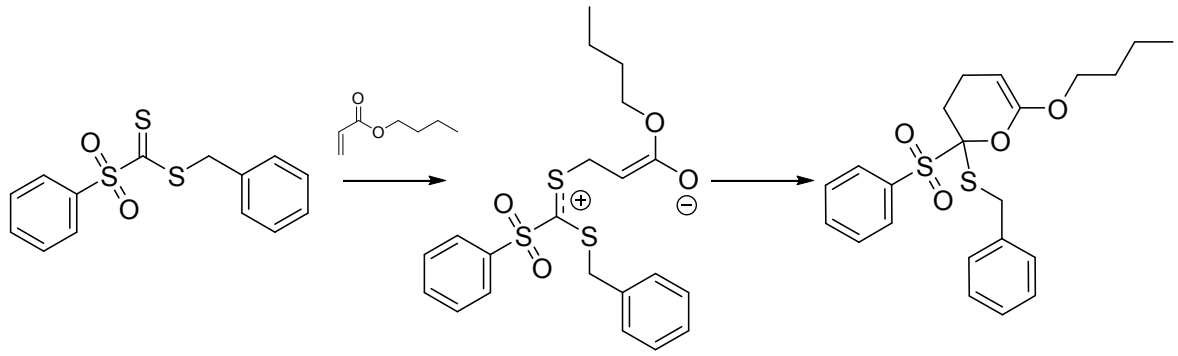

Figure 2.38 Proposed side-reaction of α-sulfonyl dithioesters with *n*-butyl acrylate.

2.6 Concluding Remarks

Such is the current *state-of-the-art* in controlled, modular synthetic polymer design and synthesis. It is the principal aim of the present investigation to use the above described electron-deficient dithioesters in a very unique way. Initially, these compounds will be utilized as RAFT agents in a radical polymerization process to achieve well-defined, linear polymeric building blocks that bear the dithioester as an end-group. Subsequently, the retained dithioester functionality will be used as a reactive heterodienophile in macromolecular conjugation reactions based upon DA chemistry. Such an atom-economical approach strives to heighten the synthetic application of DA chemistry to macromolecular science as a convenient and efficient conjugation technique leading to the realization of purposefully designed functional materials.

References

[1] Barner-Kowollik, C.; Russell, G. T. *Prog. Polym. Sci.* **2009**, *34*, 1211–1259.

[2] Hadjichristidis, N.; Pitsikalis, M.; Pispas, S.; Iatrou, H. *Chem. Rev.* **2001**, *101*, 3747–3792.

[3] Szwarc, M. *Nature* **1956**, *178*, 1168–1169.

[4] Hawker, C. J.; Bosman, A. W.; Harth, E. *Chem. Rev.* **2001**, *101*, 3661–3688.

[5] Braunecker, W. A.; Matyjaszewski, K. *Prog. Polym. Sci.* **2007**, *32*, 93–146.

[6] Ouchi, M.; Terashima, T.; Sawamoto, M. *Chem. Rev.* **2009**, *109*, 4963–5050.

[7] Moad, G.; Chong, Y. K.; Postma, A.; Rizzardo, E.; Thang, S. H. *Polymer* **2005**, *46*, 8458–8468.

[8] Moad, G.; Rizzardo, E.; Thang, S. H. *Polymer* **2008**, *49*, 1079–1131.

[9] Moad, G.; Rizzardo, E.; Thang, S. H. *Aust. J. Chem.* **2009**, *62*, 1402–1472.

[10] Fischer, H.; Souaille, M. *Macromol. Symp.* **2001**, *174*, 231–240.

[11] Tang, W.; Tsarevsky, N. V.; Matyjaszewski, K. *J. Am. Chem. Soc.* **2006**, *128*, 1598–1604.

[12] Barner-Kowollik, C.; Davis, T. P.; Heuts, J. P. A.; Stenzel, M. H.; Vana, P.; Whittaker, M. *J. Polym. Sci., Part A: Polym. Chem.* **2003**, *41*, 365–375.

[13] Haddleton, D. M.; Waterson, C.; Derrick, P. J.; Jasieczek, C. B.; Shooter, A. J. *Chem. Commun.* **1997**, 683–684.

[14] Coessens, V.; Matyjaszewski, K. *Macromol. Rapid Commun.* **1999**, *20*, 127–134.

[15] Zhang, X.; Matyjaszewski, K. *Macromolecules* **1999**, *32*, 7349–7353.

[16] Lai, J. T.; Filla, D.; Shea, R. *Macromolecules* **2002**, *35*, 6754–6756.

[17] Ferguson, C. J.; Hughes, R. J.; Pham, B. T. T.; Hawkett, B. S.; Gilbert, R. G.; Serelis, A. K.; Such, C. H. *Macromolecules* **2002**, *35*, 9243–9245.

[18] You, Y. Z.; Hong, C. Y.; Wang, W. P.; Lu, W. Q.; Pan, C. Y. *Macromolecules* **2004**, *37*, 9761–9767.

[19] Wang, R.; McCormick, C. L.; Lowe, A. B. *Macromolecules* **2005**, *38*, 9518–9525.

[20] Such, G. K.; Evans, R. A.; Davis, T. P. *Macromolecules* **2006**, *39*, 9562–9570.

[21] Kasko, A. M.; Heintz, A. M.; Pugh, C. *Macromolecules* **1998**, *31*, 256–271.

[22] Stenzel, M. H. Complex Architecture Design via the RAFT Process: Scope, Strengths and Limitations. In *Handbook of RAFT Polymerization*; Barner-Kowollik, C., Ed.; Wiley-VCH: Weinheim, 2008; pp 315–372.

[23] Stenzel, M. H.; Cummins, L.; Roberts, G. E.; Davis, T. P.; Vana, P.; Barner-Kowollik, C. *Macromol. Chem. Phys.* **2003**, *204*, 1160–1168.

[24] Benaglia, M.; Chiefari, J.; Chong, Y. K.; Moad, G.; Rizzardo, E.; Thang, S. H. *J. Am. Chem. Soc.* **2009**, *131*, 6914–6915.

[25] Malmstrom, E. E.; Hawker, C. J. *Macromol. Chem. Phys.* **1998**, *199*, 923–935.

[26] Kolb, H. C.; Finn, M. G.; Sharpless, K. B. *Angew. Chem. Int. Ed.* **2001**, *40*, 2004–2021.

[27] Rostovtsev, V. V.; Green, L. G.; Fokin, V. V.; Sharpless, K. B. *Angew. Chem. Int. Ed.* **2002**, *41*, 2596–2599.

[28] Tornoe, C. W.; Christensen, C.; Meldal, M. *J. Org. Chem.* **2002**, *67*, 3057–3064.

[29] Huisgen, R. *Angew. Chem. Int. Ed.* **1968**, *7*, 321–406.

[30] Diaz, D. D.; Punna, S.; Holzer, P.; McPherson, A. K.; Sharpless, K. B.; Fokin, V. V.; Finn, M. G. *J. Polym. Sci., Part A: Polym. Chem.* **2004**, *42*, 4392–4403.

[31] Helms, B.; Mynar, J. L.; Hawker, C. J.; Frechet, J. M. J. *J. Am. Chem. Soc.* **2004**, *126*, 15020–15021.

[32] Wu, P.; Feldman, A. K.; Nugent, A. K.; Hawker, C. J.; Scheel, A.; Voit, B.; Pyun, J.; Frechet, J. M. J.; Sharpless, K. B.; Fokin, V. V. *Angew. Chem. Int. Ed.* **2004**, *43*, 3928–3932.

[33] Binder, W. H.; Sachsenhofer, R. *Macromol. Rapid Commun.* **2008**, *29*, 952–981.

[34] Opsteen, J. A.; Hest, J. C. M. v. *Chem. Commun.* **2005**, 57–59.

[35] Quémener, D.; Davis, T. P.; Barner-Kowollik, C.; Stenzel, M. H. *Chem. Commun.* **2006**, 5051–5053.

[36] Barner-Kowollik, C.; Inglis, A. J. *Macromol. Chem. Phys.* **2009**, *210*, 987–992.

[37] Lutz, J. F. *Angew. Chem. Int. Ed.* **2007**, *46*, 1018–1025.

[38] Fournier, D.; Hoogenboom, R.; Schubert, U. S. *Chem. Soc. Rev.* **2007**, *36*, 1369–1380.

[39] Hawker, C. J.; Wooley, K. L. *Science* **2005**, *309*, 1200–1205.

[40] Sumerlin, B. S.; Vogt, A. P. *Macromolecules* **2010**, *43*, 1–13.

[41] Gauthier, M. A.; Gibson, M. I.; Klok, H. A. *Angew. Chem. Int. Ed.* **2009**, *48*, 48–58.

[42] Lutz, J. F. *Angew. Chem. Int. Ed.* **2008**, *47*, 2182–2184.

[43] Becer, C. R.; Hoogenboom, R.; Schubert, U. S. *Angew. Chem. Int. Ed.* **2009**, *48*, 4900–4908.

[44] Wittig, G.; Krebs, A. *Chem. Ber. Recl.* **1961**, *94*, 3260–3275.

[45] Agard, N. J.; Prescher, J. A.; Bertozzi, C. R. *J. Am. Chem. Soc.* **2004**, *126*, 15046–15047.

[46] Kohn, M.; Breinbauer, R. *Angew. Chem. Int. Ed.* **2004**, *43*, 3106–3116.

[47] Agard, N. J.; Baskin, J. M.; Prescher, J. A.; Lo, A.; Bertozzi, C. R. *ACS Chem. Biol.* **2006**, *1*, 644–648.

[48] Baskin, J. M.; Prescher, J. A.; Laughlin, S. T.; Agard, N. J.; Chang, P. V.; Miller, I. A.; Lo, A.; Codelli, J. A.; Bertozzi, C. R. *Proc. Natl. Acad. Sci. U.S.A.* **2007**, *104*, 16793–16797.

[49] Codelli, J. A.; Baskin, J. M.; Agard, N. J.; Berozzi, C. R. *J. Am. Chem. Soc.* **2008**, *130*, 11486–11493.

[50] Ning, X. H.; Guo, J.; Wolfert, M. A.; Boons, G. J. *Angew. Chem. Int. Ed.* **2008**, *47*, 2253–2255.

[51] Debets, M. F.; van Berkel, S. S.; Schoffelen, S.; Rutjes, F.; van Hest, J. C. M.; van Delft, F. L. *Chem. Commun.* **2010**, *46*, 97–99.

[52] Li, Z. M.; Seo, T. S.; Ju, J. Y. *Tetrahedron Lett.* **2004**, *45*, 3143–3146.

[53] Gouin, S. G.; Kovensky, J. *Synlett* **2009**, 1409–1412.

[54] McKay, C. S.; Moran, J.; Pezacki, J. P. *Chem. Commun.* **2010**, *46*, 931–933.

[55] Hoyle, C. E.; Lee, T. Y.; Roper, T. *J. Polym. Sci., Part A: Polym. Chem.* **2004**, *42*, 5301–5338.

[56] Lowe, A. B. *Polym. Chem.* **2010**, *1*, 17–36.

[57] Gress, A.; Völkel, A.; Schlaad, H. *Macromolecules* **2007**, *40*, 7928–7933.

[58] ten Brummelhuis, N.; Diehl, C.; Schlaad, H. *Macromolecules* **2008**, *41*, 9946–9947.

[59] Bertin, A.; Schlaad, H. *Chem. Mater.* **2009**, *21*, 5698–5700.

[60] Killops, K. L.; Campos, L. M.; Hawker, C. J. *J. Am. Chem. Soc.* **2008**, *130*, 5062–5064.

[61] Pounder, R. J.; Stanford, M. J.; Brooks, P.; Richards, S. P.; Dove, A. P. *Chem. Commun.* **2008**, 5158–5160.

[62] Chan, J. W.; Hoyle, C. E.; Lowe, A. B. *J. Am. Chem. Soc.* **2009**, *131*, 5751–5753.

[63] Chan, J. W.; Yu, B.; Hoyle, C. E.; Lowe, A. B. *Chem. Commun.* **2008**, 4959–4961.

[64] Chan, J. W.; Yu, B.; Hoyle, C. E.; Lowe, A. B. *Polymer* **2009**, *50*, 3158–3168.

[65] Chen, G. J.; Kumar, J.; Gregory, A.; Stenzel, M. H. *Chem. Commun.* **2009**, 6291–6293.

[66] Konkolewicz, D.; Gray-Weale, A.; Perrier, S. *J. Am. Chem. Soc.* **2009**, *131*, 18075–18077.

[67] Hensarling, R. M.; Doughty, V. A.; Chan, J. W.; Patton, D. L. *J. Am. Chem. Soc.* **2009**, *131*, 14673–14675.

[68] Koo, S. P. S.; Stamenovic, M. M.; Prasath, R. A.; Inglis, A. J.; Du Prez, F. E.; Barner-Kowollik, C.; Van Camp, W.; Junkers, T. *J. Polym. Sci., Part A: Polym. Chem.* **2010**, *48*, 1699–1713.

[69] Klemm, E.; Stöckl, C. *Makromol. Chem.* **1991**, *192*, 153–158.

[70] Shin, J.; Matsushima, H.; Chan, J. W.; Hoyle, C. E. *Macromolecules* **2009**, *42*, 3294–3301.

[71] Li, H. B.; Yu, B.; Matsushima, H.; Hoyle, C. E.; Lowe, A. B. *Macromolecules* **2009**, *42*, 6537–6542.

[72] Rosen, B. M.; Lligadas, G.; Hahn, C.; Percec, V. *J. Polym. Sci., Part A: Polym. Chem.* **2009**, *47*, 3931–3939.

[73] Rosen, B. M.; Lligadas, G.; Hahn, C.; Percec, V. *J. Polym. Sci., Part A: Polym. Chem.* **2009**, *47*, 3940–3948.

[74] Xu, J. T.; Tao, L.; Boyer, C.; Lowe, A. B.; Davis, T. P. *Macromolecules* **2010**, *43*, 20–24.

[75] Royzen, M.; Yap, G. P. A.; Fox, J. M. *J. Am. Chem. Soc.* **2008**, *130*, 3760–3761.

[76] Blackman, M. L.; Royzen, M.; Fox, J. M. *J. Am. Chem. Soc.* **2008**, *130*, 13518–13519.

[77] Devaraj, N. K.; Weissleder, R.; Hilderbrand, S. A. *Bioconjugate Chem.* **2008**, *19*, 2297–2299.

[78] Devaraj, N. K.; Upadhyay, R.; Hatin, J. B.; Hilderbrand, S. A.; Weissleder, R. *Angew. Chem. Int. Ed.* **2009**, *48*, 7013–7016.

[79] Singh, I.; Zarafshani, Z.; Lutz, J. F.; Heaney, F. *Macromolecules* **2009**, *42*, 5411–5413.

[80] Singh, I.; Vyle, J. S.; Heaney, F. *Chem. Commun.* **2009**, 3276–3278.

[81] Gutsmiedl, K.; Wirges, C. T.; Ehmke, V.; Carell, T. *Org. Lett.* **2009**, *11*, 2405–2408.

[82] Himo, F.; Lovell, T.; Hilgraf, R.; Rostovtsev, V. V.; Noodleman, L.; Sharpless, K. B.; Fokin, V. V. *J. Am. Chem. Soc.* **2005**, *127*, 210–216.

[83] Grecian, S.; Fokin, V. V. *Angew. Chem. Int. Ed.* **2008**, *47*, 8285–8287.

[84] Koyama, Y.; Yonekawa, M.; Takata, T. *Chem. Lett.* **2008**, *37*, 918–919.

[85] Lee, Y. G.; Koyama, Y.; Yonekawa, M.; Takata, T. *Macromolecules* **2009**, *42*, 7709–7717.

[86] Grundman, C.; Frommeld, H. D. *J. Org. Chem.* **1966**, *31*, 157–162.

[87] Heredia, K. L.; Tolstyka, Z. P.; Maynard, H. D. *Macromolecules* **2007**, *40*, 4772–4779.

[88] Shao, H. Y.; Crnogorac, M. M.; Kong, T.; Chen, S. Y.; Williams, J. M.; Tack, J. M.; Gueriguian, V.; Cagle, E. N.; Carnevali, M.; Tumelty, D.; Paliard, X.; Miranda, L. P.; Bradburne, J. A.; Kochendoerfer, G. G. *J. Am. Chem. Soc.* **2005**, *127*, 1350–1351.

[89] Song, W.; Wang, Y.; Qu, J.; Madden, M. M.; Lin, Q. *Angew. Chem. Int. Ed.* **2008**, *47*, 2832–2835.

[90] Song, W.; Wang, Y.; Qu, J.; Lin, Q. *J. Am. Chem. Soc.* **2008**, *130*, 9654–9655.

[91] Staudinger, H.; Bruson, H. A. *Justus Liebig's Ann. Chem.* **1926**, *447*, 97–110.

[92] Diels, O.; Alder, K. *Justus Liebig's Ann. Chem.* **1928**, *460*, 98–122.

[93] Alder, K.; Stein, G.; Finzenhagen, H. *Justus Liebig's Ann. Chem.* **1931**, *485*, 223–246.

[94] Bailey, W. J.; Economy, J.; Hermes, M. E. *J. Org. Chem.* **1962**, *27*, 3295–3299.

[95] Durmaz, H.; Colakoclu, B.; Tunca, U.; Hizal, G. *J. Polym. Sci., Part A: Polym. Chem.* **2006**, *44*, 1667–1675.

[96] Durmaz, H.; Dag, A.; Altintas, O.; Erdogan, T.; Hizal, G.; Tunca, U. *Macromolecules* **2007**, *40*, 191–198.

[97] Durmaz, H.; Karatas, F.; Tunca, U.; Hizal, G. *J. Polym. Sci., Part A: Polym. Chem.* **2006**, *44*, 499–509.

[98] Dag, A.; Durmaz, H.; Hizal, G.; Tunca, U. *J. Polym. Sci., Part A: Polym. Chem.* **2008**, *46*, 302–313.

[99] Dag, A.; Durmaz, H.; Tunca, U.; Hizal, G. *J. Polym. Sci., Part A: Polym. Chem.* **2009**, *47*, 178–187.

[100] Dag, A.; Durmaz, H.; Demir, E.; Hizal, G.; Tunca, U. *J. Polym. Sci., Part A: Polym. Chem.* **2008**, *46*, 6969–6977.

[101] Durmaz, H.; Karatas, F.; Tunca, U.; Hizal, G. *J. Polym. Sci., Part A: Polym. Chem.* **2006**, *44*, 3947–3957.

[102] Gungor, E.; Hizal, G.; Tunca, U. *J. Polym. Sci., Part A: Polym. Chem.* **2009**, *47*, 3409–3418.

[103] Chen, X. X.; Dam, M. A.; Ono, K.; Mal, A.; Shen, H. B.; Nutt, S. R.; Sheran, K.; Wudl, F. *Science* **2002**, *295*, 1698–1702.

[104] Syrett, J. A.; Mantovani, G.; Barton, W.; Price, D.; Haddleton, D. M. *Polymer Chemistry* **2010**, *1*, 102–106.

[105] Manoharan, M.; Venuvanalingam, P. *J. Phys. Org. Chem.* **1997**, *10*, 768–776.

[106] McGregor, W. M.; Sherrington, D. C. *Chem. Soc. Rev.* **1993**, *22*, 199–204.

[107] Barone, V.; Arnaud, R.; Chavant, P. Y.; Vallee, Y. *J. Org. Chem.* **1996**, *61*, 5121–5129.

[108] Kirby, G. W.; Lochead, A. W.; Williamson, S. *J. Chem. Soc. Perkin Trans. 1* **1996**, 977–984.

[109] Beslin, P.; Metzner, P. *Tetrahedron Lett.* **1980**, *21*, 4657–4658.

[110] Middleton, W. J. *J. Org. Chem.* **1965**, *30*, 1390–1394.

[111] Vyas, D. M.; Hay, G. W. *Can. J. Chem.* **1971**, *49*, 3755–3758.

[112] Vyas, D. M.; Hay, G. W. *J. Chem. Soc. Perkin Trans. 1* **1975**, 180–186.

[113] Boerma, J. A.; Nilsson, N. H.; Senning, A. *Tetrahedron* **1974**, *30*, 2735–2740.

[114] Vedejs, E.; Arnost, M. J.; Dolphin, J. M.; Eustache, J. *J. Org. Chem.* **1980**, *45*, 2601–2604.

[115] Heuzé, B.; Gasparova, R.; Heras, M.; Masson, S. *Tetrahedron Lett.* **2000**, *41*, 7327–7331.

[116] Pfund, E.; Lequeux, T.; Vazeux, M.; Masson, S. *Tetrahedron Lett.* **2002**, *43*, 2033–2036.

[117] Hilmy, K. M. H.; El-Sayed, I.; El-Kousy, S.; Slem, H. S. *Sulfur Letters* **2003**, *26*, 187–193.

[118] Heras, M.; Gulea, M.; Masson, S.; Philouze, C. *Eur. J. Org. Chem.* **2004**, 160–172.

[119] Bastin, R.; Albadri, H.; Gaumont, A. C.; Gulea, M. *Org. Lett.* **2006**, *8*, 1033–1036.

[120] Laus, M.; Papa, R.; Sparnacci, K.; Alberti, A.; Benaglia, M.; Macciantelli, D. *Macromolecules* **2001**, *34*, 7269–7275.

[121] Alberti, A.; Benaglia, M.; Laus, M.; Sparnacci, K. *J. Org. Chem.* **2002**, *67*, 7911–7914.

[122] Alberti, A.; Benaglia, M.; Guerra, M.; Gulea, M.; Hapiot, P.; Laus, M.; Macciantelli, D.; Masson, S.; Postma, A.; Sparnacci, K. *Macromolecules* **2005**, *38*, 7610–7618.

[123] Benaglia, M.; Rizzardo, E.; Alberti, A.; Guerra, M. *Macromolecules* **2005**, *38*, 3129–3140.

3

End-Group Modification

3.1 Introduction

As the applications for synthetic polymeric materials become more and more demanding, the precision with which such materials are synthesized must also follow suit. Rather than providing merely structural and physical properties to a bulk material, many applications require some form of highly specific chemical interaction between the synthetic polymer and its intended environment. As such, the incorporation of chemical functionality into polymer chains in a very well-defined fashion has been greatly facilitated by continued developments in controlled radical polymerization (CRP), the most successful of which have been ATRP[1, 2] and RAFT polymerization.[3, 4]

A very effective way in which chemical functionality is imparted to polymers formed by ATRP and RAFT polymerization is through the use of a pre-functionalized initiator or chain transfer agent respectively. Such a strategy has been shown to be very facile in producing α-functional polymer chains bearing such moieties as hydroxyl and carboxyl to name the two most common.[5–10] Another technique which has fast become a convenient pathway to functional polymers is the ω-group approach. In this technique, the reactive chain-end of a *living* polymer (a halide in the case of ATRP or a thiocarbonylthio moiety in the case of RAFT polymerization) is modified via a number of classical reactions from organic chemistry. For example, the halide chain terminus of

a polymer formed by ATRP may undergo nucleophilic subsitution with an azide,[11] thus causing an exchange of functionality and the polymer chain can then be further modified using the CuAAC.[12] In the case of polymers formed by RAFT polymerization, a number of modifications are possible; including aminolysis,[13] oxidation,[14] thermal elimination[15] and radical induced removal of the thiocarbonylthio group.[16] In all of these examples, however, the thiocarbonylthio moiety is either removed or transformed into a reactive intermediate. Herein, it will be shown that the thiocarbonylthio moiety (within the context of macromolecular science) may be used directly as a heterodienophile in Diels-Alder chemistry. Consequently, as a proof of concept, a diene functional polymer was synthesized and modified via hetero Diels-Alder (HDA) chemistry with electron-deficient dithioesters, as conceptualized in Figure 3.1.

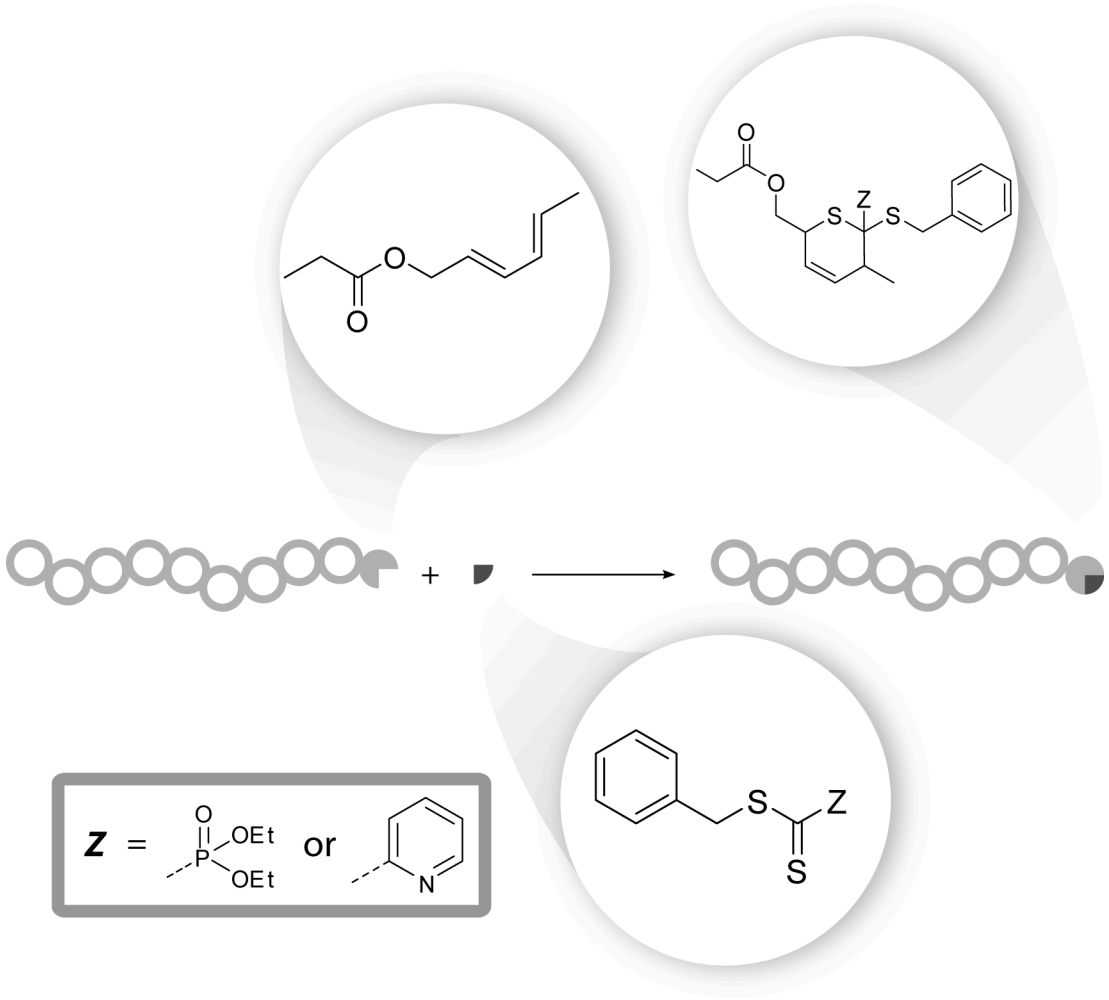

Figure 3.1 Polymer end-group modification by hetero Diels-Alder chemistry.

3.2 Experimental Section

Polymerization of ϵ-caprolactone (PCL 1)

Under a nitrogen atmosphere, a mixture of *trans*,*trans*-2,4-hexadien-1-ol (430 mg, 4.4 mmol), ϵ-caprolactone (9.3 ml, 10 g, 88 mmol), toluene (10 mL) and lipase acrylic resin (250 mg) were placed in a dried Schlenk flask. The solution was stirred at 70 °C for 1.5 hours. After cooling down to room temperature, the lipase acrylic resin was removed by filtration. The polymer **1** was precipitated from the filtrate in a cold mixture of diethylether/*n*-hexane (1:1). Yield: 9.34 g, 90 %.

SEC (THF): M_n=2550 g·mol^{-1}, *PDI*=1.37. ^{1}H NMR ($CDCl_3$): M_n=2520 g·mol^{-1}.

^{1}H NMR (300 MHz, $CDCl_3$, 25 °C): δ= 6.21 (dd; C**H**), 6.01 (ddq; C**H**), 5.71 (dq; C**H**), 5.58 (dt; C**H**), 4.53 (d; C$\mathbf{H_2}$), 4.03 (t; C$\mathbf{H_2}$), 3.60 (t; C$\mathbf{H_2}$), 2.7 (t; C$\mathbf{H_2}$), 1.5-1.7 (m; C$\mathbf{H_2}$), 1.25-1.45 ppm (m; C$\mathbf{H_2}$); ^{13}C NMR (75 MHz, $CDCl_3$, 25 °C): δ= 173.4 (**C**=O), 123.6, 130.3, 131.1, 134.7 (**C**H), 64.7 (**C**H_2), 64.0 (**C**H_2), 62.4 (**C**H_2), 34.0 (**C**H_2), 32.1 (**C**H_2), 28.2 (**C**H_2), 25.4 (**C**H_2), 24.5 (**C**H_2), 18.0 (**C**H_3) ppm.

HDA Cycloaddition between PCL 1 and BDPDF

A solution of PCL **1** (200 mg, 78 µmol), 2 equiv. of benzyl(diethoxyphosphoryl)dithioformate (BDPDF) (48 mg, 158 µmol) and 1 equiv. of zinc chloride (10 mg, 78 µmol) in 1 mL chloroform was kept at 50 °C for 24 hours. The polymer **2** was precipitated in a cold mixture of diethylether/*n*-hexane (1:1).

SEC (THF): M_n=2800 g·mol^{-1}, *PDI*=1.27.

^{1}H NMR (300 MHz, $CDCl_3$, 25 °C): δ = 7.1-7.4 (m, C**H**), 5.5-5.9 (m, C**H**), 4.0-4.8 (m, C**H**), 4.02 (t, C$\mathbf{H_2}$), 3.63 (t, C$\mathbf{H_2}$), 2.71 (t, C$\mathbf{H_2}$), 1.5-1.7 (C$\mathbf{H_2}$), 1.25-1.45 ppm (C$\mathbf{H_2}$); ^{13}C NMR (75 MHz, $CDCl_3$, 25 °C): δ = 173.4 (**C**=O), 127-130 (**C**H), 64.7 (**C**H_2), 62.4 (**C**H_2), 34.0 (**C**H_2), 28.2 (**C**H_2), 25.4 (**C**H_2), 24.5 (**C**H_2), 16.2 (**C**H_3) ppm.

HDA Cycloaddition between PCL 1 and BPDF

A solution of PCL **1** (200 mg, 78 µmol), 2 equiv. of benzyl pyridin-2-yldithioformate (BPDF) (38 mg, 158 µmol) and 1.1 equiv. of TFA (6.4 µL, 86 µmol) in 1 mL chloroform was kept at 50 °C for 2 hours. The polymer **3** was precipitated in a cold mixture of diethylether/*n*-hexane (1:1).

SEC (THF): M_n=2780 g·mol^{-1}, *PDI*=1.26.

^{1}H NMR (300 MHz, $CDCl_3$, 25 °C): δ= 8.54 (d, C**H**), 7.79 (d, C**H**), 7.66 (dd, C**H**), 7.2-7.0 (m, C**H**), 5.5-5.9 (m, C**H**), 4.34 (s, C$\mathbf{H_2}$), 4.07 (t, C$\mathbf{H_2}$), 3.66 (t, C$\mathbf{H_2}$), 2.71 (t, C$\mathbf{H_2}$), 1.5-1.7 (C$\mathbf{H_2}$), 1.25-1.38 (C$\mathbf{H_2}$), 0.78 ppm (s, C$\mathbf{H_3}$); ^{13}C NMR (75 MHz, $CDCl_3$, 25 °C): δ = 173.4 (**C**=O), 127-130 (**C**H), 64.0 (**C**H_2), 62.4 (**C**H_2), 34.0 (**C**H_2), 28.2 (**C**H_2), 25.4 (**C**H_2), 24.5 (**C**H_2) ppm.

3.3 Results and Discussion

3.3.1 Equipping a Polymer Chain with Diene Functionality

It has already been shown in the literature the ability of electron-deficient dithioesters to undergo [4+2] cycloadditions with a variety of dienes.[17–23] Extending this concept to a macromolecular species, a polymer chain bearing a suitable diene end-group was synthesized. The synthesis of such a material was achieved by the ring opening polymerization (ROP) of ϵ-caprolactone, using commercially available *trans*, *trans*- 2,4-hexadien-1-ol as the initiator. A standard method for performing such a polymerization makes use of *n*-butyl lithium or tin (II) 2-ethylhexanoate as a co-initiator at high temperatures ($>$ 100 °C). It was observed, however, that this temperature caused the *trans*, *trans*- 2,4-hexadien-1-ol to isomerize to various combinations of *trans, cis*- and *cis, cis*- species, all of which (for sterical reasons) have significantly lower reactivity towards [4+2] cycloadditions. To overcome this, the ROP was performed under enzymatic conditions.

In contrast to conventional anionic ROP (which proceeds via an active-chain end mechanism), enzymatic ROP proceeds via a monomer-activated mechanism.[24] Initiation occurs by the reaction of the lactone with the enzyme, resulting in the formation of an acyl-enzyme intermediate (enzyme activated monomer). The now activated monomer can then add to an initiator-typically water or an alcohol, resulting in the formation of a hydroxyacid or ester respectively. Propagation then proceeds via the sequentional addition of enzyme-activated monomers to the growing chain. This process allows for the synthesis of well-defined, and quantitatively end-group functional poly(esters) at lower temperatures.

As such, enzyme mediated ROP was performed using a lipase acrylic resin (*Candida antarctica*) at 70 °C, as depicted in Figure 3.2. 2,4-Hexadienoyl functional poly(ϵ-caprolactone) (PCL **1**) was thus obtained with M_n = 2550 g·mol^{-1} and *PDI* = 1.37. The ^{1}H NMR spectrum of PCL **1** (Figure 3.3) showed the presence of both the polymer backbone and the vinylic protons. A comparison of the intensities of the signals arising from the vinylic protons with the that of the terminal hydroxymethylene protons revealed the quantitative functionalization of the poly(ester).

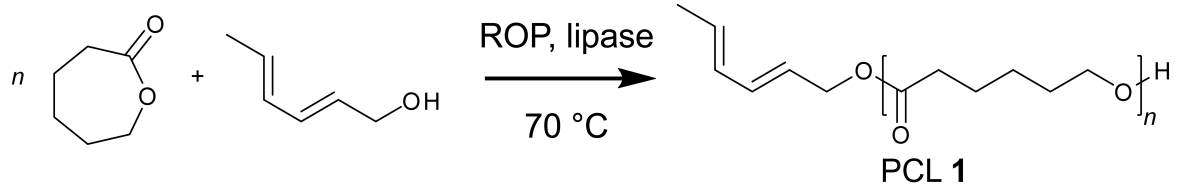

Figure 3.2 Synthesis of the diene-functional PCL **1**.

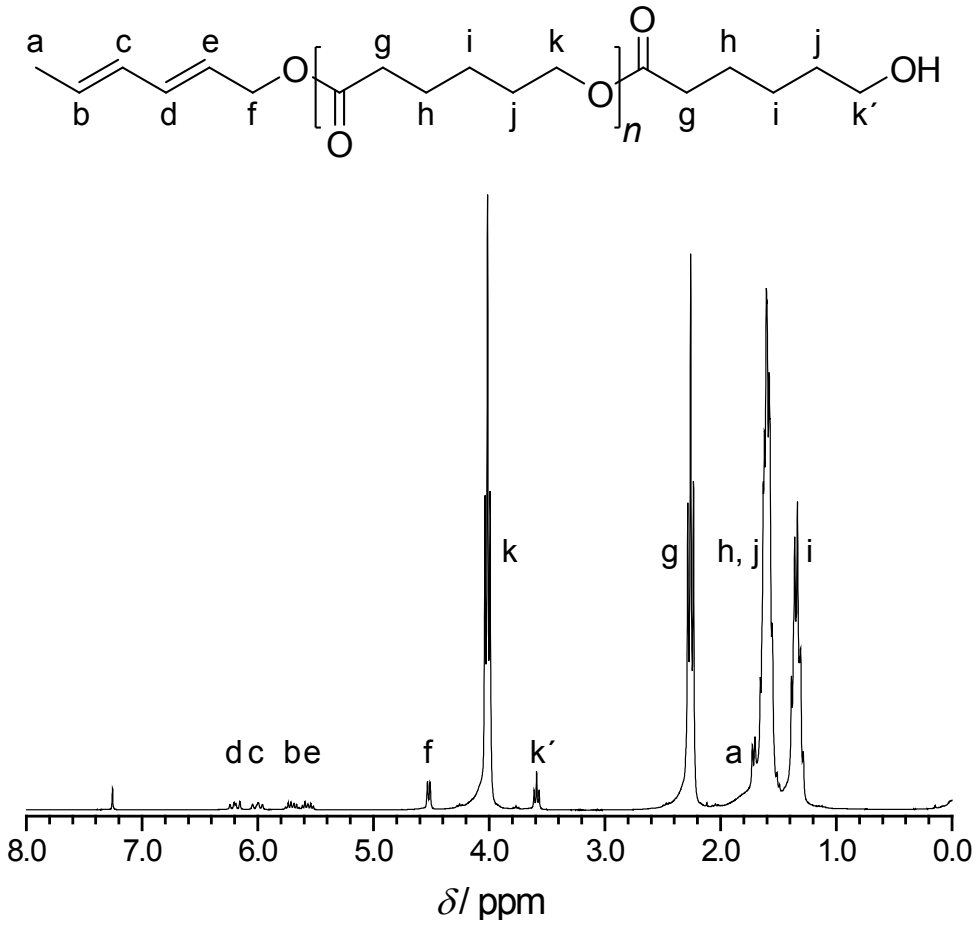

Figure 3.3 ^{1}H NMR spectrum of PCL **1**.

To further confirm its structure, PCL **1** was also analysed via electrospray ionization mass spectrometry (ESI-MS). The soft ionization method used in this system allows for the efficient ionization of macromolecules without effecting a fragmentation, resulting in much less ambiguous mass spectra. It is because of this that ESI-MS is a highly attractive technique for end-group analysis of synthetic polymers.[25] Figure 3.4a depicts the full mass spectrum of PCL **1**. The dominant series of signals can be assigned to the targeted 2,4-hexadienoyl functional poly(ester). A second and smaller series can also be observed, which is assigned to the same macromolecule in a doubly charged state. Upon inspection of a zoom region of the mass spectrum for a single repeat unit (Figure 3.4b), the purity of PCL **1** can further be confirmed. A comparison of the experimentally observed and theoretically determined *m/z* values for the peaks present in Figure 3.4b are, along with their unambiguous identification, presented in Table 3.1

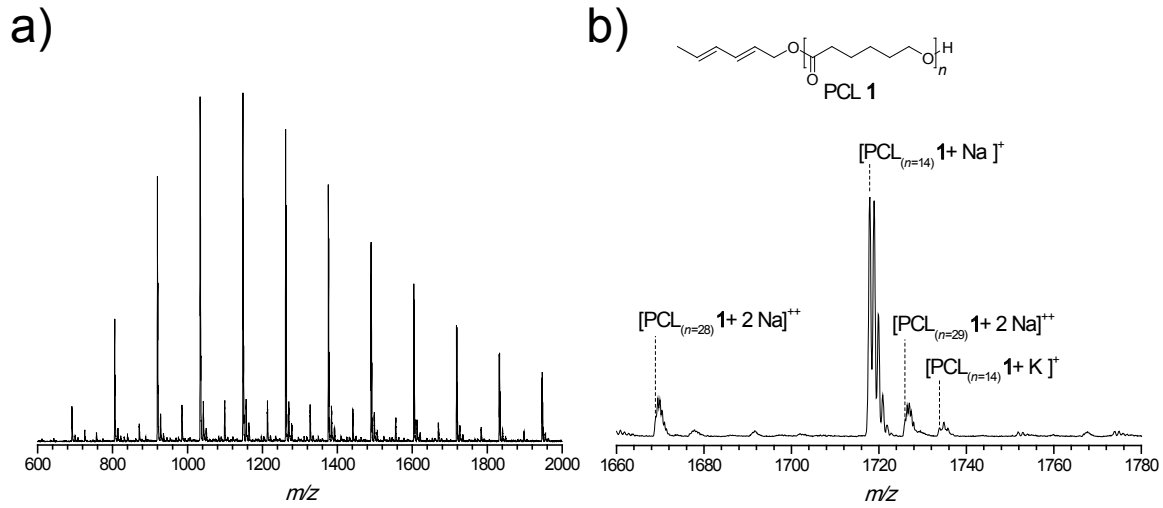

Figure 3.4 Full ESI-MS spectrum (a) and 1660-1780 *m/z* zoom region (b) of PCL **1**.

Table 3.1 Experimental and theoretical *m/z* values for the first peak in the isotopic distributions of the zoom spectrum in Figure 3.4b and their assignment.

$m/z_{\text{expt.}}$	ion assignment	formula	$m/z_{\text{theor.}}$	$\Delta m/z$
1668.9	PCL $\mathbf{1}_{(n\,=\,28)}$ + 2 Na^+	$[C_{174}H_{290}O_{57}Na_2]^{++}$	1669.0	0.1
1717.9	PCL $\mathbf{1}_{(n\,=\,14)}$ + Na^+	$[C_{90}H_{150}O_{29}Na]^+$	1718.0	0.1
1726.0	PCL $\mathbf{1}_{(n\,=\,29)}$ + 2 Na^+	$[C_{180}H_{300}O_{59}Na_2]^{++}$	1726.0	0.0
1733.9	PCL $\mathbf{1}_{(n\,=\,14)}$ + K^+	$[C_{90}H_{150}O_{29}K]^+$	1734.0	0.1

3.3.2 End-Group Modification by HDA Chemistry

With the diene-functional PCL **1** in hand, end-group modification via HDA chemistry was subsequently investigated. For this purpose, the electron-deficient dithioesters benzyl(diethoxyphosphoryl)dithioformate (BDPDF)[26] and benzyl pyridin-2-yldithioformate (BPDF)[27, 28] were synthesized following literature procedures, the structures of which are presented in Figure 3.5.

The diethoxyphosphoryl moiety of BDPDF is inherently electron-withdrawing. However, this effect is significantly enhanced upon addition of a Lewis acid, such as zinc (II) chloride ($ZnCl_2$). Thus, in invesitgating the HDA reaction between PCL **1** and BDPDF, 1 equiv. of $ZnCl_2$ was added to a chloroform solution of the two reactants and kept at 50 °C for 24 hours. The modified polymer PCL **2** was isolated by precipitation in a cold mixture of diethylether and *n*-hexane (1:1).

The HDA cycloaddition results in the formation of a 3,6-dihydro-2*H*-thiopyran ring (Figure 3.1). Due to the number of possible stereo/regioisomers of such a structure, the obtained NMR data is complex (Figure 3.6). Nevertheless, it is possible to observe a complete disappearance of signals arising from the β and ϵ position vinylic protons of PCL **1** and the appearance of signals from aromatic protons. Both of these observations are consistent with the formation of PCL **2**.

Considering that the number of possible isomers may differ in their spectroscopic properties but not in their mass, ESI-MS measurements were also performed. Figure 3.7a compares the ESI-MS spectra of PCL **1** prior to and after reaction with BDPDF. In the spectrum of PCL **1**, one series of signals dominates, which can be assigned to the different chain lengths of the functional poly(ester) **1**. In the spectrum of the modified PCL **2**, the complete series is shifted by 304 to higher *m/z* values (M_{exact} = 304.04 g·mol^{-1}). The zoom region for one repeat unit (1660-1780 *m/z*) is presented in Figure 3.7b and the detailed assignments of the peaks therein are presented in Table 3.2.

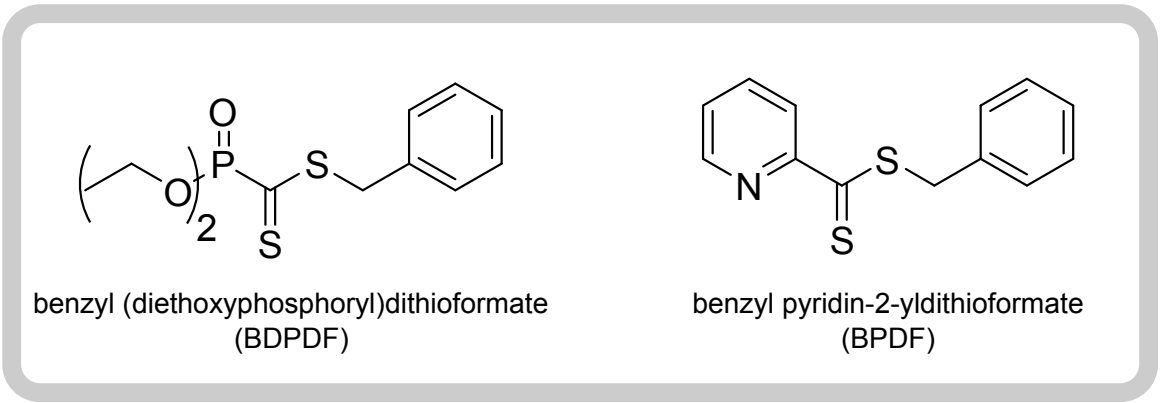

Figure 3.5 Dithioesters synthesized to behave as heterodienophiles.

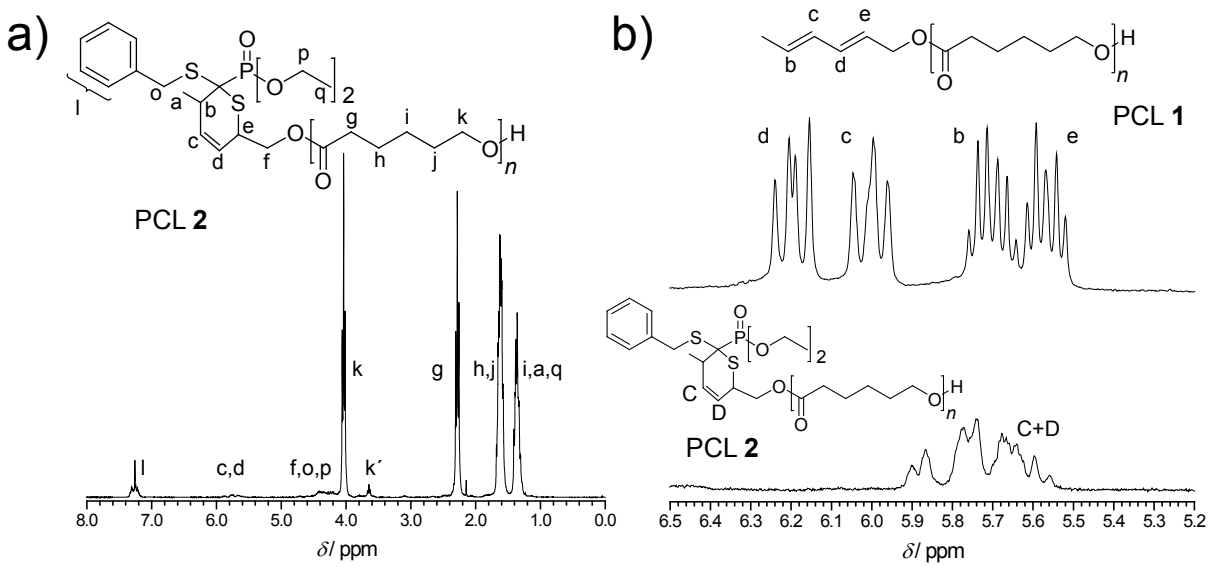

Figure 3.6 a)Full ^{1}H NMR spectrum of PCL **2**; and b) Comparison of the 6.5-5.2 ppm zoom region of the ^{1}H NMR spectra of PCL **1** and PCL **2**.

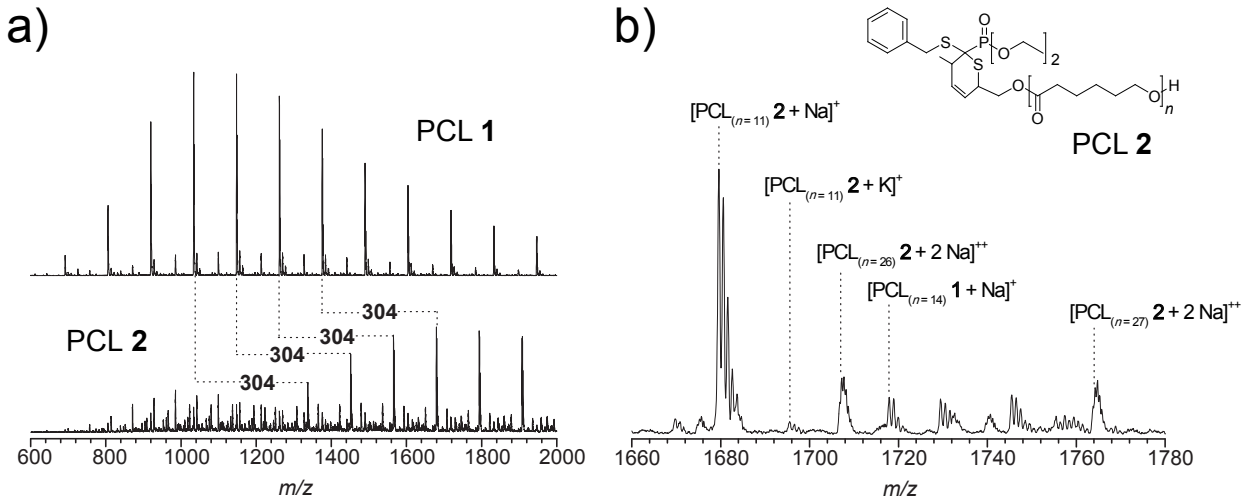

Figure 3.7 a) ESI-MS spectra of PCL prior to (**1**) and after (**2**) reaction with BDPDF; and b) 1660-1780 *m/z* zoom region of the ESI-MS spectrum of PCL **2**.

Table 3.2 Experimental and theoretical *m/z* values for the first peak in the isotopic distributions of the zoom spectrum in Figure 3.7b and their assignment.

$m/z_{expt.}$	ion assignment	formula	$m/z_{theor.}$	$\Delta m/z$
1679.6	PCL **2**$_{(n = 11)}$ + Na^+	$[C_{84}H_{137}O_{26}PS_2Na]^+$	1679.9	0.3
1695.6	PCL **2**$_{(n = 11)}$ + K^+	$[C_{84}H_{137}O_{26}PS_2K]^+$	1695.8	0.2
1706.9	PCL **2**$_{(n = 26)}$ + 2 Na^+	$[C_{174}H_{287}O_{56}PS_2Na_2]^{++}$	1706.9	0.0
1717.9	PCL **1**$_{(n = 14)}$ + Na^+	$[C_{90}H_{150}O_{29}Na]^+$	1718.0	0.1
1763.8	PCL **2**$_{(n = 27)}$ + 2 Na^+	$[C_{180}H_{297}O_{58}PS_2Na_2]^{++}$	1764.0	0.2

Concurrently, the use of BPDF as the heterodienophile was investigated in an identical fashion. In this case, however, the cycloaddition was promoted by the addition of at least 1 equiv. of trifluoroacetic acid (TFA). The TFA is used to protonate the pyridinyl group nitrogen atom, which enhances its electron withdrawing effect on the thiocarbonyl bond. The ensuing cycloaddition (which was performed at 50 °C for 2 hours), and subsequent isolation, yielded PCL **3**. Figure 3.8a depicts the ^{1}H NMR spectrum of PCL **3**, the appropriate zoom region of which is compared to that of the starting PCL **1** in Figure 3.8b. Again, the characteristic aromatic signals from the BPDF along with the already described changes in the vinylic region are clearly observed and are consistent with the formation of PCL **3**.

The ESI-MS spectra presented in Figure 3.9a clearly show the dominant series of peaks of PCL **1** shift by 245 to higher *m/z* values in PCL **3** (M_{exact} = 245.03 g·mol^{-1}). The zoom region for one repeat unit (1660-1780 *m/z*) is presented in Figure 3.9b and the detailed assignments of the peaks therein are presented in Table 3.3.

Upon inspection of the above described mass spectra (Figure 3.7 and 3.9), it may be observed that a significant quantity of the starting material PCL **1** is present. This, at first glance, would indicate the non quantitative nature of the HDA cycloaddition. However, under the applied conditions of measuring mass spectra via ESI-MS (capilliary temperature of 275 °C), the possibility of the retro Diels-Alder reaction occuring cannot be discounted. In order to determine whether or not this was indeed the case, a technique called tandem mass spectrometry (MS/MS) was employed. In this technique, a mass-selected ion pertaining to a specific species is isolated and subsequently forced to fragment by collision with a neutral gas in a process called *collision-induced*

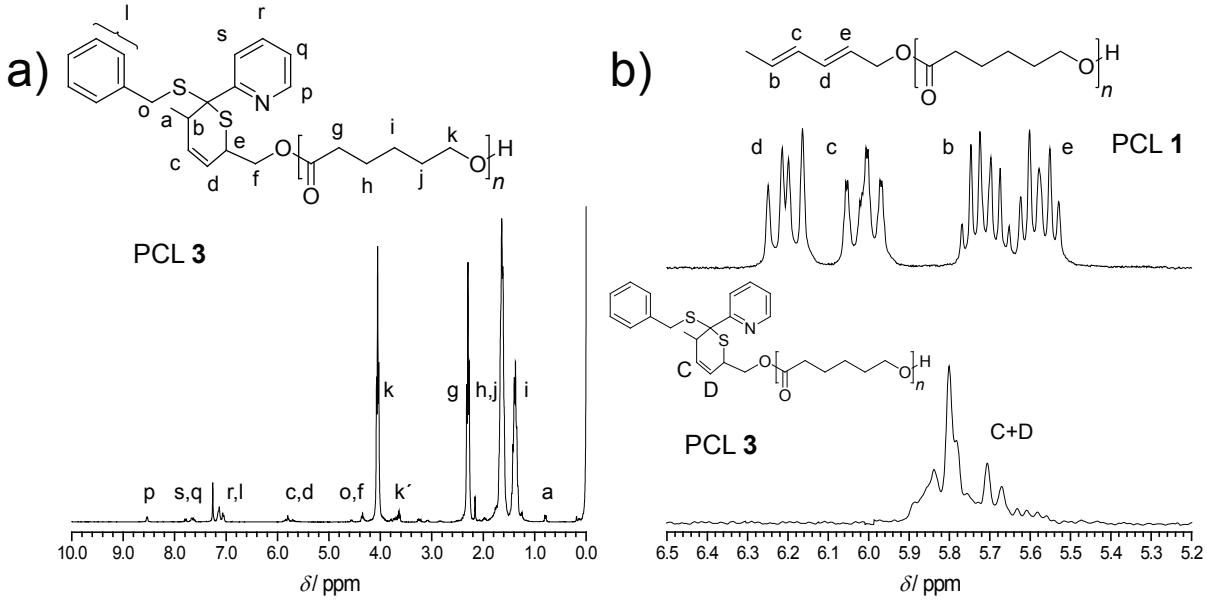

Figure 3.8 a)Full ^{1}H NMR spectrum of PCL **3**; and b) Comparison of the 6.5-5.2 ppm zoom region of the ^{1}H NMR spectra of PCL **1** and PCL **3**.

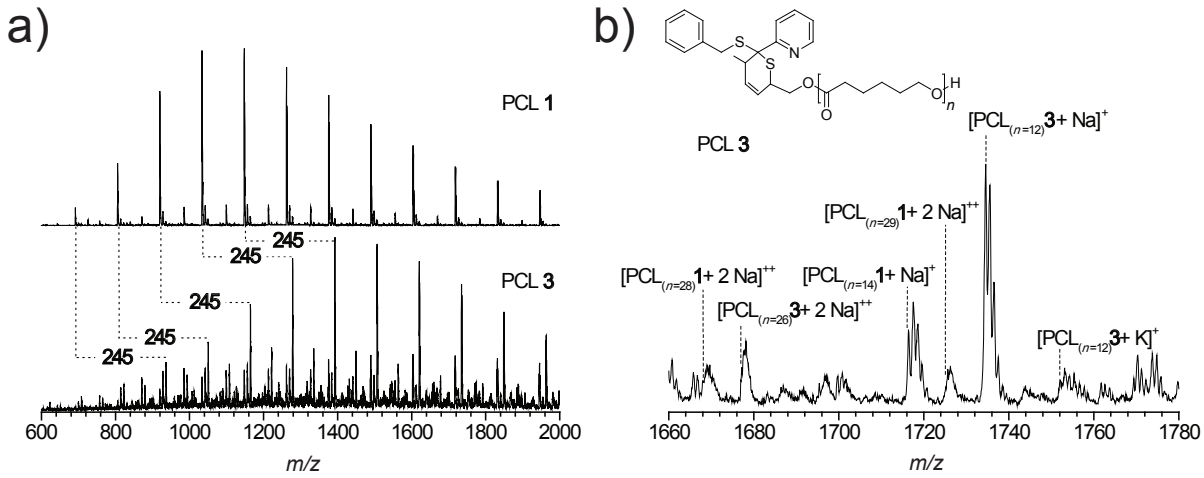

Figure 3.9 a) ESI-MS spectra of PCL prior to (**1**) and after (**3**) reaction with BPDF; and b) 1660-1780 *m/z* zoom region of the ESI-MS spectrum of PCL **3**.

Table 3.3 Experimental and theoretical *m/z* values for the first peak in the isotopic distributions of the zoom spectrum in Figure 3.9b and their assignment.

$m/z_{expt.}$	ion assignment	formula	$m/z_{theor.}$	$\Delta m/z$
1668.9	PCL $\mathbf{1}_{(n=28)}$ + 2 Na^+	$[C_{174}H_{290}O_{57}Na_2]^{++}$	1669.0	0.1
1677.0	PCL $\mathbf{3}_{(n=26)}$ + 2 Na^+	$[C_{175}H_{281}O_{53}NS_2Na_2]^{++}$	1677.4	0.4
1717.5	PCL $\mathbf{1}_{(n=14)}$ + Na^+	$[C_{90}H_{150}O_{29}Na]^+$	1718.0	0.5
1725.7	PCL $\mathbf{1}_{(n=29)}$ + 2 Na^+	$[C_{180}H_{300}O_{59}Na_2]^{++}$	1726.0	0.3
1734.6	PCL $\mathbf{3}_{(n=12)}$ + Na^+	$[C_{91}H_{141}O_{25}NS_2Na]^+$	1734.9	0.3
1750.5	PCL $\mathbf{3}_{(n=12)}$ + K^+	$[C_{91}H_{141}O_{25}NS_2K]^+$	1750.9	0.4

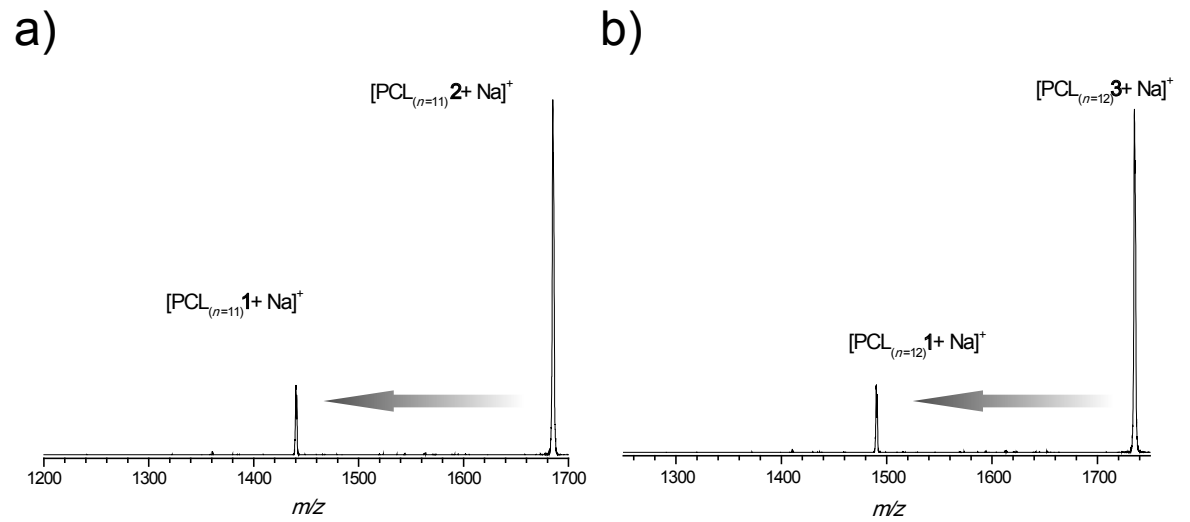

Figure 3.10 MS/MS spectra of the parent mass *m/z* = 1680 corresponding to PCL **2** (a); and the parent mass *m/z* = 1735 corresponding to PCL **3**.

dissociation (CID). The formed fragments are then separated according to their mass and analysed. The resulting MS/MS spectrum therefore consists only of product ions from the selected precursor. The MS/MS spectra of PCL **2** and **3** are presented in Figure 3.10a and 3.10b respectively. In both cases, it is observed that fragmentation of the modified PCL chains yields the starting material PCL **1**, thus confirming the ability of the ESI-MS measurement to cause a retro Diels-Alder reaction. It can therefore be established that the end-group modification of PCL **1** by HDA cycloaddition with BDPDF and BPDF is quantitative.

3.4 Conclusion

It is apparent from the above described results that electron-deficient dithioesters such as BDPDF and BPDF are able to undergo efficient HDA cycloadditions with polymer chains bearing a diene end-group. By using non-toxic catalysts and moderate temperatures, the successful polymer end-group modification by this technique stands as an initial 'proof of concept' in promoting such chemistry as a viable macromolecular conjugation tool.

References

[1] Matyjaszewski, K.; Xia, J. H. *Chem. Rev.* **2001**, *101*, 2921–2990.

[2] Ouchi, M.; Terashima, T.; Sawamoto, M. *Chem. Rev.* **2009**, *109*, 4963–5050.

[3] Moad, G.; Chong, Y. K.; Postma, A.; Rizzardo, E.; Thang, S. H. *Polymer* **2005**, *46*, 8458–8468.

[4] Barner, L.; Davis, T. P.; Stenzel, M. H.; Barner-Kowollik, C. *Macromol. Rapid Commun.* **2007**, *28*, 539–559.

[5] Coessens, V.; Pintauer, T.; Matyjaszewski, K. *Prog. Polym. Sci.* **2001**, *26*, 337–377.

[6] Lai, J. T.; Filla, D.; Shea, R. *Macromolecules* **2002**, *35*, 6754–6756.

[7] D'Agosto, F.; Hughes, R.; Charreyre, M. T.; Pichot, C.; Gilbert, R. G. *Macromolecules* **2003**, *36*, 621–629.

[8] You, Y. Z.; Hong, C. Y.; Wang, W. P.; Lu, W. Q.; Pan, C. Y. *Macromolecules* **2004**, *37*, 9761–9767.

[9] Liu, J.; Hong, C. Y.; Pan, C. Y. *Polymer* **2004**, *45*, 4413–4421.

[10] Wang, R.; McCormick, C. L.; Lowe, A. B. *Macromolecules* **2005**, *38*, 9518–9525.

[11] Coessens, V.; Matyjaszewski, K. *J. Macromol. Sci., Pure Appl. Chem.* **1999**, *A36*, 667–679.

[12] Binder, W. H.; Sachsenhofer, R. *Macromol. Rapid Commun.* **2007**, *28*, 15–54.

[13] Wang, Z. M.; He, J. P.; Tao, Y. F.; Yang, L.; Jiang, H. J.; Yang, Y. L. *Macromolecules* **2003**, *36*, 7446–7452.

[14] Dietrich, M.; Glassner, M.; Gruendling, T.; Schmid, C.; Falkenhagen, J.; Barner-Kowollik, C. *Polym. Chem.* **2010**, DOI:10.1039/b9py00273a.

[15] Chong, B.; Moad, G.; Rizzardo, E.; Skidmore, M.; Thang, S. H. *Aust. J. Chem.* **2006**, *59*, 755–762.

[16] Perrier, S.; Takolpuckdee, P.; Mars, C. A. *Macromolecules* **2005**, *38*, 2033–2036.

[17] Vyas, D. M.; Hay, G. W. *Can. J. Chem.* **1971**, *49*, 3755–3758.

[18] Vyas, D. M.; Hay, G. W. *J. Chem. Soc., Perkin Trans. 1* **1975**, 180–186.

[19] Vedejs, E.; Arnost, M. J.; Dolphin, J. M.; Eustache, J. *J. Org. Chem.* **1980**, *45*, 2601–2604.

[20] Kirby, G. W.; Lochead, A. W.; Williamson, S. *J. Chem. Soc., Perkin Trans. 1* **1996**, 977–984.

[21] Heuzé, B.; Gasparova, R.; Heras, M.; Masson, S. *Tetrahedron Lett.* **2000**, *41*, 7327–7331.

[22] Pfund, E.; Lequeux, T.; Vazeux, M.; Masson, S. *Tetrahedron Lett.* **2002**, *43*, 2033–2036.

[23] Bastin, R.; Albadri, H.; Gaumont, A. C.; Gulea, M. *Org. Lett.* **2006**, *8*, 1033–1036.

[24] Kobayashi, S. *Macromolecular Symposia* **2006**, *240*, 178–185.

[25] Fenn, J. B.; Mann, M.; Meng, C. K.; Wong, S. F.; Whitehouse, C. M. *Science* **1989**, *246*, 64–71.

[26] Laus, M.; Papa, R.; Sparnacci, K.; Alberti, A.; Benaglia, M.; Macciantelli, D. *Macromolecules* **2001**, *34*, 7269–7275.

[27] Abrunhosa, I.; Gulea, M.; Masson, S. *Synthesis* **2004**, 928–934.

[28] Alberti, A.; Benaglia, M.; Guerra, M.; Gulea, M.; Hapiot, P.; Laus, M.; Macciantelli, D.; Masson, S.; Postma, A.; Sparnacci, K. *Macromolecules* **2005**, *38*, 7610–7618.

4

An Atom-Economical Synthesis of Block Copolymers

4.1 Introduction

The generation of well-defined complex macromolecular architectures plays an important role in contemporary polymer science. The development of various CRP methods[1, 2] as well as efficient modification reactions for polymers has highly contributed to this development. In the case of the latter, the use of the CuAAC as an efficient coupling reaction has seen a great increase in recent years.[3, 4] Although other ligation strategies (which more or less fulfil the *click* criteria)[5] have been successfully employed (with CRP) in generating macromolecular conjugates,[6–8] the vast majority of examples require different functionalities for mediating controlled polymerization and for the post-polymerization coupling reaction. Consequently, either both functionalities are combined into one (initiator) molecule (e.g. alkyne and azide functionalized RAFT agents)[9, 10] or pre-prepared macromolecules are equipped with an appropriate function (e.g. bromo substitution of polymers prepared by ATRP).[11]

In Chapter 3, the end-group modification of a diene-functional polymer via HDA chemistry was explored. The heterodienophiles used, BDPDF and BPDF (depicted as structures **2a** and **2b** respectively in Figure 4.1), can also behave as chain-transfer agents (CTA) in a RAFT polymerization.[12, 13] Therefore, polymers formed in such a

process will automatically bear an active heterodienophile at the chain terminus. As such, the present chapter describes two examples for the combination of a diene terminated poly(ϵ-caprolactone) (PCL), as described in Chapter 3, and a RAFT polymerized poly(styrene) (PS) in a HDA cycloaddition yielding well-defined PCL-*b*-PS block copolymers (Figure 4.1). In this atom-economical approach, the dithioester function was sequentially used for the controlled RAFT polymerization and as the reactive heterodienophile for a polymer-polymer coupling. It has been shown in Chapter 3 that **2a** and **2b** can efficiently undergo a HDA reaction with a macromolecular diene; however the results presented herein establishes for the first time that these structures, as end-groups in polymeric systems, behave in a similar manner.

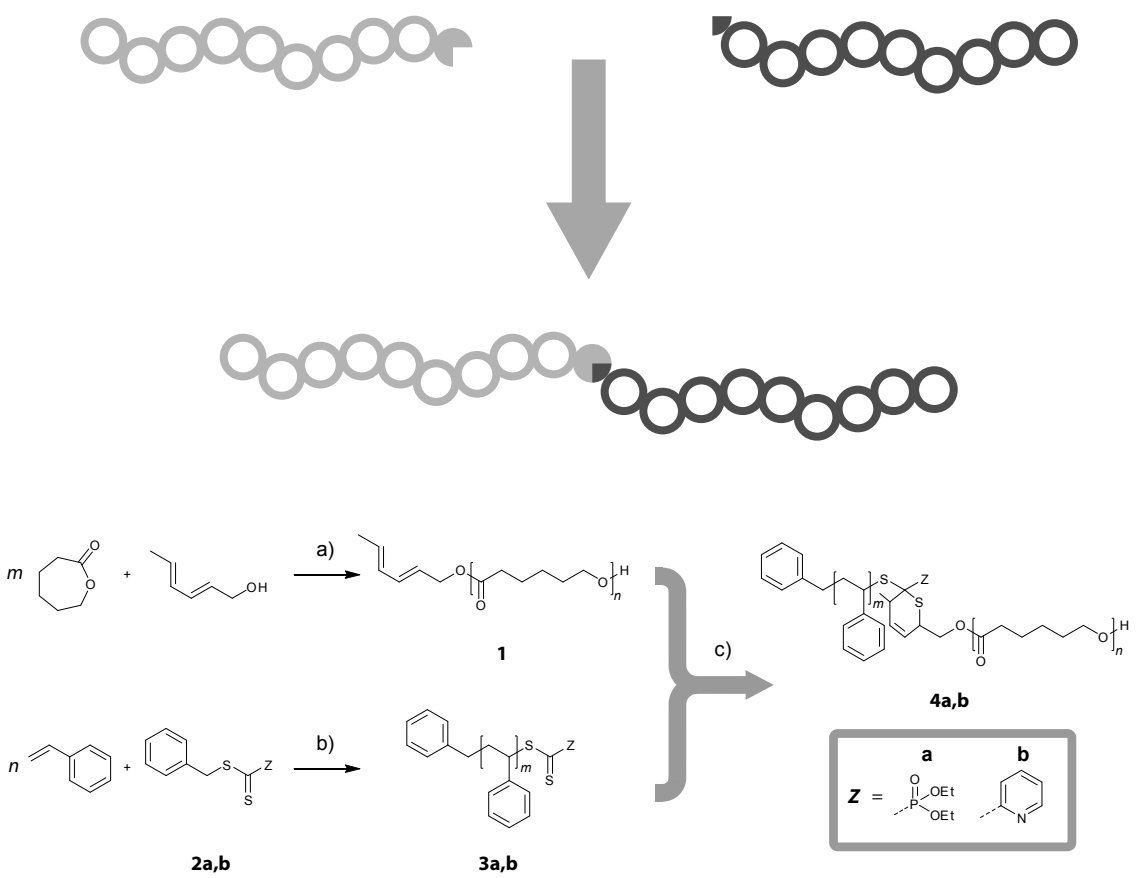

Figure 4.1 Preparation of PS **3a,b** and PCL **1** followed by their coupling via a HDA cycloaddition. (a) ROP, lipase, 70 °C; (b) RAFT polymerization, AIBN, 60 °C; (c) $ZnCl_2$ (1 equiv.), 50 °C, 24 hours for **3a** and TFA (1.1 equiv.), 50 °C, 2 hours for **3b**.

4.2 Experimental Section

The polymerization of ϵ-caprolactone is described in Chapter 3.

Styrene Polymerization

A solution of styrene (80 mL, 0.70 mol), RAFT agent **2a,b** (1.62 mmol) and AIBN (0.043 g, 0.27 mmol) was prepared in a 250 mL round bottom flask. The flask was subsequently purged with nitrogen for 30 minutes to remove any residual oxygen. The polymerization reaction was performed at 60 °C. After a certain reaction time (8.5 hours for **2a** and 11 hours for **2b**), the reaction was quenched by placing the flask in an ice/water mixture and a small amount of hydroquinone added to suspend the reaction. The polymers **3a,b** were isolated by two fold precipitation in cold methanol.

PS **3a**: $M_{n,\,SEC}$ = 2800 g·mol^{-1}, *PDI* = 1.11; $M_{n,\,NMR}$ = 2300 g·mol^{-1}

PS **3b**: $M_{n,\,SEC}$ = 2200 g·mol^{-1}, *PDI* = 1.14; $M_{n,\,NMR}$ = 2500 g·mol^{-1}

Hetero Diels-Alder Cycloaddition Between PCL 1 and PS 3a

A solution of PS **3a** (141 mg, 50 µmol), PCL **1** (128 mg, 50 µmol) and 1 equiv. zinc chloride (6.5 mg, 50 µmol) in 1.5 mL chloroform was kept at 50 °C for 24 hours. The polymer **4a** was isolated by removing the solvent *in vacuo*. SEC (THF): M_n = 5500 g·mol^{-1}, *PDI* = 1.28.

Hetero Diels-Alder Cycloaddition Between PCL 1 and PS 3b

A solution of PS **3b** (112 mg, 50 µmol), PCL **1** (128 mg, 50 µmol) and 1.1 equiv. TFA (4 µL, 55 µmol) in 1.5 mL chloroform was kept at 50 °C for 2 hours. The polymer **4b** was isolated by removing the solvent *in vacuo*. SEC (THF): M_n = 4700 g·mol^{-1}, *PDI* = 1.24.

Thermal Stability Investigation

10 mg of polymer **4b** was dissolved in 100 µL of chloroform and kept at 60 °C in a pressure resistant tube for 24 hours. After removal of the solvent *in vacuo*, the residue was analysed by SEC.

4.3 Results and Discussion

4.3.1 RAFT Polymerization with Electron-Deficient Dithioesters

The RAFT polymerization of styrene was carried out in the presence of **2a,b** and 2,2'-azobis(isobutyronitrile) (AIBN) at 60 °C (Figure 4.1). In order to provide the clearest observable change in the molecular weight distribution after conjugation, the polymerization was stopped at low monomer conversion to ensure a high dithioester end-group concentration and to achieve molecular weights comparable to that of PCL **1**. As such, PS **3a,b** were obtained with a number average molecular weight (M_n) of 2800 g·mol^{-1} and 2200 g·mol^{-1} respectively and low polydispersity indices (*PDI*) of 1.11 and 1.14 respectively (Table 4.1), which confirms the controlled character of the polymerization.

The ^{1}H NMR spectra of PS **3a** and **3b** are depicted in Figure 4.2a and 4.2b respectively. In the case of PS **3a**, one can clearly observe the presence of the ethoxymethylene protons, which confirms that the polymer bears the targeted dithioester end-group. Similarly, the ^{1}H NMR spectrum of PS **3b** reveals the presence of protons from the pyridine ring, thus confirming that it too bears the required dithioester end-group.

Comparison of the intensities of the signals arising from the end-group protons with those from the polymer backbone allows for the calculation of M_n. In doing so, the NMR derived molecular weights of PS **3a,b** were determined to be 2300 g·mol^{-1} and 2500 g·mol^{-1} respectively. The excellent agreement between these values and those derived from SEC measurements confirms the near quantitative dithioester content of both polymers. With dithioester- and diene-capped polymers in hand, the modular construction of block copolymers may be investigated.

4.3.2 Modular Construction of Block Copolymers via HDA Chemistry

The coupling reaction between **3a** and **1** via HDA cycloaddition was performed at 50 °C in chloroform solution and in the presence of zinc chloride (Figure 4.1). A complete conversion of **1** was found after a reaction time of 24 hours. Conveniently, the progress of the reaction may be qualitatively monitored by the discolouration of the reaction mixture as the chromophoric dithioester end-group is transformed into the colourless cycloadduct. Figure 4.3a shows the molar mass distribution of the obtained PCl-*b*-PS copolymer **4a**. In comparison to the starting materials **3a** and **1**, the reaction product **4a** shows an increase in molar mass (M_n = 5500 g·mol^{-1}) which is consistent with the calculated value (Table 4.1) and a distribution width between those of **3a** and

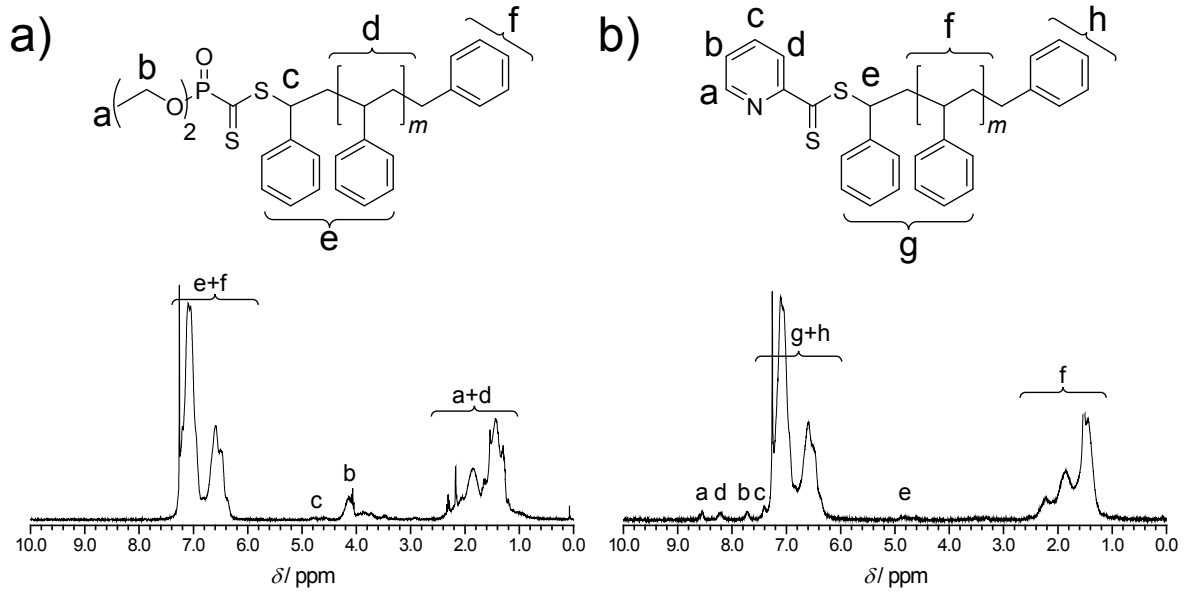

Figure 4.2 ^{1}H NMR spectra of PS **3a** (a); and PS **3b** (b).

1 (*PDI* = 1.28). It must be understood that the determination of the molecular weight of polymers via SEC is not without error and, as such, it is difficult to use this data to attain an exact 1:1 stoichiometry when attempting to react two polymer chains via their reactive end-groups. Consequently, a shoulder at about 2800 g·mol^{-1} can be observed and is attributed to remaining PS **3a**. Such occurrences of residual polymer precursor have previously been encountered and could be easily removed by further purification steps.[14, 15] Under similar conditions, using trifluoroacetic acid (TFA) as the catalyst, quantitative conversion of PS **3b** with PCL **1** was achieved in just 2 hours (Figure 4.1). The corresponding molar mass distributions are presented in Figure 4.3b, which shows an increase in molar mass (M_n = 4700 g·mol^{-1}) and a distribution width between those of **3b** and **1** (*PDI* = 1.24). A summary of the molecular weight data, as obtained via SEC measurements, is presented in Table 4.1.

Table 4.1 Polymer characterization.

Polymer	$M_{n,\,theor.}{}^{a}$/g·mol^{-1}	$M_{n,\,exp.}{}^{b}$/g·mol^{-1}	PDI^{b}
PCL **1**	—	2500^{c}	1.37^{c}
PS **3a**	—	2800	1.11
PS **3b**	—	2200	1.14
PCL-*b*-PS **4a**	5300	5500	1.28
PCL-*b*-PS **4b**	4700	4700	1.24

^{a}Calculated by the sum of the individual building blocks. ^{b}Measured by SEC in THF (calibration with linear PS standards). ^{c}Values for PCL are corrected by applying the Mark-Houwink relationship (K = 13.95 × 10^{-5} dL·g^{-1}, α = 0.786).[16]

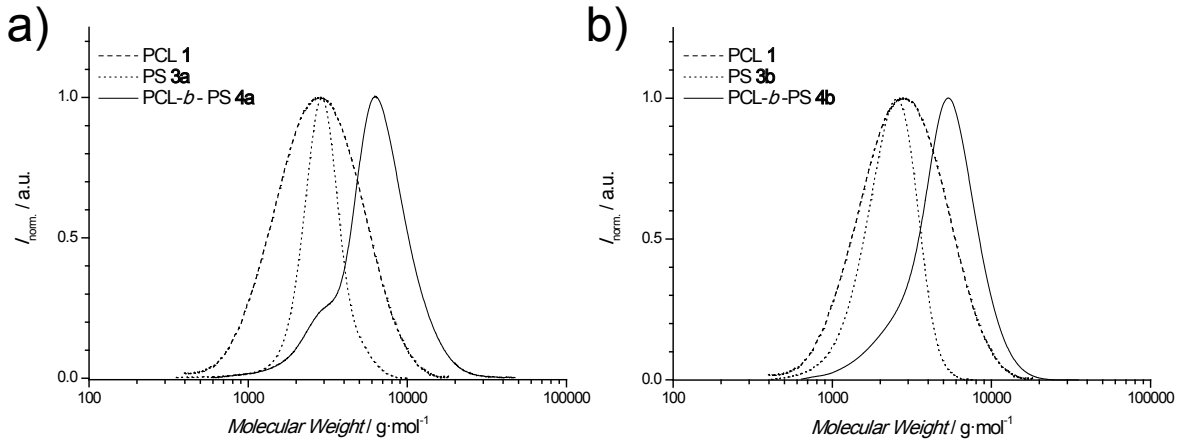

Figure 4.3 Overlay of molecular weight distributions of (a) PCL **1**, PS **3a** and PCL-*b*-PS **4a**; and of (b) PCL **1**, PS **3b** and PCL-*b*-PS **4b**.

In **4a,b**, polymer-segments are linked through the formation of a 3,6-dihydro-2*H*-thiopyran ring, the stability of which was briefly investigated. A sample of block copolymer **4b** was dissolved in chloroform, placed in a pressure-resistant tube and kept at 60 °C for 24 hours. Figure 4.4 depicts the molecular weight distribution of **4b** before and after thermal treatment. If the treatment were to promote a retro Diels-Alder reaction, a change in the molecular weight distribution to reveal more lower molecular weight material would be expected. Upon inspection of Figure 4.4, it is apparent that no decomposition occurs. More in-depth studies of the thermally activated reversibility of this chemistry may be found in Chapters 5, 11 and 12.

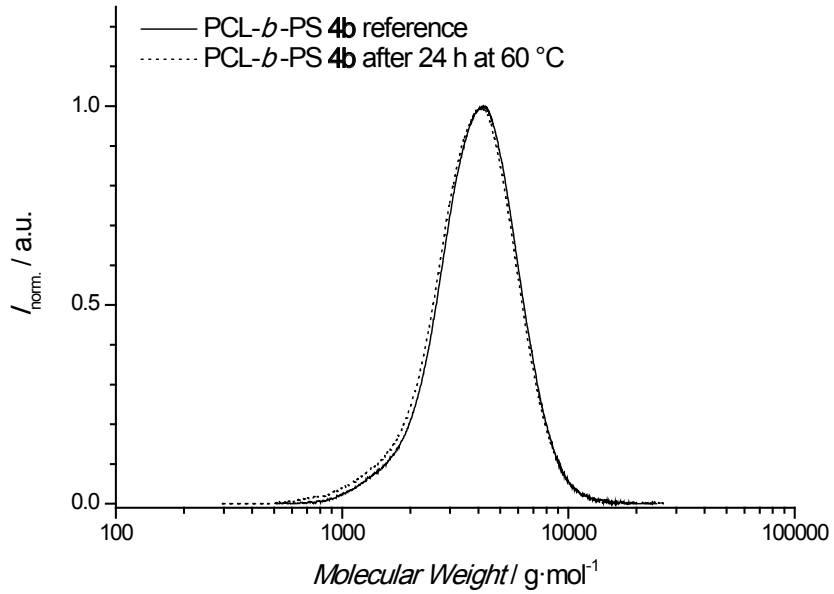

Figure 4.4 Overlay of the molecular weight distributions of PCL-*b*- PS **4b** before and after thermal treatment at 60 °C in chloroform solution.

4.4 Conclusion

It can be confirmed from the above described results that the tendency of electron-deficient dithioesters to undergo HDA cycloadditions can be successfully used to generate polymer conjugates. In two examples, PS's **3a,b**, obtained after controlled polymerization with RAFT agents **2a,b**, were used to form PCL-*b*-PS copolymers **4a,b** after reaction with 2,4-hexadienoyl terminated PCL **1**. This atom-economical method features a high selectivity, quantitative conversion, the absence of dry/inert procedures and can be performed under moderate conditions with a non-toxic catalyst in case of **2a** or with Brønsted acids in case of **2b**. It contributes therefore to the expansion of the field of efficient polymer conjugation.

References

[1] Matyjaszewski, K. *Prog. Polym. Sci.* **2005**, *30*, 858–875.

[2] Barner, L.; Davis, T. P.; Stenzel, M. H.; Barner-Kowollik, C. *Macromol. Rapid Commun.* **2007**, *28*, 539–559.

[3] Lutz, J. F. *Angew. Chem. Int. Ed.* **2007**, *46*, 1018–1025.

[4] Binder, W. H.; Sachsenhofer, R. *Macromol. Rapid Commun.* **2007**, *28*, 15–54.

[5] Kolb, H. C.; Finn, M. G.; Sharpless, K. B. *Angew. Chem. Int. Ed.* **2001**, *40*, 2004–2021.

[6] Gacal, B.; Durmaz, H.; Tasdelen, M. A.; Hizal, G.; Tunca, U.; Yagci, Y.; Demirel, A. L. *Macromolecules* **2006**, *39*, 5330–5336.

[7] Kim, T. D.; Luo, J. D.; Tian, Y. Q.; Ka, J. W.; Tucker, N. M.; Haller, M.; Kang, J. W.; Jen, A. K. Y. *Macromolecules* **2006**, *39*, 1676–1680.

[8] Durmaz, H.; Dag, A.; Altintas, O.; Erdogan, T.; Hizal, G.; Tunca, U. *Macromolecules* **2007**, *40*, 191–198.

[9] Quémener, D.; Davis, T. P.; Barner-Kowollik, C.; Stenzel, M. H. *Chem. Commun.* **2006**, 5051–5053.

[10] Ting, S. R. S.; Granville, A. M.; Quémener, D.; Davis, T. P.; Stenzel, M. H.; Barner-Kowollik, C. *Aust. J. Chem.* **2007**, *60*, 405–409.

[11] Gao, H. F.; Matyjaszewski, K. *Macromolecules* **2006**, *39*, 4960–4965.

[12] Laus, M.; Papa, R.; Sparnacci, K.; Alberti, A.; Benaglia, M.; Macciantelli, D. *Macromolecules* **2001**, *34*, 7269–7275.

[13] Alberti, A.; Benaglia, M.; Guerra, M.; Gulea, M.; Hapiot, P.; Laus, M.; Macciantelli, D.; Masson, S.; Postma, A.; Sparnacci, K. *Macromolecules* **2005**, *38*, 7610–7618.

[14] Opsteen, J. A.; van Hest, J. C. M. *Chem. Commun.* **2005**, 57–59.

[15] Hoogenboom, R.; Moore, B. C.; Schubert, U. S. *Chem. Commun.* **2006**, 4010–4012.

[16] Schindler, A.; Hibionada, Y. M.; Pitt, C. G. *J. Polym. Sci., Part A: Polym. Chem.* **1982**, *20*, 319–326.

5

Star-Shaped Polymers via RAFT-HDA Chemistry

5.1 Introduction

The relationship between the form and function of polymeric materials is the fuel that drives the development of the set of tools with which organic chemists can construct macromolecules of predetermined architecture. Some of the more notable inclusions in this *tool box* are the various forms of CRP, which aim to combine the convenience of radical chemistry with the control over molecular architecture that is offered by such techniques as living anionic polymerization.[1, 2] More recently, the combination of these techniques with *click* chemistry has significantly diversified the contents of this *tool box*, which has allowed macromolecules with complex architecture to be synthesized with great ease.[3–6] An example of such structures is star polymers.

Star polymers have been the subject of intense investigation in the field of material science due to their compact structure, unusual solution properties and unique rheological behaviour.[7, 8] Initially, living anionic polymerization has been the method of choice in the synthesis of such structures, however, very stringent reaction conditions and the limited range of monomers that may be used means that anionic polymerization is not as versatile nor as convenient as radical-based techniques. More recently,

the development of the CRP technologies has brought with it resurgence in interest in the synthesis of these architectures.[1, 2, 9]

Within the field of CRP, polymeric star architectures may be synthesized utilizing one of two general techniques: *core-first*[9–14] and *arm-first*.[15–18] The former technique involves the use of a multi-functional initiator whereby the arms of the star are grown from the core during the polymerization. With techniques such as RAFT polymerization, ATRP and NMP having been successfully shown to produce well-defined stars by the *core-first* method, the RAFT process has been shown to be more cumbersome in attaining such structures.[18] The *arm-first* technique, as it is applied to CRP, initially involved the chain extension of linear polymers with a multi-vinyl crosslinker. Another approach to the *arm-first* technique involves the 'grafting' or 'coupling' of linear polymer segments onto a multifunctional core. This latter method is limited by the selectivity and efficiency of the reactions responsible for linking the linear segments to the core. It has only been recently that, with the advent of the CuAAC[19, 20] that there has been sharp increase in the reported syntheses of well-defined star polymers via the *arm-first* method[21–26] and in polymer chemistry in general.[27–29] This *click* reaction, as defined by Sharpless et al.,[30] bears the selectivity and efficiency necessary to make an *arm-first* strategy for star polymer synthesis viable.

In addition to the above mentioned *click* reaction, the Diels-Alder cycloaddition between anthracene derivatives and maleimides has also been successfully used in the generation of a variety of well-defined polymeric architectures, including di-block copolymers,[31] tri-block copolymers,[32] graft polymers[33] and star polymers.[34] However, both of these strategies bear characteristics that may prove to be problematic in certain applications. For example, the requirement of using toxic copper catalysts in the classical *click* reaction would also have the requirement of a purification stage in the development of materials destined for biomedical application. With regard to the Diels-Alder reaction, the high temperatures required make it unsuitable for use in forming polymeric conjugates from thermally unstable compounds. Another characteristic that both techniques share is that both the core and the polymer segments need to be pre-functionalized with the appropriate complementary moieties in addition to those responsible for performing the controlled polymerization. For example, in the case of RAFT, the controlling agents must be equipped with azide/alkyne functionalities.[6, 35, 36]

An alternative strategy for synthesizing polymer conjugates that is uniquely used with RAFT chemistry was presented in Chapter 3 and in Chapter 4. Here, controlling agents bearing electron-withdrawing Z-groups (BDPDF and BPDF) were used in such a way that the thiocarbonyl functionality of the controlling agents was sequentially used for the CRP and as a reactive heterodienophile in a HDA cycloaddition with an appropriate diene. It was shown in Chapter 4 that the tendency of electron-deficient

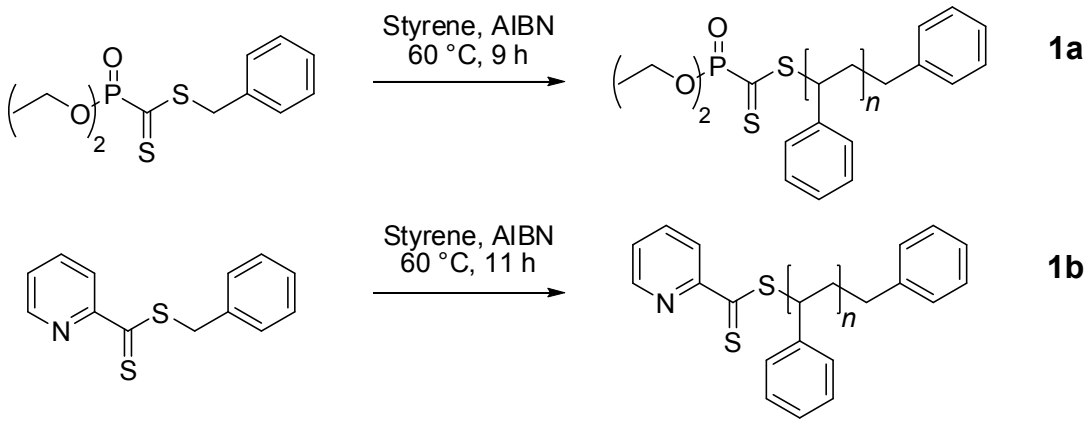

Figure 5.1 Synthesis of poly(styrene) *arms* by RAFT polymerization.

dithioesters to undergo HDA cycloadditions can be successfully used for the formation of block copolymers from dissimilar monomer families. The HDA cycloadditions are facilitated by the use of a catalyst which enhances the electron-withdrawing nature of the RAFT Z-group. This can be achieved by using $ZnCl_2$ as a Lewis acid in the case of the phosphoryl Z- group,[37] and by TFA as a Brønsted acid in the case of the pyridinyl Z- group.[38]

In order to verify the versatility of this method, it is herein reported the synthesis of star polymers by a combination of RAFT chemistry and the HDA cycloaddition. PS prepared by RAFT chemistry (Figure 5.1) is coupled to a 2-arm, 3-arm and 4-arm diene precursor (Figure 5.2) to form star polymers with 2-, 3- and 4-arms respectively (Figure 5.3). The reaction used to generate these structures was then monitored via UV/Vis spectroscopy and ^{1}H NMR spectroscopy from the perspective of the RAFT end-group and the diene respectively. Finally, in order to investigate the possibilities of induced cleavage of the 4-arm stars, the compounds were subjected to a high temperature environment for 24 hours and subsequent SEC measurements were performed.

The present contribution provides a simple and synthetically non-demanding pathway to well-defined macromolecular star-shaped architectures which provides a convenient exemplification for this new synthetic technique.

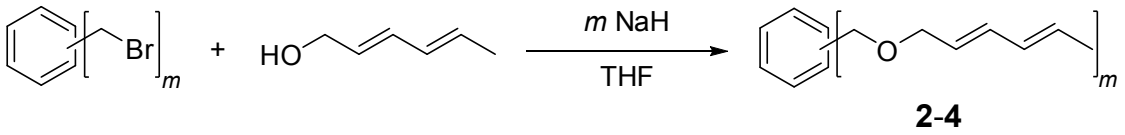

2-4

compound	*m*	substitution
2	2	1,4
3	3	1,3,5
4	4	1,2,4,5

Figure 5.2 Synthesis of *trans,trans*-(hexa-2,4-dienyloxy)methylbenzenes as star *core* molecules.

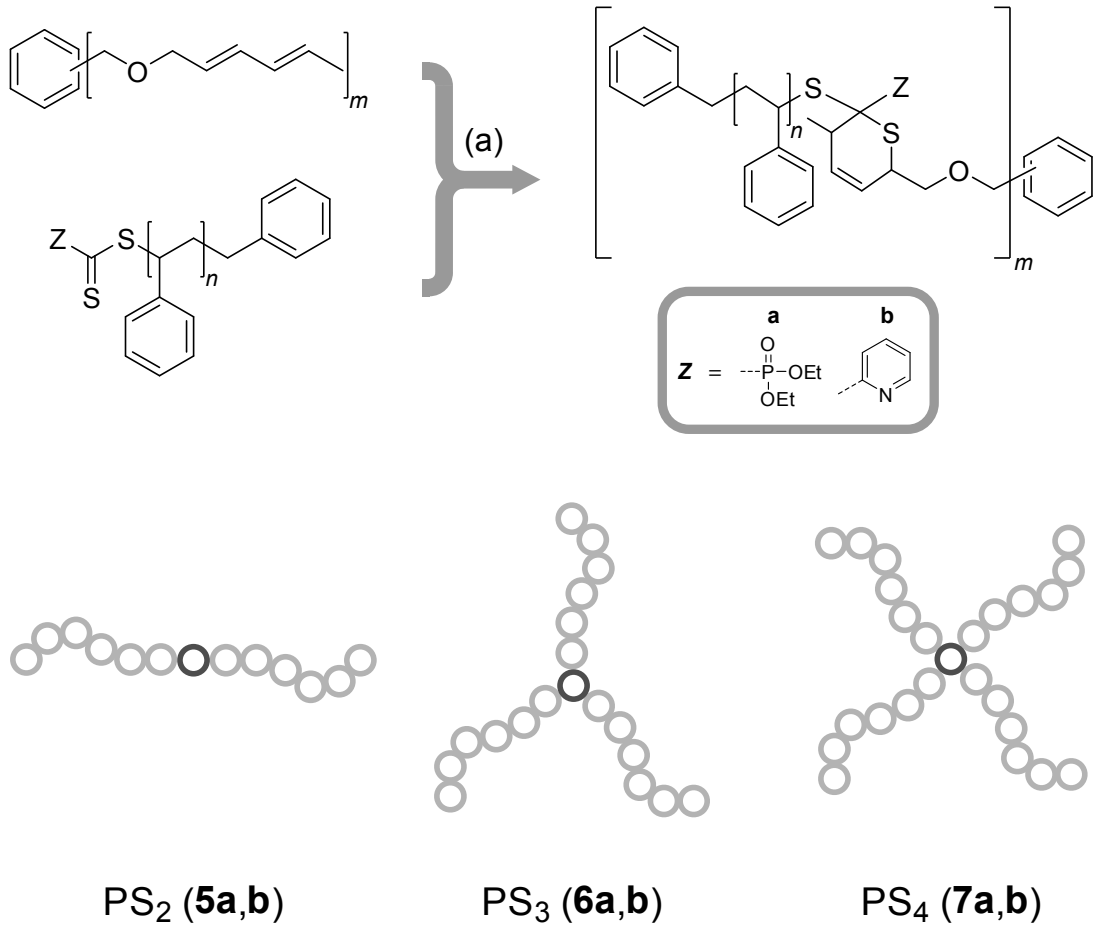

Figure 5.3 Synthesis of star polymers via HDA cycloaddition. Conditions: (a) 1.0 equiv. $ZnCl_2$ for **1a** or 1.2 equiv. of TFA for **1b**, $CHCl_3$, 50 °C, 24 h.

5.2 Experimental Section

Styrene Polymerization

A solution of styrene (80 mL, 0.70 mol), RAFT agent BDPDF or BPDF (1.62 mmol) and AIBN (0.043 g, 0.27 mmol) was prepared in a 250 mL round bottom flask. The flask was subsequently purged with nitrogen for 30 minutes to remove any residual oxygen. The polymerization reaction was performed at 60 °C. After a certain reaction time (9 hours for BDPDF and 11 hours for BPDF), the reaction was quenched by placing the flask in an ice/water mixture and a small amount of hydroquinone added to suspend the reaction. The polymers **1a,b** were isolated by two fold precipitation in cold methanol.

PS **1a**: $M_{n,\,SEC}$ = 3600 g·mol^{-1}, *PDI* = 1.10.

PS **1b**: $M_{n,\,SEC}$ = 3500 g·mol^{-1}, *PDI* = 1.15.

General Procedure for the Synthesis of (trans,trans-hexa-2,4-dienyloxy)methylbenzenes

The according bromomethylbenzene derivative (3 mmol) and sodium hydride (60 % suspension in oil, 1.1 equiv. of bromine groups) were placed in a Schlenk flask. Under a nitrogen atmosphere, THF (dry, 30 mL) was added at room temperature. At 0 °C a solution of *trans,trans*-2,4-hexadien-1-ol (1.1 equiv. of bromine groups) in 5 mL THF was added dropwise. After complete addition, the mixture was allowed to warm to room temperature and was stirred for a further 8 hours. 30 mL aqueous ammonium chloride solution (1 M) was then added in order to destroy residual sodium hydride, which was followed by a three-fold extraction with 30 mL of diethyl ether. After removal of the solvent under vacuum, the product was isolated via column chromatography (silica/*n*-hexane/ethyl acetate).

1,4-bis((*trans,trans*-hexa-2,4-dienyloxy)methyl)benzene (2). Yield: 1.0 g (83 %). R_f=0.66 (*n*-hexane/ethyl acetate = 5:1). ^{1}H NMR (300 MHz, $CDCl_3$, 25 °C): δ = 7.31 (s, 4H, arom.), 6.21 (dd, $^3J_{HH}$=15 Hz, $^3J_{HH}$ = 10 Hz, 2H, -$OCH_2CHC\mathbf{H}(CH)_2CH_3$), 6.06 (ddq, $^3J_{HH}$ = 15 Hz, $^3J_{HH}$ = 10 Hz, $^4J_{HH}$ = 1 Hz, 2H, -$OCH_2(CH)_2C\mathbf{H}CHCH_3$), 5.70 (dq, $^3J_{HH}$ = 14 Hz, $^3J_{HH}$ = 7 Hz, 2H, -$OCH_2(CH)_3C\mathbf{H}CH_3$), 5.66 (dt, $^3J_{HH}$ = 15 Hz, $^3J_{HH}$ = 6 Hz, 2H, -$OCH_2C\mathbf{H}(CH)_3CH_3$), 4.49 (s, 4H, Ph$C\mathbf{H}_2$O-), 4.02 (d, $^3J_{HH}$ = 6 Hz, 4H, -$OC\mathbf{H}_2$CH-) 1.75 (dd, $^3J_{HH}$ = 7 Hz, $^4J_{HH}$ = 1 Hz, 6H, -$C\mathbf{H}_3$) ppm. ^{13}C NMR (75 MHz, $CDCl_3$, 25 °C): δ = 138 ($\mathbf{C}_{arom}$-CH_2-), 133 ($OCH_2CH\mathbf{C}H(CH)_2CH_3$), 131 (-$OCH_2(CH)_2\mathbf{C}HCHCH_3$), 130 (-$OCH_2(CH)_3\mathbf{C}HCH_3$),

128 (**C**$_{arom}$-H), 127 (-OCH$_2$**C**H(CH)$_3$CH$_3$), 71.7 (-O**C**H$_2$CH-), 70.7 (Ph**C**H$_2$O-), 18.1 (-**C**H$_3$) ppm.

1,3,5-tris((*trans,trans*-hexa-2,4-dienyloxy)methyl)benzene (3). Yield: 0.71 g (79 %). R_f=0.55 (*n*-hexane/ethyl acetate = 5:1). ^{1}H NMR (300 MHz, $CDCl_3$, 25 °C): δ = 7.24 (s, 3H, arom.), 6.22 (ddt, $^3J_{HH}$ = 15 Hz, $^3J_{HH}$ = 11 Hz, $^4J_{HH}$ = 1 Hz, 3H, -OCH$_2$CHC**H**(CH)$_2$CH$_3$), 6.07 (ddq, $^3J_{HH}$ = 15 Hz, $^3J_{HH}$ = 10 Hz, $^4J_{HH}$ = 1 Hz, 3H, -OCH$_2$(CH)$_2$C**H**CHCH$_3$), 5.71 (dq, $^3J_{HH}$ = 14 Hz, $^3J_{HH}$ = 7 Hz, 3H, -OCH$_2$(CH)$_3$C**H**CH$_3$), 5.66 (dt, $^3J_{HH}$ = 15 Hz, $^3J_{HH}$ = 6 Hz, 3H, -OCH$_2$C**H**(CH)$_3$CH$_3$), 4.49 (s, 6H, PhC**H**$_2$O-), 4.03 (d, $^3J_{HH}$ = 6 Hz, 6H, -OC**H**$_2$CH-) 1.75 (dd, $^3J_{HH}$ = 7 Hz, $^4J_{HH}$ = 1 Hz, 9H, -C**H**$_3$) ppm. ^{13}C NMR (75 MHz, $CDCl_3$, 25 °C): δ = 139 (**C**$_{arom}$-CH$_2$-), 133 (-OCH$_2$CH**C**H(CH)$_2$CH$_3$), 131 (-OCH$_2$(CH)$_2$**C**HCHCH$_3$), 130 (-OCH$_2$(CH)$_3$**C**HCH$_3$), 127 (**C**$_{arom}$-H), 126 (-OCH$_2$**C**H(CH)$_3$CH$_3$), 71.7 (-O**C**H$_2$CH-), 70.5 (Ph**C**H$_2$O-), 18.1 (-**C**H$_3$) ppm.

1,2,4,5-tetrakis((*trans,trans*-hexa-2,4-dienyloxy)methyl)benzene (4). Yield: 0.82 g (53 %). R_f=0.50 (*n*-hexane/ethyl acetate = 5:1). ^{1}H NMR (300 MHz, $CDCl_3$, 25 °C): δ = 7.24 (s, 2H, arom.), 6.22 (ddt, $^3J_{HH}$ = 15 Hz, $^3J_{HH}$ = 11 Hz, $^4J_{HH}$ = 1 Hz, 4H, -OCH$_2$CHC**H**(CH)$_2$CH$_3$), 6.07 (ddq, $^3J_{HH}$ = 15 Hz, $^3J_{HH}$ = 10 Hz, $^4J_{HH}$ = 1 Hz, 4H, -OCH$_2$(CH)$_2$C**H**CHCH$_3$), 5.71 (dq, $^3J_{HH}$ = 14 Hz, $^3J_{HH}$ = 7 Hz, 4H, -OCH$_2$(CH)$_3$C**H**CH$_3$), 5.66 (dt, $^3J_{HH}$ = 15 Hz, $^3J_{HH}$ = 6 Hz, 4H, -OCH$_2$C**H**(CH)$_3$CH$_3$), 4.49 (s, 8H, PhC**H**$_2$O-), 4.03 (d, $^3J_{HH}$ = 6 Hz, 8H, -OC**H**$_2$CH-) 1.75 (dd, $^3J_{HH}$ = 7 Hz, $^4J_{HH}$ = 1 Hz, 9H, C**H**$_3$) ppm. ^{13}C NMR (75 MHz, $CDCl_3$, 25 °C): δ =136 (**C**$_{arom}$-CH$_2$-), 133 (-OCH$_2$CH**C**H(CH)$_2$CH$_3$), 131 (-OCH$_2$(CH)$_2$**C**HCHCH$_3$), 130 (-OCH$_2$(CH)$_3$**C**HCH$_3$), 129 (**C**$_{arom}$-H), 127 (-OCH$_2$**C**H(CH)$_3$CH$_3$), 70.5 (-O**C**H$_2$CH-), 69.2 (Ph**C**H$_2$O-), 18.0 (-**C**H$_3$) ppm.

Synthesis of Star Polymers by HDA Cycloaddition of PS 1a with Multifunctional Coupling Agents 2, 3 and 4 (5a, 6a, 7a)

A solution of PS **1a** (47 mg, 13 µmol), multifunctional coupling agent **2**, **3**, **4** (1.0 equiv. of diene) and 1 equiv. $ZnCl_2$ (1.8 mg, 13 µmol) in 200 µL chloroform was kept at 50 °C for 24 hours. The solvent was removed under vacuum and the residue directly analysed by SEC in THF.

Monitoring of the Reaction between PS 1a and 2 by UV/Vis Spectroscopy

PS **1a** (216 mg, 60 µmol) and 1.0 equiv. $ZnCl_2$ (8.2 mg, 60 µmol) were dissolved in 700 µL chloroform. The resulting solution was added to a solution of **2** (2 mg, 60 µmol) in 500 μL chloroform in a UV cuvette immediately prior to placing in the preheated (50 °C) cuvette holder of the UV/Vis spectrophotometer. The reaction was allowed to proceed at this temperature for 25 hours.

Synthesis of Star Polymers by HDA Cycloaddition of PS 1b with Multifunctional Coupling Agents 2, 3 and 4 (5b, 6b, 7b)

A solution of PS **1b** (47 mg, 13 µmol), multifunctional coupling agent **2**, **3**, **4** (1.0 equiv. of diene) and 1.2 equiv. TFA (1.2 µL, 15.6 µmol) in 200 µL chloroform was kept at 50 °C for 24 hours. The solvent was removed under vacuum and the residue directly analyzed by SEC in THF.

Monitoring of the Reaction between PS 1b and 2 via ^{1}H NMR Spectroscopy

A solution of PS **1b** (88 mg, 25 µmol) and **2** (7.5 mg, 25 µmol) in 900 µL $CDCl_3$ was prepared in a NMR tube. A solution of TFA (23 µL, 30 µmol) in 100 µL $CDCl_3$ was added immediately prior to placing the tube in the NMR spectrometer. Spectra of the reaction mixture were taken every 10 minutes over a period of 24 hours at 50 °C.

High Temperature Treatment of PS_4 (7a,b)

PS_4 **7a,b** was dissolved in toluene (2 mL) in a pressure tube and kept at 160 °C for 24 hours. The solvent was removed under vacuum and the residue directly analysed by SEC in THF.

5.3 Results and Discussion

The linear PS precursors (**1a,b**), from which the subsequent star polymers were prepared, were synthesized by the RAFT polymerization of styrene using controlling agents BDPDF and BPDF respectively (Figure 5.1). The reaction was stopped at low monomer conversion to ensure a high RAFT end-group concentration. Linear PS **1a,b** were obtained with a number average molecular weight (M_n) of 3600 g·mol^{-1} and 3500 g·mol^{-1}, and low polydispersity indices (*PDI*) of 1.10 and 1.15 respectively as determined by SEC analysis in THF.

The multi-functional coupling agents **2-4** were obtained by etherification of the corresponding bromomethylbenzenes with *trans,trans*-2,4-hexadien-1-ol (Figure 5.2). The commercially available *trans,trans*-2,4-hexadien-1-ol has been proven to be a very useful diene as its ester in the HDA approach to polymer conjugates (cf. Chapter 4). In the present Chapter, the above diene is transformed into its ether in the simple synthesis of **2-4** all of which could be obtained in good yields.

5.3.1 Synthesis and Characterization of Star Polymers using PS 1a

The coupling reactions of PS **1a** with coupling agents **2-4** were performed in chloroform solution at 50 °C in the presence of $ZnCl_2$ (1.0 equiv.), as illustrated in Figure 5.3. After a reaction time of 24 hours, the initially pink solutions (the colour of the PS by virtue of its RAFT end-group) had turned colourless. Figure 5.4 shows the SEC trace of the linear PS **1a** in comparison to those of the coupling products PS_2 **5a**, PS_3 **6a**, and PS_4 **7a**. The shift of the distributions to lower retention times with increasing arm number is clearly observed. The M_n values of the coupling products (Table 5.1) increase with arm number, however they depart further and further away from the theoretical values. This is attributed to two factors. Firstly, due to the relatively compact structure of star polymers, increases in observed molecular weight become less and less pronounced with increasing arm number. Secondly, the determination of M_n values takes into consideration remaining precursor material, which tends to skew the observed M_n to lower values and leads to an increase in *PDI* values.

The reduction in hydrodynamic volume that arises when linear polymers are arranged in star formations leads to under-estimated values for the M_n as determined from SEC measurements. As such, the synthesis of star polymers with 2-, 3- and 4-arms was performed in order to directly show the evolution of the molecular weight distributions of star polymers with increasing number of arms. Furthermore, due to the successive increase in the number of arms from the linear PS **1a** to PS_4 **7a**, it is possible to deconvolute the SEC data via peak splitting. The peak splitting technique

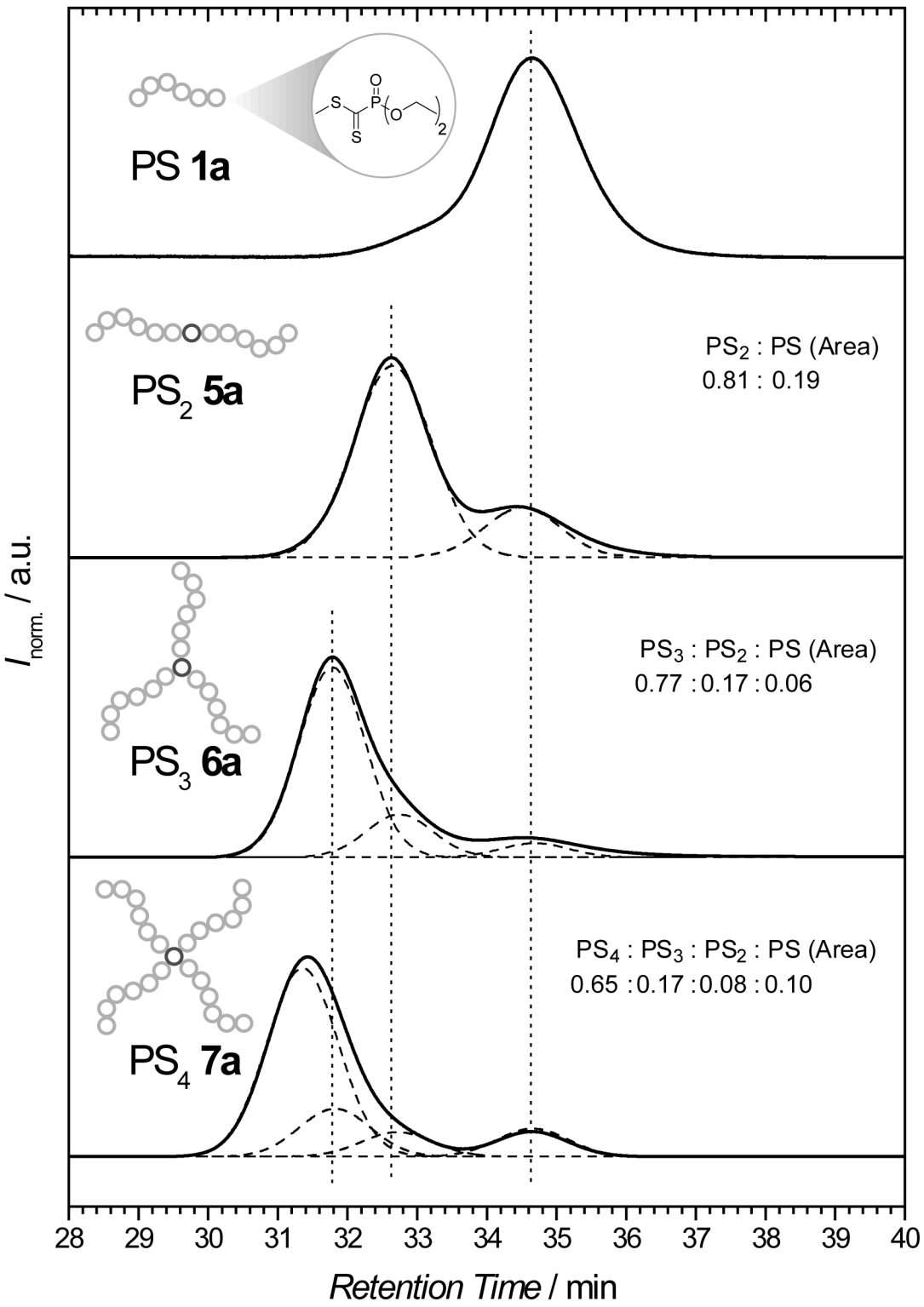

Figure 5.4 Comparative SEC traces of PS **1a** with coupling products PS_2 **5a**, PS_3 **6a** and PS_4 **7a**. The dotted lines represent the results of deconvolution via peak splitting.

Table 5.1 Characterization of PS **1a,b** and its coupling products.

Polymer	$M_{n,\,theor.}$[a] / g·mol^{-1}	$M_{n,\,SEC}$[b] / g·mol^{-1}	$M_{n,\,deconv.}$[c] / g·mol^{-1}	PDI_{SEC}[b]	$PDI_{deconv.}$[c]
PS **1a**	—	3 600	—	1.10	—
PS_2 **5a**	7 500	6 000	7 600	1.13	1.03
PS_3 **6a**	11 200	7 700	11 100	1.16	1.06
PS_4 **7a**	14 900	9 000	12 300	1.28	1.03
PS **1b**	—	3 500	—	1.15	—
PS_2 **5b**	7 300	5 600	7 300	1.16	1.04
PS_3 **6b**	10 900	7 900	10 900	1.16	1.04
PS_4 **7b**	14 500	8 810	12 900	1.24	1.03

[a]Calculated by the sum of the individual building blocks. [b]Measured by SEC in THF with RI detection (calibration with linear PS standards). [c]Values determined from deconvoluted SEC data after peak splitting using a Gaussian function.

allows the observed mass distribution of the various coupling products to be broken down into its constituent distributions. For example, the observed mass distribution of the 4-arm star PS_4 **7a,b** represents the sum of the mass distributions of the desired 4-arm star, any 3-arm and 2-arm star material that is formed in the reaction and any remaining precursor. Since the star polymers are built up successively in terms of arm number, it is possible to define the position (i.e. the retention time) of the expected side products and, using a Gaussian approximation to the individual distributions of these products, a fit to the experimental data may be achieved. The data acquired from this fitting procedure enables the estimation of the M_n and *PDI* values for the desired product by manual calculation and, may also be used to determine the fraction of styrene units that are present in the desired product.

The result of peak splitting of the SEC trace of PS_2 **5a** indicates that the area ratio of di-block PS and linear PS **1a** precursor is 0.81: 0.19 (Figure 5.4). Further analysis of the deconvoluted data indicates that the corrected value of M_n of PS_2 **5a** is in close agreement with the theoretical value (Table 5.1). The decrease in *PDI* suggested by the deconvoluted data is consistent with polymer-polymer couplings. Similar analyses were performed on the SEC traces of PS_3 **6a** and PS_4 **7a**. In the case of the former, the area ratio of 3-arm star, PS_2 and PS precursor is 0.77:0.17:0.06, indicating that 94 % of the styrene units are incorporated into a coupling product. In the case of the latter, the area ratio of 4-arm star, 3-arm star, PS_2 and PS precursor is 0.65:0.17:0.08:0.10, indicating that 90 % of the styrene units are incorporated into a coupling product. The analyses of the deconvoluted data of PS_3 **6a** and PS_4 **8a** both yield the expected decrease in *PDI* (Table 5.1). The corrected value of M_n for PS_3 **6a** shows a more dis-

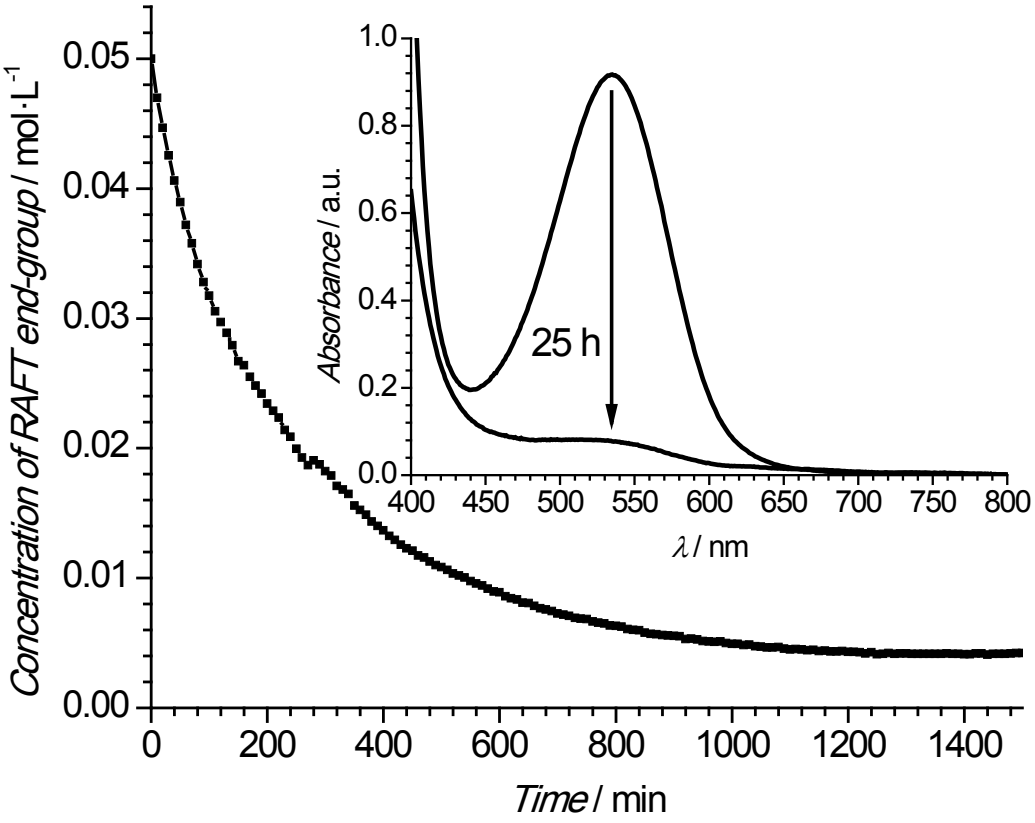

Figure 5.5 Monitoring the concentration of the RAFT end-group of PS **1a** as a function of time in its reaction with coupling agent **2**. The UV/Vis spectra prior to and after reaction are presented in the inset.

tinctive increase in molecular weight, while that of PS_4 **7a** is markedly lower than the theoretical value and is attributed to the compact structure of the star polymer in relation to its linear analogue.

The coupling reaction between PS **1a** and coupling agent **2** was also followed by UV/Vis spectroscopy. The use of this analytical technique was deemed to be ideal to follow the conversion of the chromophoric RAFT end-group (λ_{max} = 535 nm) to the colourless 3,6-dihydro-2*H*-thiopyran ring that is formed during the reaction (Figure 5.3). The inset of Figure 5.5 depicts the absorbance of the RAFT end-group of PS **1a** (λ = 400-800 nm). The monitoring of this absorbance over a period of 25 hours yielded the concentration-time relationship presented in the main section of Figure 5.5, which indicates that the conversion of the thiocarbonyl group in **1a** reached a constant value of 92 % after 24 hours. This finding is consistent, within the limitations of both methods, with the results obtained from peak splitting of the SEC traces, taking into consideration that the SEC traces are influenced by unfunctionalized PS whereas the UV/Vis spectra are not.

5.3.2 Synthesis and Characterization of Star Polymers using PS 1b

Concurrent with the previous set of investigations, PS **1b** was also reacted with coupling agents **2-4** to yield star polymers PS_2 **5b**, PS_3 **6b** and PS_4 **7b**, the SEC traces of which are presented in Figure 5.6. It is clear to observe the shift in the molecular weight distributions to lower retention times with increasing arm number. The elution peak of PS_2 **5b** is a combination of di-block PS and linear PS precursor. The result of peak splitting indicates that the area ratio of these species (PS_2 and linear PS precursor) is 0.91:0.09. Likewise, the elution peak of PS_3 **6b** is comprised of 3-arm star polymer, PS_2 polymer and linear polymer precursor, the area ratios of which is 0.86:0.11:0.03. Furthermore, the elution peak of PS_4 **7b** is comprised of 4-arm star polymer and other star material of lower functionality. The area ratio of these four species (4-arm star, 3-arm star PS_2 and linear PS precursor) is 0.81:0.10:0.05:0.04. In all cases, more that 90 % of the styrene units are incorporated in a coupling product (91 % for PS_2 **5b**, 97 % for PS_3 **7b** and 96 % for PS_4 **8b**).

Table 5.1 summarises the mass distribution data for the star polymers synthesized from PS **1b**. While the M_n values determined from SEC measurements increase with growing arm number, the M_n values determined from the deconvoluted data more distinctly show this increase. The *PDI* values of the deconvoluted data, which are distinctly lower than that of the precursor, are also consistent with the formation of star polymers.

The reaction of PS **1b** with coupling agent **2** was also performed in an NMR tube in $CDCl_3$ solvent in order to monitor the progress of the reaction by ^{1}H NMR spectroscopy. This technique was selected in preference to UV/Vis spectroscopy for two main reasons, the first of which is the fact that the presence of TFA catalyst in the reaction mixture imparts colour to the final coupling product. The second reason for using ^{1}H NMR spectroscopy is that the reaction may be monitored with respect to the coupling agent, rather than the RAFT end-group, which was the case with UV/Vis spectroscopy.

Figure 5.7 shows an overlay of ^{1}H NMR spectra of the reaction mixture of PS **1b** and coupling agent **2** at 10 minute intervals. Since a non-symmetric diene is utilized, there are two possible regioisomers of the 3,6-dihydro-2*H*-thiopyran ring in the coupling products, which contains three chiral centres. Consequently, the large number of possible stereo/regioisomers of the coupling products renders monitoring of the HDA coupling reaction via NMR spectroscopy complex. However, progress of the reaction is indicated by the disappearance of signals arising from the vinylic protons (d and e in Figure 5.7) and the disappearance of signals arising from aliphatic protons (a and b in Figure 5.7). The series of NMR spectra obtained were then used to generate Figure 5.8, which depicts the concentration of the diene functionality in the coupling agent **2**

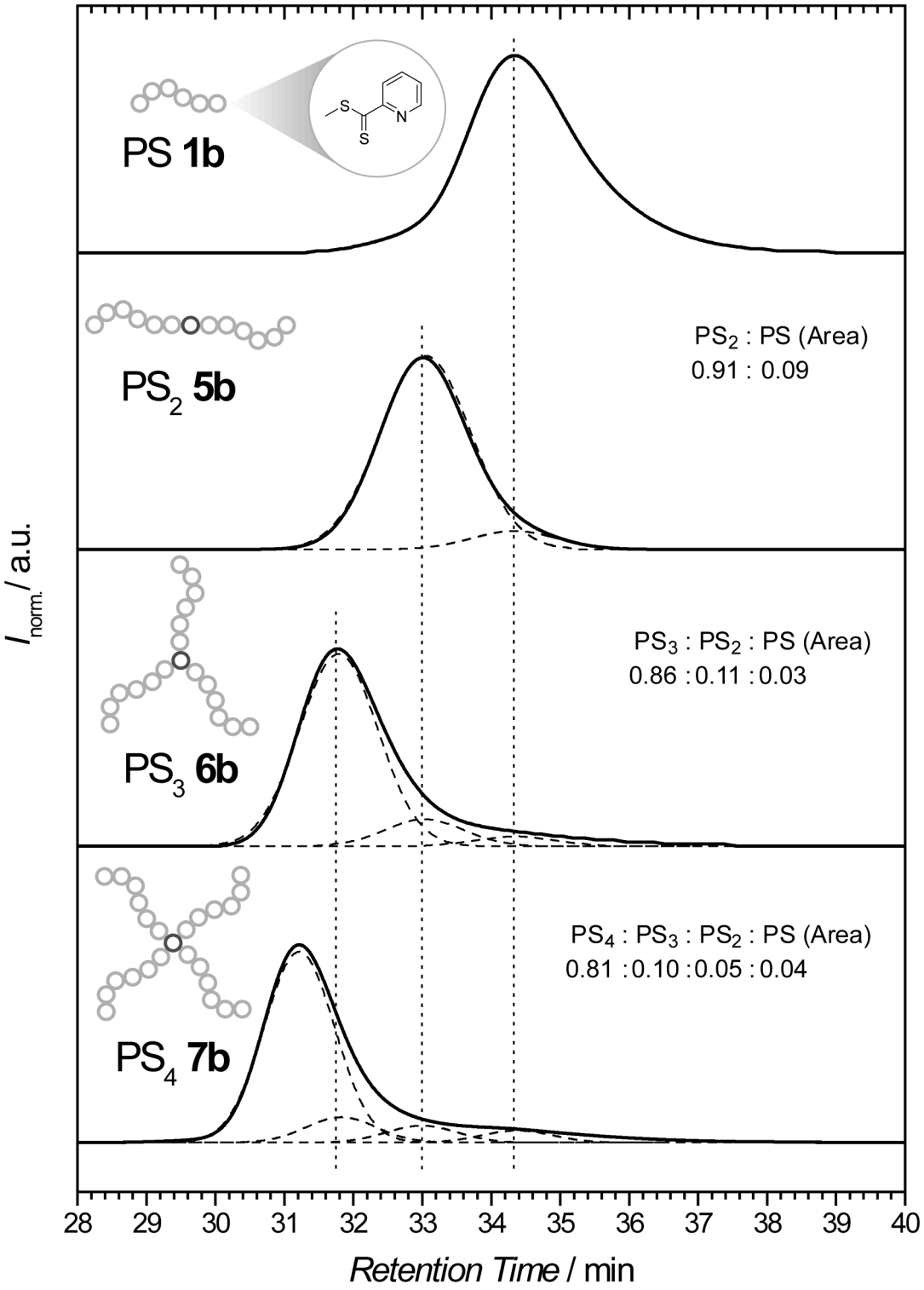

Figure 5.6 Comparative SEC traces of PS **1b** with coupling products PS_2 **5b**, PS_3 **6b** and PS_4 **7b**. The dotted lines represent the results of deconvolution via peak splitting.

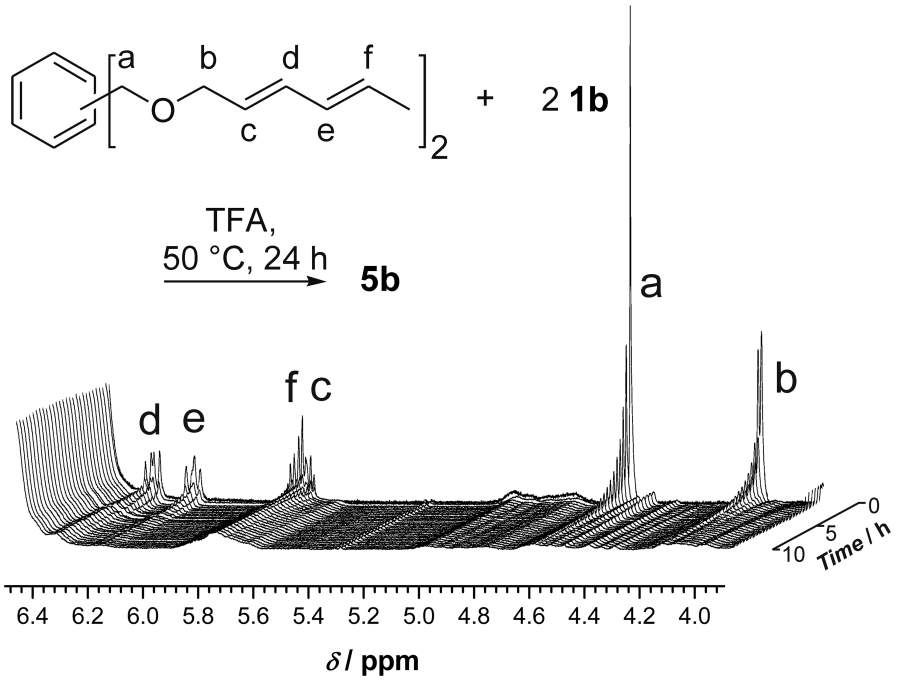

Figure 5.7 Overlay of ^{1}H NMR spectra (6.5 - 3.9 ppm region) of the reaction mixture of PS **1b** and coupling agent **2**.

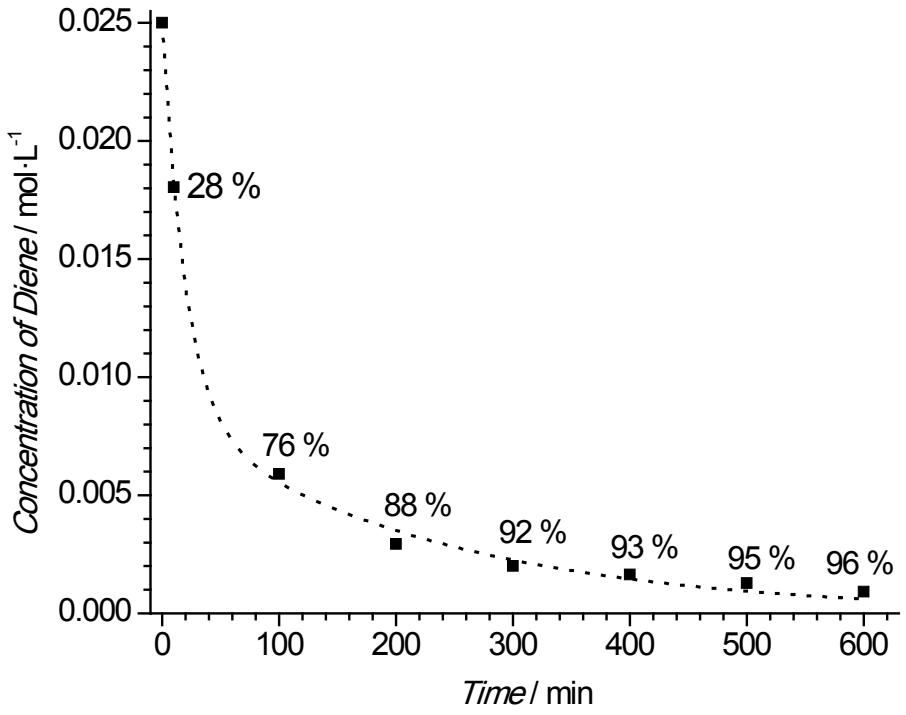

Figure 5.8 Concentration and conversion of diene with respect to time in the reaction of PS **1b** with coupling agent **2**.

as a function of time. The data suggest that a 96 % conversion of the diene is achieved in just 10 hours (91 % as approximated from SEC peak splitting) which is consistent with previous observations that the pyridinyl dithioester is, under the applied conditions, a more efficient heterodienophile than the phosphoryl dithioester (cf. Chapter 3 and Chapter 4). The consistency between the NMR results and the SEC approximation is also observed and further confirms that the pyridinyl dithioester end-group is a more effective heterodienophile by virtue of the higher conversions obtained.

5.3.3 Thermal Cleavage of Star PS_4 7a,b

It has been well established that thioacetals and thioketals undergo fragmentation under such conditions as oxidative[39] and thermal.[40] Furthermore, the 3,6-dihydro-*2H*-thiopyran ring has been shown to fragment under radical conditions and may also undergo a retro Diels-Alder reaction. Therefore, the investigation of the conditions under which the cleavage of these structures may be induced can be used in the design of macromolecular architectures with predetermined or targeted fragmentation patterns. It has been shown that the 3,6-dihydro-*2H*-thiopyran ring as a linking agent in polymer conjugates is stable for at least 24 hours at 60 °C. In the present investigation, the star polymers PS_4 **7a,b** were dissolved in an excess of toluene and subjected to thermal environments ranging from 80 °C to 160 °C. Interestingly, it was observed that the successive increase in the thermal treatment of the polymers brought about a successively increasing degree of fragmentation, with quantitative cleavage achieved after 24 hours at 160 °C.

Figure 5.9a compares the SEC traces of PS_4 **7a** and its degradation product to that of the original linear precursor PS **1a**. The M_n and *PDI* of the degradation product (3600 g·mol^{-1} and 1.09 respectively) are in excellent agreement with the corresponding values of the precursor PS **1a** (3600 g·mol^{-1} and 1.10 respectively), thus indicating the thermal treatment of the 4-arm star polymer was successful in the cleaving of all arms to recover linear PS.

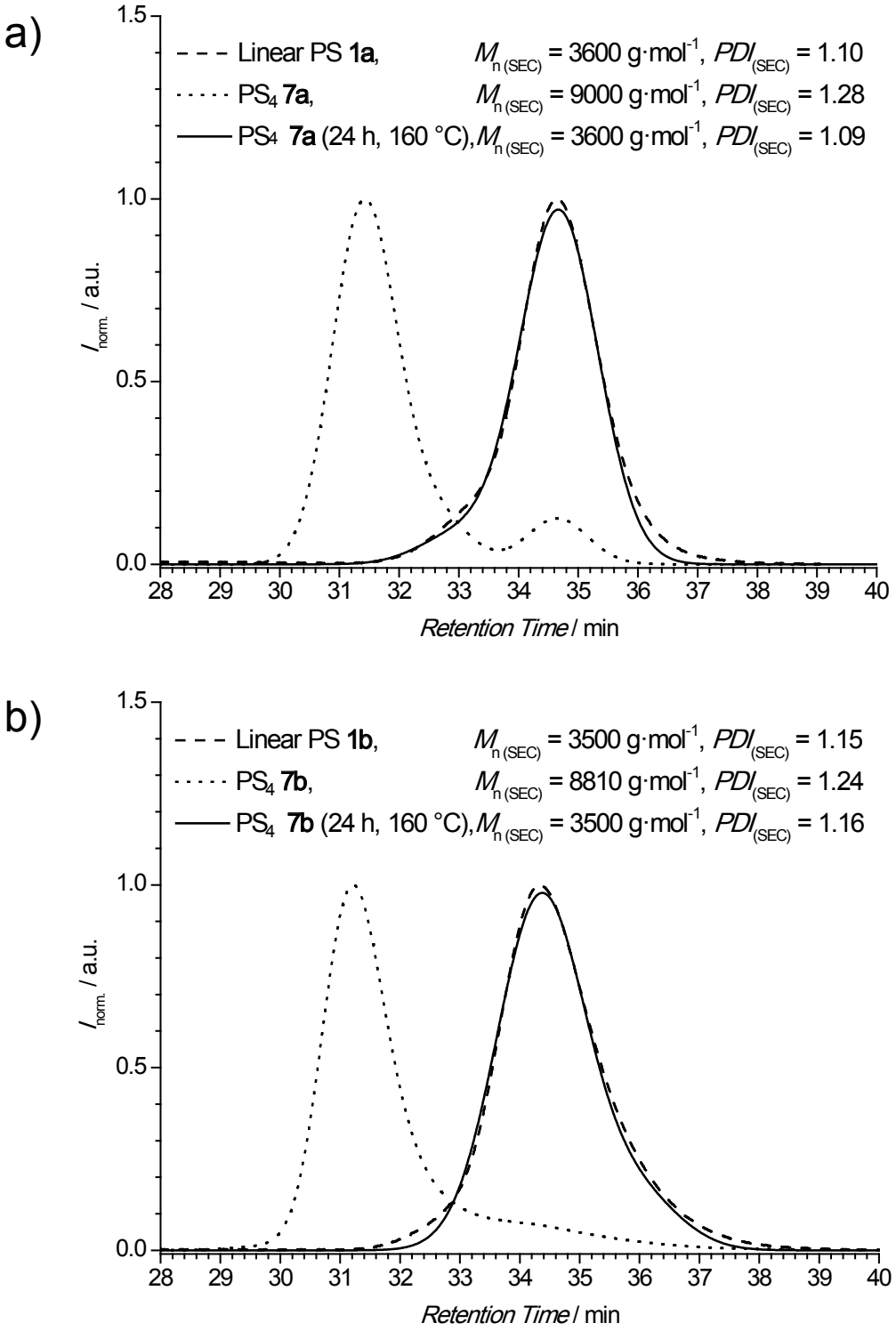

Figure 5.9 SEC traces of (a) PS **1a**, PS_4 **7a**, and its degradation product; and (b) PS **1b**, PS_4 **7b**, and its degradation product

Similarly, the complete induced fragmentation of PS_4 **7b** to its linear PS constituents was achieved at 160 °C, as is shown in Figure 5.9b. The product was found to have a M_n = 3500 g·mol^{-1} and a *PDI* of 1.08, which are consistent with the precursor PS **1b**. A more quantitative investigation into the thermal and pH stability of 3,6-dihydro-*2H*-thiopyran rings within the context of macromolecular conjugations was reported as an extension of the current work.[41] In the case of the phosphoryl dithioester, complete fragmentation was observed to occur after 24 hours at 160 °C via a combination of retro HDA cycloaddition and two un-determined, yet separate degradation mechanisms. The pyridinyl dithioester, however was found to exclusively degrade via a retro HDA mechanism after 24 hours at 180 °C. Interestingly, both systems were found to have excellent stability to strongly basic and strongly acidic conditions (pH = 0 - 14).

5.4 Conclusion

The synthesis of star polymers with up to 4 arms by a combination of RAFT chemistry and the HDA cycloaddition has proven to be successful by the above described results. In two examples, PS **1a,b** prepared by RAFT polymerizations were used to form star polymers with up to 4 arms after reaction with multi-diene containing coupling agents **2**-**4**. The present work verifies the ability of the HDA cycloaddition/ RAFT chemistry combination to be useful in the convenient synthesis of macromolecules of pre-determined complex architecture. It therefore successfully represents a viable technique that attempts to widen the synthetic *tool box* that is available to the organic chemist to advance the field of materials research.

References

[1] Matyjaszewski, K. *Prog. Polym. Sci.* **2005**, *30*, 858–875.

[2] Barner, L.; Davis, T. P.; Stenzel, M. H.; Barner-Kowollik, C. *Macromol. Rapid Commun.* **2007**, *28*, 539–559.

[3] Opsteen, J. A.; van Hest, J. C. M. *Chem. Commun.* **2005**, 57–59.

[4] Dirks, A. J. T.; van Berkel, S. S.; Hatzakis, N. S.; Opsteen, J. A.; van Delft, F. L.; Cornelissen, J.; Rowan, A. E.; van Hest, J. C. M.; Rutjes, F.; Nolte, R. J. M. *Chem. Commun.* **2005**, 4172–4174.

[5] O'Reilly, R. K.; Joralemon, M. J.; Hawker, C. J.; Wooley, K. L. *J. Polym. Sci., Part A: Polym. Chem.* **2006**, *44*, 5203–5217.

[6] Quémener, D.; Davis, T. P.; Barner-Kowollik, C.; Stenzel, M. H. *Chem. Commun.* **2006**, 5051–5053.

[7] Burchard, W. *Branched Polym. II* **1999**, *143*, 113–194.

[8] Hadjichristidis, N.; Pispas, S.; Pitsikalis, M.; Iatrou, H.; Vlahos, C. *Branched Polym. I* **1999**, *142*, 71–127.

[9] Hawker, C. J.; Bosman, A. W.; Harth, E. *Chem. Rev.* **2001**, *101*, 3661–3688.

[10] Angot, S.; Murthy, K. S.; Taton, D.; Gnanou, Y. *Macromolecules* **1998**, *31*, 7218–7225.

[11] Ueda, J.; Matsuyama, M.; Kamigaito, M.; Sawamoto, M. *Macromolecules* **1998**, *31*, 557–562.

[12] Stenzel-Rosenbaum, M.; Davis, T. P.; Chen, V.; Fane, A. G. *J. Polym. Sci., Part A: Polym. Chem.* **2001**, *39*, 2777–2783.

[13] Matyjaszewski, K. *Polym. Int.* **2003**, *52*, 1559–1565.

[14] Mayadunne, R. T. A.; Jeffery, J.; Moad, G.; Rizzardo, E. *Macromolecules* **2003**, *36*, 1505–1513.

[15] Xia, J. H.; Zhang, X.; Matyjaszewski, K. *Macromolecules* **1999**, *32*, 4482–4484.

[16] Barner-Kowollik, C.; Davis, T. P.; Heuts, J. P. A.; Stenzel, M. H.; Vana, P.; Whittaker, M. *J. Polym. Sci., Part A: Polym. Chem.* **2003**, *41*, 365–375.

[17] Lord, H. T.; Quinn, J. F.; Angus, S. D.; Whittaker, M. R.; Stenzel, M. H.; Davis, T. P. *J. Mater. Chem.* **2003**, *13*, 2819–2824.

[18] Barner-Kowollik, C.; Davis, T. P.; Stenzel, M. H. *Aust. J. Chem.* **2006**, *59*, 719–727.

[19] Rostovtsev, V. V.; Green, L. G.; Fokin, V. V.; Sharpless, K. B. *Angew. Chem. Int. Ed.* **2002**, *41*, 2596–2599.

[20] Tornoe, C. W.; Christensen, C.; Meldal, M. *J. Org. Chem.* **2002**, *67*, 3057–3064.

[21] Altintas, O.; Yankul, B.; Hizal, G.; Tunca, U. *J. Polym. Sci., Part A: Polym. Chem.* **2006**, *44*, 6458–6465.

[22] Gao, H. F.; Matyjaszewski, K. *Macromolecules* **2006**, *39*, 4960–4965.

[23] Hoogenboom, R.; Moore, B. C.; Schubert, U. S. *Chem. Commun.* **2006**, 4010–4012.

[24] Deng, G. H.; Ma, D. Y.; Xu, Z. Z. *Eur. Polym. J.* **2007**, *43*, 1179–1187.

[25] Gao, H. F.; Min, K.; Matyjaszewski, K. *Macromol. Chem. Phys.* **2007**, *208*, 1370–1378.

[26] Zhu, J.; Zhu, X. L.; Kang, E. T.; Neoh, K. G. *Polymer* **2007**, *48*, 6992–6999.

[27] Evans, R. A. *Aust. J. Chem.* **2007**, *60*, 384–395.

[28] Binder, W. H.; Sachsenhofer, R. *Macromol. Rapid Commun.* **2007**, *28*, 15–54.

[29] Fournier, D.; Hoogenboom, R.; Schubert, U. S. *Chem. Soc. Rev.* **2007**, *36*, 1369–1380.

[30] Kolb, H. C.; Finn, M. G.; Sharpless, K. B. *Angew. Chem. Int. Ed.* **2001**, *40*, 2004–2021.

[31] Durmaz, H.; Colakoclu, B.; Tunca, U.; Hizal, G. *J. Polym. Sci., Part A: Polym. Chem.* **2006**, *44*, 1667–1675.

[32] Durmaz, H.; Dag, A.; Altintas, O.; Erdogan, T.; Hizal, G.; Tunca, U. *Macromolecules* **2007**, *40*, 191–198.

[33] Gacal, B.; Durmaz, H.; Tasdelen, M. A.; Hizal, G.; Tunca, U.; Yagci, Y.; Demirel, A. L. *Macromolecules* **2006**, *39*, 5330–5336.

[34] Dag, A.; Durmaz, H.; Hizal, G.; Tunca, U. *J. Polym. Sci., Part A: Polym. Chem.* **2008**, *46*, 302–313.

[35] Quémener, D.; Le Hellaye, M.; Bissett, C.; Davis, T. P.; Barner-Kowollik, C.; Stenzel, M. H. *J. Polym. Sci., Part A: Polym. Chem.* **2008**, *46*, 155–173.

[36] Ting, S. R. S.; Granville, A. M.; Quémener, D.; Davis, T. P.; Stenzel, M. H.; Barner-Kowollik, C. *Aust. J. Chem.* **2007**, *60*, 405–409.

[37] Heuzé, B.; Gasparova, R.; Heras, M.; Masson, S. *Tetrahedron Lett.* **2000**, *41*, 7327–7331.

[38] Bastin, R.; Albadri, H.; Gaumont, A. C.; Gulea, M. *Org. Lett.* **2006**, *8*, 1033–1036.

[39] Krishnaveni, N. S.; Surendra, K.; Nageswar, Y. V. D.; Rao, K. R. *Synthesis* **2003**, 2295–2297.

[40] Yadav, J. S.; Reddy, B. V. S.; Raghavendra, S.; Satyanarayana, M. *Tetrahedron Lett.* **2002**, *43*, 4679–4681.

[41] Sinnwell, S.; Synatschke, C. V.; Junkers, T.; Stenzel, M. H.; Barner-Kowollik, C. *Macromolecules* **2008**, *41*, 7904–7912.

6

Orthogonality of RAFT-HDA Chemistry to the CuAAC

6.1 Introduction

Since the early reports in polymer science, published in 2004,[1–3] the concept of *click* chemistry has seen a great increase in its use and has become a well-established tool for the tailor-made synthesis of well-defined materials.[4–10] The characteristics of *click* reactions such as high efficiency and tolerance against a variety of functional groups and reaction conditions match perfectly with the requirements of the preparation of well-defined, multifunctional polymer architectures. In particular, the CuAAC has been proven as an ideal candidate to fulfill the *click* criteria[11] and was therefore the reaction of choice in the vast majority of *click* papers. However, Diels-Alder cycloadditions,[12, 13] nucleophilic substitution chemistry of stained rings[14] and additions to carbon-carbon multiple bonds (thiol-ene reaction)[15, 16] have also been shown as efficient orthogonal synthetic strategies and have been used alternatively to or in combination with CuAAC chemistry.

The use of RAFT as a controlled radical polymerization technique in combination with orthogonal coupling reactions has been employed for the preparation of a wide variety of well-defined architectures.[17] However, different functionalities are required for the controlled polymerization and for the post polymerization coupling

reaction which was usually achieved by the use of alkyne and azide functionalized RAFT agents.[18–20] The preceding chapters described the combination of RAFT polymerization and hetero Diels-Alder (HDA) chemistry as a versatile method for the synthesis of complex polymer architectures such as block copolymers and star-shaped polymers. In the present chapter, the RAFT HDA concept is combined with CuAAC chemistry as two consecutive coupling reactions. Through the use of an α-diene-ω-alkyne functionalized PCL, PS-*b*-PCL stars have been synthesized by either forming the PS-*b*-PCL arms first with the HDA cycloaddition and their subsequent coupling to a triazide coupling agent through the CuAAC (*arm-first*) or by forming the basic star structure first through the CuAAC of the coupling agent and the PCL, with the diblock stars achieved by the subsequent HDA cycloaddition with the PS (*core-first*). Both synthetic pathways are illustrated in Figure 6.1.

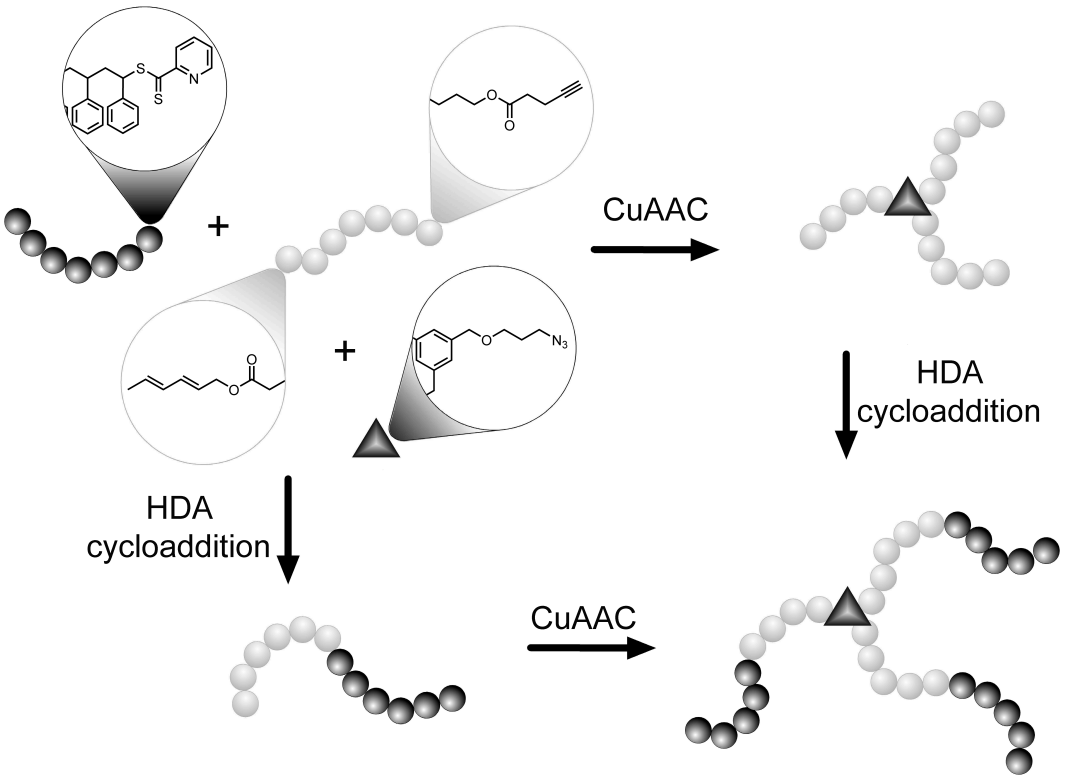

Figure 6.1 Combining the CuAAC and HDA cycloaddition in the synthesis of star-shaped block copolymers.

6.2 Experimental Section

The synthesis of PCL **1** is described in Chapter 3.

Synthesis of PCL 2

PCL **1** (4.0 g, 1.5 mmol), 4-pentynoic acid (0.44 g, 4.5 mmol) and DMAP (37 mg, 0.30 mmol) were dissolved in 30 mL dichloromethane. This solution was kept at 0 °C and DCC (0.93 g, 4.5 mmol) in 10 mL dichloromethane was added drop-wise. After complete addition, the mixture was allowed to warm up to room temperature and stirred for 18 hours. The generated urea was removed via filtration and PCL **2** was isolated by precipitation into cold methanol. ^{1}H NMR (300 MHz, $CDCl_3$, 25 °C): δ = 6.20 (dd, $^3J_{HH}$ = 15 Hz, $^3J_{HH}$ = 10 Hz, $CH_3(CH)_2C\mathbf{H}$-), 6.00 (ddq, $^3J_{HH}$ = 15 Hz, $^3J_{HH}$ = 10 Hz, $^4J_{HH}$ = 1 Hz, $CH_3CHC\mathbf{H}$-), 5.70 (dq, $^3J_{HH}$ = 15 Hz, $^3J_{HH}$ = 7 Hz, $CH_3C\mathbf{H}$-), 5.57 (dt, $^3J_{HH}$ = 15 Hz, $^3J_{HH}$ = 7 Hz, $CH_3(CH)_3C\mathbf{H}$-), 4.52 (d, $^3J_{HH}$ = 7 Hz, -CHC$\mathbf{H_2}$O-), 4.01 (t, $^3J_{HH}$ = 7 Hz, -$CH_2C\mathbf{H_2}$O-), 2.53-2.42 (m, -C$\mathbf{H_2}$C$\mathbf{H_2}$CCH), 2.26 (t, $^3J_{HH}$ = 8 Hz, -O(CO)C$\mathbf{H_2}$-), 1.94 (t, $^3J_{HH}$ = 2 Hz, -CH_2CC$\mathbf{H}$), 1.71 (d, $^3J_{HH}$ = 6 Hz, C$\mathbf{H_3}$CH-), 1.68-1.52 (m, -O(CO)CH_2C$\mathbf{H_2}$$CH_2C\mathbf{H_2}$$CH_2$), 1.39-1.29 (m, -O(CO)$CH_2CH_2C\mathbf{H_2}$$CH_2CH_2$) ppm. $M_{n,\,SEC}$ = 2580 g·mol^{-1}, PDI_{SEC} = 1.36, $M_{n,\,NMR}$ = 2680 g·mol^{-1}. End-group functionality$_{diene}$ = 98 %, end-group functionality$_{alkyne}$ = 100 %,

Synthesis of 1,3,5-tris((3-azidopropoxy)methyl)benzene 4

1,3,5-Tris(bromomethyl)benzene (3.0 g, 8.4 mmol) and sodium hydride (60 % suspension in oil, 1.1 g, 28 mmol or 1.1 equiv. of bromine groups) were placed in a Schlenk flask. Under a nitrogen atmosphere, THF (dry, 60 mL) was added at room temperature. At 0 °C a solution of 3-azido-1-propanol (2.8 g, 28 mmol or 1.1 equiv. of bromine groups) in 5 mL THF was added drop-wise. After complete addition, the mixture was allowed to warm to room temperature and was stirred for a further 8 hours. Aqueous ammonium chloride solution (30 mL, 1 M) was then added in order to destroy residual sodium hydride, which was followed by a three-fold extraction with 30 mL of diethyl ether. After removal of the solvent under vacuum, the product was isolated via column chromatography. Yield: 2.1 g (60 %). R_f = 0.29 (silica/*n*-hexane/ethyl acetate = 5:1). ^{1}H NMR (300 MHz, $CDCl_3$, 25 °C): δ = 7.22 (s, arom.), 4.49 (s, Ph(C$\mathbf{H_2}$O-)$_3$), 3.56 (t, $^3J_{HH}$ = 6 Hz, (-OC$\mathbf{H_2}$-)$_3$), 3.41 (t, $^3J_{HH}$ = 6.6 Hz, (-C$\mathbf{H_2}N_3$)$_3$), 1.88 (tt, $^3J_{HH}$ = 6.3 Hz, $^3J_{HH}$ = 6.3 Hz, (-CH_2C$\mathbf{H_2}$$CH_2$-)$_3$) ppm.

Synthesis of PS-b-PCL 5 via Hetero Diels-Alder Cycloaddition

PCL **2** (0.50 g, 0.19 mmol) and PS **3** (0.58 g, 0.19 mmol) were dissolved in 1 mL chloroform. After the addition of 0.28 mmol TFA (0.28 mL of a 1 M solution in chloroform) the solution was stirred at 50 °C for 18 hours. PS-*b*-PCL **5** was isolated by precipitation into cold methanol. ^{1}H NMR (300 MHz, $CDCl_3$, 25 °C): δ = 7.3-6.2 (m, arom.), 5.8-5.5 (m, vinyl.), 4.01 (t, $^3J_{HH}$ = 7 Hz, -$CH_2C\mathbf{H_2}O$-), 2.53-2.42 (m, -$C\mathbf{H_2}C\mathbf{H_2}$CCH), 2.26 (t, $^3J_{HH}$ = 8 Hz, -O(CO)C$\mathbf{H_2}$-), 2.2-1.1 (m, aliph.) ppm. $M_{n,\,SEC}$ = 2580 g·mol^{-1}, PDI_{SEC} = 1.36, $M_{n,\,NMR}$ = 2680 g·mol^{-1}.

Synthesis of 3-Arm PCL 6 via CuAAC

PCL **2** (0.50 g, 0.19 mmol), cupric sulfate pentahydrate (4.7 mg, 0.019 mmol), (+)-sodium L ascorbate (19 mg, 0.095 mmol) and coupling agent **4** (26 mg, 0.062 mmol) were dissolved in 1 mL *N*,*N*-dimethylformamide (DMF). The mixture was stirred at 50 °C for 18 hours. After complete reaction, the mixture was passed through a small column of basic alumina in order to remove the copper catalyst. The 3-arm PCL **6** was isolated by precipitation of the filtrate into cold methanol. ^{1}H NMR (300 MHz, $CDCl_3$, 25 °C): δ = 7.32 (s, triazole), 7.22 (s, arom.), 6.23 (dd, $^3J_{HH}$ = 15 Hz, $^3J_{HH}$ = 10 Hz, $CH_3(CH)_2C\mathbf{H}$-), 6.03 (ddq, $^3J_{HH}$ = 15 Hz, $^3J_{HH}$ = 10 Hz, $^4J_{HH}$ = 1 Hz, $CH_3CHC\mathbf{H}$-), 5.74 (dq, $^3J_{HH}$ = 15 Hz, $^3J_{HH}$ = 7 Hz, $CH_3C\mathbf{H}$-), 5.60 (dt, $^3J_{HH}$ = 15 Hz, $^3J_{HH}$ = 7 Hz, $CH_3(CH)_3C\mathbf{H}$-), 4.55 (d, $^3J_{HH}$ = 7 Hz, -CHC$\mathbf{H_2}$O-), 4.49 (s, PhC$\mathbf{H_2}$O-), 4.43 (t, $^3J_{HH}$ = 6 Hz, -triazole-C$\mathbf{H_2}CH_2CH_2O$-), 4.04 (t, $^3J_{HH}$ = 7 Hz, -$CH_2C\mathbf{H_2}$O(CO)-), 3.47 (t, $^3J_{HH}$ = 6 Hz, -triazole-$CH_2CH_2C\mathbf{H_2}$O-), 3.00 (t, $^3J_{HH}$ = 7 Hz, -O(CO)$CH_2C\mathbf{H_2}$-triazole-), 2.69 (t, $^3J_{HH}$ = 7 Hz, -O(CO)C$\mathbf{H_2}CH_2$-triazole-), 2.29 (t, $^3J_{HH}$ = 8 Hz, -O(CO)C$\mathbf{H_2}$-CH_2CH_2), 2.21-2.12 (m, -triazole-CH2C$\mathbf{H_2}CH_2$O-), 1.75 (d, $^3J_{HH}$ = 6 Hz, C$\mathbf{H_3}$CH-), 1.68-1.52 (m, -O(CO)$CH_2C\mathbf{H_2}CH_2C\mathbf{H_2}CH_2$), 1.39-1.29 (m, -O(CO)$CH_2CH_2C\mathbf{H_2}CH_2CH_2$-) ppm.

Synthesis of 3-Arm PS-b-PCL 7a via CuAAC

The synthesis of 3-arm PS-*b*-PCL **7a** was performed in a similar manner to that of the 3-arm PCL **6** except PS-*b*-PCL **5** was used as the alkyne carrying polymer.

Synthesis of 3-Arm PS-b-PCL 7b via Hetero Diels-Alder Cycloaddition

The synthesis of 3-arm PS-*b*-PCL **7b** was performed in a similar manner to that of the PS-*b*-PCL **5** except 3-arm PCL **6** was used as the diene carrying polymer and 2.5 equiv. of TFA was added.

6.3 Results and Discussion

The strategy for the synthesis of 3-arm star PS-*b*-PCL by a combination of CuAAC and HDA cycloadditions involves the preparation of an α-diene-ω-alkyne functionalized PCL, a RAFT PS equipped with an electron-deficient dithioester end-group and a triazide coupling agent as the corresponding building blocks. The diene terminated PCL **1** was obtained after ring-opening polymerization of ϵ-caprolactone using *trans*,*trans*-2,4-hexadien-1-ol as the initiator (cf. Chapter 3). The alkyne function was introduced by esterification of the terminal hydroxy group of PCL **1** with 4-pentynoic acid (Figure 6.2). The ^{1}H NMR spectrum of the obtained PCL **2** shows the presence of both the polymer backbone, the vinylic protons and the pentynoic acid ester (Figure 6.3). A comparison of the signal integrals of the protons of both end-groups reveals the quantitative functionalization of the polyester at both sites. SEC measurements indicate that the number average molar mass, M_n, increases slightly during the end-group modification which is consistent with the M_n values determined via ^{1}H NMR (Table 6.1).

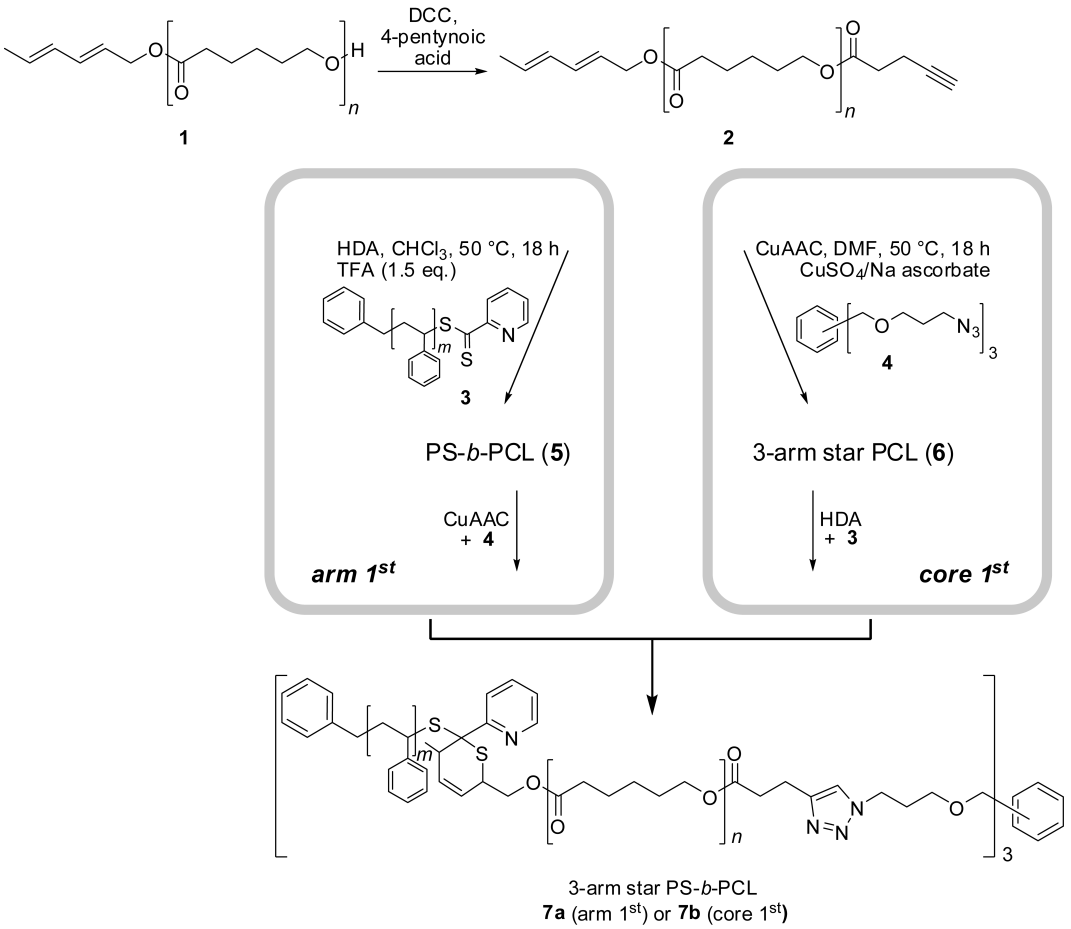

Figure 6.2 The *arm first* and *core first* approach to star block copolymer synthesis used in this investigation.

Table 6.1 Characterization of the polymeric building blocks.

Polymer	$M_{n,\,SEC}$[a] / g·mol^{-1}	PDI_{SEC}[a]	$M_{n,\,NMR}$[b] / g·mol^{-1}
PCL **1**	2400[c]	1.39[c]	2660
PCL **2**	2580[c]	1.36[c]	2680
PS **3**	2900	1.14	3070

[a]Measured by SEC in THF (calibration with linear PS standards); [b]Determined by ^{1}H NMR spectroscopy; [c]Values for PCL are corrected by applying the Mark-Houwink relationship (K = 13.95 × 10^{-5} dL·g^{-1}, α = 0.786).[21]

The RAFT polymerization of styrene was carried out in the presence of BPDF as the controlling agent. BPDF was chosen as the RAFT agent due to the good control it offers for the polymerization and for its high HDA activity. Due to the gradual decrease in the number of polymer chains bearing the RAFT end group with increasing monomer conversions in RAFT polymerizations, the polymerization was stopped at low monomer conversion to ensure a high dithioester end-group concentration. PS **3** was obtained with $M_{n,\,SEC}$ = 2900 g·mol^{-1} and *PDI* of 1.14 (Table 6.1) which is consistent with the molar mass obtained after ^{1}H NMR measurements ($M_{n,\,NMR}$ = 3070 g·mol^{-1}). For all subsequent calculations, the NMR derived molar masses were employed. The tri-functional coupling agent **4** was obtained by etherification of 1,3,5-tris(bromomethyl)benzene with 3-azido-1-propanol.

6.3.1 The Arm-First Approach

For the *arm-first* approach, PCL **2** and PS **3** were combined via a HDA cycloaddition resulting in PS-*b*-PCL **5** which was subsequently attached to the coupling agent **4** in a CuAAC. The conditions for the HDA cycloaddition between **2** and **3** are similar to those described in the preceding chapters [TFA (1.5 equiv.), chloroform solution, 18 hours]. To activate the dienophilicity of the pyridinyl dithioester, TFA is used as the catalyst in order to protonate the pyridine nitrogen atom which lowers the electron density of the aromatic ring and hence its electron withdrawing character. Due to the basic character of the pyridinyldithioester in **3**, the system was not observed to undergo any side reactions by the addition of TFA (e.g. acidic hydrolysis). Figure 6.4 shows the molar mass distributions (from SEC measurements) of the building blocks **2** and **3** as well as that of the coupling product **5**. The obtained peak of **5** is in good agreement with the theoretical value ($M_{n,theo}$ = 2680 + 3070 g·mol^{-1} = 5750 g·mol^{-1}) which is indicated in the graph as a dashed line, showing the successful formation of the block copolymer **5**. Due to the number of possible isomers of the 3,6-dihydro-2*H*-thiopyran ring which is formed in the HDA cycloaddition, the ^{1}H NMR spectrum

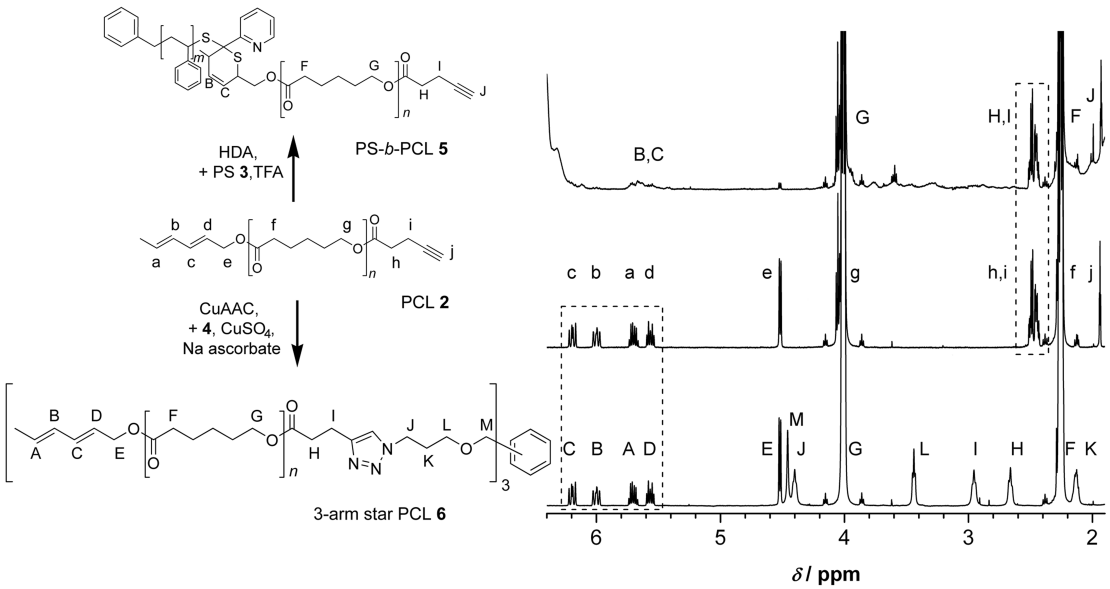

Figure 6.3 ^{1}H NMR spectra ($CDCl_3$) of PCL **2** prior to (middle), after the CuAAC (DMF, $CuSO_4$/Na ascorbate, 50 °C, 18 h) with the triazide coupling agent **4** (bottom) and after the HDA cycloaddition [$CHCl_3$, TFA (1.5 equiv.), 50 °C, 18 h] with PS **3** (top).

of the actual polymer linkage in **5** is complex. However, the signals of two of the four vinylic protons (four multiplets between 6.3 and 5.5 ppm) as well as those of the methylene group in the allyl position (doublet at 4.57 ppm) in PCL **2** disappear after the HDA reaction (Figure 6.3). According to the integral of the remaining signal of the allylester protons, 94 % of the diene end-groups in **2** have been converted. The signals of the alkyne moiety (two multiplets between 2.57-2.46 ppm) remain intact after the HDA reaction, confirming the high resistance of the alkyne function against the applied conditions.

The CuAAC of PS-*b*-PCL **5** and coupling agent **4** was performed in DMF with cupric sulfate/sodium ascorbate as the catalyst at 50 °C for 18 hours. The SEC measurement of the obtained reaction product is shown in Figure 6.4. The obtained peak corresponds to the dashed line representing the calculated molar mass [$M_{n,theo}$ = (3 × 5750 + 417) g·mol^{-1} = 17 667 g·mol^{-1}] of **7a**. The occurrence of a small tail in the lower molar mass range can be explained by residual linear chains of **2**, **3** and **5**. In the ^{1}H NMR spectrum of the reaction product, the signals of the 4-pentynoic acid ester (two multiplets between 2.57-2.46 ppm) shifted completely down field (two triplets at 3.0 and 2.7 ppm) indicating the full conversion of the alkyne moiety. A shift of the signal of the azidomethylene group in **4** from 3.4 ppm to 4.45 ppm as well as the appearance of a singlet at 7.35 ppm confirm the successful triazole formation.

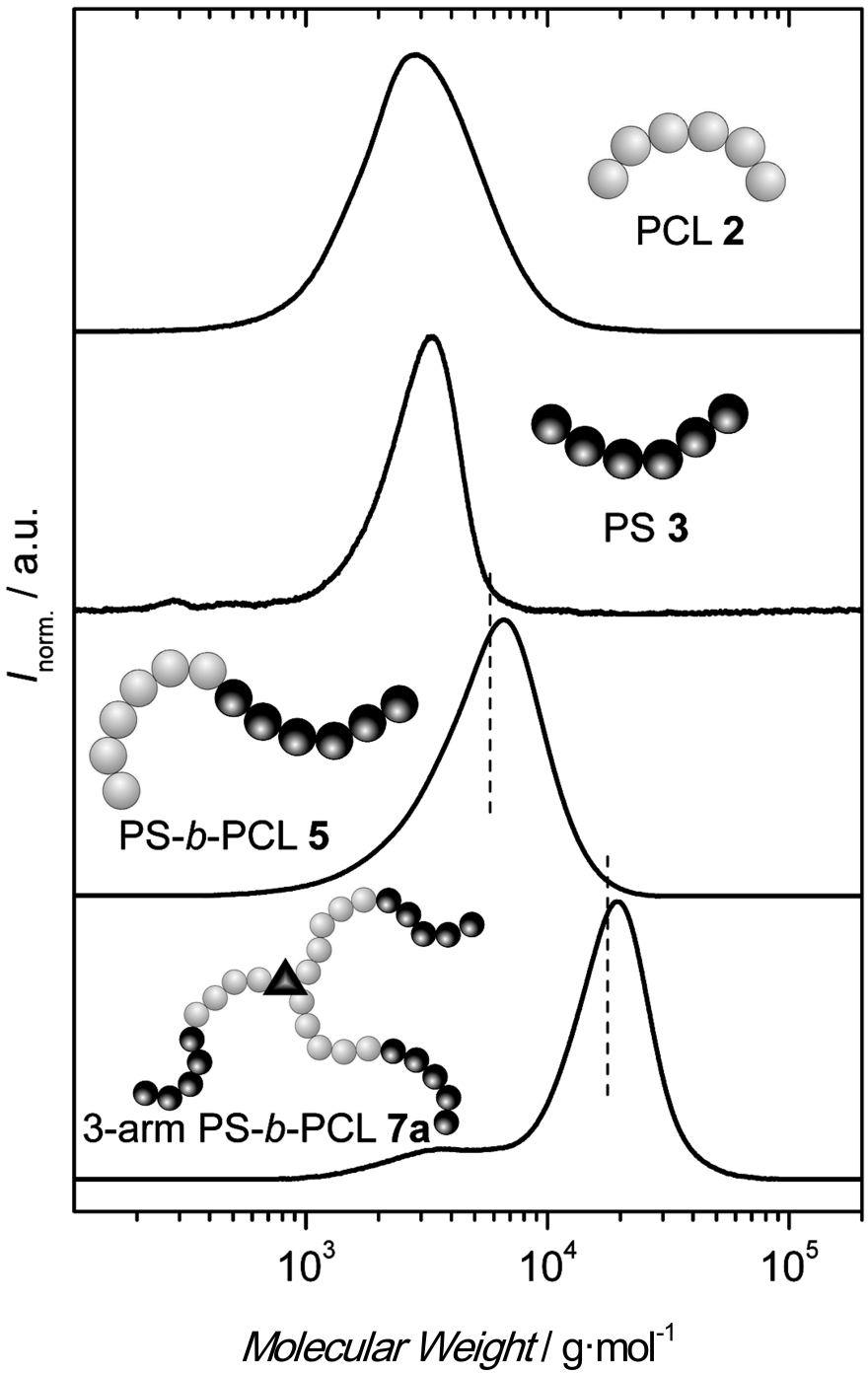

Figure 6.4 Development of the molecular weight distributions (according to SEC in THF) for the *arm-first* approach of PCL **2**, PS **3**, PS-*b*-PCL **5** and three-arm star PS-*b*-PCL **7a** (from top to bottom). The dashed lines represent the theoretical M_n, the values of which were calculated from the sum of the corresponding building blocks.

6.3.2 The Core-First Approach

For the *core-first* approach, three chains of PCL **2** were attached onto the triazide coupling agent **4** in a CuAAC and the obtained 3-arm star PCL **6** (which carries three diene end-groups) was further converted with PS **3** in a HDA cycloaddition (Figure 6.2). The resulting 3-arm star PS-*b*-PCL is identical in structure to **7a** but will be referred to in the following as **7b** due to the different synthetic method by which it was obtained. The CuAAC of PCL **2** and coupling agent **4** was performed in a similar fashion to the one described in the *arm-first* method. The resulting SEC measurement of the obtained reaction product is shown in Figure 6.5. The obtained peak is in good agreement with the theoretical value [$M_{n,theo}$ = (3 × 2680 + 417) g·mol^{-1} = 8457 g·mol^{-1}] which is indicated in the graph as a dashed line, showing the successful formation of the 3-arm star polymer **6**. In the ^{1}H NMR spectrum of the reaction product, the signals of the 4-pentynoic acid ester (two multiplets between 2.57-2.46 ppm) shifted completely down field (two triplets at 3.0 and 2.7 ppm), indicating the full conversion of the alkyne moiety (Figure 6.3). A shift of the signal of the azidomethylene group in **4** from 3.4 ppm to 4.45 ppm as well as the appearance of a singlet at 7.35 ppm, the integrals of which match exactly with those of the other PCL end-groups, confirm the successful triazole formation. The signals of the diene moiety (four multiplets between 6.3 and 5.5 ppm) as well as those of the methylene group in the allyl position (doublet at 4.57 ppm) remain intact after the CuAAC, thus confirming their resistance against the applied conditions.

The HDA cycloaddition between **6** and **3** was performed with an increased TFA concentration (2.5 equiv.) as in the experiments involved in the *arm-first* approach. In previous attempts using 1.5 equiv., only low conversions of the diene were achieved which resulted in a bimodal molar mass distribution with a high amount of residual starting material. It is suspected that due to the basic character of the triazole ring in **6**, its presence causes a decreased degree of protonated pyridinyldithioester and hence reducing its reactivity. By increasing the TFA concentration to 2.5 equiv., the reactivity of the dithioester in **3** could be improved.

Figure 6.5 shows the molar mass distributions (according to SEC measurements) of **6**, the building block **3** and the coupling product **7b**. The obtained peak of **7b** is in good agreement with the theoretical value [$M_{n,theo}$ = (8457 + 3 × 3070) g·mol^{-1} = 17 667 g·mol^{-1}] which is indicated in the graph as a dashed line, showing the successful formation of the 3-arm star block copolymer **7b**. A tailing in the lower molar mass region is slightly stronger than observed in the SEC trace of **7a**. Although the ^{1}H NMR spectrum of **7b** shows the disappearance of two of the four vinylic protons as well as of the methylene group in the allyl position of PCL **6**, the calculated conversion of the diene end-group is close to 81 %. Both the tailing in the SEC trace of **7b** and the

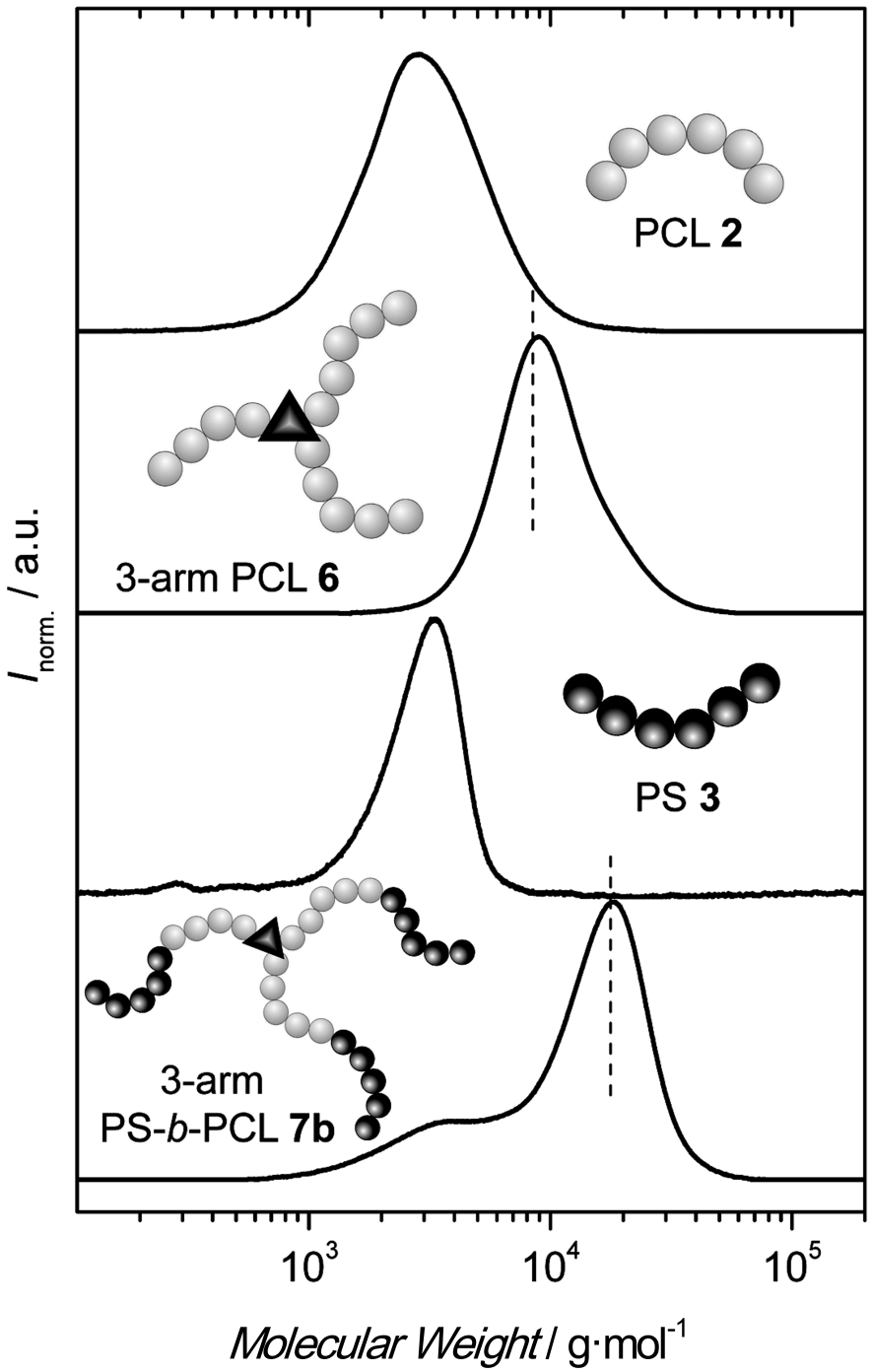

Figure 6.5 Development of the molecular weight distributions (according to SEC in THF) for the *arm-first* approach of PCL **2**, three-arm star PCL **6**, PS **3**,and three-arm star PS-*b*-PCL **7b** (from top to bottom). The dashed lines represent the theoretical M_n, the values of which were calculated from the sum of the corresponding building blocks.

reduced diene conversion observed in the *core-first* approach may be attributed to the above mentioned competition in basicity between the formed triazole ring and the pyridine moiety for the acidic catalyst.

Although not performing quite as well as the *arm-first* approach, the *core-first* approach as an additional synthetic strategy still adequately serves to exemplify the great flexibility in which tri-arm diblock star polymers may be constructed through RAFT polymerization and efficient conjugation chemistries.

6.4 Conclusion

The present chapter offers, for the first time, a direct combination of the RAFT-HDA cycloaddition with the CuAAC. Importantly, it was shown that the procedure for performing the former is comparable to, if not simpler than the CuAAC. The synthesis of 3-arm PS-*b*-PCL by a consecutive combination of the CuAAC and HDA cycloaddition was successfully accomplished via an *arm-first* and *core-first* approach. Due to the chemoselectivity of both cycloaddition reactions, it was possible to control both reaction sites. Both the *arm-first* and *core-first* approaches led to the desired product, however, due to its basic character, the presence of the triazole ring in 3-arm PCL **6** is suspected to reduce the reactivity of the pyridinyl dithioester in PS **3**. It has been shown that HDA cycloaddition and CuAAC can be successfully used in a cooperative fashion, thus establishing the combination of RAFT chemistry and efficient orthogonal coupling strategies as one of the foremost architectural tools in polymer science today.

References

[1] Wu, P.; Feldman, A. K.; Nugent, A. K.; Hawker, C. J.; Scheel, A.; Voit, B.; Pyun, J.; Frechet, J. M. J.; Sharpless, K. B.; Fokin, V. V. *Angew. Chem. Int. Ed.* **2004**, *43*, 3928–3932.

[2] Helms, B.; Mynar, J. L.; Hawker, C. J.; Frechet, J. M. J. *J. Am. Chem. Soc.* **2004**, *126*, 15020–15021.

[3] Diaz, D. D.; Punna, S.; Holzer, P.; McPherson, A. K.; Sharpless, K. B.; Fokin, V. V.; Finn, M. G. *J. Polym. Sci., Part A: Polym. Chem.* **2004**, *42*, 4392–4403.

[4] Hawker, C. J.; Wooley, K. L. *Science* **2005**, *309*, 1200–1205.

[5] Lutz, J. F.; Borner, H. G.; Weichenhan, K. *Macromol. Rapid Commun.* **2005**, *26*, 514–518.

[6] Fournier, D.; Hoogenboom, R.; Schubert, U. S. *Chem. Soc. Rev.* **2007**, *36*, 1369–1380.

[7] Binder, W. H.; Sachsenhofer, R. *Macromol. Rapid Commun.* **2007**, *28*, 15–54.

[8] Golas, P. L.; Matyjaszewski, K. *QSAR Comb. Sci.* **2007**, *26*, 1116–1134.

[9] Evans, R. A. *Aust. J. Chem.* **2007**, *60*, 384–395.

[10] Lutz, J. F. *Angew. Chem. Int. Ed.* **2007**, *46*, 1018–1025.

[11] Kolb, H. C.; Finn, M. G.; Sharpless, K. B. *Angew. Chem. Int. Ed.* **2001**, *40*, 2004–2021.

[12] Gacal, B.; Durmaz, H.; Tasdelen, M. A.; Hizal, G.; Tunca, U.; Yagci, Y.; Demirel, A. L. *Macromolecules* **2006**, *39*, 5330–5336.

[13] Dag, A.; Durmaz, H.; Hizal, G.; Tunca, U. *J. Polym. Sci., Part A: Polym. Chem.* **2008**, *46*, 302–313.

[14] Tsarevsky, N. V.; Bencherif, S. A.; Matyjaszewski, K. *Macromolecules* **2007**, *40*, 4439–4445.

[15] Killops, K. L.; Campos, L. M.; Hawker, C. J. *J. Am. Chem. Soc.* **2008**, *130*, 5062–5064.

[16] Gress, A.; Völkel, A.; Schlaad, H. *Macromolecules* **2007**, *40*, 7928–7933.

[17] Barner, L.; Davis, T. P.; Stenzel, M. H.; Barner-Kowollik, C. *Macromol. Rapid Commun.* **2007**, *28*, 539–559.

[18] Quémener, D.; Davis, T. P.; Barner-Kowollik, C.; Stenzel, M. H. *Chem. Commun.* **2006**, 5051–5053.

[19] Ting, S. R. S.; Granville, A. M.; Quemener, D.; Davis, T. P.; Stenzel, M. H.; Barner-Kowollik, C. *Aust. J. Chem.* **2007**, *60*, 405–409.

[20] Ranjan, R.; Brittain, W. J. *Macromol. Rapid Commun.* **2007**, *28*, 2084–2089.

[21] Schindler, A.; Hibionada, Y. M.; Pitt, C. G. *J. Polym. Sci., Part A: Polym. Chem.* **1982**, *20*, 319–326.

7

Ultra-fast Click Conjugation of Macromolecular Building Blocks at Ambient Temperature

7.1 Introduction

The combination of highly efficient orthogonal conjugation chemistries with CRP has increasingly been proven to be a convenient tool in the synthesis of novel polymeric materials.[1] For example, techniques such as ATRP and RAFT polymerization have successfully been combined with *click* chemistry to achieve a wide variety of structures ranging from complex architectures (e.g. blocks,[2–4] stars[5–7] and combs[8, 9]) through to conjugates of synthetic polymers and biologically important molecules such as peptides/proteins,[10–12] sugars[13, 14] and even viruses.[15] The continued development of such techniques is ultimately geared towards faster, more efficient reactions that may be performed under ambient conditions and utilizing benign or, indeed, no catalysts.

Within the realm of polymer chemistry, the CuAAC has been the most widely utilized *click* reaction, due to its high selectivity and efficiency under relatively mild

reaction conditions. One of the major limiting factors of the CuAAC is the requirement of a toxic copper catalyst. This can have a profound influence on its compatibility with many systems that are sensitive to heavy metals, particularly in biological applications.[16] Although there are examples of 'copper free' azide-alkyne cycloadditions,[17, 18] they have not obtained the overall popularity of the CuAAC.

In an attempt to address some of the issues surrounding the applicability of *click* chemistry, a number of alternative strategies have been proposed. For instance, the Diels-Alder cycloaddition between anthracene and maleimide derivatives has proven to produce excellent results in the formation of complex architectures in a modular approach.[4, 7] However, a severe drawback to this technique is the requirement of temperatures in excess of 110 °C and long reaction times (36 - 120 hours). Thus, this technique would not be appropriate for use in conjugation reactions involving proteins and nucleic acids, which can readily denature under such conditions.

With regard to the rate of the CuAAC, the vast majority of publications report reaction times of several hours at temperatures ranging from ambient to 50 °C. However, in the synthesis of star polymers via a *click* coupling method, Gao and Matyjaszewski report a 97 % conversion of all azide moieties into the 1,2,3-triazole groups within 3 hours at room temperature (using 1:1 stoichiometry).[5] Moreover, Du Prez and co-workers report the completion of a *click* reaction between azide functionalized poly(isobornyl acrylate) and 2 equiv. of alkyne functionalized poly(1-ethoxyethyl acrylate) in just 5 minutes under ambient conditions.[9] It is therefore apparent that the rate of the CuAAC can be influenced by using an excess of one of the reactants; however this approach is undesirable in the majority of cases as further purification strategies are necessary. Furthermore, there is a growing attraction in the polymer community to thiol-ene chemistry which, under certain conditions, can be completed between 5 minutes and 2 hours.[19, 20]

The preceding chapters have conceptualized and developed several examples of the use of the highly atom-economical RAFT-HDA concept in the efficient construction of block copolymers (Chapter 4), stars (Chapter 5) and has further been appropriated for the surface functionalization of polymeric microspheres.[21] In these examples, polymers prepared by RAFT polymerization in the presence of electron-deficient dithioesters have been conjugated to materials bearing a suitable diene through a HDA cycloaddition. Thus far, the reactions used have been performed at 50 °C, have taken between 2 and 24 hours to achieve completion and have made use of *trans*, *trans*-2,4-hexadien-1-ol as the diene. Herein, it will be demonstrated that a dramatic reaction rate improvement of the RAFT-HDA *click* reaction can be achieved through the use of novel cyclopentadienyl (Cp) functionalized polymers (Figure 7.1).

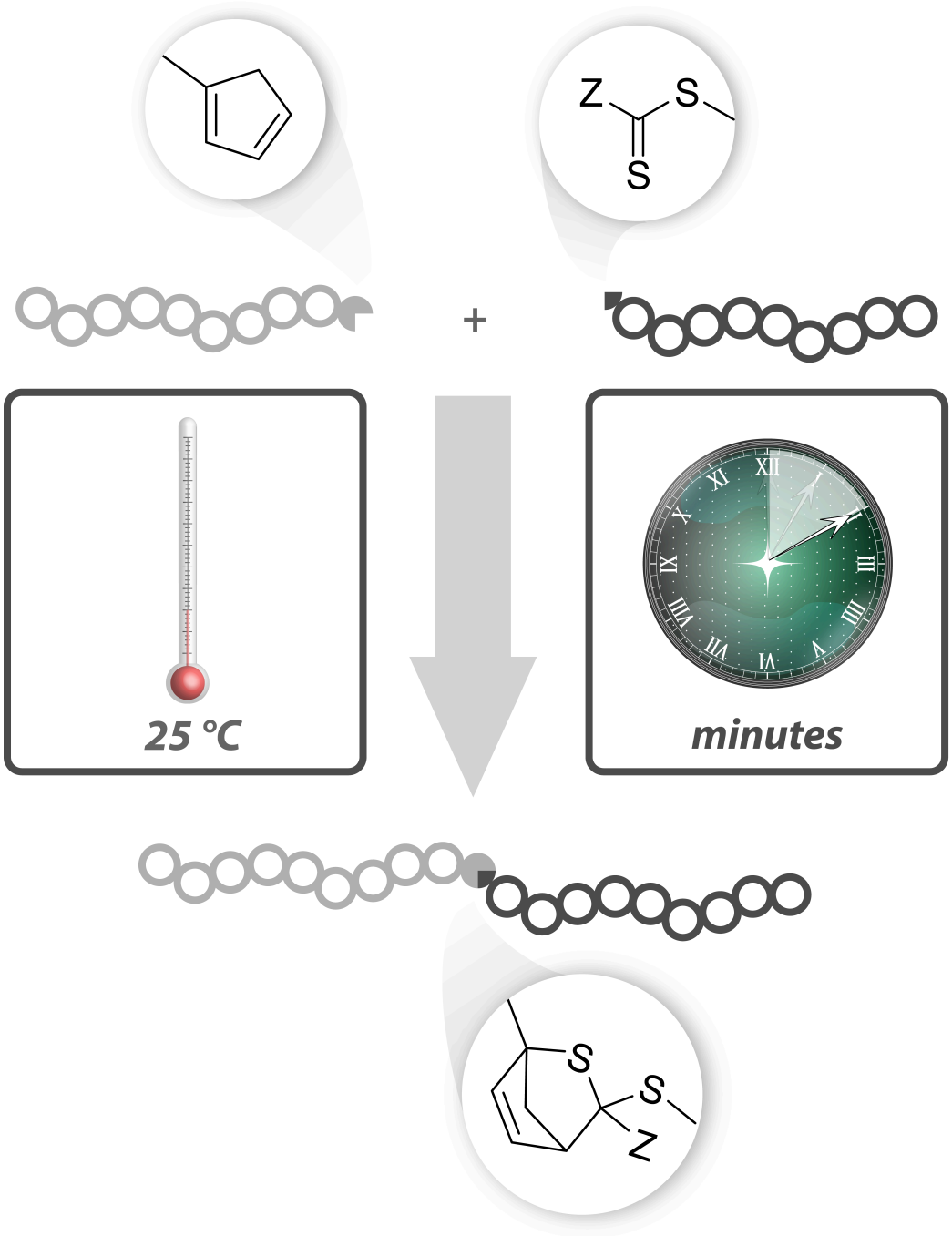

Figure 7.1 The use of novel cyclopentadienyl-functional polymers substantially increases the rate of the RAFT-HDA cycloaddition such that rapid macromolecular construction at ambient temperature is feasible.

7.2 Experimental Section

Synthesis of Tosylated Poly(ethylene glycol) monomethylether

To a stirred solution of poly(ethylene glycol) mono methyl ether (4.00 g, 2.00 mmol) in anhydrous pyridine (20 mL) was added *p*-toluenesulfonyl chloride (3.82 g, 20.0 mmol). The resulting mixture was allowed to stir at room temperature for 24 hours and then added to cold distilled water (60 mL). The polymer was extracted with dichloromethane. The organic phase was dried over $MgSO_4$ and concentrated to a volume of 20 mL. Precipitation in cold diethyl ether yielded a white solid (3.73 g, 86 %). ^{1}H NMR (400 MHz, $CDCl_3$, 25 °C): δ = 7.79 (d, $^3J_{HH}$ = 8.3 Hz, arom.), 7.31 (d, $^3J_{HH}$ = 8.3 Hz, arom.), 4.13 (t, $^3J_{HH}$ = 4.8 Hz, -$CH_2C\mathbf{H_2}$OTs), 3.62 (s, -O-(C$\mathbf{H_2}$)2-O-), 3.36 (s, -O-C$\mathbf{H_3}$), 2.43 (s, C$\mathbf{H_3}$-aryl) ppm.

Synthesis of Cyclopentadienyl Functional Poly(ethylene glycol) monomethylether

Tosylated poly(ethylene glycol) mono methyl ether (800 mg, 0.37 mmol) was dissolved in THF (5 mL) and cooled to 0 °C. To this solution was slowly added 3 equiv. sodium cyclopentadienide solution (2.0 M in THF) (0.56 mL, 1.11 mmol). The mixture was then stirred at 0 °C for 30 minutes and then overnight at room temperature. The resulting mixture was then poured into a saturated NH_4Cl solution and extracted with dichloromethane. The organic phase was washed once with cold distilled water, dried over $MgSO_4$ and concentrated to a volume of 10 mL. Precipitation in cold diethyl ether yielded a brown solid (609 mg, 80 %). ^{1}H NMR (400 MHz, $CDCl_3$, 25 °C): δ = 6.47-6.08 (m, $C_5\mathbf{H_5}$, vinylic), 3.65 (s, -O-(C$\mathbf{H_2}$-)$_2$), 3.38 (s, -O-C$\mathbf{H_3}$), 3.18 (t, ^3J = 8.5 Hz, -O-C$\mathbf{H_2}CH_2$-C_5H_5), 2.93 (m, bridge head), 2.69 (m, -O-$CH_2C\mathbf{H_2}$-C_5H_5) ppm.

RAFT Polymerization-Typical Procedure

A solution of styrene (80 mL, 0.70 mol), RAFT agent (1.62 mmol) and AIBN (0.043 g, 0.27 mmol) was prepared in a 250 mL round bottom flask. The flask was subsequently purged with nitrogen for 1 hour to remove any residual oxygen. The polymerization reaction was performed at 60 °C. The reaction was stopped by exposing the reactants to oxygen and chilling in an ice bath. The polymers were isolated by a two-fold precipitation in cold methanol.

PS **3**: $M_{n,\,SEC}$ = 2500 g·mol^{-1}, *PDI* = 1.11; $M_{n,\,NMR}$ = 3100 g·mol^{-1}

PS **4**: $M_{n,\,SEC}$ = 3300 g·mol^{-1}, *PDI* = 1.12; $M_{n,\,NMR}$ = 3300 g·mol^{-1}

P*i*BoA **5a**: $M_{n,\,SEC}$ = 3400 g·mol^{-1}, *PDI* = 1.15; $M_{n,\,NMR}$ = 3500 g·mol^{-1}

P*i*BoA **5b**: $M_{n,\,SEC}$ = 6600 g·mol^{-1}, *PDI* = 1.14; $M_{n,\,NMR}$ = 7000 g·mol^{-1}

ATRP Polymerization-Typical Procedure

To a dried Schlenk tube was added copper (I) bromide. The tube was then sealed with a septum, evacuated and back filled with nitrogen. In another Schlenk tube was added styrene and PMDETA. The resulting monomer solution was then de-oxygenated by three freeze-pump-thaw cycles and subsequently transferred to the Schlenk tube containing the copper (I) bromide via cannula. The tube was sealed under a nitrogen atmosphere and placed in a thermostatic oil bath held at 90 °C. After the polymerization mixture reached the desired temperature, 1-phenylethyl bromide (1-PEBr) was added. The initial ratio of [Styrene]:[1-PEBr]:[CuBr]:[PMDETA] was 100:1:1:1. The polymerization was stopped by cooling the tube in an ice-bath and exposing the contents to oxygen. The resulting mixture was then diluted with THF and passed through a column of neutral alumina to remove the copper catalyst. The polymer was isolated by two-fold precipitation in cold methanol.

PS **2a**: $M_{n,\,SEC}$ = 1800 g·mol^{-1}, PDI = 1.10; $M_{n,\,NMR}$ = 1800 g·mol^{-1}

PS **2b**: $M_{n,\,SEC}$ = 3500 g·mol^{-1}, PDI = 1.10; $M_{n,\,NMR}$ = 3400 g·mol^{-1}

Synthesis of Cyclopentadienyl Functional Poly(styrene)- Typical Procedure

To a stirred solution of bromide terminated poly(styrene) in THF at 0 °C was added a 10-fold excess of sodium cyclopentadienide (2.0 M in THF) drop-wise. After the addition was completed, the reaction mixture was allowed to gradually warm to room temperature and stirred overnight. The cyclopentadienyl functionalized polymer was then isolated by precipitation in cold methanol.

Cycloaddition Reactions- Typical Procedure

Cyclopentadienyl terminated polymer (10 µmol) and dithioester terminated polymer (10 µmol) was dissolved in 200 µL chloroform and agitated for 10 minutes by shaking (1.5 equiv. TFA was added where PS **4** and PS **5a,b** were used). The solvent was then removed under reduced pressure and the residue analysed by SEC in THF.

7.3 Results and Discussion

7.3.1 Synthesis of ω-Cyclopentadienyl Functional Polymers

Adapting approaches widely utilized in the synthesis of cyclopentadienyl ligands[22] and alkylated cyclopentadiene compounds,[23, 24] the use of sodium cyclopentadienide (NaCp) in a nucleophilic substitution reaction was investigated as a route to ω-Cp functionalized polymer chains. For this purpose, appropriately end-group functional polymers are required such that the substitution reaction may take place. Commencing with the most convenient of starting points, the use of the quantitatively hydroxyl-functional (and commercially available) poly(ethylene glycol) monomethylether (PEG) was considered.

Initially, the provision of a more efficient leaving group on the PEG chain was achieved via a standard tosylation procedure (Figure 7.2). The ^{1}H NMR spectrum of the tosylated PEG (Figure 7.3a) shows the presence of the tosyl end-group (one singlet at 2.43 ppm, a triplet at 4.13 ppm and two doublets at 7.79 and 7.31 ppm). Integration of these signals with respect to those arising from the α-methoxy end-group protons (3.36 ppm) revealed the quantitative nature of the transformation.

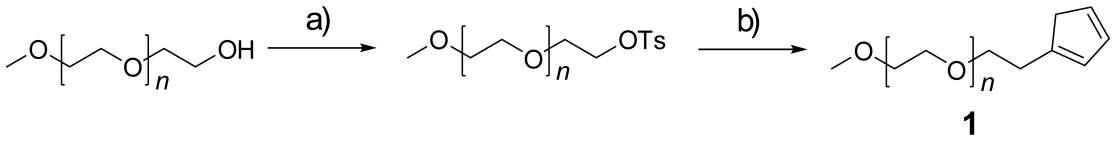

Figure 7.2 Synthesis of ω-cyclopentadienyl poly(ethylene glycol). Conditions: a) TsCl, pyridine, RT; b) NaCp (2.0 M in THF), THF, 0 °C-RT. Ts = Tosyl.

Substitution of the tosyl end-group with Cp functionality was achieved by reaction with 3 equiv. of NaCp in THF (Figure 7.2). The ^{1}H NMR spectrum presented in Figure 7.3b clearly shows the presence of the Cp end-group (signals at 6.47-6.08 ppm, 2.93 ppm and 2.69 ppm). Comparative integration of these signals reveal the quantitative functionalization of the polymer and that the substitution has taken place (with equal preference) at the 1- and 2- position of the Cp ring.*

Having established the feasibility of the above nucleophilic substitution reaction on a commercial polymer, a more versatile approach was sought with a view to gain access to a wider variety of Cp-functional materials. As such, ATRP was envisaged to provide a facile route to achieve such outcomes. Polymerization via this technique results in well-defined polymer chains that bear ω-halide functionality and it has been well documented in the literature the nucleophilic substitution of this functionality with

*Although a mixture of isomers are produced, only the chemical structure of the 1-isomer is presented throughout for reasons of brevity.

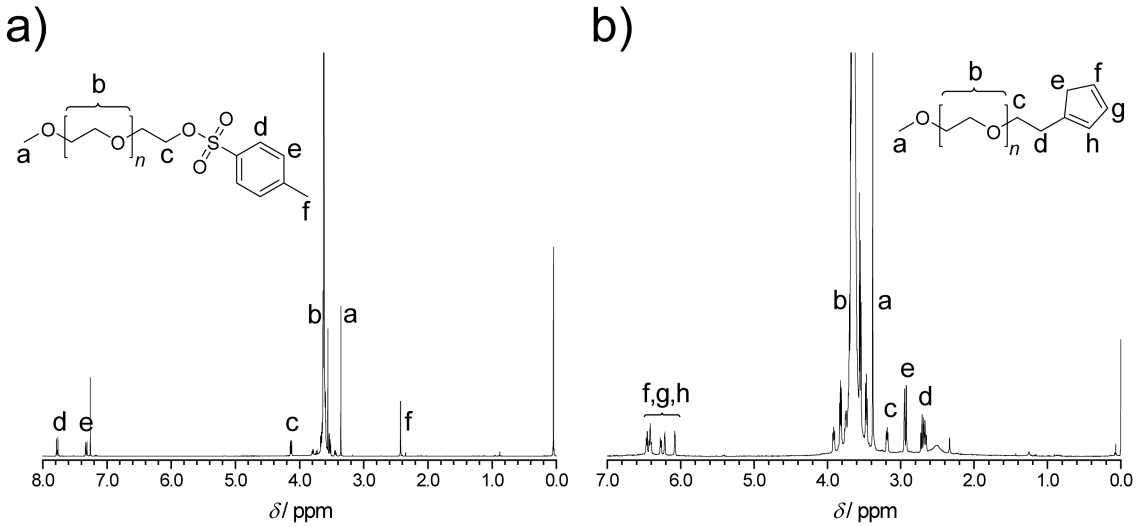

Figure 7.3 ^{1}H NMR spectra of a) tosylated PEG, and b) PEG-Cp.

sodium azide.[25] It was therefore expected that Cp-substitution could be achieved following a similar strategy.

ATRP of styrene was performed in bulk at 90 °C using 1-PEBr as the initiator (Figure 7.4). The polymerization was stopped at low conversion (< 30 %) to ensure high bromide content in the resulting polymers (two different molecular weights of PS-Br). The ^{1}H NMR spectrum of the higher molecular weight PS-Br ($M_{n,SEC}$ = 3500 g·mol^{-1}), presented in Figure 7.5a, clearly shows the presence of the α-bromo proton (multiplet at 4.4 ppm). Integration of this signal with respect to that arising from the methyl-group protons of the initiator (0.9 ppm) confirms the high bromide functionality (92 %).

Conversion of two different molecular weights of PS-Br into the corresponding ω-Cp functional PS **2a,b** was performed in a similar fashion to that of the PEG (Figure 7.4). The ^{1}H NMR spectrum of PS **2b** is depicted in Figure 7.5b. It is observed that the signal appearing at 4.4 ppm in the spectrum of PS-Br is observed to completely shift to 3.2 ppm after the transformation. The multiplet appearing between 6.2-5.7 ppm in addition to the appearance of a signal at 2.9 ppm provides complete confirmation

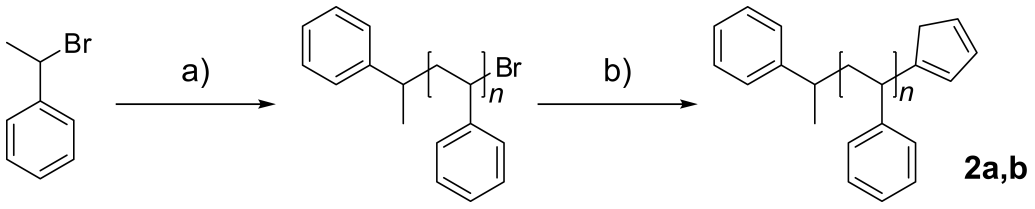

Figure 7.4 Synthesis of ω-cyclopentadienyl poly(styrene) via ATRP. Conditions: a) ATRP of styrene, CuBr/PMDETA, 90 °C; b) NaCp (2.0 M in THF), THF, 0 °C-RT. **2a** and **2b** represent poly(styrene)s of different molecular weights.

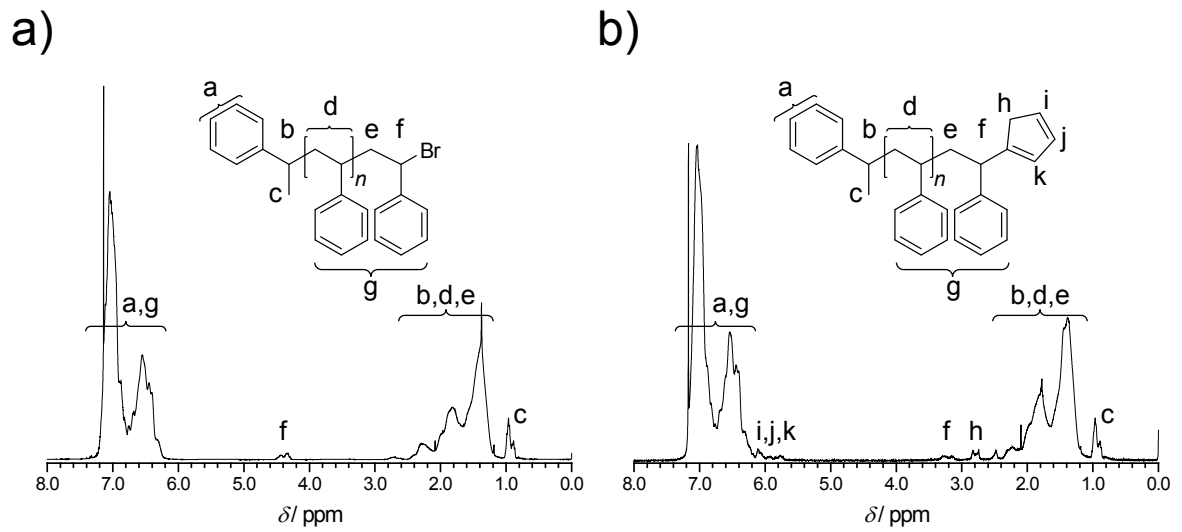

Figure 7.5 ^{1}H NMR spectra of a) PS-Br, and b) PS-Cp.

of the quantitative formation of the targeted Cp-functional polymer. The molecular weight assessments of PS **2a,b** are presented in Table 7.1.

7.3.2 Synthesis of Dienophilic Polymers via RAFT Polymerization

As dienophiles in the RAFT-HDA *click* reaction, BDPDF was used to prepare PS **3** and BPDF was used to prepare PS **4** by RAFT polymerization. Importantly, BPDF was also successfully utilized in the controlled synthesis of poly(isobornyl acrylate) (P*i*BoA) **5a,b**, the first example of this polymer being prepared by a RAFT process and the first example of this transfer agent mediating controlled polymerization of a monomer other than styrene. The structures of these polymeric building blocks are illustrated in Figure 7.6.

The ^{1}H NMR spectra of PS **3**, PS **4** and P*i*BoA **5a** are presented in Figure 7.7. In the case of PS **3**, the signal arising from ethoxy-group protons (-OC**H$_2$**CH$_3$) at 4.0 ppm confirms the presence of the targeted dithioester end-group. Analgously, in the cases where BPDF was used as the controlling agent, the series of signals appearing above 7.5 ppm arising from the protons of the pyridine ring confirm the presence of the required dithioester functionality. The molecular weight assessment of these building blocks is presented in Table 7.1. The corresponding molecular weights as determined by NMR analysis are in good agreement with the SEC data, however, the NMR derived molecular weights were used for all calculations.

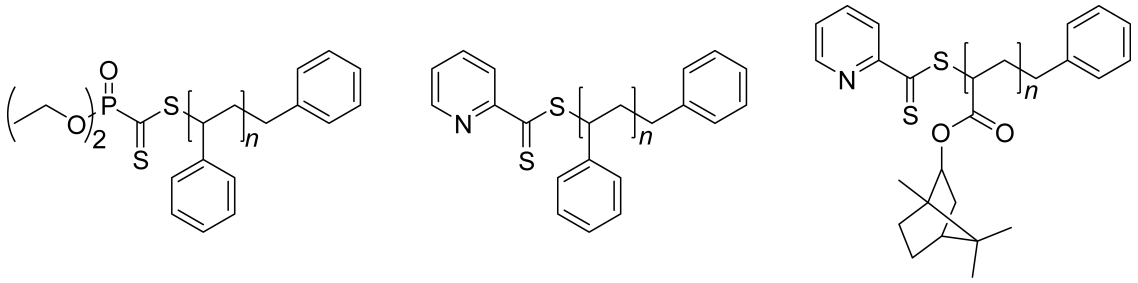

3 **4** **5a,b**

Figure 7.6 Polymers prepared by RAFT polymerization serving as dienophiles in the RAFT-HDA *click* reaction. **5a** and **5b** represent poly(isobornyl acrylate)s of different molecular weights.

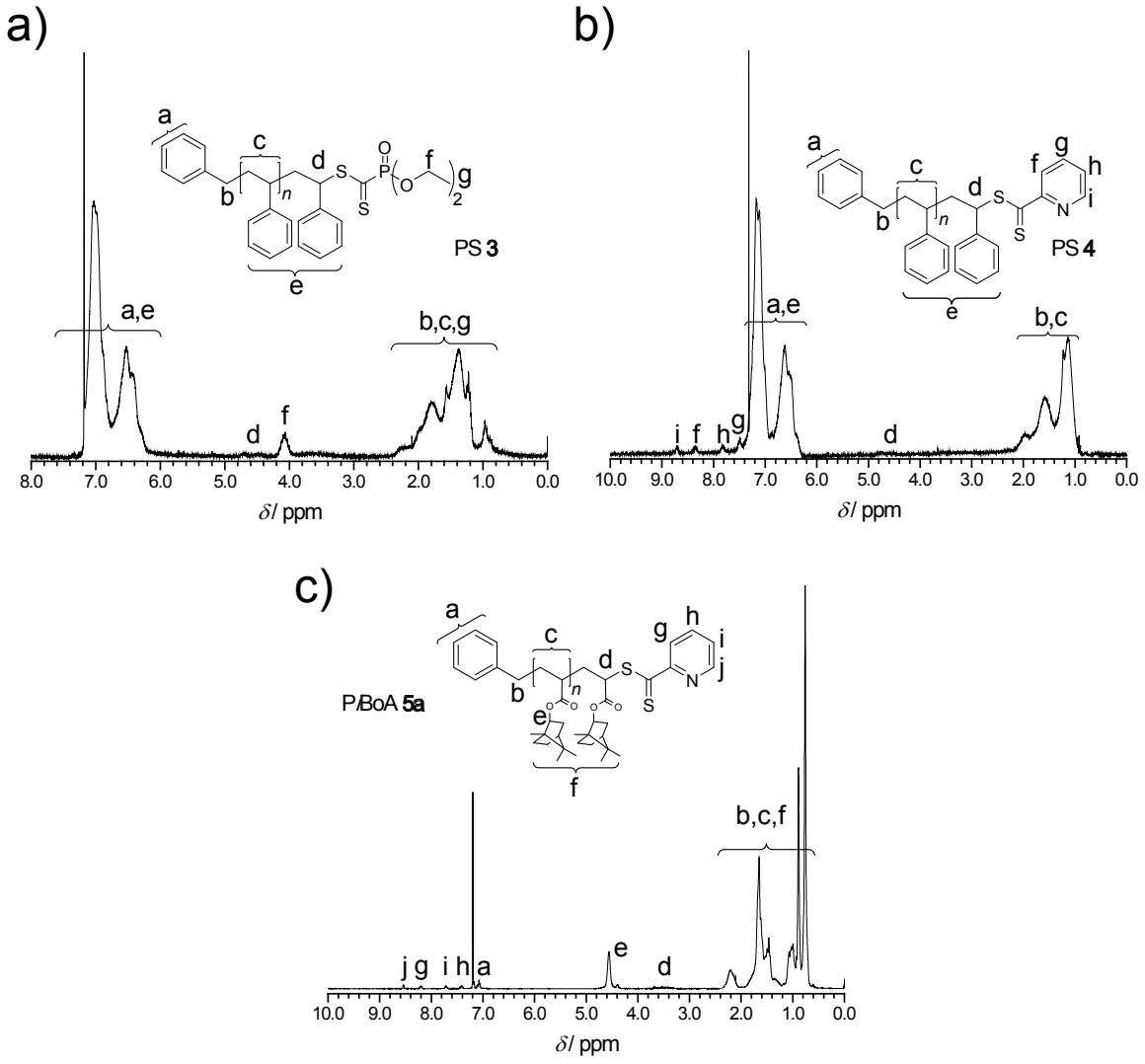

Figure 7.7 ^{1}H NMR spectra of PS **3** (a), PS **4** (b), and and P*i*BoA **5a** (c).

Table 7.1 Polymeric building block characterization.

Polymer	$M_{n,\,SEC}$[a] / g·mol^{-1}	$M_{n,\,NMR}$[b] / g·mol^{-1}	PDI_{SEC}[c]
1	2800	2100	1.04
2a	1800	1800	1.10
2b	3500	3400	1.10
3	2500	3100	1.11
4	3300	3300	1.12
5a	3400[d]	3500	1.15
5b	6600[d]	7000	1.14

[a]Measured by SEC in THF against linear PS standards [b]Determined by ^{1}H NMR spectroscopy; [c]Polydispersity index. [d]Values for P*i*BoA are corrected by applying the Mark-Houwink-Sakurada relationship ($K = 5.00 \times 10^{-5}$ dL·g^{-1}, $\alpha = 0.745$).

7.3.3 Ultra-fast Construction of Block Copolymers via HDA Cycloaddition

As an initial validation of this approach to achieve ultra-fast *click* couplings; and to ascertain the required reaction conditions, a series of simple model reactions were performed in which PS **3** and **4** were reacted with PS **2a,b** in chloroform solution at ambient temperature. These examples are classified as model reactions by the simple fact that both precusor polymers are PS. Although the polymers that result after coupling aren't technically block copolymers, the direct molecular weight determination of the coupling products to those of the precursor building blocks against a PS calibration in SEC measurements can be deemed to be accurate.

In the case of PS **4**, 1.5 equiv. of TFA was added to catalyse the reaction. After shaking for 10 minutes, the solvent was removed *in vacuo* and the residue directly analyzed by SEC. The reaction scheme for two selected examples is presented in Figure 7.8. The SEC analyses, as depicted in Figure 7.9a , b and c, show a clear and qualitatively complete shift of the molecular weight distrbutions to lower retention times (with respect to those of the starting materials). This indirectly indicates an increase in molecular weight, the extent of which is in excellent agreement with the predicted values as determined by the sum of the molecular weights of the individual blocks (Table 7.2). Such a methodology was then utilized for all subsequent couplings.

Figure 7.9 present overlays of the SEC traces of the individual polymeric building blocks and those of the corresponding room-temperature stable coupling products for all reactions performed. In all cases, a clear shift of the trace to lower retention times indicates successful block formation, which is consistent with the data presented in

Table 7.2 Block copolymer characterization.[a]

Polymer	$M_{n,\,theor.}$[b] / g·mol^{-1}	$M_{n,\,SEC}$[c] / g·mol^{-1}	PDI_{SEC}[d]
2a-*b*-**3**	4900	4800	1.15
2a-*b*-**4**	5100	5400	1.12
2b-*b*-**4**	6700	6900	1.11
2b-*b*-**5a**	6900	7000	1.17
2b-*b*-**5b**	10400	10300	1.15
1-*b*-**3**	5200	5500	1.10
1-*b*-**4**	5400	6000	1.13
1-*b*-**5a**	5600	6100	1.15

[a] All reactions resulting in block copolymers were performed in chloroform at ambient temperature and pressure and were complete within 10 minutes. [b] Calculated from the sum of the NMR-derived values of the molecular weights of the respective building blocks; [c] Measured by SEC in THF against linear PS standards; [d] Polydispersity index.

Table 7.2. It is important to note that in the preceding chapters, $ZnCl_2$ has been required to catalyse the HDA cycloaddition when using BDPDF. In the present study, however, it was found that the coupling reaction proceeded to completion within 10 minutes without the addition of catalyst. This is attributed to the high Diels-Alder activity of the Cp end-group.

In order to further evaluate the efficiency of block copolymer formation, the SEC distributions of the coupling products were deconvoluted using the procedure introduced in Chapter 5. In all cases, a greater than 90 % area fraction of the coupling product SEC trace is representative of the *block* structure. The remaining small fractions of seemingly un-reacted starting materials are most certainly a result of non-quantitative end-group functionalization of the precusor homopolymers which, in an ω-functionalization strategy for CRP, is an impossibility.

In order to assess the rate of the HDA coupling in a more quantitative fashion via SEC analysis, it is necessary to enforce a cessation of the HDA reaction at specific time intervals. The results presented in the preceding chapters indicate that the pyridinyl dithioester is the more efficient heterodienophile, thus it was with polymers bearing this end-group that the kinetics of the rapid cycloaddition was investigated. Unlike the phosphoryl dithioester end-group, which is permanently electron-withdrawing, the pyridinyl dithioester end-group must be activated by protonation in order to undergo rapid HDA chemistry. Therefore, the pyridinyl dithioester serves as a molecular switch, which offers great control over the conjugation reaction. This was utilized advantageously in determining the rate of block formation.

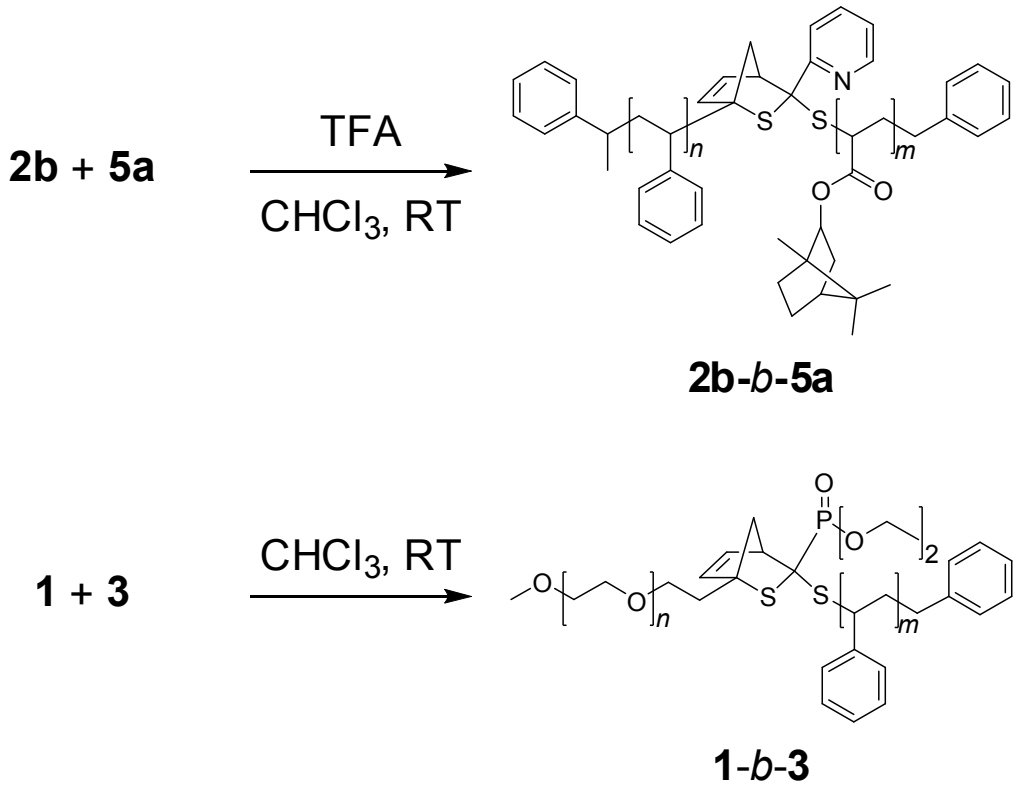

Figure 7.8 Selected examples of the formation of block copolymers by ultrafast HDA chemistry. PS-*b*-P*i*BoA **2b**-*b*-**5a** (top), and PEG-*b*-PS **1**-*b*-**3** (bottom).

In a control run, PS **4** and PS **2a** were dissolved in chloroform without the addition of TFA. The mixture was allowed to stand at room temperature for 1 hour, after which the solvent was removed *in vacuo* and the residue directly analyzed by SEC. The resulting SEC trace was identical to that of a freshly prepared mixture of PS **4** and PS **2a**, and consistent with the traces of the individual segments. It has been documented that pyridinyl dithioesters can react with butadiene derivatives without catalysis;[26] however the reaction is slow to the point that it may be neglected for the present study.

A stock solution of PS **4** and PS **2a** in chloroform was then prepared and distributed amongst four vials. The progress of the rapid HDA cycloaddition was then monitored by stopping the reaction and analysing the crude reaction mixture via SEC. This was achieved by direct precipitation after the allotted time in cold basic methanol, which served to neutralize the acidic catalyst and recover the formed block copolymer. Given that no further reaction can take place to an appreciable extent during the time required to recover the polymer and prepare a sample in THF for SEC analysis, it can be expected (with a high degree of confidence) that the SEC data will give an accurate depiction of the progress of the coupling reaction.

Figure 7.10 depicts an overlay of the SEC traces of the starting materials PS **4** and PS **2a** along with those of the crude reaction mixtures after 10 seconds, 1, 5 and 10 minutes.

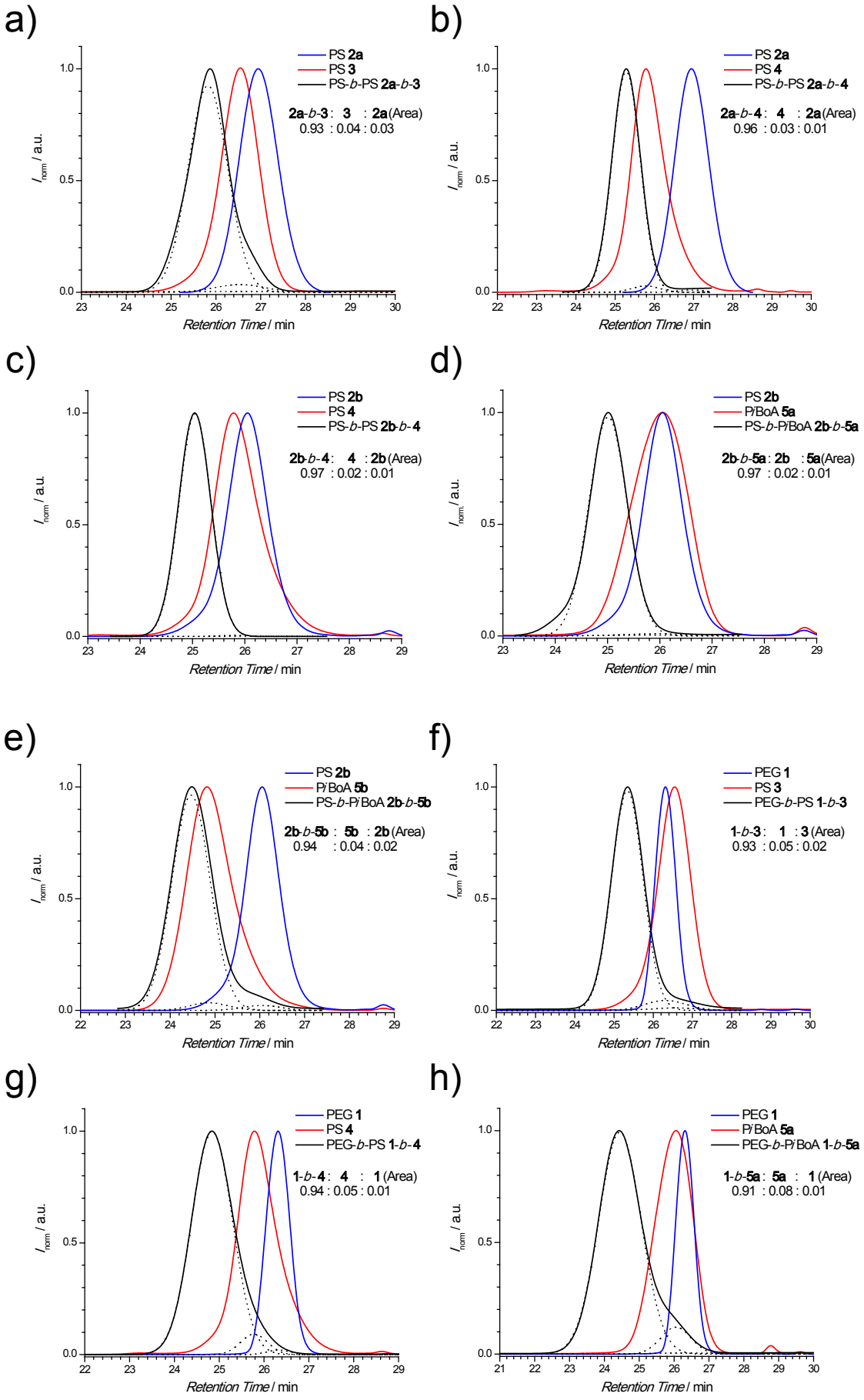

Figure 7.9 Overlay of SEC traces showing the formation of block copolymers via ultra-fast RAFT-HDA chemistry.

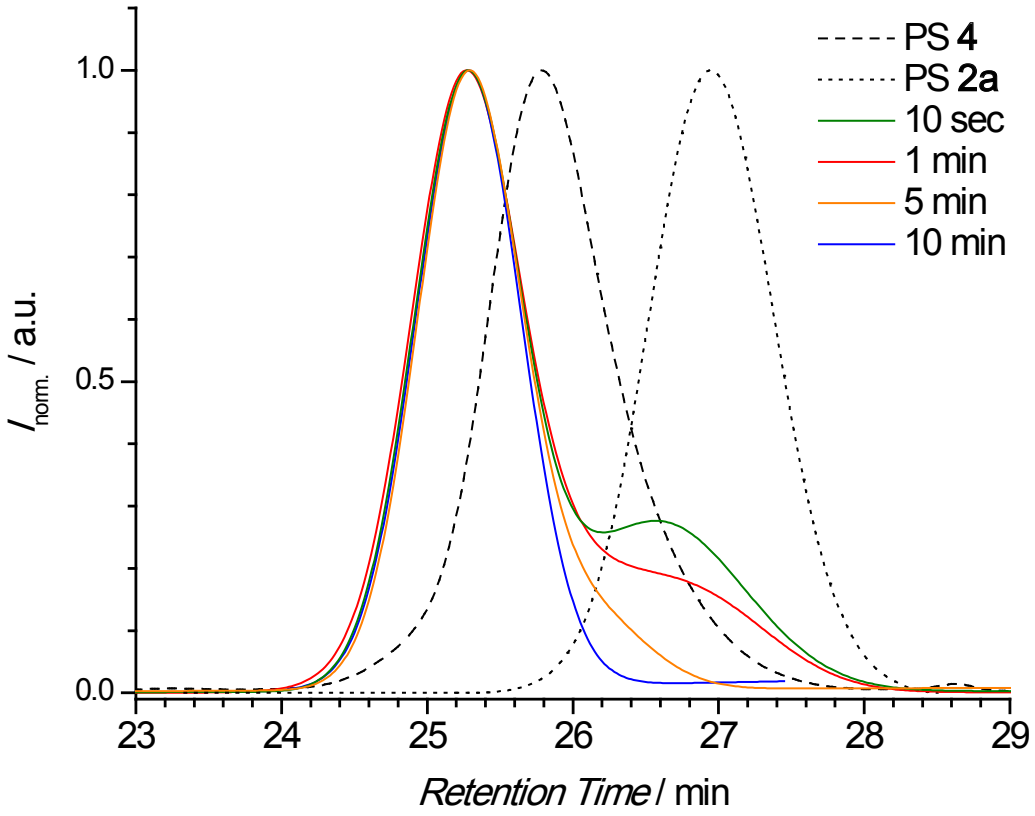

Figure 7.10 Overlay of SEC traces showing the progress of the HDA reaction between PS **4** and PS **2a**.

Inspection of Figure 7.10 clearly demonstrates that the majority of the block copolymer structure is formed within the first 10 seconds of the reaction, with quantitative conversion achieved within 10 minutes.

7.4 Conclusion

In summary, an efficient and extremely rapid room temperature conjugation strategy to access pure block copolymer structures which proceed without the addition of a catalyst has been presented. In addition, the present chapter describes a technique for the preparation of novel ω-Cp functionalized polymers, which are easily accessible via ATRP. Thus, the *click* concept presented herein allows the ultra-fast conjugation of virtually all polymer strands accessible via RAFT and ATRP. Furthermore, the provision of Cp-functionality at very well-defined positions on a polymer chain will provide further routes to the efficient functionalization of a variety of substrates, such as fullerenes and carbon nanotubes.

References

[1] Binder, W. H.; Sachsenhofer, R. *Macromol. Rapid Commun.* **2008**, *29*, 952–981.

[2] Opsteen, J. A.; van Hest, J. C. M. *Chem. Commun.* **2005**, 57–59.

[3] Quémener, D.; Davis, T. P.; Barner-Kowollik, C.; Stenzel, M. H. *Chem. Commun.* **2006**, 5051–5053.

[4] Durmaz, H.; Colakoclu, B.; Tunca, U.; Hizal, G. *J. Polym. Sci., Part A: Polym. Chem.* **2006**, *44*, 1667–1675.

[5] Gao, H. F.; Matyjaszewski, K. *Macromolecules* **2006**, *39*, 4960–4965.

[6] Wang, G. W.; Luo, X. L.; Liu, C.; Huang, J. L. *J. Polym. Sci., Part A: Polym. Chem.* **2008**, *46*, 2154–2166.

[7] Dag, A.; Durmaz, H.; Hizal, G.; Tunca, U. *J. Polym. Sci., Part A: Polym. Chem.* **2008**, *46*, 302–313.

[8] Gacal, B.; Durmaz, H.; Tasdelen, M. A.; Hizal, G.; Tunca, U.; Yagci, Y.; Demirel, A. L. *Macromolecules* **2006**, *39*, 5330–5336.

[9] Van Camp, W.; Germonpre, V.; Mespouille, L.; Dubois, P.; Goethals, E. J.; Du Prez, F. E. *React. Funct. Polym.* **2007**, *67*, 1168–1180.

[10] Parrish, B.; Breitenkamp, R. B.; Emrick, T. *J. Am. Chem. Soc.* **2005**, *127*, 7404–7410.

[11] Lutz, J. F.; Börner, H. G.; Weichenhan, K. *Macromolecules* **2006**, *39*, 6376–6383.

[12] Lutz, J. F.; Börner, H. G.; Weichenhan, K. *Aust. J. Chem.* **2007**, *60*, 410–413.

[13] Ladmiral, V.; Mantovani, G.; Clarkson, G. J.; Cauet, S.; Irwin, J. L.; Haddleton, D. M. *J. Am. Chem. Soc.* **2006**, *128*, 4823–4830.

[14] Ting, S. R. S.; Granville, A. M.; Quemener, D.; Davis, T. P.; Stenzel, M. H.; Barner-Kowollik, C. *Aust. J. Chem.* **2007**, *60*, 405–409.

[15] Sen Gupta, S.; Raja, K. S.; Kaltgrad, E.; Strable, E.; Finn, M. G. *Chem. Commun.* **2005**, 4315–4317.

[16] Le Drournaguet, B.; Velonia, K. *Macromol. Rapid Commun.* **2008**, *29*, 1073–1089.

[17] Agard, N. J.; Prescher, J. A.; Bertozzi, C. R. *J. Am. Chem. Soc.* **2004**, *126*, 15046–15047.

[18] van Berkel, S. S.; Dirks, A. T. J.; Debets, M. F.; van Delft, F. L.; Cornelissen, J.; Nolte, R. J. M.; Rutjesa, F. *ChemBioChem* **2007**, *8*, 1504–1508.

[19] Campos, L. M.; Killops, K. L.; Sakai, R.; Paulusse, J. M. J.; Damiron, D.; Drockenmuller, E.; Messmore, B. W.; Hawker, C. J. *Macromolecules* **2008**, *41*, 7063–7070.

[20] Chan, J. W.; Yu, B.; Hoyle, C. E.; Lowe, A. B. *Chem. Commun.* **2008**, 4959–4961.

[21] Nebhani, L.; Sinnwell, S.; Inglis, A. J.; Stenzel, M. H.; Barner-Kowollik, C.; Barner, L. *Macromol. Rapid Commun.* **2008**, *29*, 1431–1437.

[22] Coolbaugh, T. S.; Coots, R. J.; Santarsiero, B. D.; Grubbs, R. H. *Inorg. Chim. Acta* **1985**, *98*, 99–105.

[23] Christie, S. D. R.; Man, K. W.; Whitby, R. J.; Slawin, A. M. Z. *Organometallics* **1999**, *18*, 348–359.

[24] Dillmore, W. S.; Yousaf, M. N.; Mrksich, M. *Langmuir* **2004**, *20*, 7223–7231.

[25] Coessens, V.; Matyjaszewski, K. *J. Macromol. Sci. Part A Pure Appl. Chem.* **1999**, *A36*, 667–679.

[26] Bastin, R.; Albadri, H.; Gaumont, A. C.; Gulea, M. *Org. Lett.* **2006**, *8*, 1033–1036.

8

Modular Access to High Molecular Weight Block Copolymers

8.1 Introduction

The conjugation of end-group functionalized macromolecular building blocks via efficient coupling reactions has been a topic of high interest in recent years. However, the vast majority of publications in this field almost exclusively make use of oligomeric materials with molecular weights of less than 10 000 $g \cdot mol^{-1}$.[1, 2] As conjugative chemistries become more and more efficient, such as the CuAAC[3] and the herein reported ultra-fast RAFT-HDA cycloaddition, the limiting factor in producing well-defined macromolecular conjugates is no longer the conjugation step, but rather the chemistries involved in the generation of the end-group functionalized macromolecular building blocks. For example, the most frequented method for preparing *clickable* polymers has been the nucleophilic substitution of the terminal halogen inherent to materials formed by the ATRP process with an azide. While the substitution reaction itself has been proven to be very efficient,[4] the retention of active halogen end-groups in ATRP polymers is significantly less so.[5] Even with the relatively recent development of the ARGET-ATRP process,[6] there still exists a limit to the degree of functionalization that may be obtained.

A viable alternative is to incorporate the required functionalities into ATRP initiators or RAFT chain transfer agents (CTA).[7, 8] While such an approach provides highly

end-functional polymers without the need for post-polymerization functionalization strategies, it does however warrant special consideration regarding the compatibility of the *click* moiety with the polymerization process. While - in general - *click* reactions have been proven to be very efficient in the conjugation of two synthetic macromolecular species with relatively low molecular weight, there is a severe shortage of studies in which high molecular weight block copolymers are produced.

Herein, a significant improvement in macromolecular engineering via the *click* approach is reported. Through the use of the ultra-fast RAFT-HDA *click* reaction, block copolymers of PS and P*i*BoA become accessible with molecular weights ranging from 34 000 g·mol^{-1} to over 100 000 g·mol^{-1}. The overall synthetic strategy is illustrated in Figure 8.1. The left-hand side of Figure 8.1 depicts the various methodologies utilized in the generation of Cp-capped PS. RAFT polymerization is used to produced hydroxyl-terminated PS (PS-OH **3**, **4**), which is then converted into the bromide-functionalized species PS-Br **3**, **4**. ATRP is concurrently used to produce PS of a similar structure (PS-Br **2**). The corresponding Cp-capped polymers PS-Cp **2**, **3**, **4** were subsequently achieved via nucleophilic substitution.

The right-hand side of Figure 8.1 illustrates the synthesis of the electron-deficient dithioester capped P*i*BoA **1a-c**. Finally, polymers from the left-hand side of the figure are *clicked* to those from the right-hand side to produce well-defined block copolymers in a very efficient and straight-forward manner. It is worthwhile noting that there are relatively few reports on the synthesis of P*i*BoA containing block copolymers. The most recent include the work of Du Prez et al.[9] who have reported the ATRP of *i*BoA and its subsequent chain extension to achieve such structures and the use of the ultra-fast RAFT-HDA *click* approach was presented in Chapter 7.

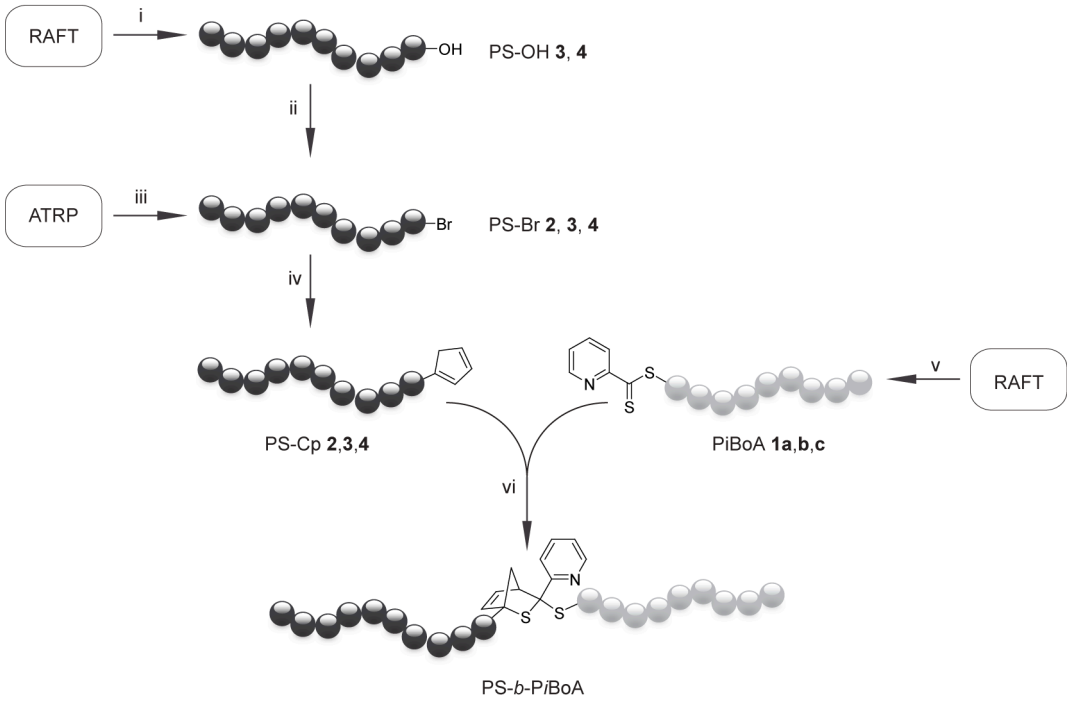

Figure 8.1 General synthetic strategy for producing well-defined block copolymers via the RAFT-HDA *click* reaction. The reaction conditions were as follows: i) RAFT polymerization of styrene, 4-cyano-1-hydroxypent-4-yl dithiobenzoate/ACP, 65 °C; ii) BPiB/TEA; iii) ATRP of styrene, MPB/CuBr/PMDETA, 110 °C; iv) NaCp/THF, 0 °C-RT; v) RAFT polymerization of *i*BoA, BPDF/AIBN, 60 °C; vi) HDA cycloaddition, TFA/$CHCl_3$, RT.

8.2 Experimental Section

Synthesis of PiBoA 1a-c

A mixture of *i*BoA, BPDF and AIBN was deoxygenated by purging with nitrogen for 40 min. The polymerization reaction was performed at 60 °C for 24 hours. The reaction was stopped by chilling in an ice bath and exposure to oxygen. The resulting polymers were isolated by two-fold precipitation in cold methanol. The specifics for each of the three polymerizations are as follows:

P*i*BoA **1a** - $[M]_o$:$[RAFT]_o$:$[AIBN]_o$ = 230:1:0.2, $M_{n,\,SEC}$ = 5400 g·mol^{-1}, *PDI* = 1.15, conversion = 11.0 %;
P*i*BoA **1b** - $[M]_o$:$[RAFT]_o$:$[AIBN]_o$ = 400:1:0.2, $M_{n,\,SEC}$ = 10 100 g·mol^{-1}, *PDI* = 1.14, conversion = 12.1 %;
P*i*BoA **1c** - $[M]_o$:$[RAFT]_o$:$[AIBN]_o$ = 600:1:0.2, $M_{n,\,SEC}$ = 22 500 g·mol^{-1}, *PDI* = 1.10, conversion = 18.3 %.

Synthesis of PS-Cp 2

A mixture of styrene and PMDETA was prepared and deoxygenated by three consecutive freeze-pump-thaw cycles. The degassed solution was subsequently transferred into a Schlenk tube containing CuBr under nitrogen via a cannula. The resulting mixture was then sealed under nitrogen and placed in a thermostatic oil bath set to 110 °C. A deoxygenated solution of MBP in styrene was then added and the resulting mixture was allowed to stir for 70 minutes. The polymerization was stopped by chilling the contents in an ice bath and exposure to oxygen. THF was subsequently added to dilute the mixture which was then passed through a short column of neutral alumina to remove the copper catalyst. Bromide terminated PS (PS-Br **2**) was then isolated by 2-fold precipitation in cold methanol. The initial ratios of the respective components were $[M]_o$:$[MBP]_o$:$[CuBr]_o$:$[PMDETA]_o$ = 1280:1:1:0.5, conversion = 25 %,
PS-Br **2**: $M_{n,SEC}$ = 29 500 g·mol^{-1}, *PDI* = 1.07.

To a stirred solution of PS-Br **2** in anhydrous THF at 0 °C a 10-fold excess of NaCp (2.0 M in THF) was added dropwise. The resulting mixture was allowed to stir at 0 °C for 30 minutes before allowing to gradually warm to ambient temperature. Stirring was allowed to continue overnight and the resulting Cp-functionalized polymer PS-Cp **2** was isolated by two-fold precipitation in cold methanol.
PS-Cp **2**: $M_{n,\,SEC}$ = 29 500 g·mol^{-1}, *PDI* = 1.07.

Synthesis of PS-Cp 3,4

A solution of 4,4'-azobis(4-cyanopentanol) (ACP)[10] and 4-cyano-1-hydroxypent-4-yl dithiobenzoate (RAFT-OH)[11] in styrene was deoxygenated by purging with nitrogen for 40 minutes. The polymerization reaction was performed at 65 °C for 16.5 and 24 hours respectively for **3** and **4**. The initial concentrations of the respective components were as follows: for **3** - $[M]_o$:$[RAFT\text{-}OH]_o$:$[ACP]_o$ = 436:1:0.17, conversion = 10 % and for **4** - $[M]_o$:$[RAFT\text{-}OH]_o$:$[ACP]_o$ = 1090:1:0.5, conversion = 70 %. The polymerization was stopped by chilling the reaction mixture in an ice bath and exposure to oxygen. The resulting hydroxyl functionalized polymers (PS-OH **3**, **4**) were isolated by two-fold precipitation in cold methanol.
PS-OH **3** $M_{n,\,SEC}$ = 3590 g·mol^{-1}, *PDI* = 1.06;
PS-OH **4** $M_{n,\,SEC}$ = 79 100 g·mol^{-1}, *PDI* = 1.08.

A mixture of the PS-OH **3** or **4** (0.0082 M) and TEA (2 equiv.) in anhydrous THF was chilled to 0 °C under nitrogen. A solution of 2-bromopropionyl bromide (BPiB) in anhydrous THF (0.016 M, 2 equiv.) was added dropwise. Upon addition, a white precipitate formed. The mixture was allowed to warm to ambient temperature and stirred overnight. The solids were subsequently removed by filtration and the filtrate added dropwise to stirred cold methanol. The precipitated polymer was removed by filtration, dissolved in THF and re-precipitated in cold methanol. The resulting bromide terminated polymers (PS-Br **3**, **4**) were then dissolved in anhydrous THF (0.02 M) and chilled to 0 °C under nitrogen. NaCp (2.0 M in THF, 10 equiv.) was added to this solution in a dropwise fashion. The resulting mixture was stirred at 0 °C for 30 minutes before gradually warming to ambient temperature. Stirring was continued for 24 hours at ambient temperature before Cp terminated polymers PS-Cp **3**,**4** were isolated by two-fold precipitation in cold methanol.
PS-Cp **3** $M_{n,\,SEC}$ = 3650 g·mol^{-1}, *PDI* = 1.06;
PS-Cp **4** $M_{n,\,SEC}$ = 79 100 g·mol^{-1}, *PDI* = 1.08.

RAFT-HDA Cycloaddition Between PS and PiBoA - Typical Procedure

Cp terminated polymer (10 µmol) and dithioester capped polymer (10 µmol) were dissolved in 1.0 mL chloroform. After the addition of 1.5 equiv. TFA, the mixture was agitated for 10 minutes by shaking. In the case of the high molecular weight PS-Cp **4** and P*i*BoA **1c**, 2.0 mL of solvent was used and the resulting solution agitated for 2 hours. The resulting block copolymers were isolated by precipitation in cold methanol and analyzed via SEC (THF).

8.3 Results and Discussion

8.3.1 Synthesis of Macromolecular Building Blocks and Their Subsequent Coupling

With a number of highly efficient coupling reactions at our disposal, the principal focus for producing conjugates of two macromolecular species is on the methodology by which they are equipped with the appropriate chemical function. In terms of synthetic polymers, the most widely employed technique in producing highly functional materials is by CRP, typically ATRP and RAFT polymerization. In the current study, ATRP was initially used to produce PS with a high level of bromide end-group functionality. By targeting a very high molecular weight and stopping the polymerization at low monomer conversion, PS-Br **2** was obtained with M_n = 29 500 g·mol^{-1} and *PDI* = 1.07 according to the SEC assessment. The presence of the bromide functionality was confirmed by ^{1}H NMR spectroscopy. Cp functionality was imparted onto the polymer by nucleophilic substitution of the bromide with NaCp in anhydrous THF. The quantitative nature of the substitution was again confirmed by ^{1}H NMR spectroscopy.

Concurrently, a series of P*i*BoA's with varying molecular weights were prepared via RAFT polymerization of *i*BoA in the presence of BPDF as the controlling agent. The molecular weight assessment of the series is presented in Table 8.1. P*i*BoA **1a-c** were subsequently coupled to PS-Cp **2** via the ultra-fast RAFT-HDA cycloaddition in chloroform solution. The data presented in Table 8.1 outlines the M_n values for the various block copolymers and the individual building blocks from which they were synthesized. Block copolymers with molecular weights ranging from 34 600 g·mol^{-1} to 51 700 g·mol^{-1} and of narrow polydispersity were successfully formed, as indicated by the excellent agreement between the measured M_n value for the blocks and the sum of corresponding values for the individual segments. Furthermore, the top three SEC chromatograms of Figure 8.2 show the traces of the formed block copolymers in relation to those of the individual building blocks. A clear shift to lower retention times of the traces and the lack of any pronounced shoulders also indicates successful and efficient block formation, which is consistent with the data presented in Table 8.1. It should be noted that all block copolymers formed in the current investigation have not been fractionated prior to SEC analysis.

8.3.2 Extension to Higher Molecular Weights

Attempts to produce higher molecular weight blocks via this approach were not as successful as those already described. PS was synthesized via ATRP with M_n =

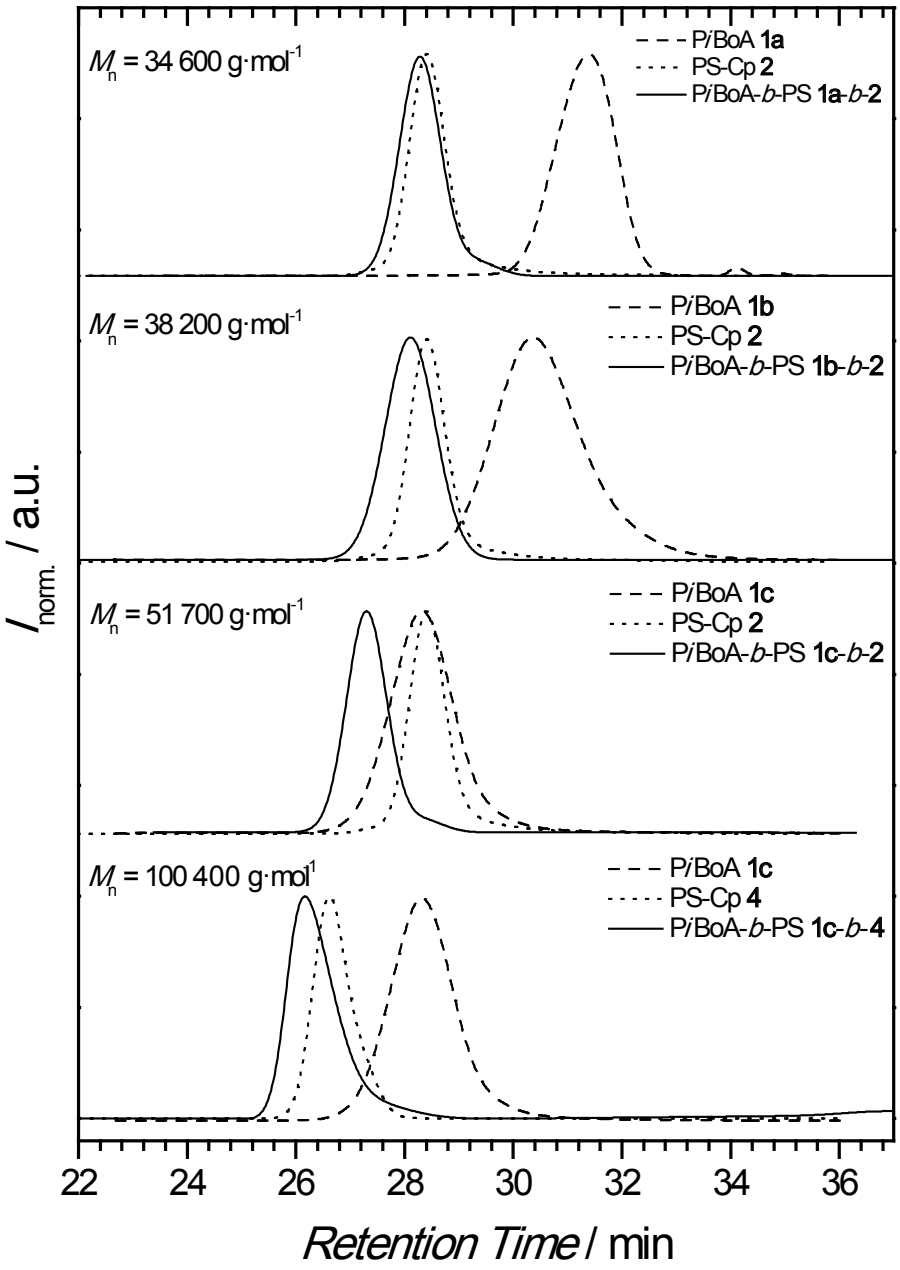

Figure 8.2 Overlay of SEC traces showing the formation of P*i*BoA-*b*-PS of various molecular weights. The M_n value given is that of the respective block copolymers.

Table 8.1 Characterization of the macromolecular building blocks and final copolymers prepared via RAFT-HDA conjugation.[a]

P*i*BoA[b]			PS			P*i*BoA-*b*-PS		
Polymer	$M_{n,\,SEC}$ / g·mol^{-1}	*PDI*	Polymer	$M_{n,\,SEC}$ / g·mol^{-1}	*PDI*	Polymer	$M_{n,\,SEC}$ / g·mol^{-1}	*PDI*
1a	5400	1.15	**2**	29 500	1.07	**1a**-*b*-**2**	34 600	1.10
1b	10 100	1.14	**2**	29 500	1.07	**1b**-*b*-**2**	38 200	1.09
1c	22 500	1.10	**2**	29 500	1.07	**1c**-*b*-**2**	51 700	1.12
1a	5400	1.15	**3**	3600	1.06	**1a**-*b*-**3**	8 900	1.10
1c	22 500	1.10	**4**	79 100	1.08	**1c**-*b*-**4**	100 400	1.13

[a]Measured by SEC in THF against linear PS standards [b]Values for P*i*BoA are corrected by applying the Mark-Houwink-Sakurada relationship ($K = 5.00 \times 10^{-5}$ dL·g^{-1}, $\alpha = 0.745$).

50 000 g·mol^{-1} and *PDI* = 1.12. Due to its high molecular weight, determination of the end-group functionality via ^{1}H NMR spectroscopy proved to be difficult and unreliable. However, the subsequent substitution of the bromide functionality was quantitative as determined via the same technique. The resulting polymer was then *clicked* to P*i*BoA **1c** and the subsequent SEC analysis revealed significant amounts of starting material remaining (Figure 8.3a). This lack of success was attributed to diminishing bromide functionality in PS prepared via ATRP as higher and higher molecular weights were targeted. In order to circumvent this problem, RAFT-OH was used to mediate the RAFT polymerization of styrene, initiated by the hydroxyl-containing azo-initiator ACP. The combination of this RAFT CTA and initiator has already been proven to be highly effective in producing polymers with a very high degree of hydroxyl functionalization.[12] The general strategy in the present study was to convert the terminal hydroxyl moiety of the resulting PS-OH chains to a Cp function via nucleophilic substitution of a bromide intermediate (Figure 8.1). As a control, low molecular weight polymer (PS-Cp **3**) was initially prepared via this method so that the various chemical transformations could be verified via ^{1}H NMR spectroscopy. Figure 8.4 shows the respective ^{1}H NMR spectra for the different stages of the synthesis.

The bottom spectrum in Figure 8.4 depicts the starting hydroxyl-terminated polymer (PS-OH **3**), clearly indicating the signal arising from the protons in α-position to the hydroxyl group at 3.2 ppm. After the reaction with BPiB (producing PS-Br **3**), this signal is observed to shift to 3.9 ppm and a new signal appears at 4.25 ppm due to the proton in α-position to the bromide moiety, as depicted in the centre spectrum. The upper spectrum of Figure 8.4 shows the polymer resulting from the nucleophilic substitution of PS-Br **3** with NaCp (PS-Cp **3**). The presence of peaks due to the proton in α-position to the Cp ring at 3.5 ppm, the Cp bridge-head protons at 2.9 ppm

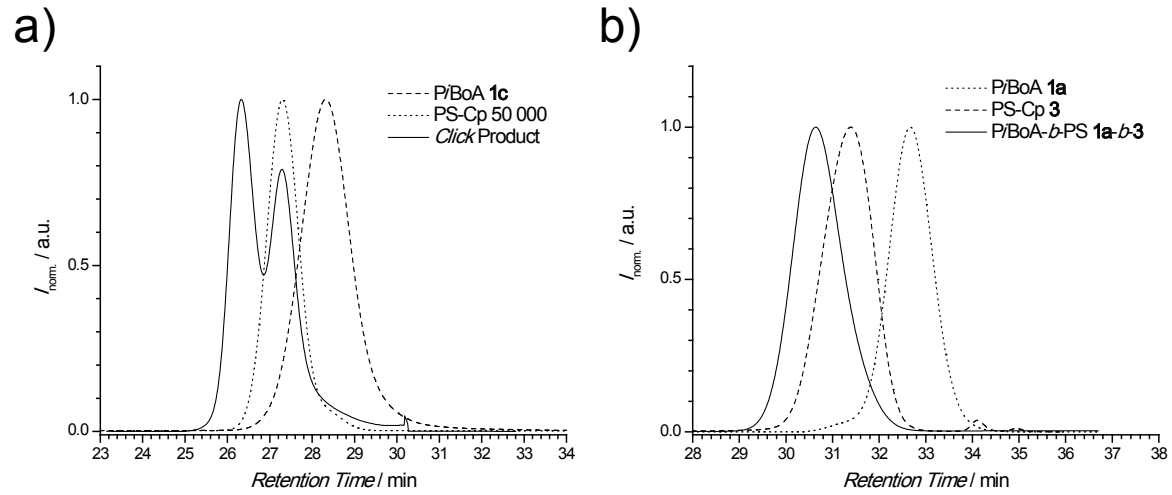

Figure 8.3 a) Overlay of SEC traces showing the initial attempt of synthesizing a high molecular weight P*i*BoA-*b*-PS. In this example, PS-Cp with M_n = 50 000 g·mol^{-1} was synthesized by ATRP; b) Overlay of SEC traces showing the formation of P*i*BoA-*b*-PS **1a**-*b*-**3** from the precursors P*i*BoA **1a** and PS-Cp **3**.

and vinylic protons at around 6.0 ppm are all consistent with the formation of PS-Cp **3**. The final polymer was subsequently reacted with P*i*BoA **1a** and the corresponding block copolymer (P*i*BoA-*b*-PS **1a**-*b*-**3**) was formed successfully, the SEC traces of which are presented in Figure 8.3b. It is noteworthy that the final reaction step of PS-Br **3** with NaCp also resulted in the removal of the dithioester function at the opposite end of the polymer chain, as indicated by the disappearance of the protons of the benzyl group at 7.78 ppm. It is most likely that - being rather a strong base - the Cp anion reacted with the terminal dithioester group and converted it into a thiol. Nevertheless, the clear and complete changes that are observed in the ^{1}H NMR spectra confirm the quantitative nature of each transformation.

As a further validation of the *click* reaction - beyond the data shown in Figure 8.2 and Table 8.1 - the starting polymers and the formed block were characterized by UV/Vis spectroscopy. Figure 8.5a illustrates the comparative absorbance profile of PS-Br **3** and PS-Cp **3**. It can be clearly observed that the absorbance of the dithioester end-group of PS-Br **3** at λ_{max} = 500 nm completely disappears after it is transformed into PS-Cp **3**, further indicating the above mentioned removal of the dithioester end group. Figure 8.5b shows the comparative absorbance profile of P*i*BoA **1a** and the conjugate product P*i*BoA-*b*-PS **1a**-*b*-**3**. The starting dithioester-capped P*i*BoA has a pink colour (λ_{max} = 506 nm) which is due to the presence of the thiocarbonyl moiety. The HDA cycloaddition alters this chromaphoric structure and, thus, the final block copolymer has a distinctly different colour, which is clearly demonstrated.

Having established the validity of this strategy (as outlined in Figure 8.4), high molecular weight PS-Cp **4** was subsequently prepared (M_n = 79 100 g·mol^{-1}, *PDI* = 1.08) and

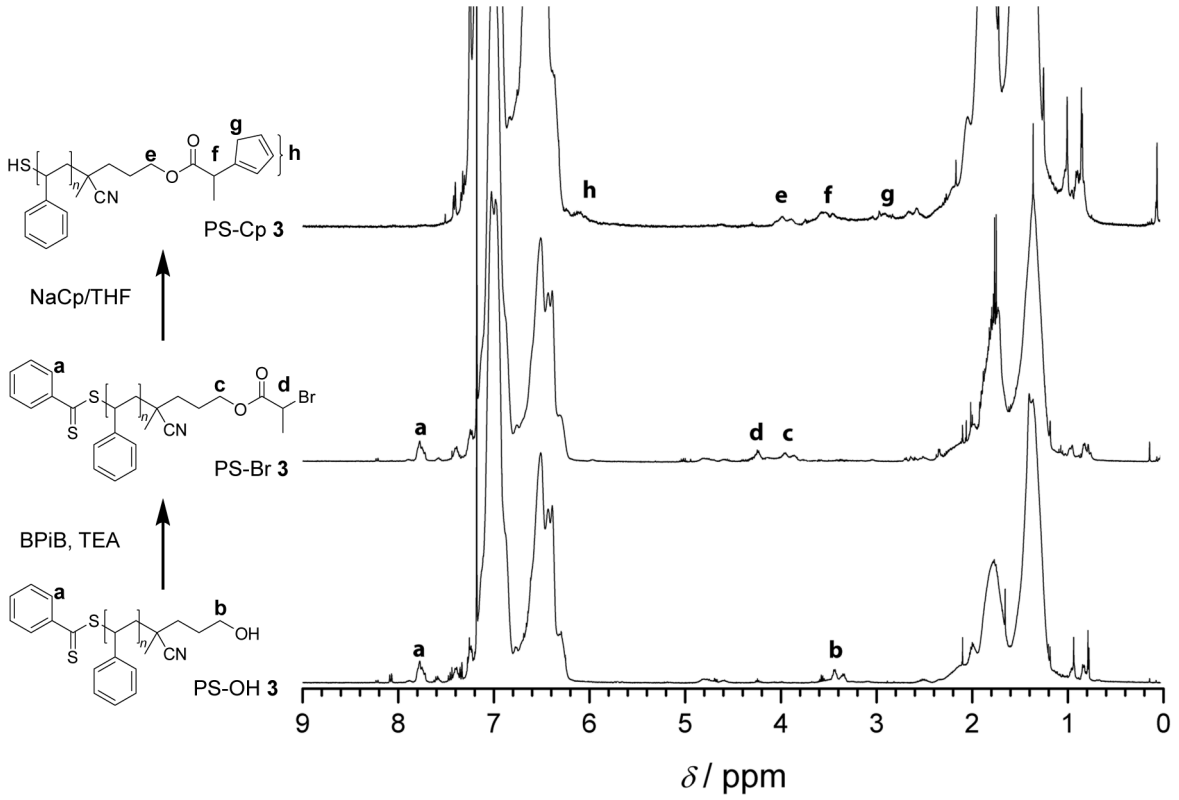

Figure 8.4 Detail of the synthetic pathway from hydroxyl-functionalized PS to Cp-functionalized PS with accompanying ^{1}H NMR spectra for the products of each stage.

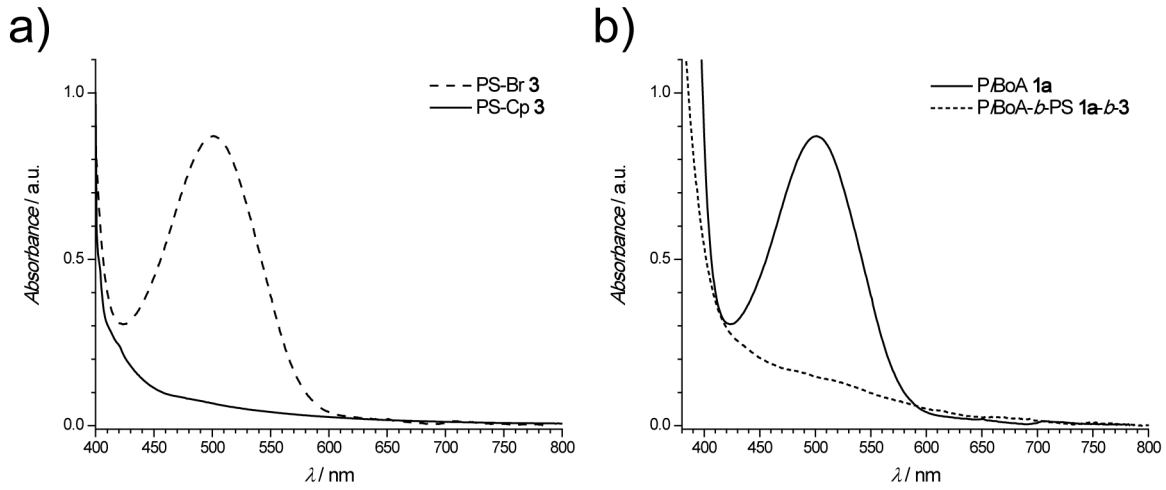

Figure 8.5 Overlay of UV/Vis spectra showing the transformation of a) PS-Br **3** into PS-Cp **3**; and b) P*i*BoA **1a** into the *click* product P*i*BoA-*b*-PS **1a**-*b*-**3**.

reacted with P*i*BoA **1c**. Due to the significantly higher molecular weight, the conjugation reaction was performed under higher dilution and allowed to proceed for 2 hours with vigourous agitation (at ambient temperature). The molecular weight of the resulting block copolymer is in good agreement with the theoretical value (see Table 8.1) and the bottom series of SEC traces in Figure 8.2 shows a clear shift to lower retention time for the *click* product. A minor tailing in the trace of the product towards higher retention times can be observed, indicative of some remaining starting material. However, the degree of tailing is very slight and, taking into consideration the relevant entry in Table 8.1, the high efficiency of the conjugation is thus verified. The molecular weight achieved (100 400 g·mol^{-1}) represents the largest linear block copolymer synthesized in a modular fashion from singly functionalized building blocks.

8.4 Conclusion

The results presented herein successfully extend block copolymer synthesis via a modular approach to unprecedentedly high molecular weights. Through the use of CRP techniques and RAFT-HDA *click* chemistry, PS-*b*-P*i*BoA copolymers were synthesized with molecular weights ranging from 34 000 g·mol^{-1} to over 100 000 g·mol^{-1} at ambient temperature in short reaction times. It has been shown that through the use of efficient synthetic strategies that extend beyond the final *click* reaction, the construction of large molecular weight macromolecules from singly functionalized materials is possible and provides further proof of the versatility of modular synthetic approaches in macromolecular engineering.

References

[1] Binder, W. H.; Sachsenhofer, R. *Macromol. Rapid Commun.* **2007**, *28*, 15–54.

[2] Binder, W. H.; Sachsenhofer, R. *Macromol. Rapid Commun.* **2008**, *29*, 952–981.

[3] Evans, R. A. *Aust. J. Chem.* **2007**, *60*, 384–395.

[4] Coessens, V.; Matyjaszewski, K. *J. Macromol. Sci., Pure Appl. Chem.* **1999**, *A36*, 667–679.

[5] Lutz, J. F.; Matyjaszewski, K. *J. Polym. Sci., Part A: Polym. Chem.* **2005**, *43*, 897–910.

[6] Jakubowski, W.; Kirci-Denizli, B.; Gil, R. R.; Matyjaszewski, K. *Macromol. Chem. Phys.* **2008**, *209*, 32–39.

[7] Opsteen, J. A.; van Hest, J. C. M. *Chem. Commun.* **2005**, 57–59.

[8] Quémener, D.; Davis, T. P.; Barner-Kowollik, C.; Stenzel, M. H. *Chem. Commun.* **2006**, 5051–5053.

[9] Dervaux, B.; Van Camp, W.; Van Renterghem, L.; Du Prez, F. E. *J. Polym. Sci., Part A: Polym. Chem.* **2008**, *46*, 1649–1661.

[10] Clouet, G.; Knipper, M.; Brossas, J. *Polym. Bull.* **1984**, *11*, 171–174.

[11] Thang, S. H.; Chong, Y. K.; Mayadunne, R. T. A.; Moad, G.; Rizzardo, E. *Tetrahedron Lett.* **1999**, *40*, 2435–2438.

[12] Lima, V.; Jiang, X. L.; Brokken-Zijp, J.; Schoenmakers, P. J.; Klumperman, B.; Van Der Linde, R. *J. Polym. Sci., Part A: Polym. Chem.* **2005**, *43*, 959–973.

9

Versatile Synthesis of Cyclopentadienyl-Functional Materials

9.1 Introduction

The ability to generate very well-defined end-group functional macromolecules is a central theme in modern polymer synthesis. Arguably being the most convenient and effective technique whereby such structures may be synthesized is CRP, in particular ATRP[1] and RAFT polymerization.[2] In the simplest case, the polymerization of a monomer by either of these techniques results in polymer chains bearing precisely controlled end-groups (a halide in the case of ATRP, or a thiocarbonyl thio moiety in the case of RAFT) which may then be subsequently utilized to polymerize a second monomer, directly yielding the corresponding block copolymer.[3, 4] More recently, however, much attention has been drawn to the use of such technology to impart additional functionality onto the ends of polymer chains, typically within the context of polymer conjugative chemistry (*click* chemistry).[5]

The use of a CRP process alone or in conjunction with some form of pre- or post-polymerization transformation (such as nucleophilic substitution or esterification) has enabled the generation of a wide variety of polymer chains that bear such functionalities as azide,[6] alkyne,[7] alkene,[8] thiol,[9] hydroxyl,[10, 11] amine[12] and carboxyl[13] to name but a few. Now, with the almost ubiquitous presence of *click* chemistry within

the field of CRP, along with a more generic demand for functional polymers, the development of the technologies involved in preparing such functional macromolecules is becoming increasingly important.

Imparting cyclopentadienyl (Cp) functionality onto polymer chains can be a challenging exercise, owing to its high reactivity. Yet, such structures would find enormous applicability in the direct catalyst-free and ambient temperature functionalization of such intensely investigated materials as fullerenes, carbon nanotubes and graphenes. Unlike other polymer conjugation technologies, the use of Cp-functional polymers in Diels-Alder reactions with the wide variety of available dienophiles would allow one to have precise control over the conditions under which chemical linkages are formed and broken. The beginnings of this concept were realized in Chapters 7 and 8 with the use of Cp-functional polymers in ultra-fast polymer conjugations. Despite this, there have only been very few and rather limited examples of imparting Cp functionality onto polymeric materials reported in the literature.

In organic synthesis, the predominant method for preparing substituted cyclopentadienes has been the nucleophilic substitution of alkyl halides or tosylates with sodium cyclopentadienide (NaCp).[14–16] Other possibilities include the use of oxycylopentadienyl dianions[17] or cyclopentadienylmagnesium bromide as a Grignard reagent.[18] In polymer chemistry, there have been numerous reports on the functionalization of chloromethylated poly(styrene)-divinylbenzene resin with a Cp end-group for use in Diels-Alder reactions with fullerenes.[19–21] Another approach, reported by Müllen and colleagues[22] involved the addition of NaCp to poly(styrene) (PS) bearing partial chloromethyl functionality along the polymer chain to yield the corresponding Cp-functional polymer. In a further example from the same authors, dimethylfulvene was added to the lithiated aromatic rings of a PS chain to also impart Cp functionality.[23] As alluded to earlier, the functionalization of PS prepared by ATRP and poly(ethylene glycol) monomethyl ether with NaCp through nucleophilic substitution of the respective bromide and tosylated end-groups was presented in Chapters 7 and 8.

Although being successful, the above polymeric systems have lacked other chemical functionality that could potentially participate in side reactions with NaCp. Although Mrksich et al.[24] reported the addition of NaCp to methyl bromoacetate to yield the corresponding methyl ester functional Cp derivative, NaCp can also participate in a reaction with esters in which the alkoxy substituent is replaced by the Cp anion.[25, 26] NaCp also reacts with other carbonyl containing compounds (ketones and aldehydes) to yield fulvenes.[27] Furthermore, Sillion et al. presented an excellent model study of the reaction of NaCp with benzyl bromide, the results of which indicated that numerous side reactions take place.[28]

A comparatively little explored method to achieve Cp functionalization is the use of nickelocene ($NiCp_2$) as the substituting agent. Characterized by a rather covalent Ni-

Cp bond, $NiCp_2$ may be considered to be a much less harsh reagent when compared to NaCp, which is much more ionic in nature. $NiCp_2$ has been successfully used in the synthesis of highly crowded Cp derivatives,[29] Cp ligands bearing fluorinated 'ponytails',[30] and has been proven to be efficient in the preparation of Cp-functional polymeric supports (such as Merrifield's resin).[31] The decision to use $NiCp_2$ in these applications was borne out of consideration of the various ill-desired side reactions that are encountered via the use of NaCp. Selective substitution of halogenated esters via the $NiCp_2$ route has, however, not been reported.

Herein, the effectiveness of $NiCp_2$ in quantitatively converting a variety of bromide end-functional polymers into the corresponding Cp functional polymers at ambient temperature without any side product formation is reported (Figure 9.1). A comparison of this strategy with one involving the use of NaCp is presented for ATRP prepared PS, poly(methyl methacrylate) (PMMA), poly(methyl acrylate) (PMA) and poly(isobornyl acrylate) (P*i*BoA).

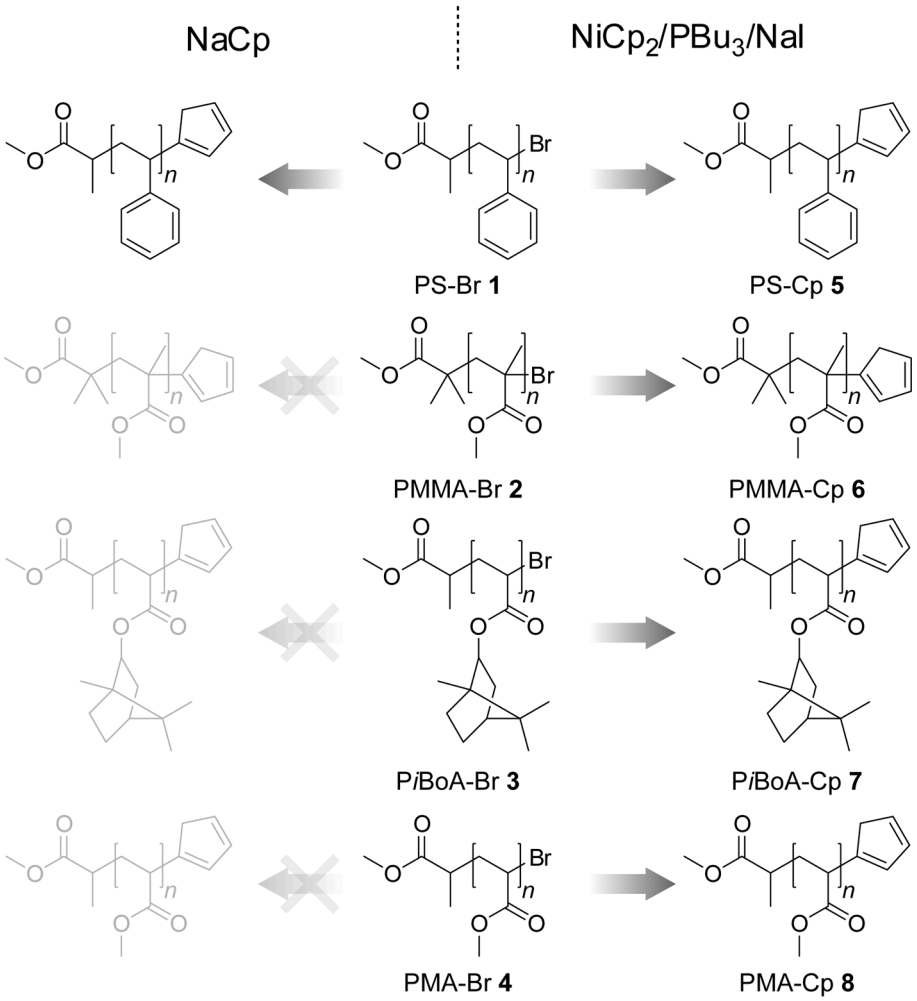

Figure 9.1 General synthetic strategy to cyclopentadienyl functionalization of polymer chains.

9.2 Experimental Section

ATRP of Styrene

To a dried Schlenk tube was added copper (I) bromide, which was then sealed with a rubber septum, evacuated and backfilled with nitrogen. To another Schlenk tube was added styrene and PMDETA and equipped with a rubber septum. The monomer/ligand mixture was then deoxygenated by three consecutive freeze-pump-thaw cycles and subsequently transferred to the copper (I) bromide via cannula. The tube was sealed under a nitrogen atmosphere and placed in a thermostatic oil bath held at 90 °C. After the polymerization mixture reached the desired temperature, methyl 2-bromopropanoate (MBP) was added. The initial ratio of [styrene]:[MBP]:[CuBr]:[PMDETA] was 100:1:1:1. The polymerization was stopped by cooling the mixture in an ice-bath and exposure to oxygen. After dilution with THF, the mixture was passed through a short column of neutral alumina to remove the copper catalyst. PS was isolated by two-fold precipitation in cold methanol. SEC (THF): M_n = 1600 g·mol^{-1}, *PDI* = 1.06.

ATRP of Methyl Methacrylate

To a dried Schlenk tube was added copper (I) bromide, copper (II) bromide and 2,2'-bipyridine (bpy) which was then sealed with a rubber septum, evacuated and backfilled with nitrogen. To another Schlenk tube was added methyl methacrylate (MMA) and acetone (50:50) and equipped with a rubber septum. The monomer solution was then deoxygenated by three consecutive freeze-pump-thaw cycles and subsequently transferred to the first Schlenk tube via cannula. The tube was sealed under a nitrogen atmosphere and placed in a thermostatic oil bath held at 50 °C. After the polymerization mixture reached the desired temperature, methyl 2-bromo-2-methylpropanoate (MBMP) was added. The initial ratio of [MMA]:[MBMP]:[CuBr]:[$CuBr_2$]:[bpy] was 50:2:0.105:0.0125:0.25. The polymerization was stopped by cooling the mixture in an ice-bath and exposure to oxygen. The mixture was passed through a short column of neutral alumina to remove the copper catalyst. PMMA was isolated by two-fold precipitation in cold *n*-hexane. SEC (THF): M_n = 2700 g·mol^{-1}, *PDI* = 1.09.

ATRP of Isobornyl Acrylate

To a dried Schlenk tube was added copper (I) bromide which was then sealed with a rubber septum, evacuated and backfilled with nitrogen. To another Schlenk tube was added isobornyl acrylate (*i*BoA) and ethyl acetate (4:1) along with PMDETA

and equipped with a rubber septum. The monomer solution was then deoxygenated by three consecutive freeze-pump-thaw cycles and subsequently transferred to the first Schlenk tube via cannula. The tube was sealed under a nitrogen atmosphere and placed in a thermostatic oil bath held at 77 °C. After the polymerization mixture reached the desired temperature, MBP was added. The initial ratio of [*i*BoA]:[MBP]:[CuBr]:[PMDETA] was 100:1:0.5:0.75. The polymerization was stopped by cooling the mixture in an ice-bath and exposure to oxygen. The mixture was passed through a short column of neutral alumina to remove the copper catalyst. P*i*BoA was isolated by two-fold precipitation in cold methanol. SEC (THF): M_n = 4200 g·mol^{-1}, *PDI* = 1.22.

ATRP of Methyl Acrylate

To a dried Schlenk tube was added copper (I) bromide and bpy, which was then sealed with a rubber septum, evacuated and backfilled with nitrogen. To another Schlenk tube was added methyl acrylate (MA) and anisole (67:33) and equipped with a rubber septum. The monomer solution was then deoxygenated by three consecutive freeze-pump-thaw cycles and subsequently transferred to the copper (I) bromide via cannula. The tube was sealed under a nitrogen atmosphere and placed in a thermostatic oil bath held at 90 °C. After the polymerization mixture reached the desired temperature, MBP was added. The initial ratio of [MA]:[MBP]:[Cu(I)Br]:[bpy] was 200:1:1:2. The polymerization was stopped by cooling the mixture in an ice-bath and exposure to oxygen. After dilution with THF, the mixture was passed through a short column of neutral alumina to remove the copper catalyst. PMA was isolated by two-fold precipitation in cold methanol. SEC (THF): M_n = 2800 g·mol^{-1}, *PDI* = 1.29.

Reaction of Bromide Terminated Polymers with NaCp - Typical Procedure

A solution of bromide terminated polymer (0.18 mmol) in anhydrous THF (2.0 mL) was prepared under a nitrogen atmosphere. To this solution was added a 2-fold excess, and in a second experiment a 10-fold excess, of NaCp. The reaction mixture was stirred overnight at ambient temperature. The polymeric material was then isolated by precipitation in an appropriate solvent.

Reaction of Bromide Terminated Polymers with $NiCp_2$ - Typical Procedure

A solution of bromide terminated polymer (0.18 mmol), tributylphosphine (0.36 mmol, 2 equiv.) and sodium iodide (1.08 mmol, 6 equiv.) in anhydrous THF (2.0 mL) was prepared under a nitrogen atmosphere. Separately, a stock solution of

$NiCp_2$ in anhydrous THF (0.18 mol·L^{-1}) was prepared under a nitrogen atmosphere. The $NiCp_2$ solution (2.0 mL, 4 equiv.) was then added to the polymer solution and allowed to stir overnight at ambient temperature. At the end of the reaction, the mixture was passed through a short column of basic alumina to remove the precipitated nickel (II) bromide and the polymer recovered by precipitation. The resulting polymer was then dissolved in chloroform and washed three times with distilled water. The Cp-functional polymers were then isolated by precipitation from the chloroform solution into an appropriate solvent.

9.3 Results and Discussion

9.3.1 Reactions with NaCp

Extrapolating from the immediately preceding chapters, the use of NaCp to achieve the desired substitution reaction was initially trialled on PS-Br **1**, PMMA-Br **2**, P*i*BoA-Br **3** and PMA-Br **4** (Figure 9.1). ATRP was performed to low monomer conversions (< 30 %) to ensure a high bromide end-group fidelity of the above mentioned polymers. The molecular weight assessments for these starting polymers are included in Table 9.1.

Figure 9.2 depicts the ^{1}H NMR spectra of the reaction products from the treatment of PS-Br **1** with a 2-fold excess and a 10-fold excess of NaCp. It may be observed that using a 2-fold excess does produce the desired Cp-capped polymer, however a small amount of starting material remains, as indicated by the presence of a signal (labelled e*) at around 4.5 ppm. Using a 10-fold excess produces quantitative conversion into the desired Cp-capped polymer, a result which is consistent with the findings presented in Chapter 7.

Despite this favourable result, the use of NaCp with the poly(acrylates) and poly(methacylate) proved to be problematic. Figure 9.3 shows the ESI-MS spectra of PMMA-Br **2** and those of the respective reaction products after treatment with a 2-fold excess and a 10-fold excess of NaCp. As can clearly be observed, a number of different products are formed, none of which are the desired Cp-capped polymer (marked by the dotted lines). It is interesting to note that higher excesses of the NaCp leads to the formation of different products. As of yet, the products cannot be conclusively identified and, not being the principal focus of the current investigation, these

Table 9.1 Polymer characterization.[a]

polymer	$M_{n,\,SEC}$[b] / g·mol^{-1}	PDI[c]
PS-Br **1**	1600	1.06
PMMA-Br **2**	2700	1.09
P*i*BoA-Br **3**	4200	1.22
PMA-Br **4**	2800	1.29

[a]Measured by SEC in THF against linear PS standards [b]Values have been corrected by applying the Mark-Houwink-Sakurada relationship PMMA: $K = 12.8 \times 10^{-5}$ dL·g^{-1}, $\alpha = 0.690$; P*i*BoA : $K = 5.00 \times 10^{-5}$ dL·g^{-1}, $\alpha = 0.745$); PMA: $K = 8.35 \times 10^{-5}$ dL·g^{-1}, $\alpha = 0.768$). [c]Polydispersity index.

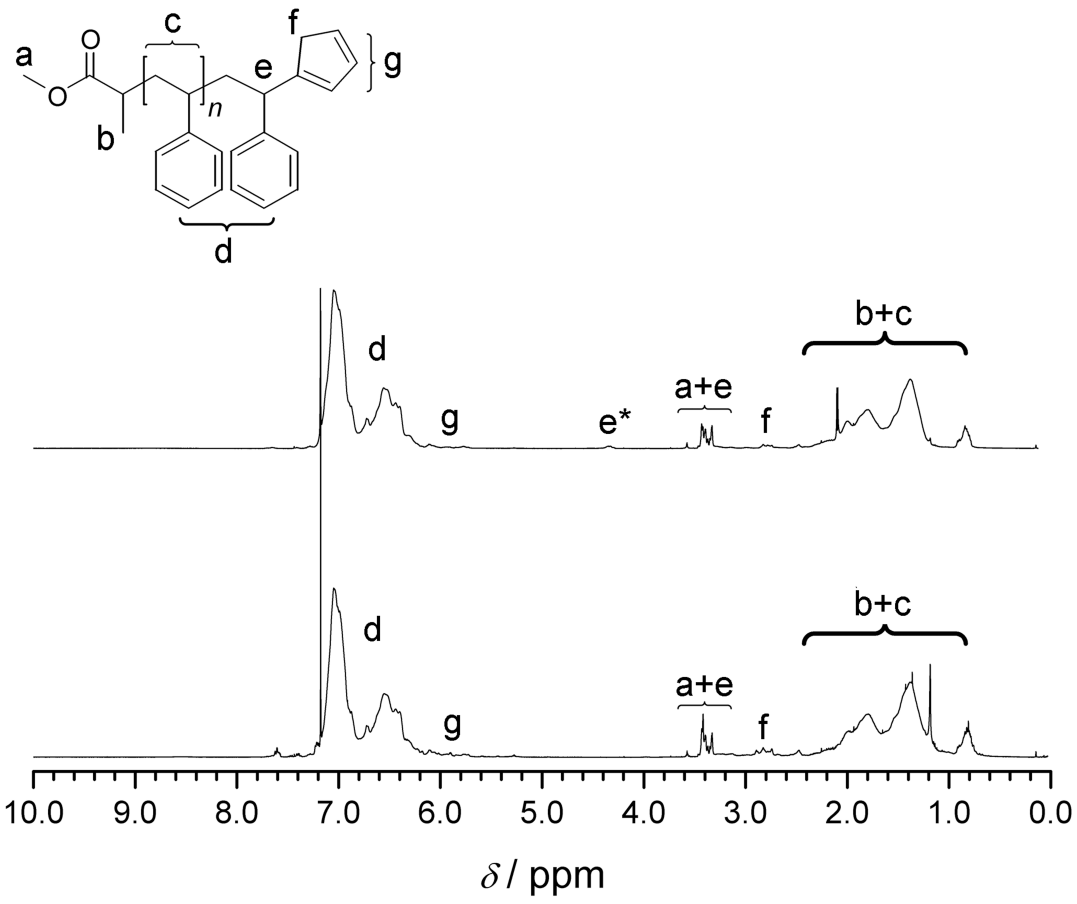

Figure 9.2 ^{1}H NMR spectra of the reaction products of PS-Br **1** with a 2-fold excess (top) and a 10-fold excess (bottom) of NaCp. The signal labelled *e** represents the α-bromo proton of remaining starting material.

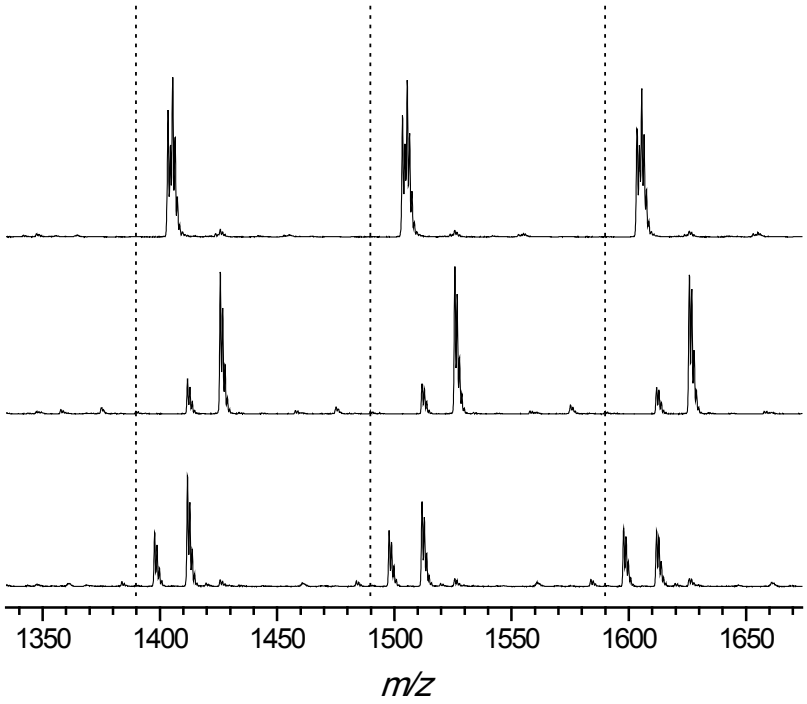

Figure 9.3 ESI-MS spectra of PMMA-Br **2** (top) and the reaction products after treatment with a 2-fold excess(middle) and a 10-fold excess (bottom) of NaCp. The dotted lines represent the *m/z* values at which the desired Cp-functional polymer is expected.

products remain as unidentified. However, the analysis still clearly shows that NaCp cannot be used to achieve the desired outcome.

Figure 9.4 compares the ESI-MS spectra of P*i*BoA-Br **3** and the reaction product after treatment with a 10-fold excess of NaCp. Similarly, a number of unidentified products are observed. It should also be noted that precipitation of the polymer after the treatment proved to be problematic and the recorded spectra was of the solid residue remaining after the reaction mixture solvent was removed under reduced pressure.

Figure 9.5 depicts the ESI-MS spectra of the PMA-Br **4** and those of the reaction products after treatment with a 2-fold excess and a 10-fold excess of NaCp. Interestingly, using a 2-fold excess of NaCp, the dominant series have *m/z* values that are in excellent agreement with the theoretical values of the required Cp-capped polymer. However none of the characteristic signals arising from a Cp-moiety were detected in the ^{1}H NMR spectrum. Increasing to a 10-fold excess, however, results in the formation of many more (unidentified) and different side-products. It should be noted here that ^{1}H NMR spectra were recorded for all NaCp experiments, however none revealed any signals characteristic of a Cp-moiety (excluding the PS example).

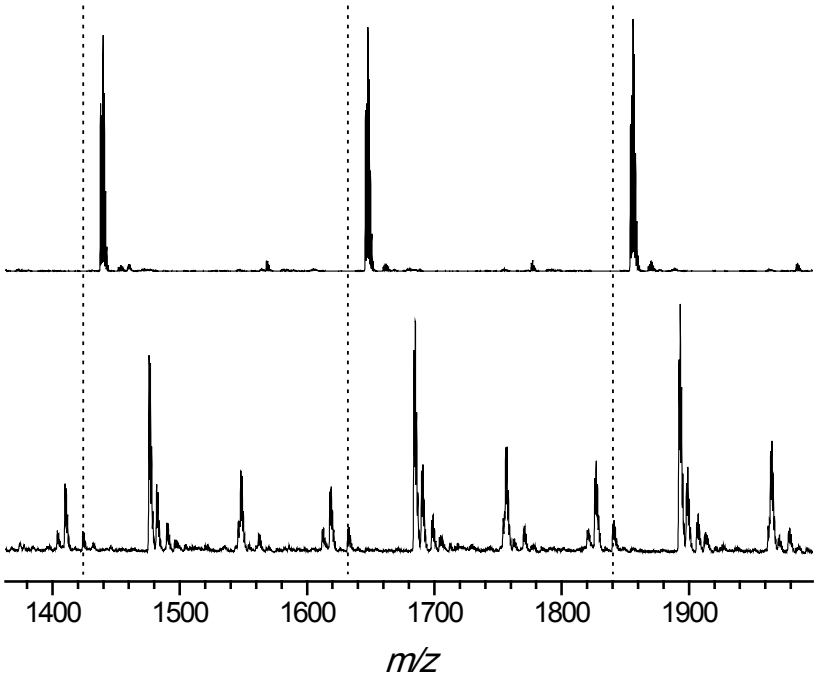

Figure 9.4 ESI-MS spectra of P*i*BoA-Br **3** (top) and the reaction product after treatment with a 10-fold excess (bottom) of NaCp. The dotted lines represent the *m/z* values at which the desired Cp-functional polymer is expected.

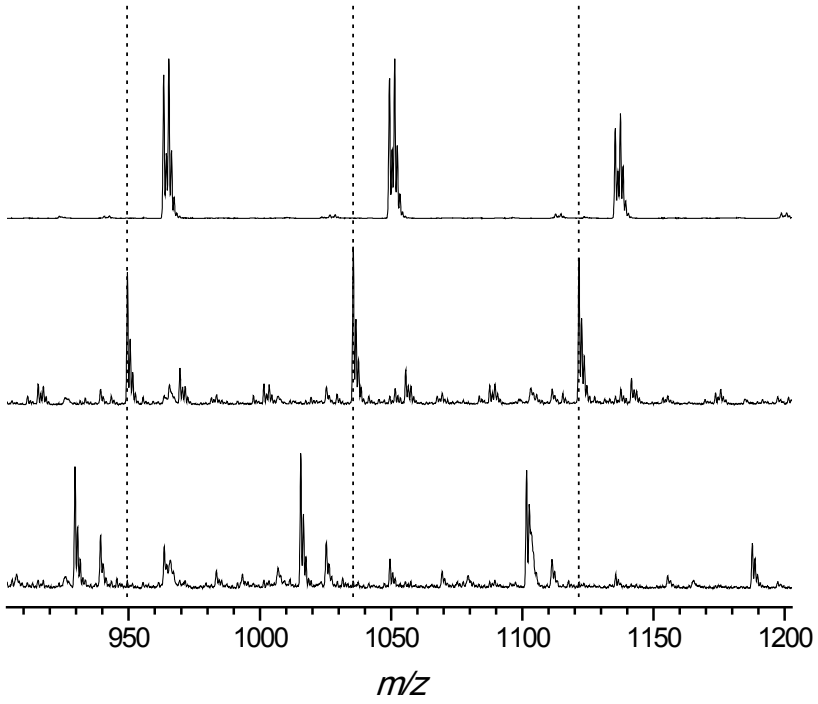

Figure 9.5 ESI-MS spectra of PMA-Br **4** (top) and the reaction products after treatment with a 2-fold excess (middle) and a 10-fold excess (bottom) of NaCp. The dotted lines represent the *m/z* values at which the desired Cp-functional polymer is expected.

9.3.2 Reactions with $NiCp_2$

In need of an alternate pathway, the use of $NiCp_2$ as the source of the Cp unit was considered (Figure 9.1). It has previously been encountered that in performing the chloride/bromide to Cp transformation with $NiCp_2$ alone, sluggish reaction times or indeed no reaction at all can be observed. However, it has been documented that the addition of triphenylphosphine and sodium iodide as a halogen metathesis reagent (if required) greatly enhances the substitution reaction.[30, 31] As such, this approach was applied in the present circumstance.

In a typical experiment; the bromide terminated polymer, sodium iodide (6.0 equiv.) and, in this case, tributylphosphine (PBu3, 2.0 equiv.) were dissolved in anhydrous THF under a nitrogen atmosphere. To the resulting mixture, a solution of $NiCp_2$ (4.0 equiv.) also in anhydrous THF was added and the now green solution was allowed to stir overnight at ambient temperature. The progression of the reaction is characterized by the change in solution colour to deep purple and the precipitation of nickel (II) bromide. It was interesting to observe that the change from green to purple occurred within the space of seconds for the poly(acrylates); a few minutes for the poly(methacrylate) and a few hours for the poly(styrene). At the end of the reaction, the mixture was passed through a short column of basic alumina and precipitated in an appropriate solvent. Chloroform solutions of the recovered polymers were then subjected to a water wash, after which the purified polymers were recovered once again by precipitation. This procedure was also performed on a 10 g scale with identical results obtained. The molecular weight assessments for the starting polymers are included in Table 9.2.

The reaction of PS-Br **1** with the $NiCp_2/PBu_3/NaI$ reagent cleanly led to the required PS-Cp **5**, as clearly shown by the ^1H NMR spectroscopic analysis (Figure 9.6). It is noted that the bottom ^1H NMR spectrum presented in Figure 9.6 is identical to that presented in the bottom of Figure 9.2, which corresponds to the same transformation, however utilizing the NaCp route. This example provides the inital proof that $NiCp_2$ may be used to substitute a bromide functionality for a Cp functionality on a polymer chain-end. Whether this process may be applied to polymers with potentially cross-reactive moieties, the followíng examples must show.

Figure 9.7 depicts the ESI-MS spectra of the starting PMMA-Br **2** alongside that of the reaction product, PMMA-Cp **6**. The dominant species in the spectrum of the starting material is clearly the required bromide-terminated polymer. One may also observe the presence of a small quantity of impurities, all but one of which can be assigned to inescapable side-products of the ATRP process and have been previously encountered in the literature.[32] The remaining unidentified product may be inferred to be another bromide-terminated species, based upon the characteristic isotopic pattern of

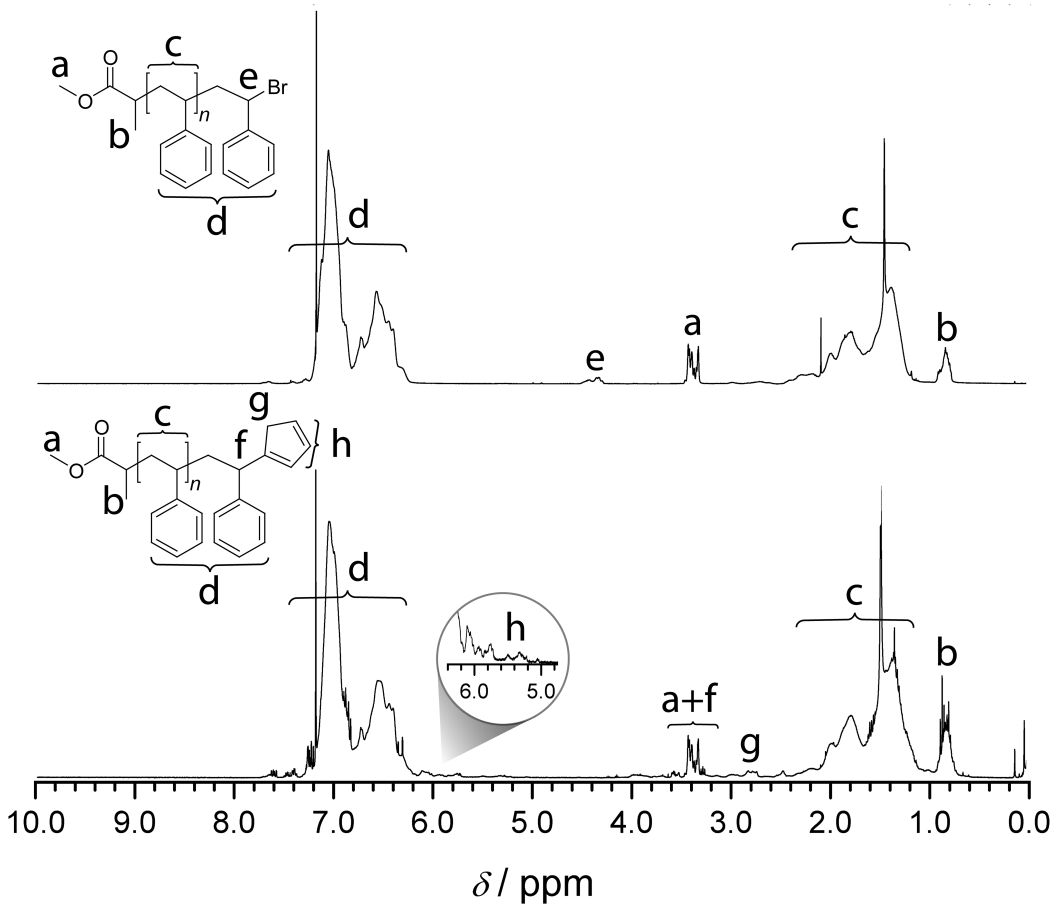

Figure 9.6 ^{1}H NMR spectra of PS-Br **1** (top) and PS-Cp **5** (bottom).

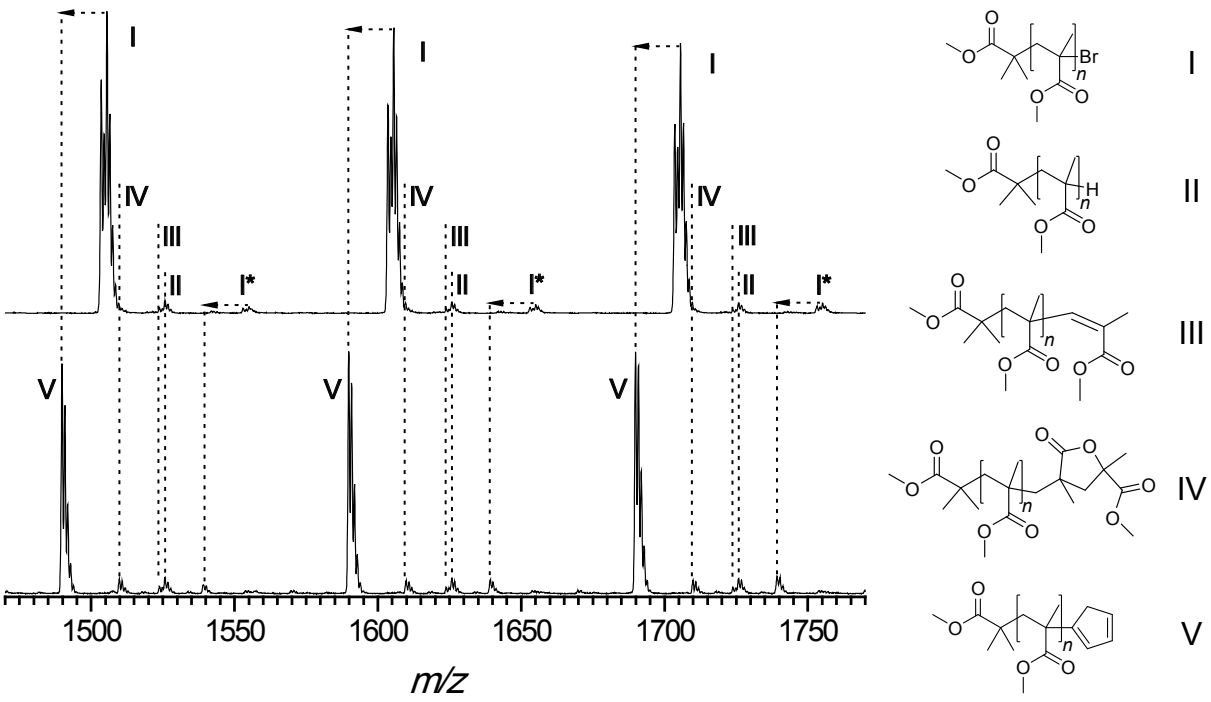

Figure 9.7 ESI-MS spectra of PMMA-Br **2** (top) and PMMA-Cp **6** (bottom).

its signal. Regardless, the ATRP-derived side products are of no significance in the investigation of this concept. After the transformation, the signals for all bromide-terminated species are observed to shift to lower *m/z* values in accordance with the formation of the desired Cp-functional species. Figure 9.8 illustrates a zoom region (*m/z* = 1480-1576) of Figure 9.7, which further clarifies the efficient transformation. Specific molecular ion assignments are presented in Table 9.2. It is highlighted here that the side-products of the ATRP are carried through the functionalization procedure, thus the presented ESI-MS data confirms the quantitative transformation.

The results of a ^{1}H NMR spectroscopic analysis (Figure 9.9) reveal that Cp-functionality has indeed been imparted to the polymer chain by virtue of the appear-

Table 9.2 Experimental and theoretical *m/z* values for the first peak in the isotopic distributions of the zoom spectrum in Figure 9.8 and their assignment.

$m/z_{\text{expt.}}$	ion assignment	formula	$m/z_{\text{theor.}}$	$\Delta m/z$
1503.5	$\mathbf{2}_{(n=13)} + Na^+$	$[C_{70}H_{113}BrO_{28}Na]^+$	1503.7	0.2
1489.8	$\mathbf{6}_{(n=13)} + Na^+$	$[C_{75}H_{118}O_{28}Na]^+$	1489.8	0.0
1525.8	**II** + Na^+	$[C_{75}H_{122}O_{30}Na]^+$	1525.8	0.0
1523.8	**III** + Na^+	$[C_{75}H_{120}O_{30}Na]^+$	1523.8	0.0
1509.6	**IV** + Na^+	$[C_{74}H_{118}O_{30}Na]^+$	1509.8	0.2
1553.0	**V*** + Na^+	-	-	-

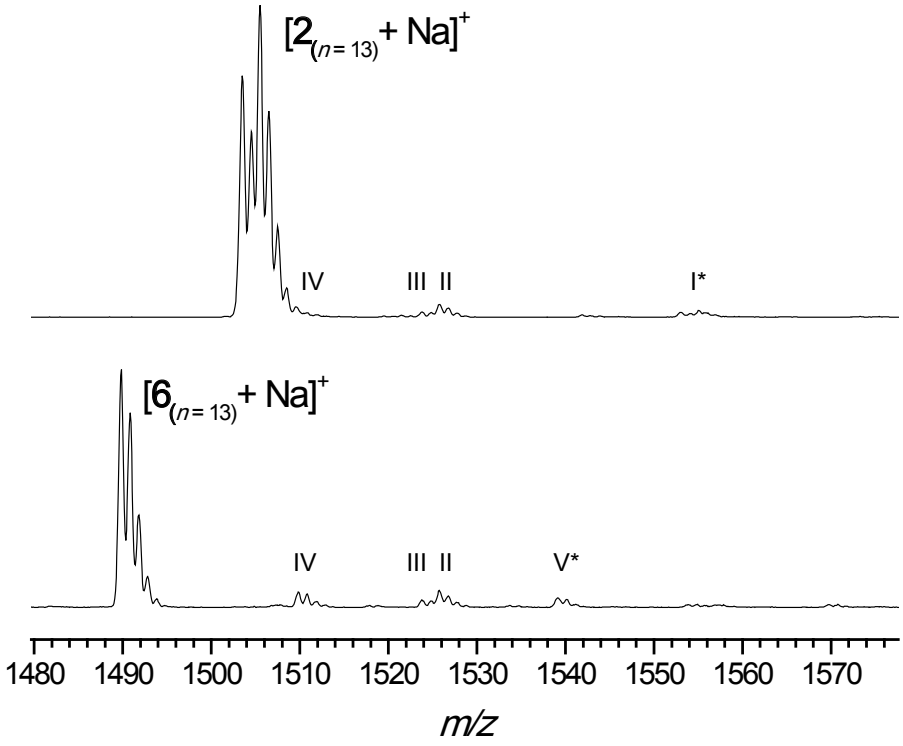

Figure 9.8 ESI-MS spectra (1480 - 1576 *m/z* zoom region) of PMMA-Br **2** (top) and PMMA-Cp **6** (bottom). Note the clear change in the isotopic pattern from bromide terminated species to Cp-terminated species that occurs. The roman-numeric labelling is carried over from Figure 9.7.

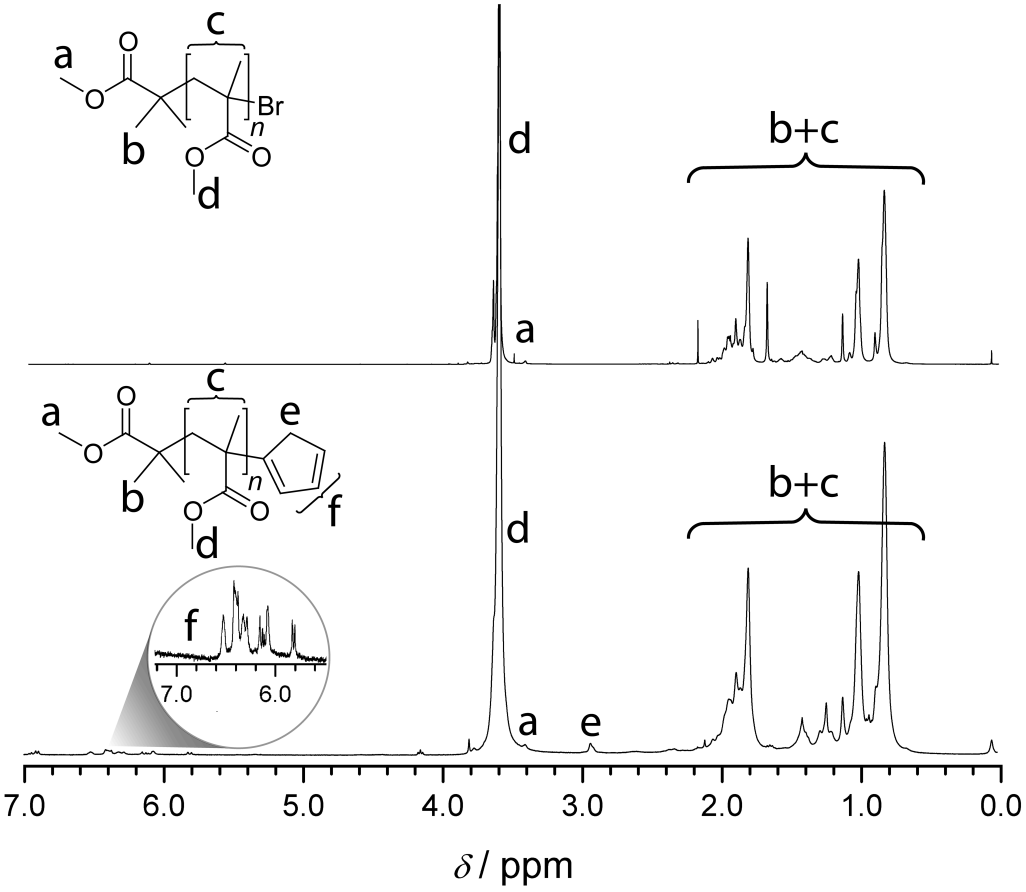

Figure 9.9 ^{1}H NMR spectra of PMMA-Br **2** (top) and PMMA-Cp **6** (bottom).

ance of characteristic signals at 6.6-5.8 ppm and 2.9 ppm. It should be noted here that although the reaction product contains a mixture of the 1-, 2- and 5- substituted cyclopentadienes, only the chemical structure for the 1-isomer is presented for reasons of brevity.

Similar success was also achieved in the case of P*i*BoA. Figure 9.10 depicts the ESI-MS spectra recorded for the starting P*i*BoA-Br **3** and the substitution product P*i*BoA-Cp **7**. Comparable to the PMMA example, a number of unidentified side-products are present resulting from the ATRP process; however these are present in very minor quantities. Nevertheless, a clear and complete transformation is observed. Figure 9.11 presents a zoom region (*m/z* = 1590-1820) of Figure 9.10. The signal labeled *a* is assigned to an unidentified (yet bromide containing) species. The experimental *m/z* values are compared to those of the theoretical structures in Table 9.3. It is observed that the signal labeled *a* shifts to lower *m/z* values in agreement with a transformation from bromide to Cp functionality (signal labelled as *a**). Upon close inspection of the data presented in Table 9.3, the *m/z* value of *a** is close to that of **3**. However, the change in the isotopic pattern that occurs from *a* to *a** leads to the conclusion that **3** and *a** are different species. Therefore, the quantitative transformation is confirmed.

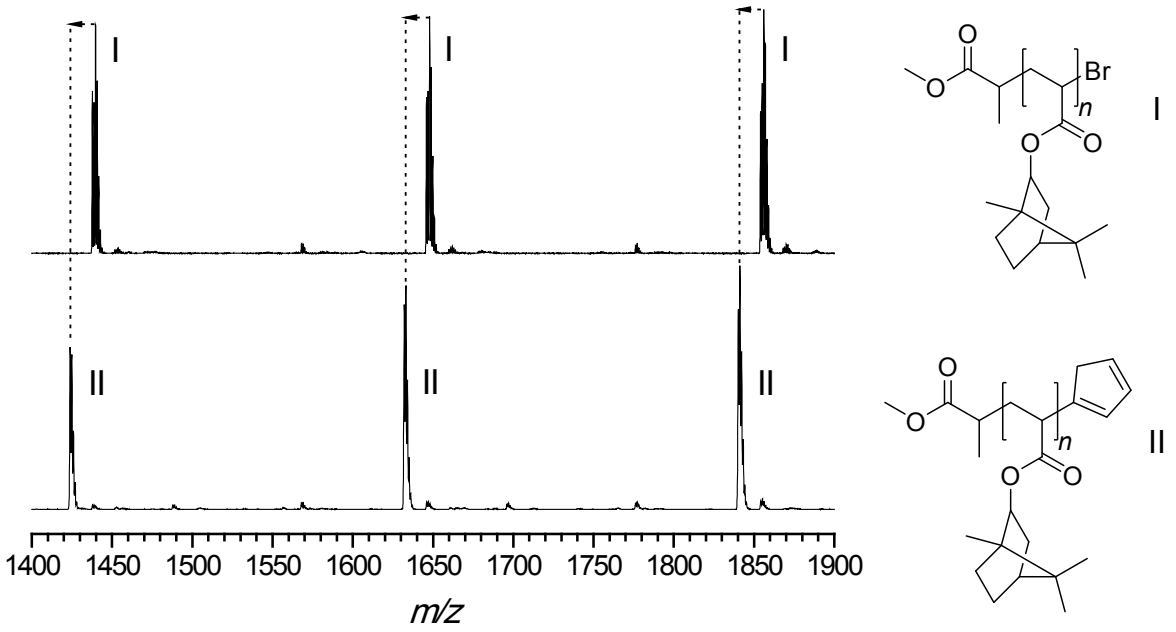

Figure 9.10 ESI-MS spectra of P*i*BoA-Br **3** (top) and P*i*BoA-Cp **7** (bottom).

The above substitution was further confirmed via ^{1}H NMR spectroscopy, the results of which are presented in Figure 9.12. The signal for the proton (in α-position to the bromide terminus) appearing at 4.1 ppm is observed to completely shift to 3.4 ppm after the substitution. The characteristic Cp signals at 6.4-5.8 ppm and 2.9 ppm are also clearly observed, nicely complementing the ESI-MS analysis and thus proving the efficient functionalization of the polymer.

Table 9.3 Experimental and theoretical *m/z* values for the first peak in the isotopic distributions of the zoom spectrum in Figure 9.11 and their assignment.

$m/z_{\text{expt.}}$	ion assignment	formula	$m/z_{\text{theor.}}$	$\Delta m/z$
1645.9	$\mathbf{3}_{(n=7)} + Na^+$	$[C_{95}H_{147}BrO_{16}Na]^+$	1650.0	0.1
1659.8	**a**	-	-	-
1632.1	$\mathbf{7}_{(n=7)} + Na^+$	$[C_{100}H_{152}O_{16}Na]^+$	1632.1	0.0
1646.1	**a***	-	-	-

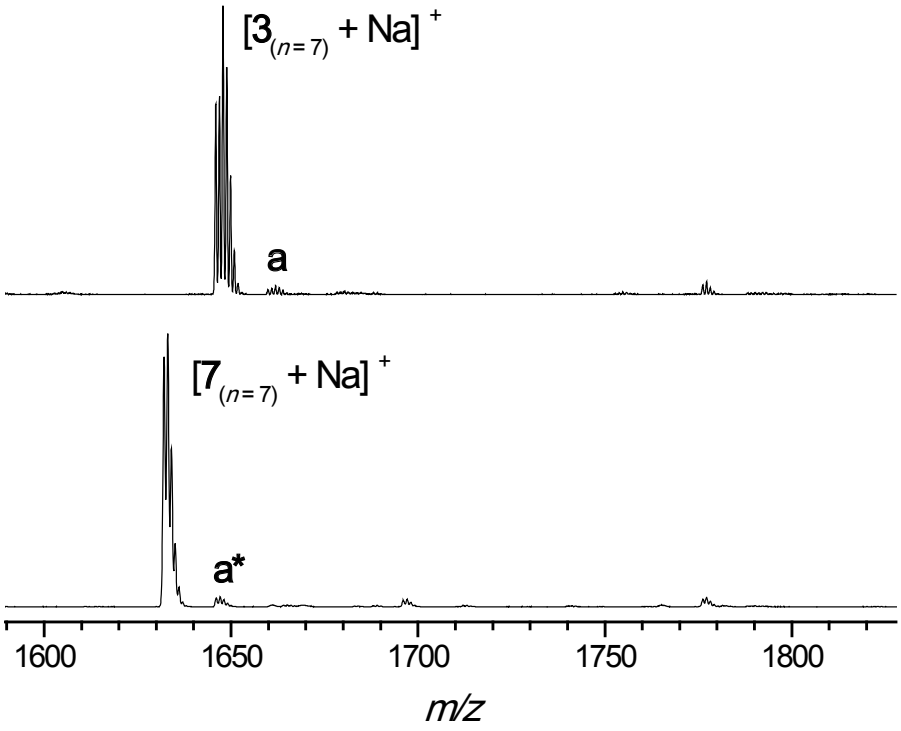

Figure 9.11 ESI-MS spectra (1590 - 1820 *m/z* zoom region) of P*i*BoA-Br **2** (top) and P*i*BoA-Cp **7** (bottom). Note the clear change in the isotopic pattern from bromide terminated species to Cp-terminated species that occurs. The signals labelled **a** and **a*** indicate an un-identified, yet bromide functional species and its substitution product respectively.

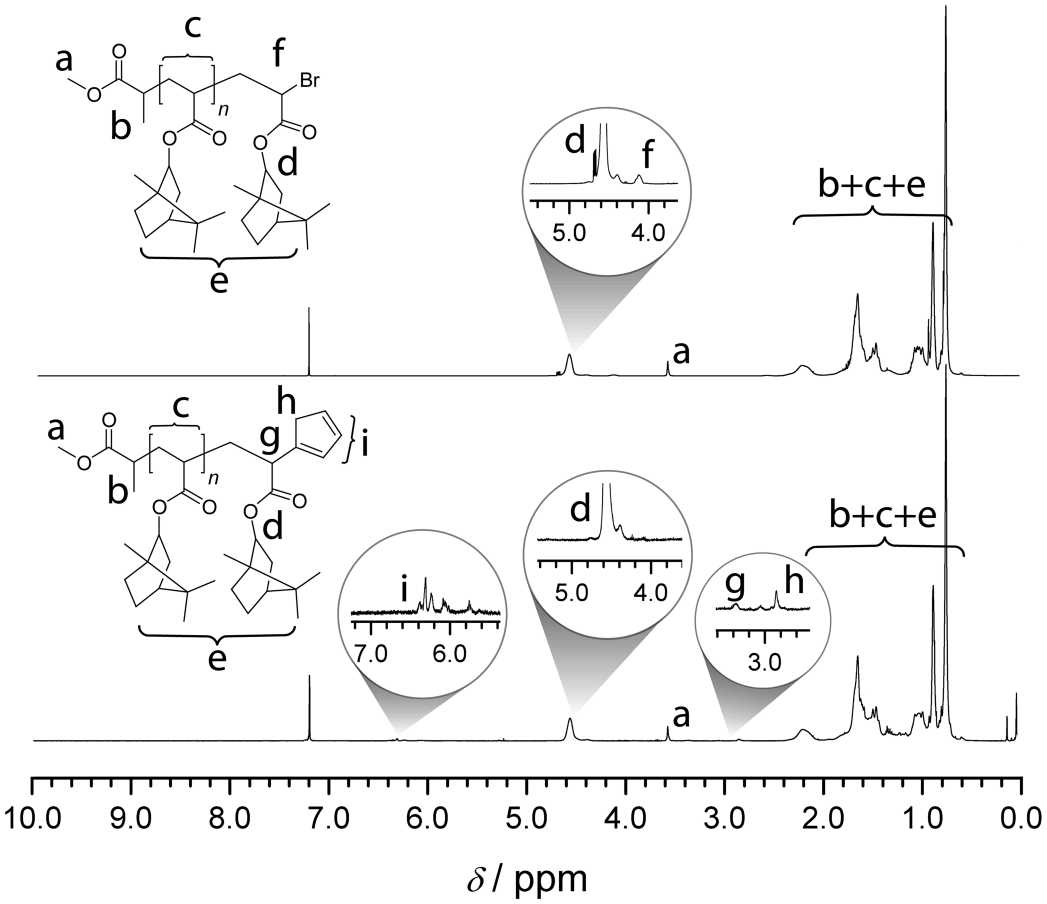

Figure 9.12 ^{1}H NMR spectra of P*i*BoA-Br **3** (top) and P*i*BoA-Cp **7** (bottom).

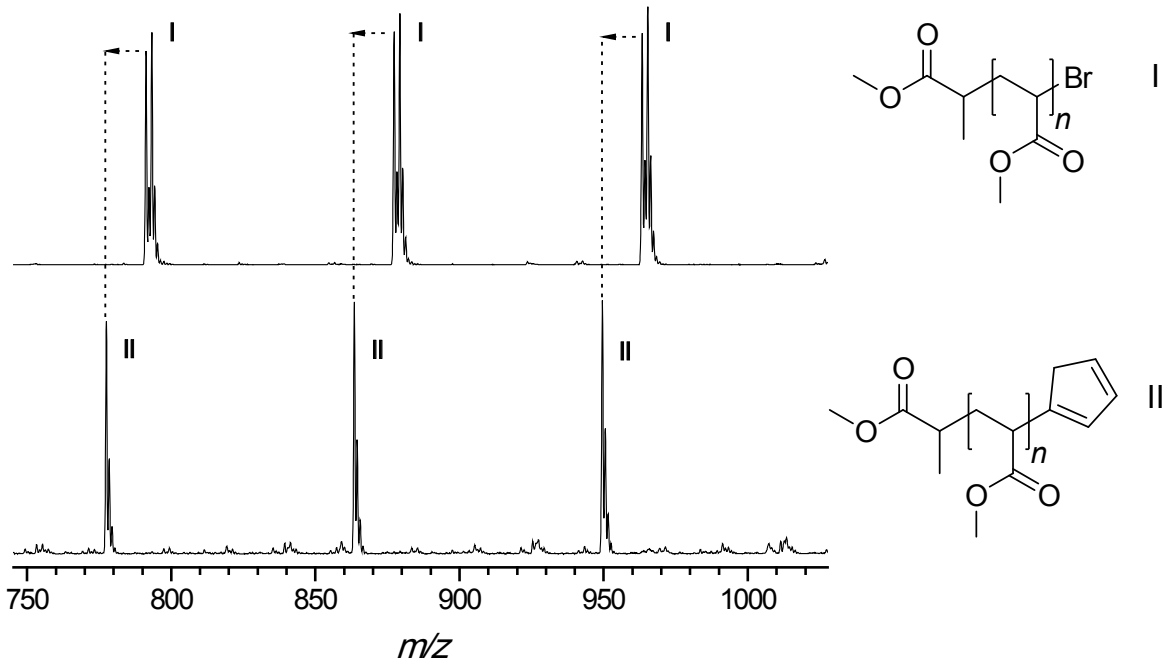

Figure 9.13 ESI-MS spectra of PMA-Br **4** (top) and PMA-Cp **8** (bottom).

Figure 9.13 depicts the ESI-MS spectra of PMA-Br **4** and PMA-Cp **8**. The dominant species in the spectrum of the starting material (bromide functional polymer) is observed to completely shift to lower *m/z* values in accordance with the formation of the required Cp-capped polymer. A zoom of the 844-946 *m/z* region is presented in Figure 9.14, the experimental *m/z* values of which are compared to those of the theoretical structures in Table 9.4. Figure 9.15 shows the ^{1}H NMR spectra of PMA-Br **4** alongside that of PMA-Cp **8**. The transformation is characterized by the disappearance of the signal of the proton in the α-position to the terminal bromide (labelled *e*) and the appearance of peaks at 6.4-5.8 ppm and 2.9 ppm, assignable to the Cp functionality.

Table 9.4 Experimental and theoretical *m/z* values for the first peak in the isotopic distributions of the zoom spectrum in Figure 9.14 and their assignment.

$m/z_{\text{expt.}}$	ion assignment	formula	$m/z_{\text{theor.}}$	$\Delta m/z$
877.3	$\mathbf{4}_{(n=8)} + Na^+$	$[C_{36}H_{55}BrO_{18}Na]^+$	877.2	0.1
865.5	$\mathbf{8}_{n=8} + Na^+$	$[C_{41}H_{60}O_{18}Na]^+$	864.4	0.1

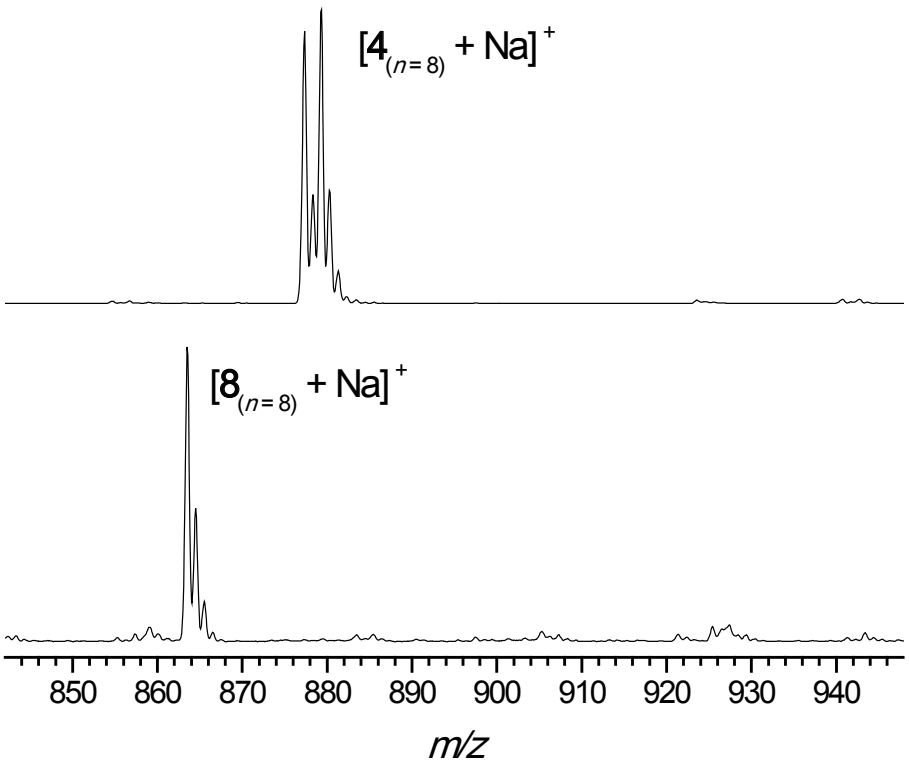

Figure 9.14 ESI-MS spectra (844 - 946 *m/z* zoom region) of PMA-Br **4** (top) and PMA-Cp **8** (bottom). Note the clear change in the isotopic pattern from bromide terminated species to Cp-terminated species that occurs.

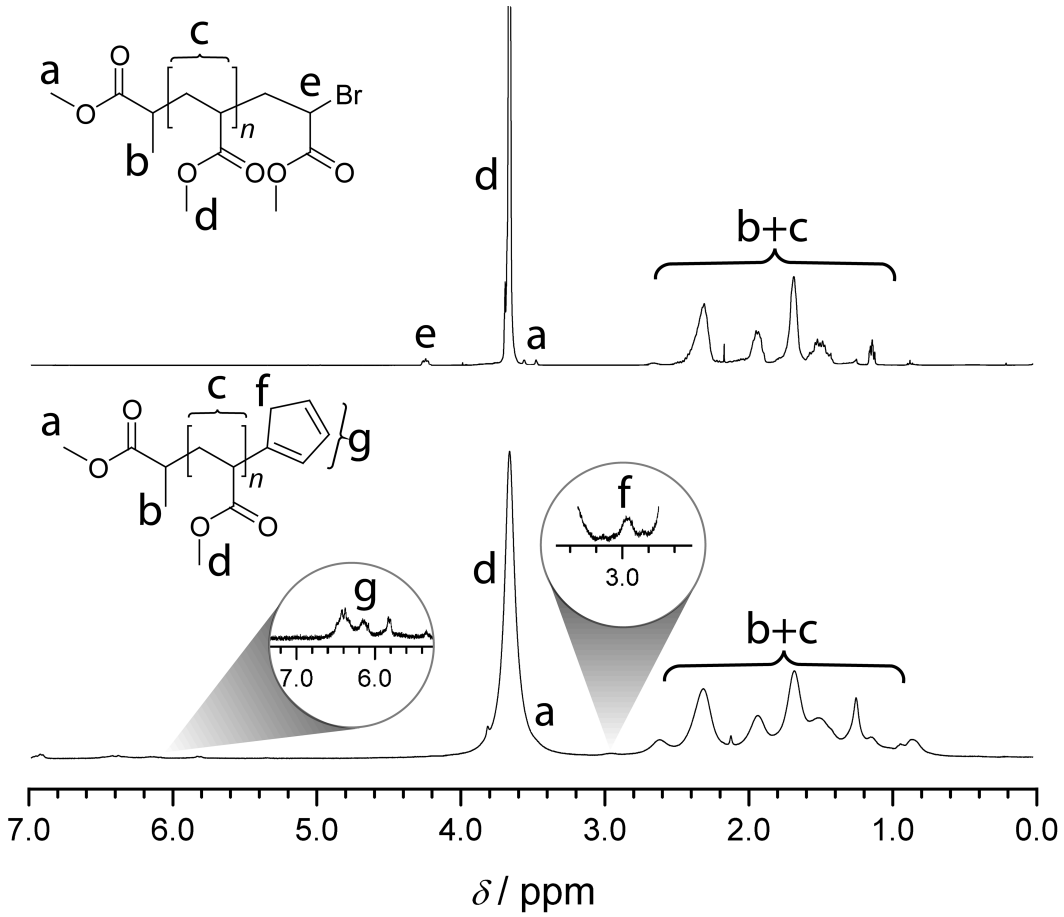

Figure 9.15 ^{1}H NMR spectra of PMA-Br **4** (top) and PMA-Cp **8** (bottom).

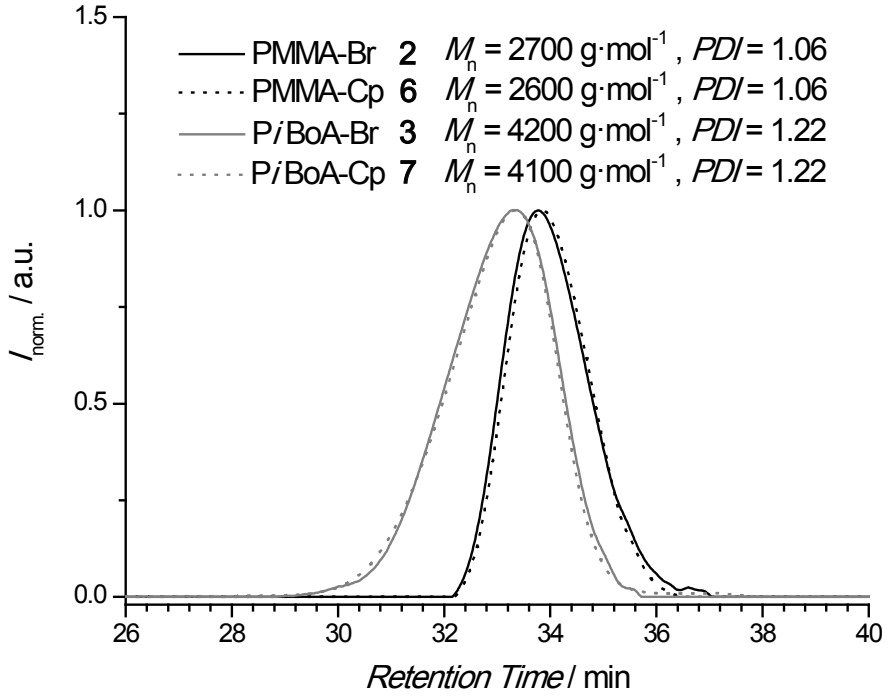

Figure 9.16 Overlay of SEC traces of PMMA-Br **2** and PMMA-Cp **6** (black); and of P*i*BoA-Br **3** and P*i*BoA-Cp **7** (gray).

As a further test of the efficient transformations, a comparative SEC analysis was performed between PMMA-Br **2** and PMMA-Cp **6**; and between P*i*BoA-Br **3** and P*i*BoA-Cp **7**. As a diene, cyclopentadiene is very reactive such that it readily dimerizes at ambient temperature via a Diels-Alder mechanism. Thus, there is potential for the presently investigated Cp-capped polymers to also undergo some degree of dimerization, a phenomomenon which would be readily observable in a SEC analysis. Figure 9.16 shows such an analysis. It is very clear that no dimerization has occurred in either system, which is consistent with earlier findings (Chapter 7).

9.4 Conclusion

In summary, a selective, efficient and mild strategy for equipping a variety of polymer chains (prepared via ATRP) with a highly reactive Cp moiety has been presented. The numerous side reactions that can occur in the presence of NaCp are avoided and, more importantly, the multitude of ester functional groups that exist in poly(acrylates) and poly(methacrylates) have been shown to be essentially inert to the functionalization system employed. It is envisaged that such provision of Cp-functional polymers would bring the concept of ambient temperature and catalyst-free conjugations to a broader platform.

References

[1] Matyjaszewski, K.; Xia, J. H. *Chem. Rev.* **2001**, *101*, 2921–2990.

[2] Perrier, S.; Takolpuckdee, P. *J. Polym. Sci., Part A: Polym. Chem.* **2005**, *43*, 5347–5393.

[3] Zhu, J.; Zhu, M. L.; Zhou, D.; Chen, J. Y.; Wang, X. Y. *Eur. Polym. J.* **2004**, *40*, 743–749.

[4] Dervaux, B.; Van Camp, W.; Van Renterghem, L.; Du Prez, F. E. *J. Polym. Sci., Part A: Polym. Chem.* **2008**, *46*, 1649–1661.

[5] Binder, W. H.; Sachsenhofer, R. *Macromol. Rapid Commun.* **2008**, *29*, 952–981.

[6] Coessens, V.; Matyjaszewski, K. *J. Macromol. Sci., Pure Appl. Chem.* **1999**, *A36*, 667–679.

[7] Quémener, D.; Davis, T. P.; Barner-Kowollik, C.; Stenzel, M. H. *Chem. Commun.* **2006**, 5051–5053.

[8] Campos, L. M.; Killops, K. L.; Sakai, R.; Paulusse, J. M. J.; Damiron, D.; Drockenmuller, E.; Messmore, B. W.; Hawker, C. J. *Macromolecules* **2008**, *41*, 7063–7070.

[9] Li, M.; De, P.; Gondi, S. R.; Sumerlin, B. S. *J. Polym. Sci., Part A: Polym. Chem.* **2008**, *46*, 5093–5100.

[10] Coessens, V.; Matyjaszewski, K. *Macromol. Rapid Commun.* **1999**, *20*, 127–134.

[11] Gruendling, T.; Dietrich, M.; Barner-Kowollik, C. *Aust. J. Chem.* **2009**, *62*, 806–812.

[12] Matyjaszewski, K.; Nakagawa, Y.; Gaynor, S. G. *Macromol. Rapid Commun.* **1997**, *18*, 1057–1066.

[13] Lai, J. T.; Filla, D.; Shea, R. *Macromolecules* **2002**, *35*, 6754–6756.

[14] Coolbaugh, T. S.; Coots, R. J.; Santarsiero, B. D.; Grubbs, R. H. *Inorg. Chim. Acta* **1985**, *98*, 99–105.

[15] Christie, S. D. R.; Man, K. W.; Whitby, R. J.; Slawin, A. M. Z. *Organometallics* **1999**, *18*, 348–359.

[16] Ben Romdhane, H.; Chaabouni, M. R.; Grenier-Loustalot, M. F.; Delolme, F.; Mison, P.; Sillion, B. *Polymer* **2000**, *41*, 3183–3191.

[17] Liu, L. T.; Zhang, W. X.; Wang, C.; Wang, C. Y.; Xi, Z. F. *Angew. Chem. Int. Ed.* **2009**, *48*, 8111–8114.

[18] Sai, M.; Sorneya, H.; Yorimitsu, H.; Oshima, K. *Org. Lett.* **2008**, *10*, 2545–2547.

[19] Nie, B.; Rotello, V. M. *J. Org. Chem.* **1996**, *61*, 1870–1871.

[20] Nie, B.; Rotello, V. *J. Phys. Chem. Solids* **1997**, *58*, 1897–1899.

[21] Ge, Z. X.; Duchamp, J. C.; Cai, T.; Gibson, H. W.; Dorn, H. C. *J. Am. Chem. Soc.* **2005**, *127*, 16292–16298.

[22] Stork, M.; Koch, M.; Klapper, M.; Müllen, K.; Gregorius, H.; Rief, U. *Macromol. Rapid Commun.* **1999**, *20*, 210–213.

[23] Nenov, N.; Koch, M.; Klapper, M.; Müllen, K. *Polym. Bull.* **2002**, *47*, 391–398.

[24] Dillmore, W. S.; Yousaf, M. N.; Mrksich, M. *Langmuir* **2004**, *20*, 7223–7231.

[25] Rausch, M. D.; Hart, W. P.; Macomber, D. W. *J. Macromol. Sci. Chem.* **1981**, *A16*, 243–250.

[26] Blankenbuehler, M. T.; Selegue, J. P. *J. Organomet. Chem.* **2002**, *642*, 268–274.

[27] Chajara, K.; Ottosson, H. *Tetrahedron Lett.* **2004**, *45*, 6741–6744.

[28] Ben Romdhane, H.; Chaabouni, M. R.; Grenier-Loustalot, M. F.; Delolme, F.; Mison, P.; Sillion, B. *Polymer* **2000**, *41*, 1633–1639.

[29] Rufanov, K. A.; Kazennova, N. B.; Churakov, A. V.; Lemenovskii, D. A.; Kuzmina, L. G. *J. Organomet. Chem.* **1995**, *485*, 173–178.

[30] Hughes, R. P.; Trujillo, H. A. *Organometallics* **1996**, *15*, 286–294.

[31] Leadbeater, N. E. *Tetrahedron Lett.* **2002**, *43*, 691–693.

[32] Gruendling, T.; Guilhaus, M.; Barner-Kowollik, C. *Macromol. Rapid Commun.* **2009**, *30*, 589–597.

10

Visualizing the Efficiency of Modular Block Copolymer Construction

10.1 Introduction

Despite their relative simplicity, block copolymers are highly sought after materials due to their ability to form well-defined micro-domains in both solution and in bulk.[1] Such a property makes these materials highly useful in a wide variety of fields, including nanolithography,[2–4] photonics,[5] controlled drug delivery[6] and nanotechnology in general. However, such 'high-demand' applications are substantially varied in their requirements, thus a rather broad range of high purity block copolymers are in need of being readily accessible.

A versatile technique by which block copolymers may be synthesized is by modular construction. This technique is largely centred on the application of highly efficient organic chemical transformations to polymer chains synthesized by, primarily, CRP. Techniques such as ATRP[7, 8] and RAFT polymerization[9, 10] are very well suited to the generation of well-defined polymeric architectures that bear one or a multitude of synthetic handles, which may be effectively manipulated to achieve larger structures through conjugation. While anionic polymerization remains the dominant method of producing block copolymers (either by sequential polymerization or coupling reactions), the variety of monomers that may be polymerized is not as vast as what can be polymerized by CRP.[11–13]

While the transfer of synthetic organic chemistry techniques to polymer science has been a highly successful enterprise, the use of the associated purification techniques (e.g. column chromatography, distillation, recrystallization) has not been possible. As such, every effort has been made to directly synthesize high purity block copolymers[14–16] by employing only the most efficient chemical transformations that are on offer (often categorized as *click* chemistry).[17] However, characterization of such efficiency is usually glossed over in conventional SEC analyses and is not reliably quantified.

Liquid adsorption chromatography at critical conditions (LACCC) can be a very effective technique whereby macromolecules are separated by the chemical heterogeneity rather than their size.[18–27] Thus, in the analysis of block copolymers (**A**-*b*-**B**) in which critical conditions are applied for the **A** segment; the elution behaviour of the block will be solely dependent upon the **B** segment. Thus the **A** segment may be considered to be chromatographically invisible. However, some publications question and even challenge the validity of this assumption.[28–30] Nevertheless, this phenomenon may be advantageously used in establishing the efficiency of modular block copolymer construction where the conjugation of two homopolymers of significantly disparate molecular weight cannot convincingly be established by conventional SEC alone. By transferring eluates from the LACCC dimension to an SEC system (generically referred to as two-dimensional or 2D chromatography),[22] a 2D-chromatogram (a two-dimensional projection of a three-dimensional surface) is thus obtained that provides information on both the chemical heterogeneity and size of the synthesized block copolymers. Critical conditions are strongly related to the polymer system under investigation. As such, for every different polymer that is in need of being analysed by such a technique, the critical conditions must be individually determined.

Such an analysis has been effectively utilized by Matyjaszewski and co-workers in establishing the efficiency of linear and star shaped block copolymer formation through a chain extension approach with various incarnations of ATRP.[31–33] Furthermore, Falkenhagen and Müller used the technique to characterize block copolymers formed by sequential living anionic polymerization.[34] Pasch, in addition to the study of block copolymers formed by living anionic polymerization, explored the generation of poly(styrene)-*block*- poly(isoprene) copolymers by coupling separately synthesized poly(styrene) and poly(isoprene), also using anionic chemistry.[35] Although the coupling process required three days, it nevertheless provided the inspiration to evaluate the efficiency of more rapid and versatile conjugation techniques.

Herein, a comprehensive assessment of the efficiency of formation and the resulting purity of block copolymers synthesized via an ultra rapid modular approach (specifically RAFT-HDA chemistry), as depicted in Figure 10.1 is reported. Initially, Cp-functional poly(methyl methacrylate) (PMMA **1**) and a series of pyridin-

2-yldithioformate-functional poly(isobornyl acrylate)s (P*i*BoA **2**, **3** and **4**) were synthesized via ATRP and RAFT polymerization respectively and their end-group functionalities determined via electrospray ionization mass spectrometry (ESI-MS) and ^{1}H NMR spectroscopy. This allowed for an initial prediction of the expected compositions of the crude block copolymer mixtures working under the assumption of quantitative conjugation. After a reaction time of 10 minutes at ambient temperature, the crude block copolymer reaction mixtures were directly analysed via conventional SEC, LACCC and 2D LACCC-SEC to assess their purity. Finally, it will be shown how a simple deconvolution of the SEC traces of the crude block copolymer mixtures can be used to also achieve reliable composition data.

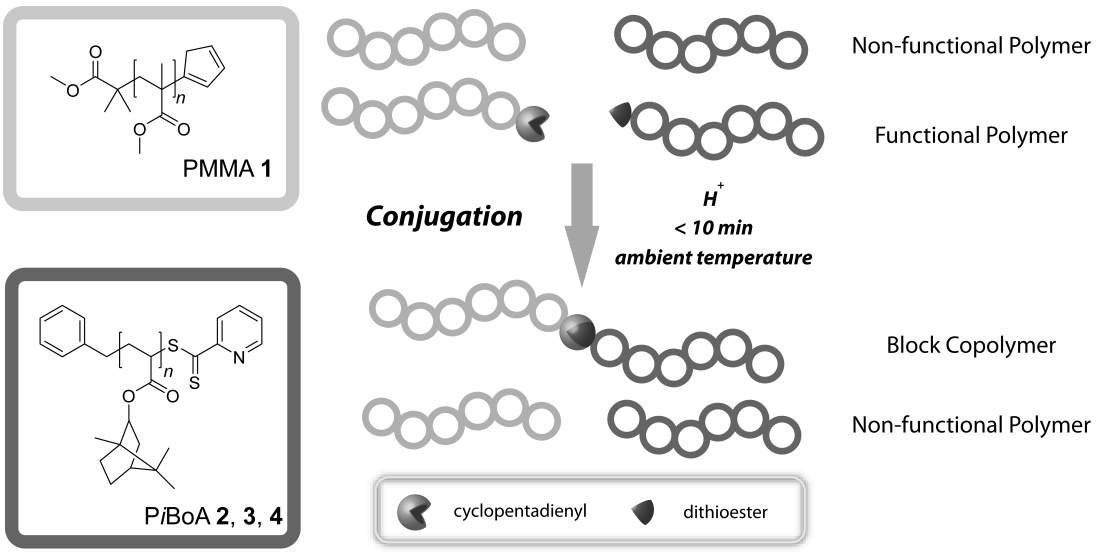

Figure 10.1 Schematic overview of the conjugation of polymer chains via their respective chain-end functionalities.

10.2 Experimental Section

RAFT Polymerization of Isobornyl Acrylate

A mixture of *i*BoA, BPDF and AIBN was deoxygenated by purging with nitrogen for 40 minutes. The polymerization reaction was performed at 60 °C for 24 hours. The reaction was stopped by chilling in an ice bath and exposure to oxygen. The resulting polymers were isolated by two-fold precipitation in cold methanol. The specifics for each of the three polymerizations are as follows:

PiBoA **2**- $[M]_o$:$[RAFT]_o$:$[AIBN]_o$ = 230:1:0.2, M_n = 4600 g·mol^{-1}, conversion = 10 %;
P*i*BoA **3**- $[M]_o$:$[RAFT]_o$:$[AIBN]_o$ = 400:1:0.2, M_n = 8900 g·mol^{-1}, conversion = 10.5 %;
P*i*BoA **4**- $[M]_o$:$[RAFT]_o$:$[AIBN]_o$ = 650:1:0.2, M_n = 32000 g·mol^{-1}, conversion = 22 %.

Preparation of PMMA 1

To a dried Schlenk tube was added copper (I) bromide, copper (II) bromide and bpy which was then sealed with a rubber septum, evacuated and backfilled with nitrogen. To another Schlenk tube was added methyl methacrylate (MMA) and acetone (50:50) and equipped with a rubber septum. The monomer solution was then deoxygenated by three consecutive freeze-pump-thaw cycles and subsequently transferred to the first Schlenk tube via cannula. The tube was sealed under a nitrogen atmosphere and placed in a thermostatic oil bath held at 50 °C. After the polymerization mixture reached the desired temperature, methyl 2-bromo-2-methylpropanoate (MBMP) was added. The initial ratio of [MMA]:[MBMP]:[CuBr]:[$CuBr_2$]:[bpy] was 50:2:0.105:0.0125:0.25. The polymerization was stopped by cooling the mixture in an ice-bath and exposure to oxygen. The mixture was passed through a short column of neutral alumina to remove the copper catalyst. PMMA was isolated by two-fold precipitation in cold *n*-hexane. A solution of bromide terminated polymer (0.18 mmol), tributylphosphine (0.36 mmol, 2 equiv.) and sodium iodide (1.08 mmol, 6 equiv.) in anhydrous THF (2.0 mL) was prepared under a nitrogen atmosphere. Separately, a stock solution of $NiCp_2$ in anhydrous THF (0.18 M) was prepared under a nitrogen atmosphere. The $NiCp_2$ solution (2.0 mL, 4 equiv.) was then added to the polymer solution and allowed to stir overnight at ambient temperature. At the end of the reaction, the mixture was passed through a short column of basic alumina to remove the precipitated nickel (II) bromide and the polymer recovered by precipitation. The resulting polymer was then dissolved in chloroform and washed three times with distilled water. The Cp-capped polymer was then isolated by precipitation from the chloroform solution into cold *n*-hexane. SEC (THF): M_n = 3200 g·mol^{-1}, *PDI* = 1.10.

Conjugation Reactions-Typical Procedure

PMMA **1** (10 µmol) and P*i*BoA precursor were dissolved in chloroform (200 µL) such that an equimolar solution (based upon functional polymer) was obtained. For example, PMMA **1** (10 µmol, 97 % functionality) was mixed with P*i*BoA **2** (10.2 µmol, 95 % functionality). After the addition of TFA (1.5 equiv.), the solution was agitated by shaking for 10 minutes at ambient temperature, after which the solvent was removed under reduced pressure to yield crude block copolymer mixtures, which were then directly analysed without any purification.

10.3 Results and Discussion

In characterizing the success of block copolymer formation through a modular approach, it is of paramount importance to first determine the starting chain-end functionalities of the respective homopolymer precursors. A substantially versatile range of such polymeric building blocks may be (and has been) synthesized by CRP processes.[36] Despite the highly effective level of control in terms of molecular weight and chain-end functionality offered by such processes as ATRP and RAFT polymerization, it is nevertheless impossible to achieve truly quantitatively ω-functional polymer chains.

ATRP and RAFT polymerization are often erroneously labeled as *living* free radical polymerization, however the fact of the matter is that in both of these processes, various ill-desired termination, transfer and elimination reactions are not completely suppressed, thus a certain (albeit low) proportion of the total polymer that is recovered will be *dead* polymer, that is polymer chains that do not bear the targeted functionality. Such species usually cannot be preparatively separated from functional polymer and are thus carried through subsequent chemical transformations. Therefore, when it comes to the conjugation of two polymer chains via their respective chain-ends, the subsequent SEC analysis will ideally show the appropriate shift of the molecular weight distribution to higher molecular weights along with some additional tailing or even a pronounced hump towards lower molecular weight.[37] Without knowing the starting chain-end fidelity, one cannot be certain which proportion of the SEC tailing is attributable to remaining *dead* polymer chains, since a non-quantitative conjugation process would also lead to such an observation. Of course, other techniques such as NMR and FT-IR spectroscopy can be used to monitor the change in chemical functionality from the starting homopolymers to the final conjugate. Yet such analyses are typically dependent upon signals from small functional groups on the ends of long polymer chains. The higher the molecular weight of the polymers utilized become, the signal-to-noise ratio of the signals of interest becomes smaller, thus (of course after a certain limit) decreasing the accuracy of any quantitative analysis that may be performed. UV detection, on the other hand is very sensitive and non-chain length dependent. However, this detection method is restricted to those species that absorb UV light and cannot therefore be applied to all compounds synthesized in the present investigation.

For this study, PMMA **1** was prepared via ATRP and the bromide end-group subsequently and directly transformed into a Cp moiety via the facile procedure using nickelocene described in Chapter 9. Typically, the chain-end functionality of such polymers is determined via a ^{1}H NMR spectroscopic analysis in which the integrals of signals arising from end-group protons are compared. Due to the nature of PMMA

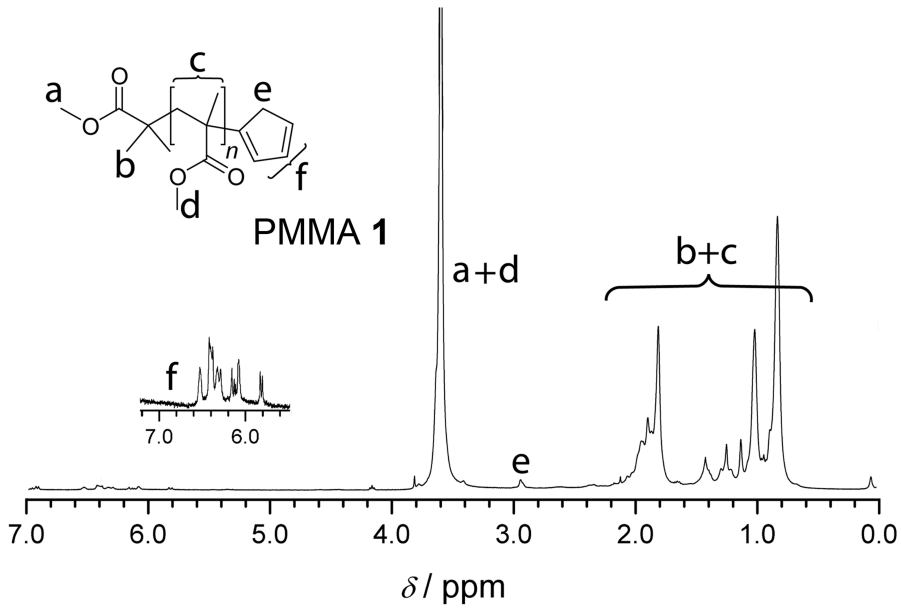

Figure 10.2 ^{1}H NMR spectrum of PMMA **1**.

1, such an analysis cannot be reliably performed due to the lack of end-group protons that do not have overlapping signals with those that form part of the polymer backbone (Figure 10.2).

As such, PMMA **1** was determined to contain 3 ± 0.60 wt% *dead* polymer via quantitative integration of its mass spectrum (recorded via ESI-MS) following a previously reported procedure (Figure 10.3).[38] In this technique, only the singly charged species were used for the integration. It is important to note that ionization occurs along the polymer backbone, a process that is not significantly influenced by the nature of the polymer end-group.[38] Furthermore, it has been reported that the mole-fraction determination of ESI-MS data in (meth)acrylate-type systems is systematically independent of chain length.[39] As reported, the error associated with this technique was estimated to be < 20 %. Thus, for the present investigation the maximum error of 20 % was taken as a conservative estimate.

Concurrently, a series of poly(isobornyl acrylate)s (P*i*BoA **2**, **3**, **4**) were synthesized via RAFT polymerization mediated by BPDF. Such a system produces polymer chains bearing the electron deficient dithioester end-group that is required for ultra-fast HDA cycloadditions. The molecular weights and functionalities (as determined by ^{1}H NMR spectroscopy) of these polymers are presented in Table 10.1. As the molecular weight of a polymer increases, so does the error involved in determining end-group functionality via integration of its NMR spectrum. The ^{1}H NMR spectrum of the lowest molecular weight P*i*BoA **2** is observed to have a good signal-to-noise ratio (Figure 10.4). Additionally, an ESI-MS analysis was able to be performed on P*i*BoA **2**, the results of which are presented in Figure 10.5. The ^{1}H NMR spectrum of P*i*BoA **3**

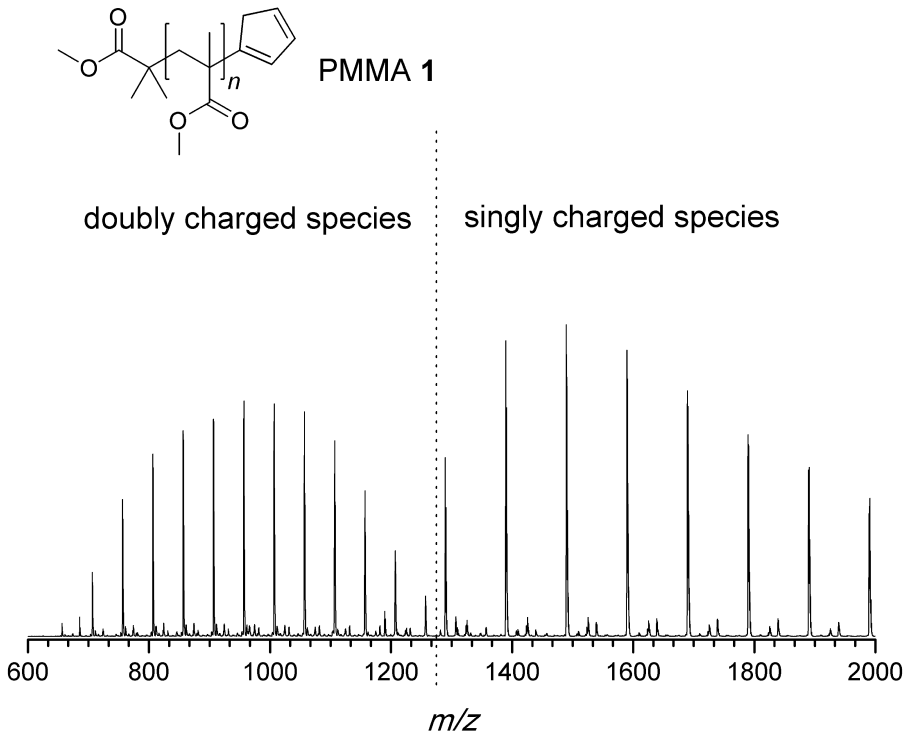

Figure 10.3 Full ESI-MS spectrum of PMMA **1**.

(Figure 10.6) is also observed to have a good signal-to-noise ratio. In both the above cases, the reproducibility of the determination of functionalization was estimated to contain an error of ± 5 % (based on the variations of the repeated integration result). The NMR spectrum of the higher molecular weight P*i*BoA **4** (Figure 10.7) was observed to have significantly lower signal-to-noise ratio and the reproducibility of its analysis by integration was estimated to have an error of ± 15 % (also obtained by repeated integration). The ^{1}H NMR spectra were all recorded with 128 scans.

Keeping in line with the most widely used technique in characterizing block copolymer formation, conventional SEC was employed to initially analyse the formed

Table 10.1 Molecular weight and functionality characterization of the starting homopolymers.[a]

polymer	$M_{n,\,SEC}$ / g·mol^{-1}	PDI^b	Fraction of *Dead* Polymer Chains / %
PMMA **1**	3200	1.10	3.0 ± 0.60[c]
P*i*BoA **2**	4600	1.09	5.0 ± 0.25[d]
P*i*BoA **3**	8900	1.24	7.0 ± 0.35[d]
P*i*BoA **4**	32 000	1.08	6.0 ± 0.90[d]

[a]Measured by SEC in THF against linear PMMA standards. [b]Polydispersity index. [c]Determined via quantitative integration of the mass spectrum recorded by ESI-MS. [d]Determined via ^{1}H NMR spectroscopy.

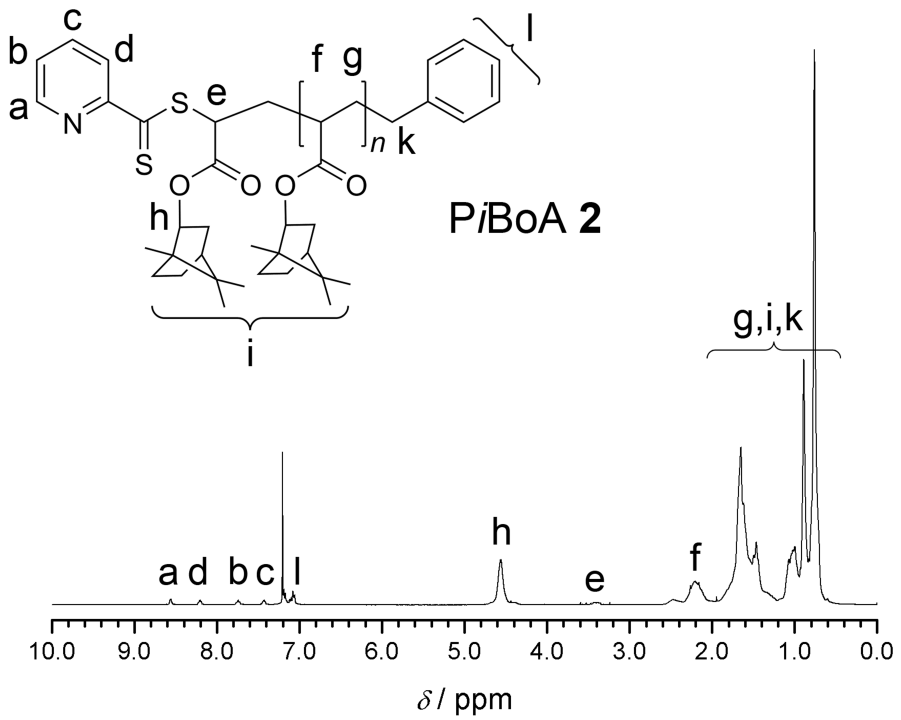

Figure 10.4 ^{1}H NMR spectrum of P*i*BoA **2**.

copolymers. The left hand side of Figure 10.8 shows an overlay of the SEC traces of the various homopolymer precursors and of the respective block copolymers. In all cases, a clear shift to lower retention times may be observed, providing a qualitative indication of successful block formation. A comparison of the SEC determined molecular weights of the generated block copolymers and the predicted values (Table 10.2) also confirms the success of the conjugation. It may also be observed that a slight degree of tailing towards higher retention times is present in all of the examples, indicating the presence of seemingly unreacted starting materials. Upon first glance, it may seem that the conjugation reaction did not proceed quantitatively, as is the general interpretation of such results. However, as discussed previously, a small proportion of the starting homopolymers are not able to undergo the conjugation reaction for the simple reason that they do not carry the required dithioester or Cp functionality. Thus, a slight degree of tailing is expected. It is therefore necessary to determine whether such tailing is solely due to this *dead* polymeric material or if the conjugation reaction is indeed non-quantitative. Another limitation to the sole use of SEC to characterize the modular formation of block copolymers arises when there is a large difference in the molecular weight (or more precisely the hydrodynamic volume) of the two precursor homopolymers. Upon close inspection of the SEC section of Figure 10.8, it is apparent that as the molecular weight of the P*i*BoA increases, the observable shift in retention time of the formed block copolymer becomes smaller. Taking a purely mathematical perspective on the convolution of two Gaussian-type distributions, the greatest shift will be observed when both starting components are

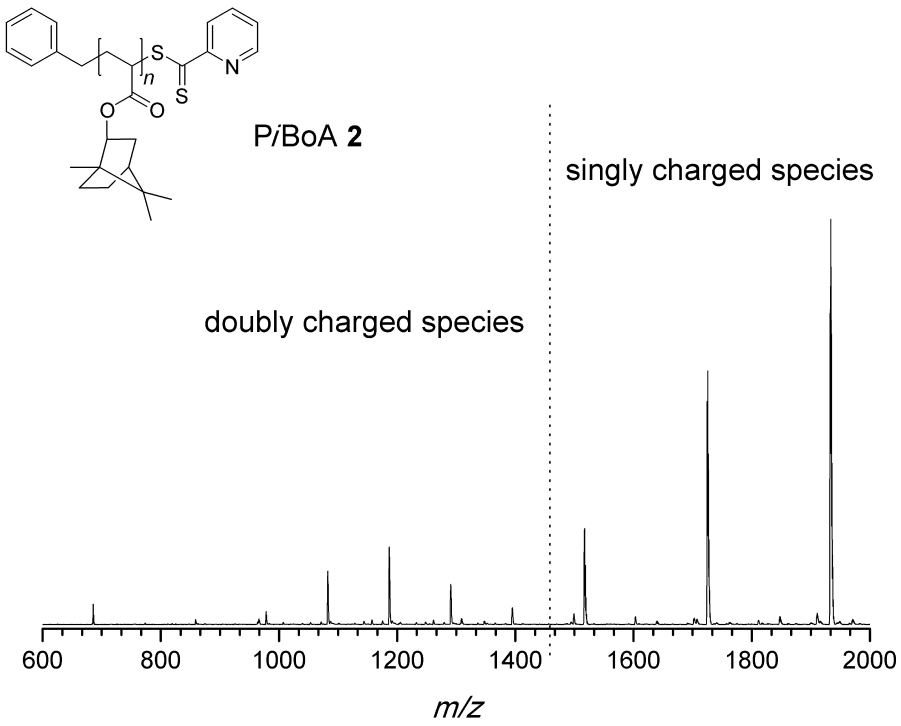

Figure 10.5 Full ESI-MS spectrum of P*i*BoA **2**.

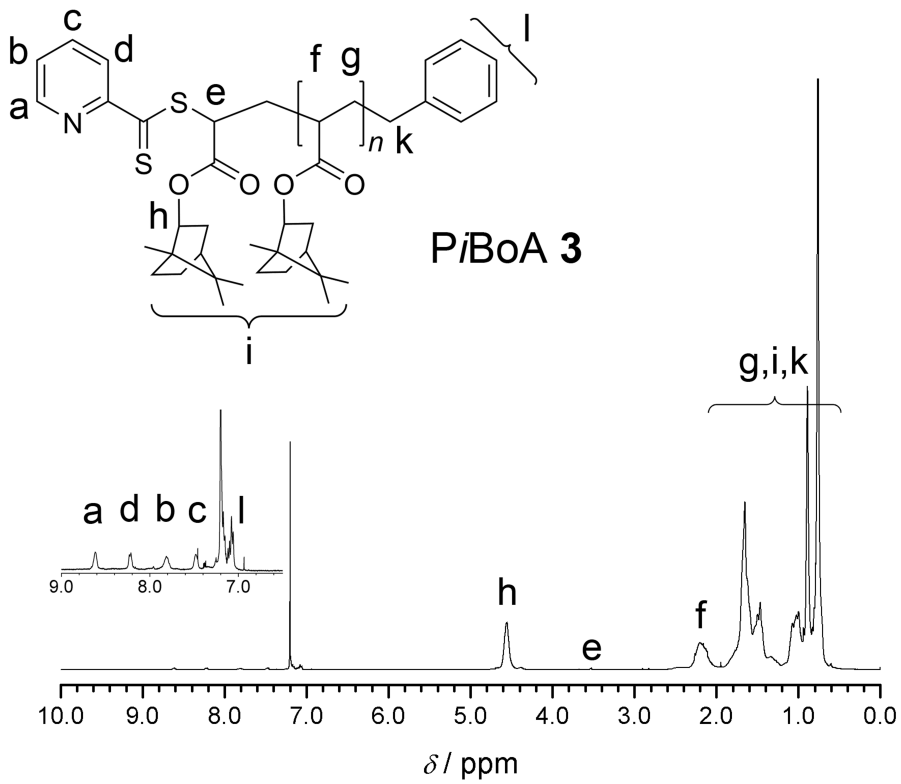

Figure 10.6 ^{1}H NMR spectrum of P*i*BoA **3**.

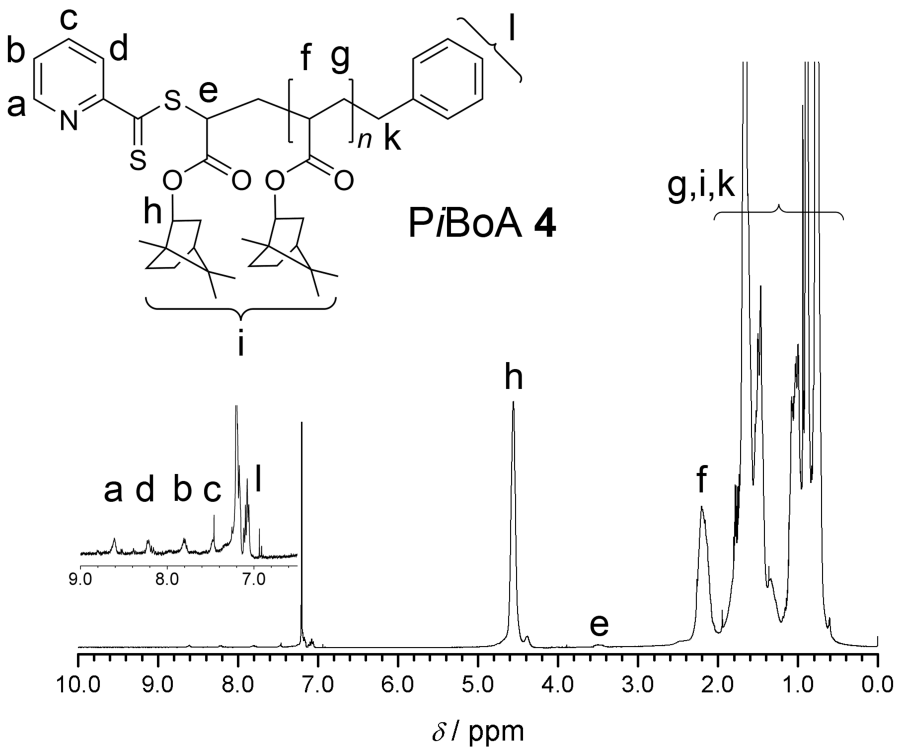

Figure 10.7 ^{1}H NMR spectrum of P*i*BoA **4**.

very close to one another, if not identical. It is therefore highly useful in this case to separate the block copolymers from the P*i*BoA homopolymers via their chemical composition in addition to their hydrodynamic volume. For this, an LACCC analysis was performed in which the critical conditions for P*i*BoA were utilized.

Under the critical conditions for a specific polymer, the enthalpic and entropic interactions of that polymer with the stationary phase of the chromatographic column compensate each other, resulting in polymer chains eluting according to their chemical heterogeneity and independently of their size. Consequently, under the critical conditions of P*i*BoA, the elution behaviour of the block copolymers **5**, **6** and **7** should differ from that of the corresponding P*i*BoA homopolymers. In reality, the compensating enthalpic and entropic effects can be less than perfect, resulting in the analyte

Table 10.2 SEC characterization of block copolymers.

polymer	$M_{n,\,SEC}$[a] / g·mol^{-1}	PDI[b]	$M_{n,\,theor.}$[c] / g·mol^{-1}
PMMA-*b*-P*i*BoA **5**	7500	1.10	7800
PMMA-*b*-P*i*BoA **6**	11 900	1.12	12 100
PMMA-*b*-P*i*BoA **7**	34 200	1.10	35 200

[a]Measured by SEC in THF against linear PMMA standards. [b]Polydispersity index. [c]Determined by the sum of the SEC determined molecular weights of the precursor polymers.

eluting either slightly in size exclusion mode or in adsorption mode. The right hand side of Figure 10.8 depicts the results of a LACCC analysis of all polymers and block copolymers synthesized under the critical conditions of P*i*BoA. Inspection of these results reveal: (1) P*i*BoA **2**, **3**, and **4** appear at a similar elution volume, thus confirming that the analysis has indeed been performed under the appropriate critical conditions; (2) PMMA **1** appears at a different elution volume to the P*i*BoA homopolymers, thus establishing the expectation that the block copolymers should also have a significantly different elution behaviour; and (3) the block copolymers **5**, **6** and **7** do indeed display a substantially different elution behaviour compared to the P*i*BoA homopolymers, thus allowing for the presence of unreacted P*i*BoA homopolymer to be observed in the crude reaction mixtures. It should be noted that the HPLC column used for the LACCC analysis was thoroughly flushed with pure THF after each measurement. Upon monitoring the detector output during this process, no pronounced signals could be observed, indicating that no residual polymer was retained on the column. A cautionary note concerning the evaluation of data from ELSD is centred on the potentially non-linear response with mass. Although not crucial in the present investigation, such detectors should be carefully calibrated, a process which makes an already laborious technique that much more involved.

Upon combining the techniques of LACCC and SEC, contour plots of the synthesized block copolymers may be generated that provide information on both its chemical composition and size. Such a characterization of block copolymers has been reported in the literature;[31–35, 40] however the present investigation provides the first comprehensive analysis of the efficiency and purity of block copolymers formed via a rapid modular pathway, of which 2D LACCC-SEC is but one element. Furthermore, this analysis enables the generation of a three-dimensional rendering of the block copolymers, thus aiding in the visualization of the efficiency of the modular conjugation.

Figure 10.9 depicts the 2D chromatograms of the various block copolymers overlayed with those of the respective P*i*BoA homopolymers from which they were synthesized. The main 2D contour of Figure 10.9a appearing at a LACCC elution volume of around 2.6 mL represents the PMMA-*b*-P*i*BoA **5**. Associated with this contour is a much smaller contour that appears at a LACCC elution volume of around 3.1 mL and a higher SEC retention time (indicating a smaller hydrodynamic volume). This is attributed to remaining P*i*BoA **2** homopolymer. Integration of these regions provided quantitative information pertaining to the composition of the crude block copolymer mixture. In doing so, the remaining P*i*BoA in the mixture was determined to be 3.0 ± 1.0 wt%. Based upon the functionalities of the starting homopolymers (Table 10.1) and assuming a 100 % efficient conjugation reaction, it is possible to calculate the expected composition of the crude block copolymer mixture (an example calculation is included in Chapter 14). Therefore, the quantitative conjugation of P*i*BoA **2** and

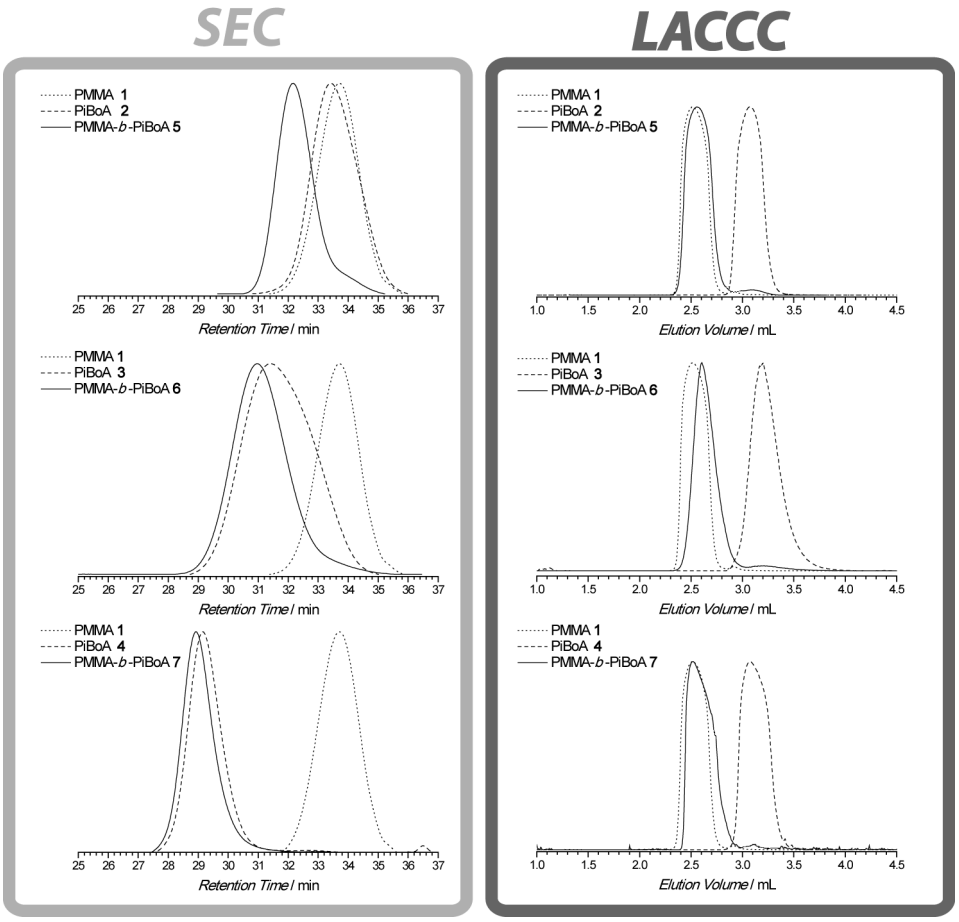

Figure 10.8 SEC characterization (left) and LACCC characterization under the critical conditions of P*i*BoA (right) of the various homopolymers and block copolymers synthesized in this study.

PMMA **1** would yield a mixture which would have an expected composition of 95.8 $\pm$ 0.4 wt% block copolymer, 3.0 $\pm$ 0.15 wt % P*i*BoA and 1.2 $\pm$ 0.24 wt% PMMA. Thus, the excellent agreement between the predicted block composition and that which was determined via the 2D chromatographic analysis confirms that the conjugation reaction (within experimental error) is quantitative, and that the remaining unreacted P*i*BoA homopolymer is solely due to polymer which did not bear the required dithioester functionality. Adjacent to the contour plot in Figure 10.9a is a three-dimensional representation of the PMMA-*b*-P*i*BoA **5** in comparison to that of the starting P*i*BoA **2**, which provides a very clear visualization of the efficient chemical transformation that has taken place.

Moving to a higher molecular weight P*i*BoA, it becomes noticeable that the separation that is achieved in the SEC dimension is not as pronounced as that which can be seen in the conventional SEC traces. This can readily be explained by the fact that the 2D-chromatographic analysis of these polymers made use of a high speed SEC column (operated under a necessarily fast eluent flow rate - 3.0 mL·min^{-1}) for the

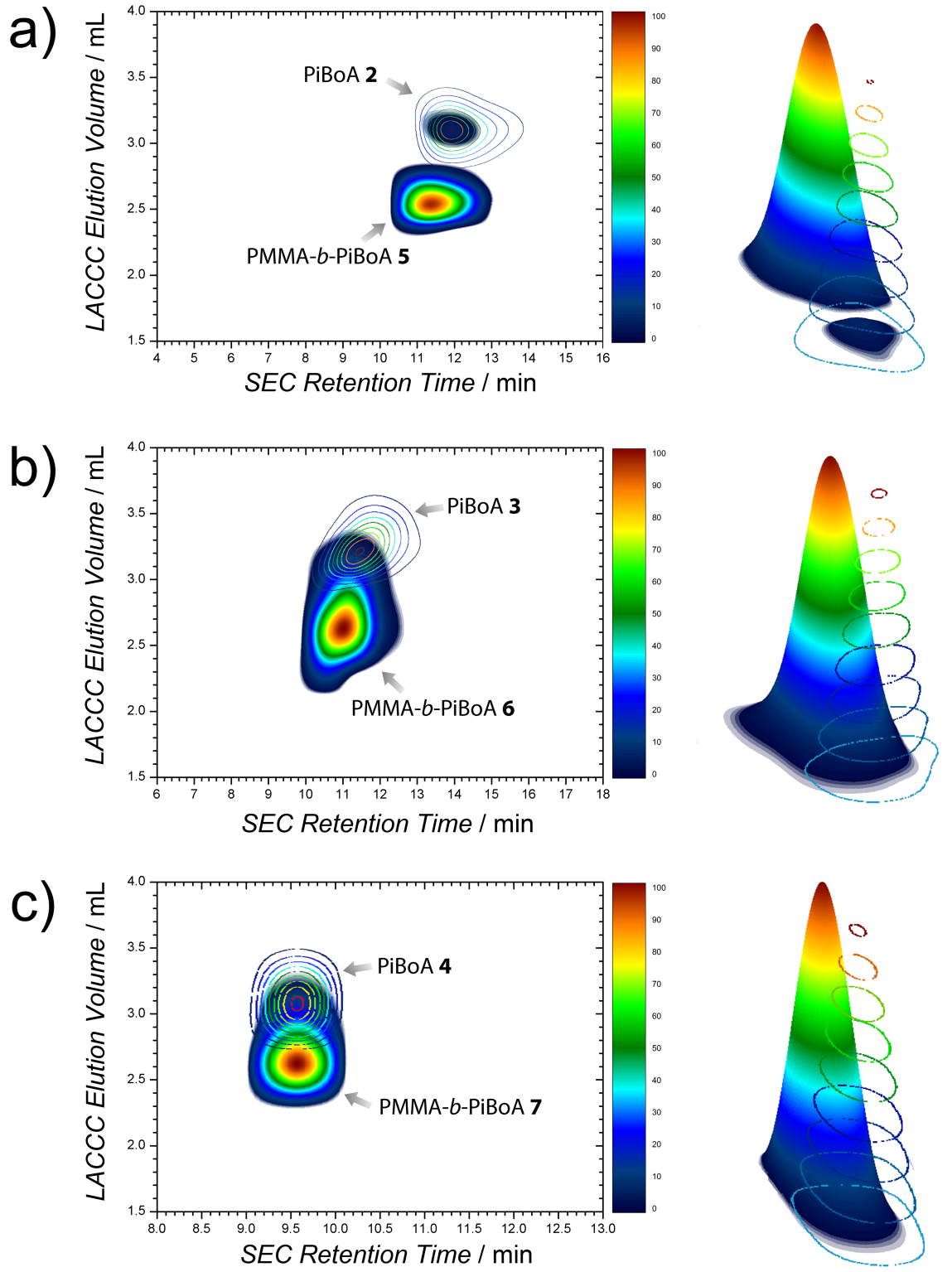

Figure 10.9 2D LACCC-SEC chromatograms and corresponding three dimensional renderings of a) PMMA-*b*-P*i*BoA **5**; b) PMMA-*b*-P*i*BoA **6**; and c) PMMA-*b*-P*i*BoA **7**; all overlayed with their respective P*i*BoA precursors.

second dimension. Nevertheless, a slight shift in the SEC dimension is still discernible (Figure 10.9b). More importantly, the feature to take note of is the comparatively large shift in elution volume in the LACCC dimension (P*i*BoA **3** - 3.2 mL, PMMA-*b*-P*i*BoA **6** - 2.6 mL). The use of the high resolution SEC system convincingly shows the appropriate shifts in retention time (Figure 10.8).

Upon inspection of Figure 10.9b, there is some overlap between the contour attributable to the block copolymer and that which is attributable to residual P*i*BoA. It is noted that the peaks associated with the block copolymers **6** and **7** in the LACCC analysis (Figure 10.8) are slightly broader than that of **5**, which contributes to this observation. However, with the aid of the superimposed contour of the precursor P*i*BoA **3**, one can distinguish the two contours with relative ease and thus establish integration limits. It is this overlap, however, that reduces the accuracy of the integrations that may be performed on these contours. Nevertheless, integration reveals that the crude block copolymer mixture contains around 4.4 ± 1.6 wt% unreacted P*i*BoA **3**, which is still in good agreement with the predicted value of 5.0 ± 0.25 wt%, which was determined as outlined previously.

Figure 10.9c presents the 2D-chromatograms and three-dimensional renderings of the PMMA-*b*-P*i*BoA **7** block copolymer and the precursor P*i*BoA **4**. Two contours were detected in the analysis of the 2D-chromatogram of the block copolymer. The major contour, centred at a LACCC elution volume of around 2.55 mL is associated with the targeted block copolymer. The minor contour centred about a LACCC elution volume of 3.1 mL is representative of remaining unreacted P*i*BoA **4**, the amount of which was determined to be 5.2 ± 1.9 wt% by integration, which is in good agreement with the predicted value of 5.5 ± 0.83 wt% (Table 10.3).

Where block copolymers are separated from their P*i*BoA precursors primarily in the LACCC dimension, separation of the said blocks from their PMMA precursors occurs in the SEC dimension. Figure 10.10 depicts the 2D-chromatograms of the synthesized block copolymers overlayed with that of the common precursor PMMA **1**.* It can readily be observed that as the molecular weight of the block copolymer increases, their separation from PMMA **1** in the SEC dimension markedly increases. It is at this point that it should be noted that in all cases the P*i*BoA component of the block copolymers ranges from being roughly 1.5 times to 10 times larger than the PMMA component in terms of molecular weight. Thus, in achieving a stoichiometric ratio between the two components for the conjugation reactions, a higher mass of the P*i*BoA component is required than that of the PMMA component. For this reason, it is anticipated that the mass fraction of residual PMMA in the crude block copolymer mixtures will be rather small. Therefore, under the assumption of quantitative

*Ideally, Figure 10.9 and 10.10 should be combined, however the PSS software used to process the presented data does not allow for the overlay of more than one 2D-chromatogram.

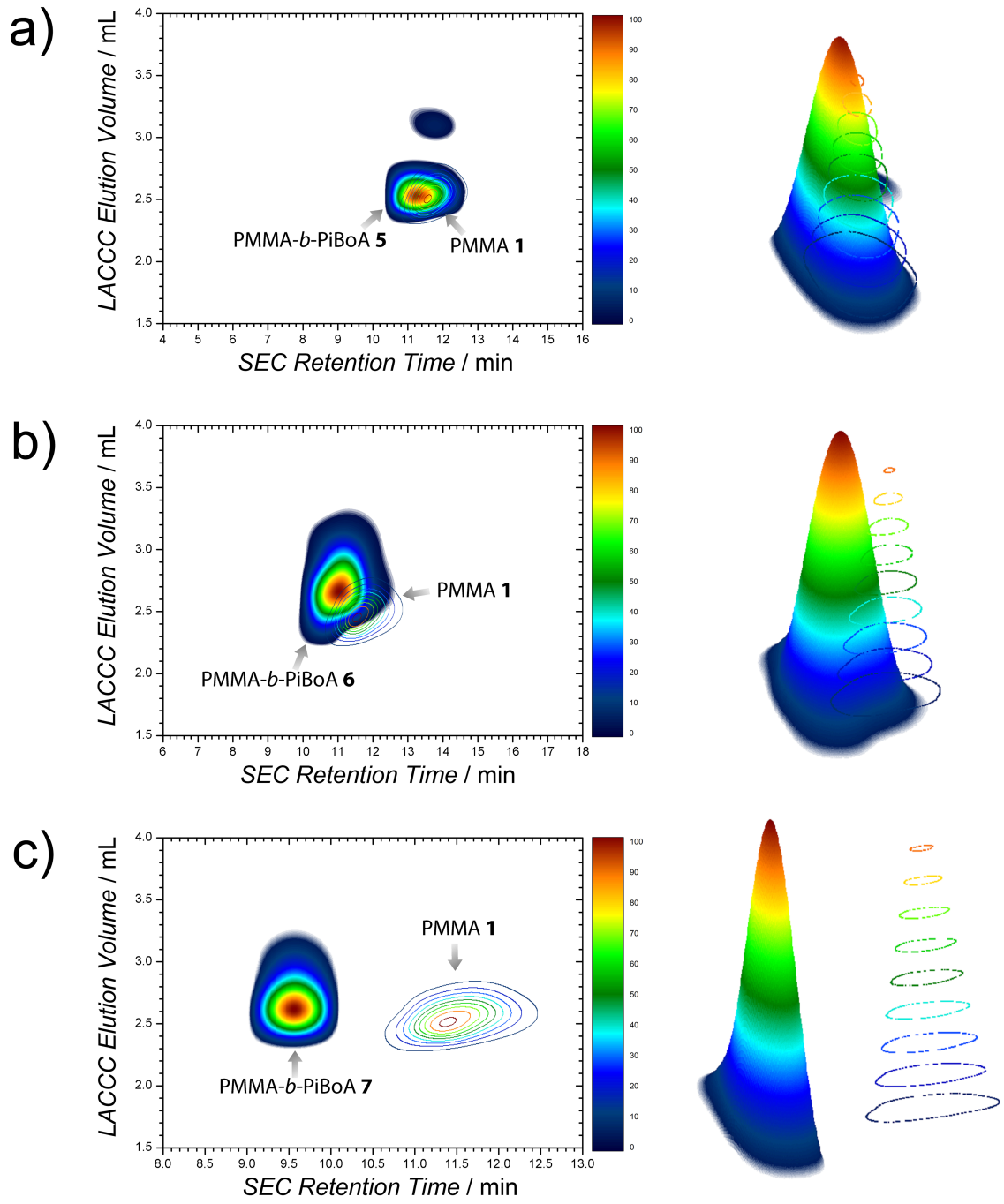

Figure 10.10 2D LACCC-SEC chromatograms and corresponding three dimensional renderings of a) PMMA-*b*-P*i*BoA **5**; b) PMMA-*b*-P*i*BoA **6**; and c) PMMA-*b*-P*i*BoA **7**; all overlayed with their respective PMMA precursors. Note the different scales of the SEC dimension.

conjugation efficiency, the predicted residual PMMA compositions of the three block copolymers (PMMA-*b*-P*i*BoA **5**, **6** and **7**) are only 1.2 ± 0.24 wt%, 1.0 ± 0.2 wt% and 0.3 ± 0.06 wt% respectively. In the case of blocks **5** and **6**, the degree of overlap between the contours of the block copolymers and the PMMA residue render its quantification via the presently used 2D chromatographic technique not possible (Figure 10.10a,b). In the case of block **7**, the much larger separation as observed in Figure 10.10c would be highly conducive to a quantitative analysis by integration; however the predicted value of 0.3 ± 0.06 wt% residual PMMA was found to lie below to detection limits of the 2D LACCC-SEC system utilized. Thus the lack of any detectable contour at a LACCC elution volume of 2.5 mL and SEC retention time of 11.5 minutes provides a good indication that if any unreacted PMMA precursor remained in the crude reaction mixture, its quantity would be very low indeed, which supports the assumption of quantitative conjugation efficiency.

It should be noted that the error associated with integrating such 2D-chromatograms is largely omitted from the literature. Indeed, establishing systematic error limits for such a coupled technique is no trivial task. What one can readily determine, however, is the reproducibility of the chromatographic technique. As such, after multiple analyses [eluting each sample twice and repeated integration (5 times) of the 2D chromatograms], the above presented composition of the block copolymer mixtures are averages, with the maximum and minimum values providing an estimate for the (statistical) error of the analysis. As such, the (statistical) error associated with the determination of the residual P*i*BoA content in the three block copolymer mixtures averaged to ± 35 %.

While the 2D LACCC-SEC analysis of the block copolymers formed via a modular pathway proves the high efficiency of the synthesis, the analytical technique is rather labour intensive and must be fine-tuned for every individual sample that is analysed. As such, it cannot be considered to be a standard nor a practical high throughput analytical method. In lieu of access to such a technique, it was discovered that a simple deconvolution of the conventional SEC traces of the block copolymers yielded comparably accurate composition data. Deconvolution of SEC traces has been used in the literature for the analysis of the modular construction of block copolymers and star-shaped polymers,[41–46] however its reliability has not been validated. Furthermore, in some instances in the literature, the area fractions of the deconvoluted peaks have been interpreted to give the fraction of polymer chains or the molar fraction of a certain component. This is incorrect as the SEC traces are mass distributions,[†] not number distributions. As such, this technique provides mass fraction data and to interpret it in any other way is misleading and false.

[†]More specifically, SEC traces from RI-detection are relative to both mass and incremental changes in refractive index.

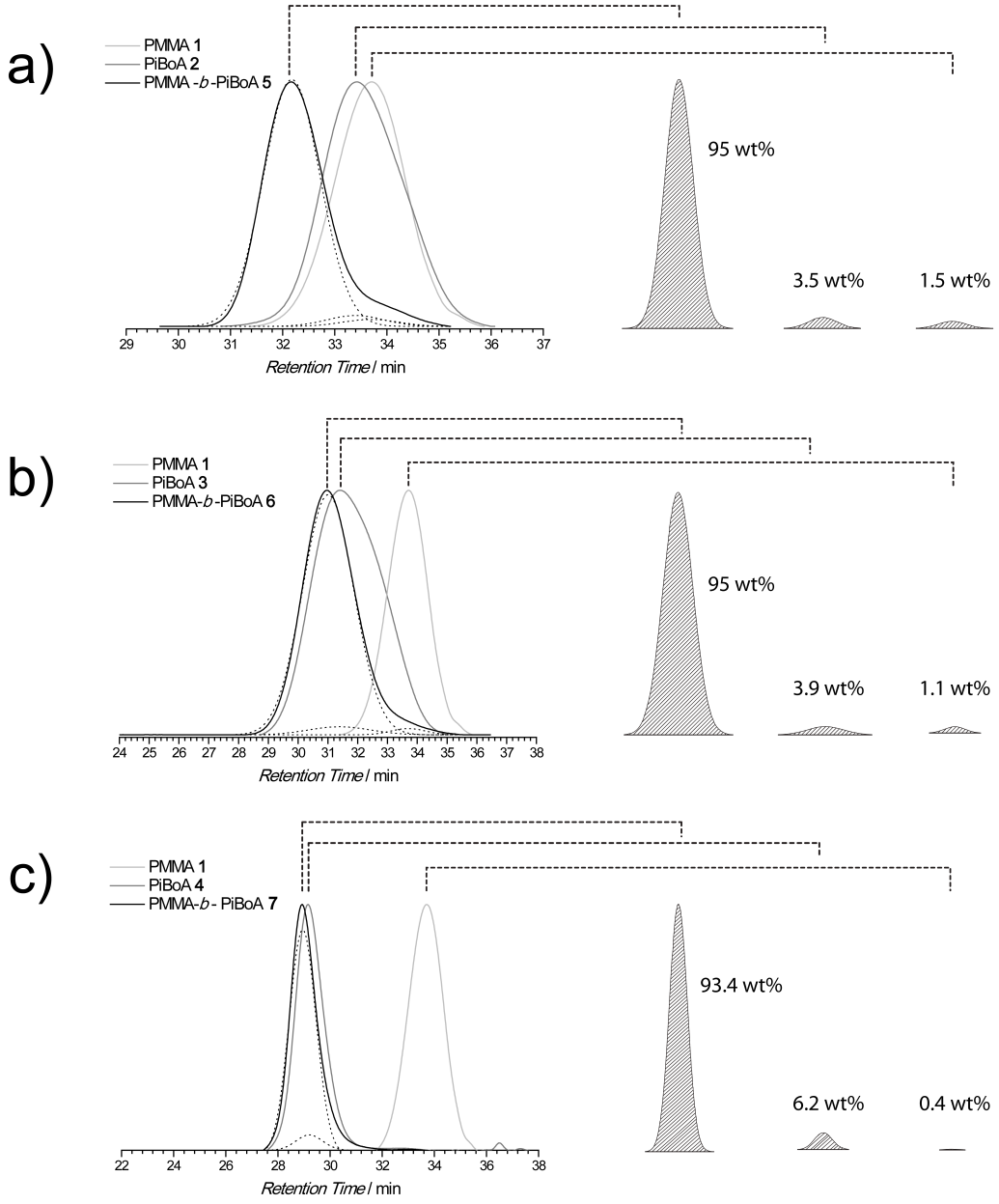

Figure 10.11 SEC trace deconvolution produces reliable estimations of the composition of crude block copolymer mixtures. The correlation coefficients (R^2) of the peak fittings are a) 0.998; b) 0.999; and c) 0.999, with 1.0 representing a perfect fit. The above presented values are conservatively estimated to contain a 1 % error resulting from the deconvolution on top of the 10 % error of the SEC measurements (see main text for an explanation).

Table 10.3 Crude block copolymer reaction mixture compositions obtained by three independent methodologies.

	2D LACCC-SEC[a] / wt%		Deconvolution[b] / wt%			Prediction[c] / wt%		
	Block + PMMA	P*i*BoA	Block	P*i*BoA	PMMA	Block	P*i*BoA	PMMA
5	97.0 ± 1.0	3.0 ± 1.0	95.0	3.5	1.5	95.8 ± 0.4	3.0 ± 0.15	1.2 ± 0.24
6	95.6 ± 1.6	4.4 ± 1.6	95.0	3.9	1.1	94.0 ± 0.5	5.0 ± 0.25	1.0 ± 0.20
7	94.8 ± 1.9	5.2 ± 1.9	94.3	6.2	0.4	94.2 ± 1.5	5.5 ± 0.83	0.3 ± 0.06

[a]Determined via integration of contours in the 2D LACCC-SEC chromatograms.[b]Determined via integration of the deconvoluted peaks of the SEC analysis. As the iterative nature of the deconvolution minimizes error, the 1 % error associated with the fit is introduced on top of the 10 % error of the original SEC measurements.[c]Determined via calculation (working on the assumption of 100 % conjugation efficiency), taking into account the different degrees of functionalization of the respective precursors.

In the case of block copolymer formation, the SEC traces of the precursor homopolymers are used to guide the fitting of associated peaks in the SEC trace of the crude block copolymer mixture. Figure 10.11 shows the results of such a deconvolution, in which the areas under the fitted traces relate to the mass fractions of their respective components. In all cases, greater than 90 wt% of the crude block copolymer mixtures are the targeted block copolymers. Naturally, there is a limit to the sensitivity, and thus the accuracy of SEC RI traces for constituents present in minute quantities. It is therefore understandable that a deconvolution of SEC traces as presently described will likewise contain error. However, the fitting of peaks is an iterative procedure in which the error (of fitting) is reduced to a minimum, as indicated by the correlation coefficients (R^2), as given in Figure 10.11. In all cases, the convergence status of all fits was given as converged and all fitted data lied within 1 % of the original data (as established by a 95 % confidence interval). This error comes on top of the inherent error of the SEC measurement which, on the system utilized, is conservatively estimated to be 10 %. It is also important to note that the deconvolution procedure is not dependent upon the SEC calibration as it is the SEC elugrams that are deconvoluted, not the calibrated molecular weight distributions.

A comparison of the composition data obtained from the 2D LACCC-SEC analysis, SEC trace deconvolution and the predicted values is presented in Table 10.3. Upon inspection, it is very clear that there is good agreement between the predicted values and those obtained from the two independent analytical methods. It is possible that the apparent close agreement of the presented values is pure coincidence as there is a degree of uncertainty in their determination, attributable to the inherent error of the analytical techniques and potential detector non-linearities. A seemingly attractive way around this dilemma appears to be a 'spiking' experiment, where known

amounts of additional homopolymer are added to the analyte. However, such a procedure will not eliminate the potential disparity in (ELS) detector signal between the block copolymer and its precursors. As a 100 % pure block copolymer is neither theoretically nor practically achievable for the system studied, a 'spiking' approach will not provide individual confirmed compositions, leaving the obtained results open to interpretation. To the best of our knowledge, the only technique potentially capable of affording unambiguous compositions with regard to the detector response is a coupling of LACCC-SEC to (quantitative) ^{1}H NMR spectroscopy, which allows the integration of every LACCC fraction via NMR.[47] Clearly, such an extremely complicated and expensive technique is not applicable for routine characterization efforts of block copolymers.

Overall, the reproducibility within (statistical) experimental error that is observed between the three data sets reported herein suggests that there is a good correlation. It is unlikely that the deconvolution on three separate, independently prepared and analysed block copolymer samples yields individual component contributions that are by mere coincidence in agreement with the LACCC-SEC and the predicted compositions. It should be stressed that block copolymers represent some of the simplest macromolecular architectures that may be analysed by 2D LACCC-SEC. However, for much more complicated polymeric mixtures, the presently described deconvolution method would not be able to be used in its place. Nevertheless, considering the wide applicability and, therefore, importance of high purity block copolymers, the low-cost and convenient SEC deconvolution technique provides a reliable means of assessing the purity of such structures.

10.4 Conclusion

The present contribution has, for the first time, provided a 2D-chromatographic analysis of the rapid, modular construction of block copolymers, which has fast become the method of choice in the synthesis of such materials. A combination of conventional SEC, LACCC and 2D LACCC-SEC was used to quantitatively visualize the formation of novel PMMA-*b*-P*i*BoA copolymers from highly functional precursors. In addition to further confirming the quantitative nature of the conjugation chemistry utilized, characterization of the composition of the crude block copolymer mixtures was also achieved. Through this analysis and calculable predictions, the low cost deconvolution of SEC traces was found to obtain comparable composition data within experimental error.

References

[1] Abetz, V.; Boschetti-de Fierro, A.; Gohy, J.-F. Morphologies in Block Copolymers. In *Controlled and Living Polymerizations: Methods and Applications*; Müller, A. H. E., Matyjaszewski, K., Eds.; Wiley-VCH Verlag GmbH & Co.: Weinheim, 2009; pp 493–554.

[2] Tang, C. B.; Lennon, E. M.; Fredrickson, G. H.; Kramer, E. J.; Hawker, C. J. *Science* **2008**, *322*, 429–432.

[3] Bang, J.; Jeong, U.; Ryu, D. Y.; Russell, T. P.; Hawker, C. J. *Adv. Mater.* **2009**, *21*, 4769–4792.

[4] Ji, S. X.; Liu, C. C.; Liu, G. L.; Nealey, P. F. *ACS Nano* **2010**, *4*, 599–609.

[5] Paquet, C.; Kumacheva, E. *Mater. Today* **2008**, *11*, 48–56.

[6] Kataoka, K.; Harada, A.; Nagasaki, Y. *Adv. Drug Deliver. Rev.* **2001**, *47*, 113–131.

[7] Braunecker, W. A.; Matyjaszewski, K. *Prog. Polym. Sci.* **2007**, *32*, 93–146.

[8] Ouchi, M.; Terashima, T.; Sawamoto, M. *Chem. Rev.* **2009**, *109*, 4963–5050.

[9] Moad, G.; Rizzardo, E.; Thang, S. H. *Polymer* **2008**, *49*, 1079–1131.

[10] Moad, G.; Rizzardo, E.; Thang, S. H. *Aust. J. Chem.* **2009**, *62*, 1402–1472.

[11] Okamoto, A.; Shimanuki, Y.; Mita, I. *Eur. Polym. J.* **1982**, *18*, 545–548.

[12] Hadjichristidis, N.; Pispas, S.; Floudas, G. A. *Block Copolymers: Synthetic Strategies, Physical Properties and Applications*; John Wiley & Sons, Inc.: Hoboken, 2002.

[13] Gitsov, I.; Simonyan, A.; Vladimirov, N. G. *J. Polym. Sci., Part A: Polym. Chem.* **2007**, *45*, 5136–5148.

[14] Opsteen, J. A.; van Hest, J. C. M. *Chem. Commun.* **2005**, 57–59.

[15] Durmaz, H.; Colakoclu, B.; Tunca, U.; Hizal, G. *J. Polym. Sci., Part A: Polym. Chem.* **2006**, *44*, 1667–1675.

[16] Quémener, D.; Davis, T. P.; Barner-Kowollik, C.; Stenzel, M. H. *Chem. Commun.* **2006**, 5051–5053.

[17] Kolb, H. C.; Finn, M. G.; Sharpless, K. B. *Angew. Chem. Int. Ed.* **2001**, *40*, 2004–2021.

[18] Belenky, B. G.; Gankina, E. S.; Tennikov, M. B.; Vilenchik, L. Z. *J. Chromatogr.* **1978**, *147*, 99–110.

[19] Glöckner, G.; Vandenberg, J. H. M. *J. Chromatogr.* **1991**, *550*, 629–638.

[20] Glöckner, G.; Stickler, M.; Wunderlich, W. *Fres. Zeitschr. Anal. Chem.* **1988**, *330*, 46–49.

[21] Pasch, H.; Gallot, Y.; Trathnigg, B. *Polymer* **1993**, *34*, 4986–4989.

[22] Kilz, P.; Kruger, R. P.; Much, H.; Schulz, G. *Chromatographic Characterization of Polymers* **1995**, *247*, 223–241.

[23] Pasch, H. *Adv. Polym. Sci.* **1997**, *128*, 1–45.

[24] Berek, D. *Prog. Polym. Sci.* **2000**, *25*, 873–908.

[25] Stoll, D. R.; Li, X. P.; Wang, X. O.; Carr, P. W.; Porter, S. E. G.; Rutan, S. C. *J. Chromatogr. A* **2007**, *1168*, 3–43.

[26] Dugo, P.; Cacciola, F.; Kumm, T.; Dugo, G.; Mondello, L. *J. Chromatogr. A* **2008**, *1184*, 353–368.

[27] Berek, D. *Anal. Bioanal. Chem.* **2010**, *396*, 421–441.

[28] Lee, W.; Cho, D. Y.; Chang, T. Y.; Hanley, K. J.; Lodge, T. P. *Macromolecules* **2001**, *34*, 2353–2358.

[29] Park, I.; Park, S.; Cho, D. Y.; Chang, T. Y.; Kim, E.; Lee, K. Y.; Kim, Y. J. *Macromolecules* **2003**, *36*, 8539–8543.

[30] Philipsen, H. J. A. *J. Chromatogr. A* **2004**, *1037*, 329–350.

[31] Li, M.; Jahed, N. M.; Min, K.; Matyjaszewski, K. *Macromolecules* **2004**, *37*, 2434–2441.

[32] Min, K.; Gao, H. F.; Matyjaszewski, K. *J. Am. Chem. Soc.* **2005**, *127*, 3825–3830.

[33] Gao, H. F.; Min, K.; Matyjaszewski, K. *Macromol. Chem. Phys.* **2006**, *207*, 1709–1717.

[34] Falkenhagen, J.; Much, H.; Stauf, W.; Müller, A. H. E. *Macromolecules* **2000**, *33*, 3687–3693.

[35] Mass, V.; Bellas, V.; Pasch, H. *Macromol. Chem. Phys.* **2008**, *209*, 2026–2039.

[36] Binder, W. H.; Sachsenhofer, R. *Macromol. Rapid Commun.* **2008**, *29*, 952–981.

[37] Barner-Kowollik, C. *Macromol. Rapid Commun.* **2009**, *30*, 1625–1631.

[38] Koo, S. P. S.; Junkers, T.; Barner-Kowollik, C. *Macromolecules* **2009**, *42*, 62–69.

[39] Günzler, F.; Wong, E. H. H.; Koo, S. P. S.; Junkers, T.; Barner-Kowollik, C. *Macromolecules* **2009**, *42*, 1488–1493.

[40] Wong, E. H. H.; Stenzel, M. H.; Junkers, T.; Barner-Kowollik, C. *Macromolecules* **2010**, DOI: 10.1021/ma100263k.

[41] Altintas, O.; Yankul, B.; Hizal, G.; Tunca, U. *J. Polym. Sci., Part A: Polym. Chem.* **2006**, *44*, 6458–6465.

[42] Gao, H. F.; Matyjaszewski, K. *Macromolecules* **2006**, *39*, 4960–4965.

[43] Durmaz, H.; Dag, A.; Altintas, O.; Erdogan, T.; Hizal, G.; Tunca, U. *Macromolecules* **2007**, *40*, 191–198.

[44] Altintas, O.; Demirel, A. L.; Hizal, G.; Tunca, U. *J. Polym. Sci., Part A: Polym. Chem.* **2008**, *46*, 5916–5928.

[45] Altintas, O.; Hizal, G.; Tunca, U. *J. Polym. Sci., Part A: Polym. Chem.* **2008**, *46*, 1218–1228.

[46] Durmaz, H.; Dag, A.; Hizal, A.; Hizal, G.; Tunca, U. *J. Polym. Sci., Part A: Polym. Chem.* **2008**, *46*, 7091–7100.

[47] Hiller, W.; Pasch, H.; Sinha, P.; Wagner, T.; Thiel, J.; Wagner, M.; Müllen, K. *Macromolecules* **2010**, *43*, 4853–4863.

11

Reversible Diels-Alder Chemistry as a Modular Polymeric Colour Switch

11.1 Introduction

A rising demand for complex and precisely engineered materials can be observed in such rapidly growing fields as biomedicine and nanoscience. Although CRP processes, such as ATRP[1] and RAFT polymerization[2] allow for the generation of well-defined architectures, it has been its recent combination with the concept of *click* chemistry that has provided a powerful tool in meeting such demands.[3] Indeed, the modern day chemist has a number of tools available to carry out ultra-rapid and mild conjugation chemistry with functionalities such as azide-alkyne,[4] thiol-ene,[5, 6] thiol-isocyanate,[7] tetrazine-alkene,[8] thio-bromo,[9] nitrile oxide,[10] aminooxy-aldehyde/ketone,[11] tetrazole-alkene[12] and dithioester-diene (Chapter 7, 8), to name but a few.[13] Within this framework of reactions, polymers can be viewed as molecular building blocks providing convenient modular access to complex functional materials.

Aside from orthogonal and ultra-rapid conjugation, significant attention has been drawn to the development of polymeric systems capable of reversibly switching between different physical and/or chemical states in response to external stimuli (e.g. temperature or pH). Indeed, such polymers would bear mendable[14] and

recyclable[15] features which could be translated into materials for applications in, for example, smart windows, displays, and switches.[16–19] Such stimuli responses include the thermally driven reversibility of covalent bonds, as is the case for Diels-Alder (DA) chemistry[20–22] or the cleavage of alkoxyamines,[23] photo- induced reversibility as in the case of olefin cycloadditions,[24] and pH driven reversibility as in the case of boronic-salicylic hydroxamic acid coupling.[25] However, the controlled incorporation of reversible covalent bonds into polymer chain remains challenging and as of yet only limited examples have been reported in the literature.

The predominant method in polymer chemistry in producing thermo-reversible covalent bonds is undoubtedly the DA reaction, which offers precise control under which chemical linkages are formed and broken. Indeed, the DA reaction has been utilized in polymer science as a method of producing reversibly cross-linked gels,[26] polymers featuring self-healing abilities,[27] surface modifications[28] and even as a polymerization technique itself.[29, 30] Recently, the reversible release of arms from a star molecule could be demonstrated for seven cycles in a DA - retro DA reaction between maleimides and furan, although this was only demonstrated on a small-molecule scale.[31] However, very recently Haddleton and coworkers obtained a relatively low efficiency of 50 % reformation of the maleimide-furan-cycloadduct linking two polymers after a reheating cycle.[32]

In search of improved efficiencies, the ultra-rapid RAFT-HDA *click* reaction is herein utilized in a reversible fashion: In this approach, electron deficient dithioesters are used as reactive heterodienophiles in a HDA cycloaddition. This versatile concept has been employed in the synthesis of complex macromolecular architectures such as blocks (Chapter 4), stars (Chapter 5) and star-shaped block copolymers (Chapter 6). It has also been employed in the modification of silicon surfaces[33] and surface-functionalized polymeric microspheres.[34] Since dithioesters are coloured by virtue of the forbidden $\pi \rightarrow \pi^*$ transition of the C=S moiety, one benefits - in addition to the high efficiency (at 1:1 stoichiometry) of the rapid HDA reaction - from two advantages: (1) The reaction progress can be directly monitored by UV/Vis spectroscopy, as the concentration of the dithioester is directly proportional to its absorption; and (2) a system where the controlled release of the dithioester behaves as a modular polymeric colour switch.

In Chapter 5, it was shown the RAFT-HDA reaction can be quantitatively reversed upon thermal treatment. However, in this case an open-chain diene was utilized, the cycloadduct of which required temperatures greater than 120 °C to achieve reversion. At these temperatures, the dithioesters that are released readily decompose, thus cycling between the *clicked* and *unclicked* states is not possible. However, the use of the more reactive Cp function allows for a reduction in the temperature range in which the forward and reverse HDA reaction can take place. As such, a thermally induced

polymeric colour switch that is based upon a completely reversible HDA system is reported (Figure 11.1).

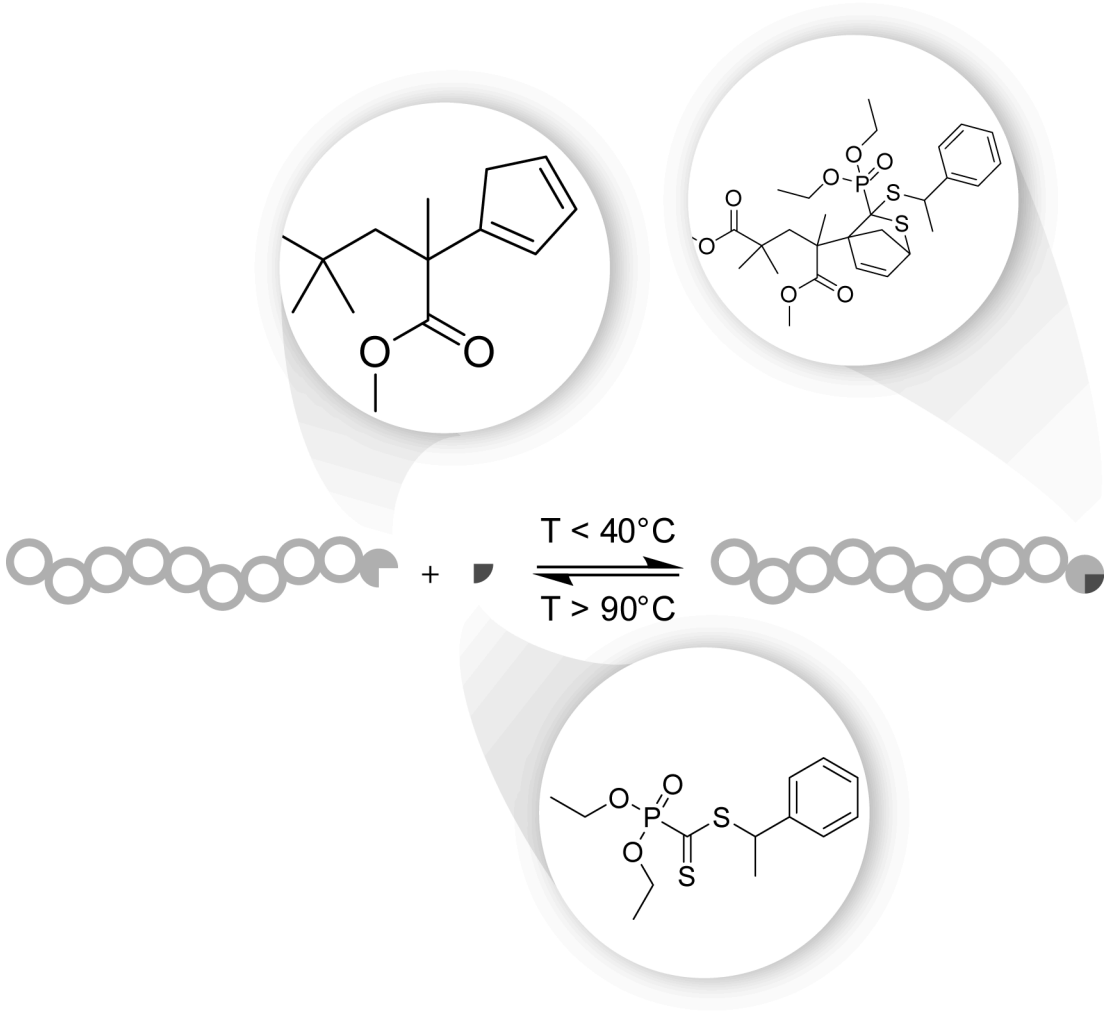

Figure 11.1 Exploring the reversibility of the RAFT-HDA *click* reaction within the context of colour switching materials.

11.2 Experimental Section

PMMA-Cp **1** ($M_{n,SEC}$ = 2500 g·mol^{-1}, *PDI* = 1.06) was synthesized according to the procedure outlined in Chapter 9. The dithioester 1-phenylethyl(diethoxyphosphoryl)dithioformate **2** was synthesized according to a literature procedure.[35]

Synthesis of PMMA Cycloadduct 3

A mixture of PMMA-Cp **1** (500 mg, 0.2 mmol) and **2** (64 mg, 0.2 mmol) was dissolved in 2 mL toluene in a glass sample tube and sealed. The catalyst-free reaction was allowed to proceed at ambient temperature for 72 hours under gentle agitation. The cycloadduct **3** was isolated by precipitation in cold *n*-hexane as a white solid.

UV/Vis Monitoring of the HDA/retro-HDA Cycloaddition

The polymeric cycloadduct **3** (50 mg) was dissolved in toluene (3 mL), filtered and placed in a UV/Vis cuvette. A small magnetic stirrer bar and $ZnCl_2$ (1 mg, 7.3 µmol) were added and the cuvette placed in the UV/Vis spectrophotometer. Starting at a temperature of 25 °C, the absorbance of the mixture (λ = 574 nm) was recorded every 5 minutes using a 0.16 °C·min^{-1} heating rate and, in another run, a 0.25 °C·min^{-1} heating rate. Upon reaching 100 °C, the temperature was ramped down at the same rate, with the absorbance measured until the temperature returned to 25 °C, at which point the heating/cooling cycle was repeated.

ESI-MS Analysis

The ESI-MS spectra depicted in Figure 11.7 were generated in the following fashion: 200 mg of the polymeric cycloadduct **3** was prepared and an initial ESI-MS spectrum was recorded (A). The remaining 195 mg of **3** was dissolved in 1 mL of toluene, filtered and placed with a stirrer in a closed standard SEC glass sample tube. This tube was subsequently heated under stirring to 100 °C and kept at this temperature for 30 minutes. 0.2 mL of the mixture at 100 °C was removed via a syringe and directly precipitated in 2 mL of cold *n*-hexane (B). The reaction mixture in the glass sample tube was subsequently allowed to cool to ambient temperature and the teflon cap was replaced with a fresh one. $ZnCl_2$ (1 mg, 7.3 µmol) was added and the reaction mixture was stirred overnight. 0.2 mL of the solution was precipitated in 2 mL of cold *n*-hexane (C). The sample tube with the remaining 0.6 mL of the reaction mixture was subsequently heated up again to 100 °C and kept at this temperature for 30 minutes.

0.3 mL of the mixture at 100 °C was removed via a syringe and directly precipitated in 2 mL of cold *n*-hexane (D). The reaction mixture was then allowed to cool to ambient temperature and was stirred overnight. Data for point E was subsequently obtained after precipitation in 2 mL of cold *n*-hexane.

11.3 Results and Discussion

The Cp-capped poly(methyl methacrylate) (PMMA-Cp) **1** (that was introduced in Chapter 9) and the hetero dienophile 1-phenylethyl (diethoxyphosphoryl) dithioformate **2** were synthesized as previously reported. The use of cyclopentadiene as a highly reactive end-group moiety was borne out of consideration of faster HDA reactions at ambient temperature and its ease of incorporation into the polymer chain by nickelocene as the source of the Cp unit. The initial coupling reaction between PMMA-Cp **1** and the dithioester **2** was performed in toluene at ambient temperature (Figure 11.2). It should be noted that the cycloadduct **3** contains a mixture of isomers, however only one chemical structure is presented throughout for reasons of brevity. Regardless, such isomers are present in every DA reaction and are of no importance proving the concept of modular switching.

Figure 11.3 depicts the ESI-MS spectra of the starting PMMA-Cp **1** alongside that of the reaction cycloadduct **3**. The dominant species in the spectrum of the starting material is clearly the required Cp-terminated polymer. One may also observe the presence of a small quantity of impurities, all but one of which can be assigned to inescapable side products of the ATRP process. The remaining unidentified product **I*** may be inferred to be another bromide-terminated species, based upon the characteristic isotopic pattern of its signal. Additionally, all observed products have been previously encountered in Chapter 9. The presence of small quantities of the starting material in the product spectrum arises due to the retro-HDA reaction occurring under the conditions of the measurement, an observation that has been previously verified (Chapter 3). A comparison of the experimental and theoretical *m/z* values is presented in Table 11.1.

After confirming its structure, the absorbance of a toluene solution of **3** was measured at various temperatures (λ = 400 - 650 nm) and compared to that of the pure dithioester **2** (Figure 11.4). As expected, the equilibrium (Figure 11.2) was observed to be strongly temperature dependent with an increase in absorbance occuring with

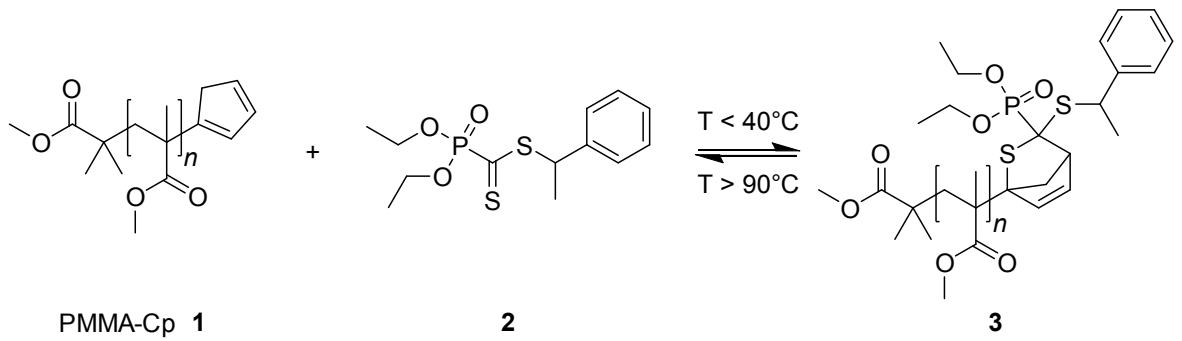

Figure 11.2 Polymeric colour-switch system based upon Diels-Alder chemistry.

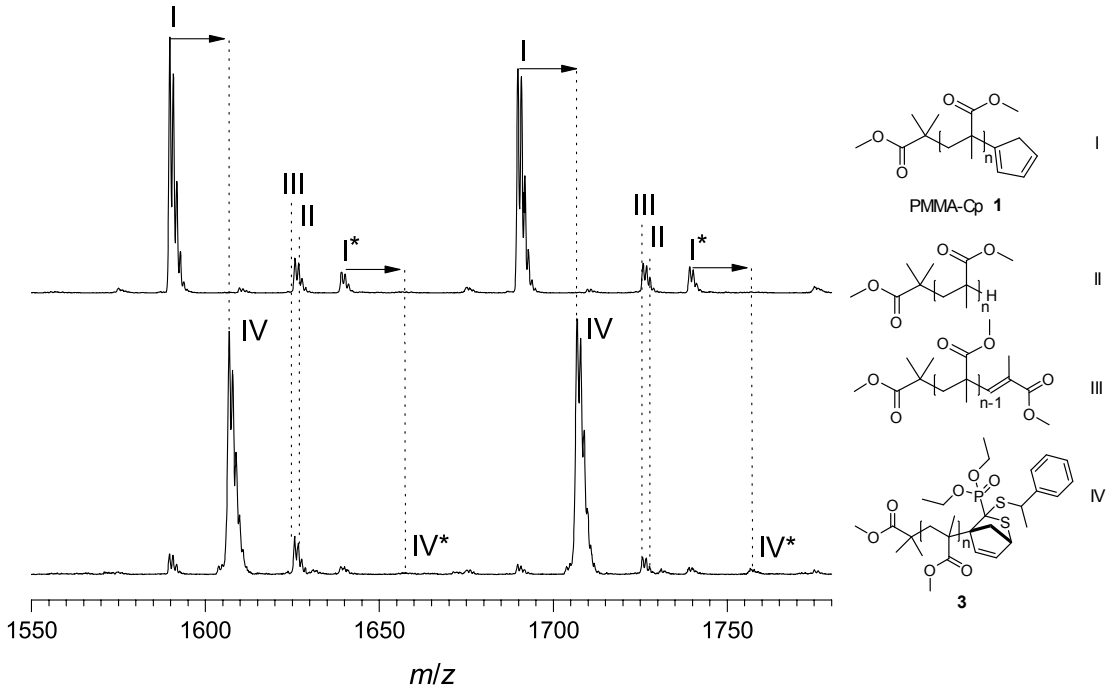

Figure 11.3 ESI-MS spectra of PMMA-Cp **1** and its HDA cycloadduct **3**. Within the presented *m/z* range, it should be noted that the number of monomer repeat units of **I** differs from that of **IV**.

increasing temperature. The remaining absorptivity of **3** does not impair the ability to monitor an efficient, subsequent switching behaviour of the system.

At ambient temperature only the cycloadduct **3** is present, whereas at temperatures over 90 °C only the starting components PMMA-Cp **1** and **2** are observed. Note that the process only functions because the HDA reaction occurs rapidly at ambient temperature. Importantly and clearly a requirement for colour switching, the dithioester **2** and the Cp-capped polymer **1** have both been proven to be thermally stable within the employed temperature range (20°C-100°C).

Table 11.1 Experimental and theoretical *m/z* values for the first peak in the isotopic distributions of Figure 11.3 in the *m/z* range between 1680-1780 and their assignment.

$m/z_{expt.}$	ion assignment	formula	$m/z_{theor.}$	$\Delta m/z$
1689.8	$\mathbf{I}_{(n=15)} + Na^+$	$[C_{85}H_{134}O_{32}Na]^+$	1689.9	0.1
1739.4	**I*** + Na^+	-	-	-
1726.0	**II** + Na^+	$[C_{85}H_{138}O_{34}Na]^+$	1725.9	0.1
1723.9	**III** + Na^+	$[C_{85}H_{136}O_{34}Na]^+$	1723.9	0.0
1707.8	$\mathbf{IV}_{(n=12)} + Na^+$	$[C_{83}H_{129}O_{29}PS_2Na]^+$	1707.8	0.0
1757.4	**IV*** + Na^+	-	-	-

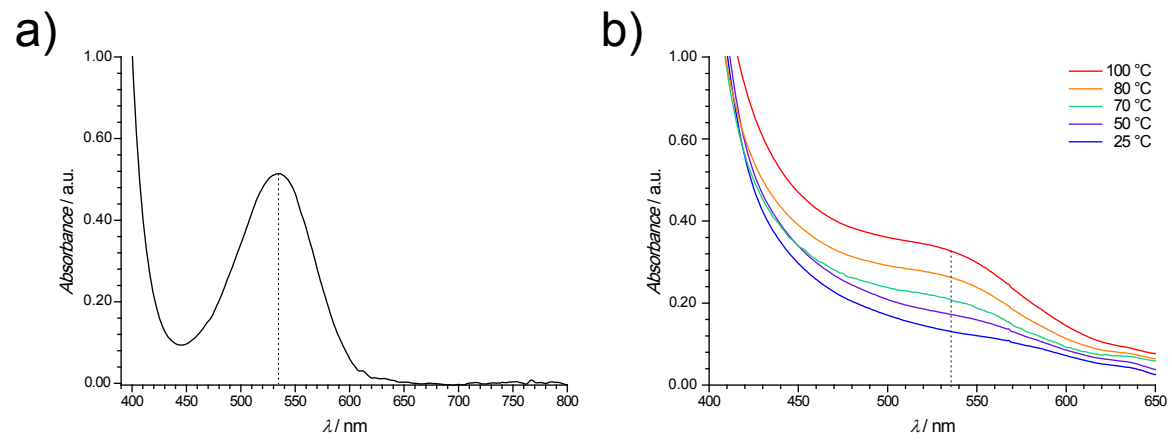

Figure 11.4 a) UV/Vis spectrum of the pure dithioester **2**. The absorbance reaches its maximum at $\lambda_{max.}$ = 534 nm; b) UV/Vis spectra of the cycloadduct **3** in toluene (0.05 mol·L^{-1}). Due to the occurence of the retro HDA reaction, the concentration of the free dithioester **2** increases with temperature. The dotted line indicates the maximum absorbance of **2**.

For a detailed investigation of a newly prepared solution of cycloadduct **3** in toluene (0.05 mol·L^{-1}) it is important to give the system enough time to reach its thermodynamic equilibrium between cycloadduct and its components for each temperature. For this reason, the UV/Vis spectroscopic investigations were conducted using the temperature cycle mode (between 25°C and 100°C) of the employed UV/Vis spectrophotometer with a relatively slow heating and cooling rate (0.16 °C·min^{-1}). It should be clearly noted that the addition of a catalyst is not a requirement for the quantitative formation/reformation of the cycloadduct **3**, however catalytic amounts of $ZnCl_2$ and a small stirrer were added to accelerate the cycloadduct reformation and to ensure the thermodynamic equilibrium for the complete cycle.

Subsequently, the absorbance of the sample was measured at one constant wavelength (λ = 574 nm) with the cooling phase started without any interruption after the heating stage. During the course of experimentation, a temperature dependence of the absorbance of **2** at $\lambda_{max.}$ = 534 nm was observed. Although reversible, such an occurence would falsify subsequent measurements during the colour-switch investigation. Thus, λ = 574 nm was identified as a wavelength in which there is no notable variation in the absorption between 20 °C and 100 °C. The complete cycle was repeated several times, the results of which are presented in Figure 11.5. The results clearly reveal a regular switching behaviour. For the switching analysis, the normalized absorbance of **3** has been set to zero. At higher temperatures, by contrast, a change of the thermodynamic equilibrium towards the building blocks (**1** and **2**) of the cycloadduct **3** can be observed, which ultimately leads to the presence of only **1** and **2** at 100 °C.

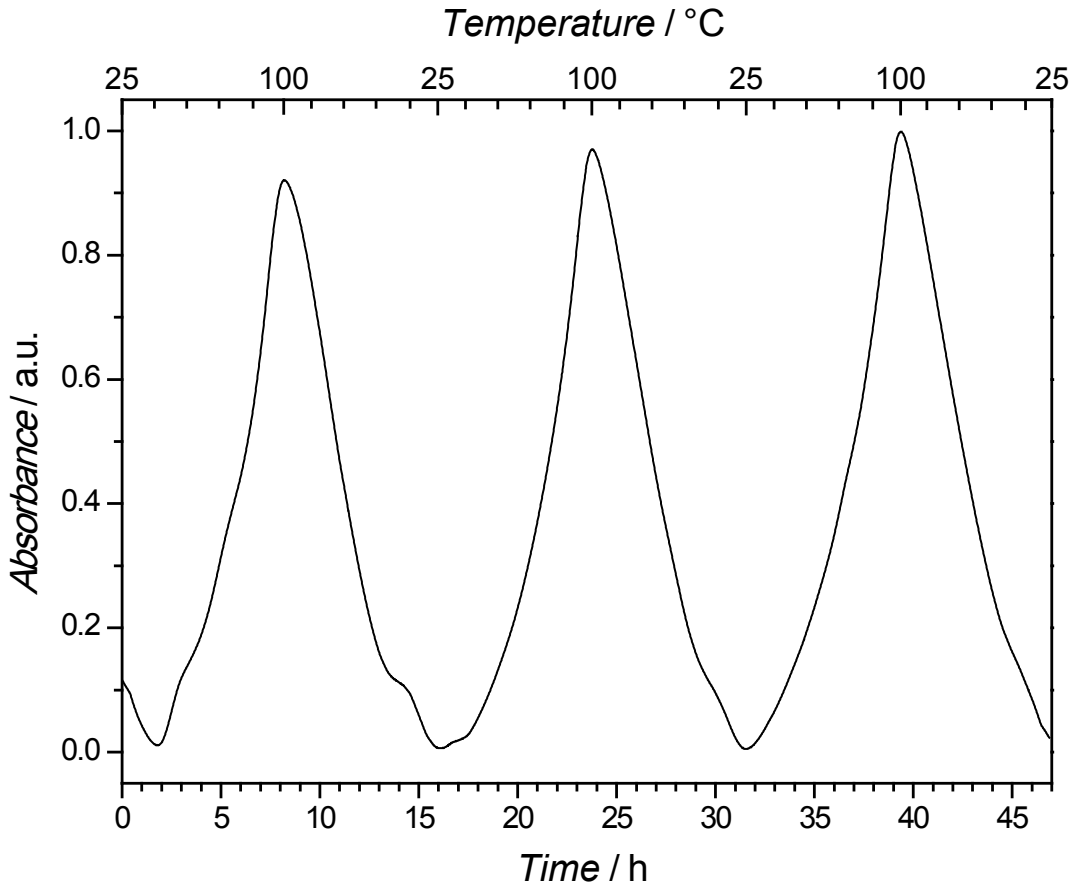

Figure 11.5 UV/Vis absorbance vs. temperature profile of the colour-switching polymeric system. The reversibility of the HDA *click* reaction is - within experimental error - quantitative. Note the clear switching behaviour of the system (heating/cooling rate: 0.16 °C·min^{-1}).

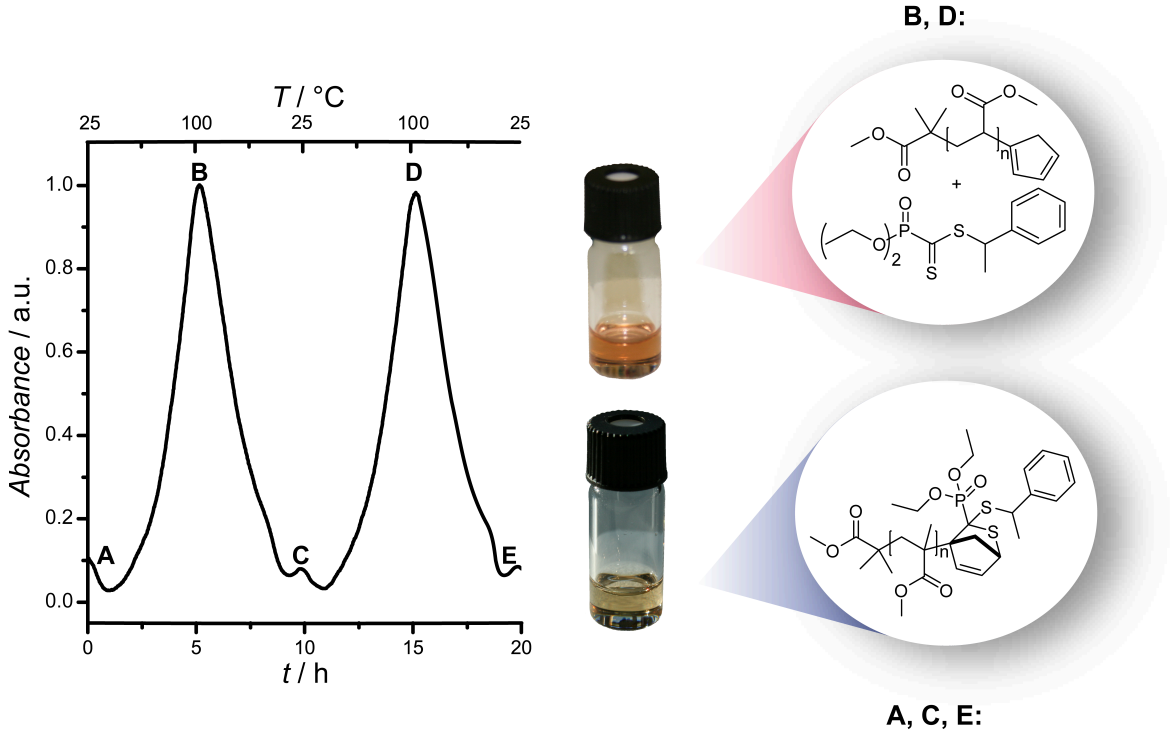

Figure 11.6 A complete reversibility of the switching system is demonstrated at a heating/cooling rate of 0.25 °C·min^{-1} for two cycles. Note the colour change from ambient temperature (**A**, **C**, **E**) to 100 °C (**B** and **D**).

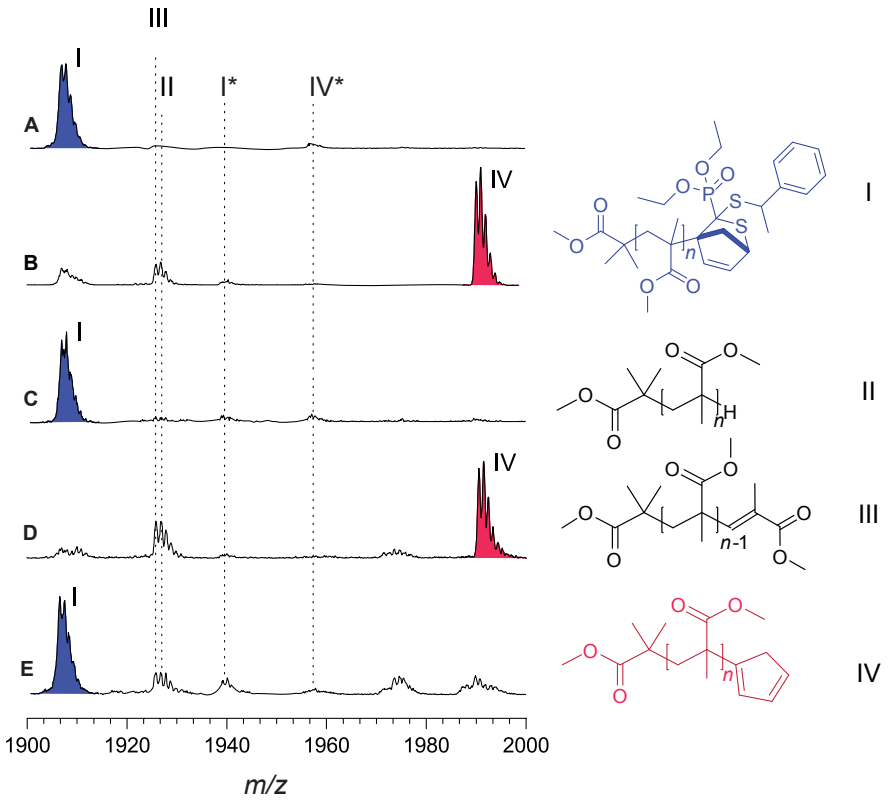

Figure 11.7 ESI-MS study to further confirm the reversibility of the HDA reaction. The structure of the building block **1** alternates with the structure of the cycloadduct **3**. The data **A** to **E** correspond to the likewise defined temperatures in the UV/Vis spectrum (Figure 11.6). Within the presented *m/z* range, it should be noted that the number of repeat units of **I** differs from that of **IV**.

Table 11.2 Experimental and theoretical *m/z* values for the first peak in the isotopic distributions of Figure 11.7 and their assignment.

$m/z_{expt.}$	ion assignment	formula	$m/z_{theor.}$	$\Delta m/z$
1907.8	$\mathbf{I}_{(n = 15)} + Na^+$	$[C_{98}H_{153}O_{35}PS_2Na]^+$	1907.9	0.1
1939.6	**I*** + Na^+	-	-	-
1925.9	**II** + Na^+	$[C_{100}H_{162}O_{40}Na]^+$	1926.0	0.1
1923.9	**III** + Na^+	$[C_{100}H_{160}O_{40}Na]^+$	1924.0	0.1
1989.9	$\mathbf{IV}_{(n = 18)} + Na^+$	$[C_{100}H_{158}O_{38}Na]^+$	1990.0	0.1
1957.5	**IV*** + Na^+	-	-	-

Similar success was also achieved by employing another heating/cooling rate: 0.25 °C·min^{-1} and, indeed, the UV/Vis data in Figure 11.6 indicates again - within the limits of experimental error - a quantitative reversibility of the employed switching system. To achieve a more detailed understanding of the HDA-process and to further prove its complete reversibility, an ESI-MS study was performed to obtain mass data for the data points **A**-**E**, as defined in Figure 11.6.

The results of the ESI-MS study are presented in Figure 11.7 and as theoretically expected, the structures of the building block **1** clearly alternates with the cycloadduct **3**, effectively correlating with the UV/Vis data. It should be noted that the acquisition of the data for **B** and **D** proved to be challenging, as one needs to precipitate the polymer out of a 100 °C solution without giving the system enough time to form **3** again. This practical reason might explain small residues of **1** in **B** and **D**. A comparison of the experimental and theoretical *m/z* values is presented in Table 11.2.

11.4 Conclusion

In summary, the highly efficient use of (retro-) HDA chemistry in a polymeric modular colour-switching material has been demonstrated. UV/Vis spectroscopic data, underpinned by an ESI-MS study, confirmed from the above presented results that the phosphoryl dithioester cycloadduct **3** indeed undergoes complete formation and re-formation and, moreover, the detailed reaction progress could be mapped on a molecular level for several complete switching cycles. The novel temperature guided colour switch, being based upon a modular polymeric retro-HDA reaction, can be efficiently controlled by external thermal stimulation. The provision of such a system, able to change physical and chemical properties in a controlled, fully reversible and predictable fashion, will greatly facilitate the fabrication of novel, stimuli-responsive materials.

References

[1] Matyjaszewski, K.; Xia, J. H. *Chem. Rev.* **2001**, *101*, 2921–2990.

[2] Perrier, S.; Takolpuckdee, P. *J. Polym. Sci., Part A: Polym. Chem.* **2005**, *43*, 5347–5393.

[3] Barner-Kowollik, C.; Inglis, A. J. *Macromol. Chem. Phys.* **2009**, *210*, 987–992.

[4] Rostovtsev, V. V.; Green, L. G.; Fokin, V. V.; Sharpless, K. B. *Angew. Chem. Int. Ed.* **2002**, *41*, 2596–2599.

[5] Pounder, R. J.; Stanford, M. J.; Brooks, P.; Richards, S. P.; Dove, A. P. *Chem. Commun.* **2008**, 5158–5160.

[6] Lowe, A. B. *Polym. Chem.* **2010**, *1*, 17–36.

[7] Klemm, E.; Stöckl, C. *Makromol. Chem.* **1991**, *192*, 153–158.

[8] Blackman, M. L.; Royzen, M.; Fox, J. M. *J. Am. Chem. Soc.* **2008**, *130*, 13518–13519.

[9] Rosen, B. M.; Lligadas, G.; Hahn, C.; Percec, V. *J. Polym. Sci., Part A: Polym. Chem.* **2009**, *47*, 3931–3939.

[10] Gutsmiedl, K.; Wirges, C. T.; Ehmke, V.; Carell, T. *Org. Lett.* **2009**, *11*, 2405–2408.

[11] Heredia, K. L.; Tolstyka, Z. P.; Maynard, H. D. *Macromolecules* **2007**, *40*, 4772–4779.

[12] Song, W.; Wang, Y.; Qu, J.; Madden, M. M.; Lin, Q. *Angew. Chem. Int. Ed.* **2008**, *47*, 2832–2835.

[13] Inglis, A. J.; Barner-Kowollik, C. *Macromol. Rapid Commun.* **2010**, *31*, 1247–1266.

[14] Bergman, S. D.; Wudl, F. *J. Mater. Chem.* **2008**, *18*, 41–62.

[15] Gandini, A.; Belgacem Mohamed, N. Recent Contributions to the Realm of Polymers from Renewable Resources. In *Materials, Chemicals, and Energy from Forest Biomass*; ACS Symposium Series; American Chemical Society: Washington, DC, 2007; pp 48–60.

[16] Bange, K.; Gambke, T. *Adv. Mater.* **1990**, *2*, 10–16.

[17] Gazotti, W. A.; Casalbore-Miceli, G.; Geri, A.; Berlin, A.; De Paoli, M. A. *Adv. Mater.* **1998**, *10*, 1522–1525.

[18] Rosseinsky, D. R.; Mortimer, R. J. *Adv. Mater.* **2001**, *13*, 783–793.

[19] Yoshioka, T.; Ogata, T.; Nonaka, T.; Moritsugu, M.; Kim, S. N.; Kurihara, S. *Adv. Mater.* **2005**, *17*, 1226–1229.

[20] Imai, Y.; Itoh, H.; Naka, K.; Chujo, Y. *Macromolecules* **2000**, *33*, 4343–4346.

[21] Chen, X. X.; Dam, M. A.; Ono, K.; Mal, A.; Shen, H. B.; Nutt, S. R.; Sheran, K.; Wudl, F. *Science* **2002**, *295*, 1698–1702.

[22] Goiti, E.; Heatley, F.; Huglin, M. B.; Rego, J. M. *Eur. Polym. J.* **2004**, *40*, 1451–1460.

[23] Higaki, Y.; Otsuka, H.; Takahara, A. *Macromolecules* **2006**, *39*, 2121–2125.

[24] Chen, Y.; Chen, K. H. *J. Polym. Sci., Part A: Polym. Chem.* **1997**, *35*, 613–624.

[25] Roberts, M. C.; Hanson, M. C.; Massey, A. P.; Karren, E. A.; Kiser, P. F. *Adv. Mater.* **2007**, *19*, 2503–2507.

[26] Liu, Y. L.; Hsieh, C. Y.; Chen, Y. W. *Polymer* **2006**, *47*, 2581–2586.

[27] Reutenauer, P.; Buhler, E.; Boul, P. J.; Candau, S. J.; Lehn, J. M. *Chem. Eur. J.* **2009**, *15*, 1893–1900.

[28] Gousse, C.; Gandini, A.; Hodge, P. *Macromolecules* **1998**, *31*, 314–321.

[29] Bailey, W. J.; Economy, J.; Hermes, M. E. *J. Org. Chem.* **1962**, *27*, 3295–3299.

[30] Kamahori, K.; Tada, S.; Ito, K.; Itsuno, S. *Macromolecules* **1999**, *32*, 541–547.

[31] Aumsuwan, N.; Urban, M. W. *Polymer* **2009**, *50*, 33–36.

[32] Syrett, J. A.; Mantovani, G.; Barton, W. R. S.; Price, D.; Haddleton, D. M. *Polym. Chem.* **2010**, *1*, 102–106.

[33] Nebhani, L.; Gerstel, P.; Atanasova, P.; Bruns, M.; Barner-Kowollik, C. *J. Polym. Sci., Part A: Polym. Chem.* **2009**, *47*, 7090–7095.

[34] Nebhani, L.; Sinnwell, S.; Inglis, A. J.; Stenzel, M. H.; Barner-Kowollik, C.; Barner, L. *Macromol. Rapid Commun.* **2008**, *29*, 1431–1437.

[35] Sinnwell, S.; Synatschke, C. V.; Junkers, T.; Stenzel, M. H.; Barner-Kowollik, C. *Macromolecules* **2008**, *41*, 79004–7912.

12

Rapid Bonding/Debonding on Demand: Reversibly Cross-Linked Polymers via Diels-Alder Chemistry*

12.1 Introduction

The design of reversibly linked and cross-linked polymeric materials that are able to change their physical characteristics rapidly, within a well-defined temperature interval and in a cyclic fashion, continues to be a highly investigated area in materials research.[1, 2] Lying at the core of such research is the exploitation of reversible covalent bonds within a polymer network. To date, there has been a wealth of chemistries that have been investigated within this context, such as thiol-driven sulphide coupling,[3] photo-reversible olefin cycloadditions,[4] carbene dimerization,[5] nucleophilic addition of isocyanates with imidazoles[6] and thermally cleavable alkoxyamines.[7] However, the most widely investigated technique by far has been Diels-Alder (DA) chemistry.[8–14] The use of DA cycloadditions (most specifically those between various maleimide and furan derivatives) in such technology has

*This work was carried out as part of an industrial collaboration with Evonik Degussa GmbH and has been appropriated for inclusion in the research thesis of L. Nebhani, being a co-author in its publication.

greatly been facilitated by both the commercial availability and chemical accessibility of such functional groups. To illustrate two very recent examples, low molecular weight star-shaped molecules were prepared by Aumsuwan and Urban[15] in which a maleimide-furan cycloadduct formed the linkage between the arms of the star and its core. From a variable-temperature ^{1}H NMR and ATR-IR spectroscopic analysis, the forward star-forming DA reaction was determined to proceed at 40 °C. The stars could subsequently be un-made through a 90 °C retro-DA reaction. In the other example, Haddleton and coworkers synthesized maleimide- and furan-capped polymers via ATRP which could be linked (60 °C, 24 h) and un-linked (110 °C, 24 h).[16]

The preceding chapters have explored the use of HDA chemistry as a polymeric conjugation method. Of particular importance are the results presented in Chapter 11, in which the reversibility of the HDA cycloaddition (with Cp functionality serving as the diene) was successfully exploited in producing a polymeric colour switch system. While the forward reaction is swift, the resulting cycloadducts are temperature stable up to a relatively moderate temperature range (60-90 °C), depending on the dithioester-Cp combination utilized. Beyond this temperature, an effective retro-DA reaction sets in, leading to a quantitative reformation of the starting materials.

A characteristic of DA chemistry that renders it highly attractive in such technologies is the wide variety of diene-dienophile pairs that can potentially be utilized, which allows one to fine-tune the temperature profile in which bonding and debonding take place. To date, particularly ultra-rapid (hetero-) DA chemistry has not been reported in the preparation of reversibly cross-linked polymeric structures. Thus, it is herein reported the synthesis of a novel poly(methyl methacrylate) (PMMA) chain bearing Cp functionality at both chain ends and a tri-functional pyridinyldithioformate linker molecule, which are able to rapidly and reversibly cross-link on demand within a highly accessible temperature range (Figure 12.1).

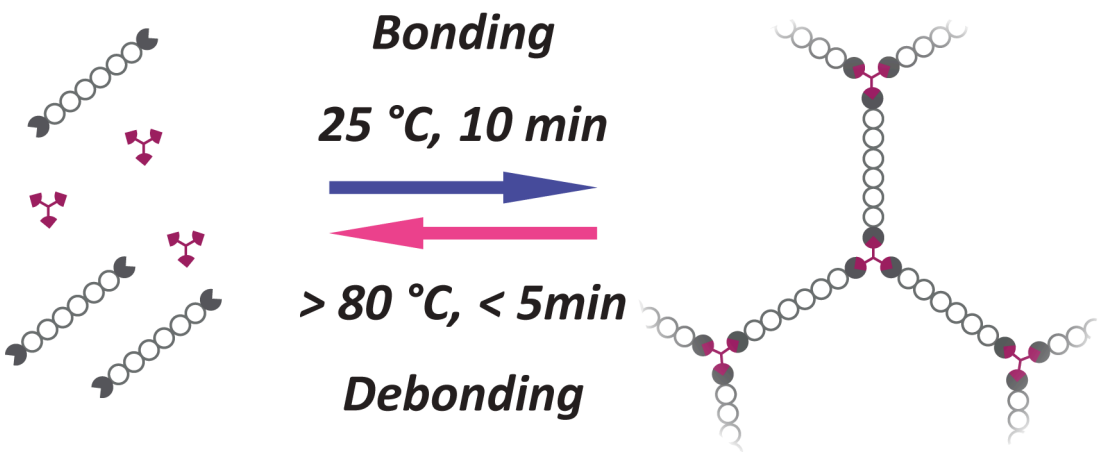

Figure 12.1 Rapid bonding/debonding on demand.

12.2 Experimental Section

Synthesis of Bis(cyclopentadienyl) Poly(methyl methacrylate) (PMMA-Cp_2)

Methyl methacrylate (MMA), 1,2-bis(bromoisobutyryloxy)ethane (Initiator),[17] copper (I) bromide (CuBr), copper (II) bromide ($CuBr_2$) and 2,2'-bipyridine (bpy) were added to a round bottom flask in the ratio 50/1/0.105/0.01250/0.25. Acetone was subsequently added such that the resulting mixture was 50 vol% acetone. Nitrogen was then bubbled through the mixture for 40 minutes to remove residual oxygen. The mixture was subsequently sealed under nitrogen and placed in a thermostatted oil bath set to 50 °C. After 2 hours, the polymerization was stopped by cooling the mixture in an ice-bath and exposure to oxygen. The mixture was then passed through a short column of neutral alumina to remove the copper catalyst. α, ω-functional poly(methyl methacrylate) (PMMA-Br_2) was isolated by two-fold precipitation in cold *n*-hexane. $M_{n,\,SEC}$ = 3500 g·mol^{-1}, PDI = 1.2.

α, ω-functional PMMA-Br_2, sodium iodide, tributylphosphine and nickelocene in the ratio 1/12/4/8 were dissolved, under nitrogen, in anhydrous THF such that the solution was 0.1 M with respect to the polymer. The ambient temperature reaction was allowed to proceed for at least 12 hours before the reaction mixture was passed through a short column of basic alumina. PMMA-Cp_2 was the isolated by a two-fold precipitation in cold *n*-hexane.

Synthesis of 4-((pyridine-2-carbonothioylthio)methyl) benzoic acid

STEP I: A mixture of 2-(chloromethyl)pyridine hydrochloride (1.64 g, 10 mmol), sodium phenylsulfinate (2.46 g, 15 mmol), and catalytic amount of tetrapropyl ammonium bromide (0.53 g, 2 mmol), DBU (1.52 g, 10 mmol) in CH_3CN (10 mL), was refluxed for 12 hours. The solvent was subsequently removed under vacuum and the residue was dissolved in CH_2Cl_2, washed with brine, dried over $MgSO_4$ and the solvent removed. The crude product was obtained in quantitative yield, as a white solid and was used without purification in the next step.

STEP II: A mixture of sulfone (1.9 g, 8.51 mmol) (from Step I) and elemental sulfur (0.78 g, 24.3 mmol) was placed into THF (10 mL) under magnetic stirring. After addition of *t*-BuOK (2.72 g, 24.3 mmol), the colour of the solution changed to dark brown. The reaction was stirred at ambient temperature for 12 hours. Subsequently, 4-methylbenzoic acid (2.6 g, 12.15 mmol) in THF (10 mL) was added dropwise to the solution and stirring was continued for a further 5 hours. The colour consequently changed to reddish-pink. The product was washed with aqueous HCl (2 N) and extracted in CH_2Cl_2. The crude product was finally purified by extraction with acetone

(45 % yield). ^{1}H NMR (DMSO-d_6, 250 MHz, 25 °C): δ = 13.0 (s, 1H, -COO**H**), 8.62-8.64 (m, 1H, pyr**H**), 7.95-8.26 (m, 2H, Ar**H**), 7.87-7.91 (m, 2H, pyr**H**), 7.67-7.71 (m, 1H, pyr**H**), 7.51-7.54 (m, 2H, Ar**H**), 4.63 (s, 2H, S-C**H$_2$**) ppm. ^{13}C NMR (DMSO-d_6, 100 MHz, 25 °C): δ = 226.1 (Py-**C**(S)-S-), 166.9 (Ar-**C**(O)-OH), 155.4 (**C**$_{Py}$), 148.3 (**C**$_{Py}$), 140.7 (**C**$_{Ar}$), 137.8 (**C**$_{Py}$), 129.5 (**C**$_{Ar}$), 129.4 (**C**$_{Ar}$), 127.9 (**C**$_{Ar}$), 121.9 (**C**$_{Py}$), 40.1 (Ar-**C**H$_2$-S-) ppm.

Synthesis of the Trifunctional Linker

1,1,1-Tris(hydroxymethyl)propane (TMP) (0.072 g, 0.536 mmol), 4-(Dimethylamino)-pyridinium-4-toluene sulfonate (DPTS) (0.118 g, 0.402 mmol) and (dimethylamino)pyridine (DMAP) (0.025 g, 0.201 mmol) were dissolved in 10 mL of CH_2Cl_2. 4-((pyridine-2-carbonothioylthio)methyl) benzoic acid (0.581 g, 2.01 mmol) were dissolved in 3 mL DMF and then added to the solution. After 10 minutes, dicyclohexylcarbodiimide (DCC) (0.622 g, 3.01 mmol) in 2 mL of dichloromethane was added to the solution. The reaction mixture was stirred overnight at ambient temperature. It was subsequently filtered, evaporated and the remaining product was purified by column chromatography over silica gel eluting with *n*-hexane/ethyl acetate (6:4) to obtain pure tri-linker as a red solid, yielding 0.301 g (59 %). ^{1}H NMR (250 MHz, $CDCl_3$, 25 °C): δ = 8.61-8.59 (d, 3H, pyr**H**), 8.32-8.29 (d, 3H, pyr**H**), 7.94-7.91 (d, 6H, Ar**H**), 7.83-7.76 (m, 3H, pyr**H**), 7.50-7.47 (m, 3H, pyr**H**), 7.44-7.41 (d, 6H, Ar**H**), 4.57 (s, 6H, -S-C**H$_2$**), 4.47 (s, 6H, -O-C**H$_2$**), 1.79-1.70 (q, 2H, -C**H$_2$**CH$_3$), 1.07-1.00 (t, 3H, -CH$_2$C**H$_3$**) ppm. ^{13}C NMR ($CDCl_3$, 100 MHz, 25 °C): δ = 226.09 (Py-**C**(S)-S-), 164.44 (Ar-**C**(O)-OH), 155.14 (**C**$_{Py}$), 146.39 (**C**$_{Py}$), 140.02 (**C**$_{Ar}$), 135.99 (**C**$_{Py}$), 128.86 (**C**$_{Ar}$), 128.47 (**C**$_{Ar}$), 125.89 (**C**$_{Py}$), 121.30 (**C**$_{Ar}$), 64.06 (-**C**H$_2$S-), 39.71 (-**C**H$_2$O-), 24.59 (**C**$_q$), 22.76 (-**C**H$_2$CH$_3$), 6.6 (-CH$_2$**C**H$_3$) ppm. ESI-MS + Na (*m/z*) calculated :970.12; found: 970.08.

Cross-linking (bonding) between PMMA-Cp$_2$ and Trifunctional Linker

PMMA-Cp$_2$ and trifunctional linker were mixed in 1:1 ratio with respect to functional groups in chloroform such that the concentration of polymer was 0.05 M. 1.5 equiv. TFA was added and the resulting mixture shaken at ambient temperature for 10 minutes. The solvent was removed and the residue directly analysed by SEC prior to gelation.

De-linking (Debonding) between PMMA-Cp$_2$ and Trifunctional Linker

The resulting cross-linked polymer was placed in toluene and heated to above 80 °C for 5 minutes. During this time, the colourless toluene turned pink in colour, indica-

tive of the release of the trifunctional linker via a retro DA cycloaddition and the polymer dissolved.

Re-Cross-Linking (Re-bonding) between PMMA-Cp2 and Trifunctional Linker

The non-cross-linked polymer was dissolved in chloroform as described above and additional TFA added (1.5 equiv.). The solvent was removed within the space of 1 minute and the residue directly analysed by SEC prior to gelation.

Solid State Cross-linking

PMMA-Cp_2 and trifunctional linker were mixed in 1:1 ratio with respect to functional groups. Upon the addition of 1.5 equiv. TFA, the mixture was thoroughly mixed with a mortar and pestle. Fully cross-linked (i.e. completely insoluble) material resulted within the space of seconds.

12.3 Results and Discussion

In the current study, reversibly cross-linked polymeric structures were generated utilizing rapid HDA chemistry. Unlike the majority of reports, in which maleimide and furan DA chemistry is used as the reversible linking mechanism, the present use of the highly reactive Cp moiety and pyridinyldithioformate allows for facile ambient temperature conjugations to be performed within the space of several minutes at ambient temperatures rather than several hours at elevated temperatures. Herein, α, ω-Cp-functional PMMA is reversibly and rapidly cross-linked by reaction with a tri-pyridinyldithioformate functional linker molecule. Bis(cyclopentadienyl) poly(methyl methacrylate) (PMMA-Cp_2) was synthesized from the corresponding dibromo precursor (Figure 12.2). Dibromo poly(methyl methacrylate) (PMMA-Br_2) was obtained via ATRP of methyl methacrylate using the difunctional initiator 1,2-bis(bromoisobutryloxy)ethane. Subsequently, the PMMA-Br_2 was transformed into the targeted PMMA-Cp_2 via nucleophilic substitution of the bromide chain termini with cyclopentadienyl moieties via the facile nickelocene pathway, as developed in Chapter 9. The quantitative conversion of PMMA-Br_2 into PMMA-Cp_2 was monitored via ESI-MS, which is a very convenient technique in determining low molecular weight polymer end-group functionalization. Figure 12.3 depicts the comparison of the ESI-MS spectra of the starting PMMA-Br_2 and PMMA-Cp_2. As can be observed, a shift of the dominant series of signals to lower *m/z* values is complete and consistent with the targeted transformation. All minor species, which are associated with various minor by-products of the ATRP process such as bimolecular coupling and elimination species, are carried through the substitution process. A comparison of the experimentally observed and the theoretically calculated *m/z* values for a representative peak in both spectra are presented in Table 12.1.

The dienophilic tri-functional linker is based upon the dithioester 4-((pyridine-2-carbonothioylthio)methyl) benzoic acid, the synthesis of which has been appropriated from a two step procedure reported in the literature.[18] In the first step, commercially available 2-(chloromethyl)pyridine hydrochloride was transformed into the corresponding sulfone by reaction with sodium phenylsulfinate in the presence of DBU and tetrapropyl ammonium bromide. The targeted sulfone was isolated in

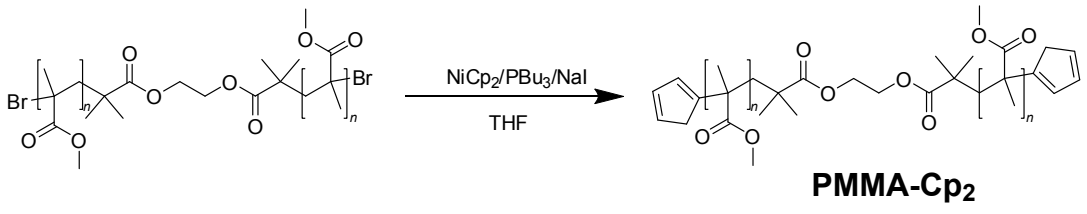

Figure 12.2 Synthesis of α,ω-Cp-functional PMMA.

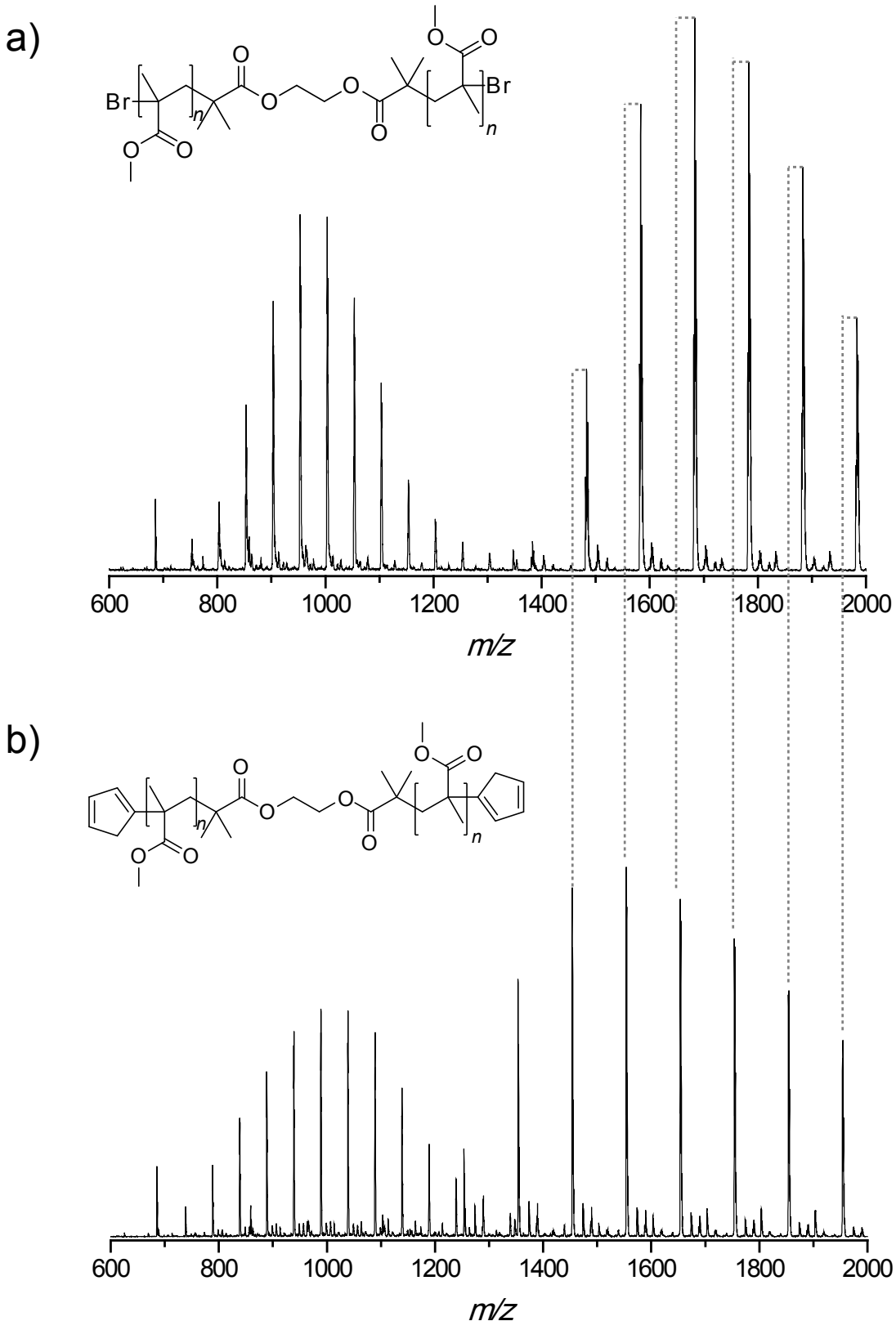

Figure 12.3 ESI-MS spectra of the starting α-ω-functional PMMA-Br_2 (a) and the corresponding α-ω-functional PMMA-Cp_2 (b). Note that both a single and double charged distribution of the polymeric materials are visibile. Minor impurities due to side-products formed in the ATRP process (bimolecular termination and elimination) are also visible.

Table 12.1 Experimental and theoretical *m/z* values for the first peak in the isotopic distributions of a representative signal in Figure 12.3 and their assignment.

$m/z_{\text{expt.}}$	ion assignment	formula	$m/z_{\text{theor.}}$	$\Delta m/z$
1481.2	PMMA-$Br_{2\ (n\,=\,11)}$ + Na^+	$[C_{65}H_{104}Br_2O_{26}Na]^+$	1481.5	0.3
1453.6	PMMA-$Cp_{2\ (n\,=\,11)}$ + Na^+	$[C_{75}H_{114}O_{26}Na]^+$	1453.7	0.1

quantitative yields and used without further purification for the next step. The second step was carried out by reacting the above sulfone with sulfur (S_8) in the presence of potassium tert-butoxide and subsequent alkylation with 4-methylbenzoic acid yielded the desired 4-((pyridine-2-carbonothioylthio)methyl) benzoic acid. The trifunctional linker was obtained via esterification of 1,1,1-tris(hydroxymethyl)propane with 4-((pyridine-2-carbonothioylthio)methyl)) benzoic acid in the presence of DCC, 4-(dimethylamino)-pyridinium-4-toluene sulfonate (DPTS) and DMAP. The overall synthetic strategy is illustrated in Figure 12.4. The tri-functional linker was purified via column chromatography and the purity was determined by ^{1}H NMR spectroscopy and ESI-MS (Figure 12.5).

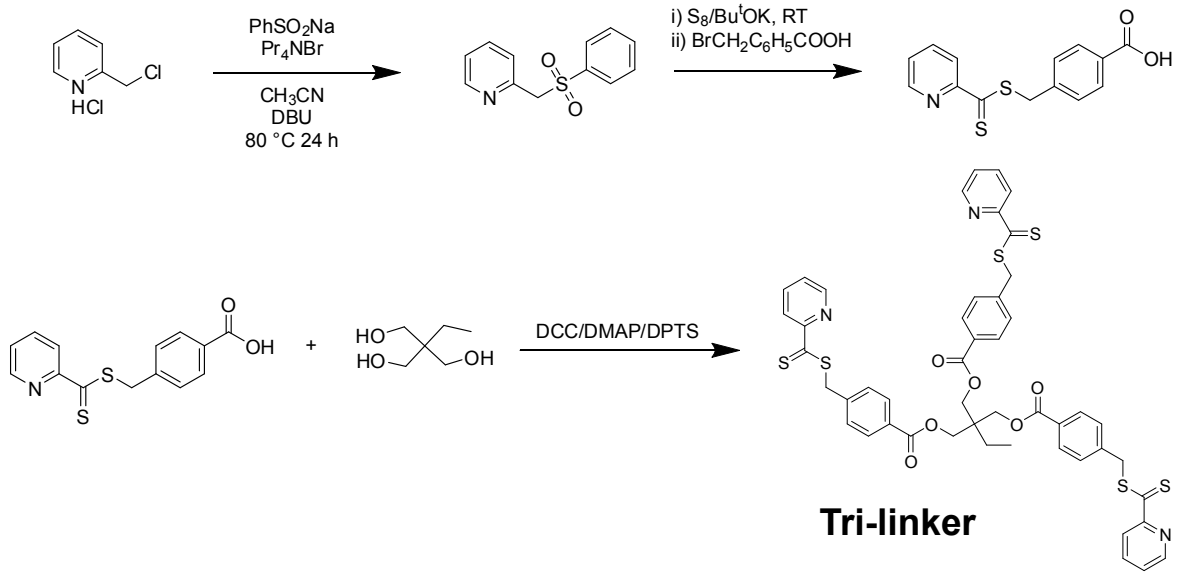

Figure 12.4 Synthetic pathway to the Tri-Linker.

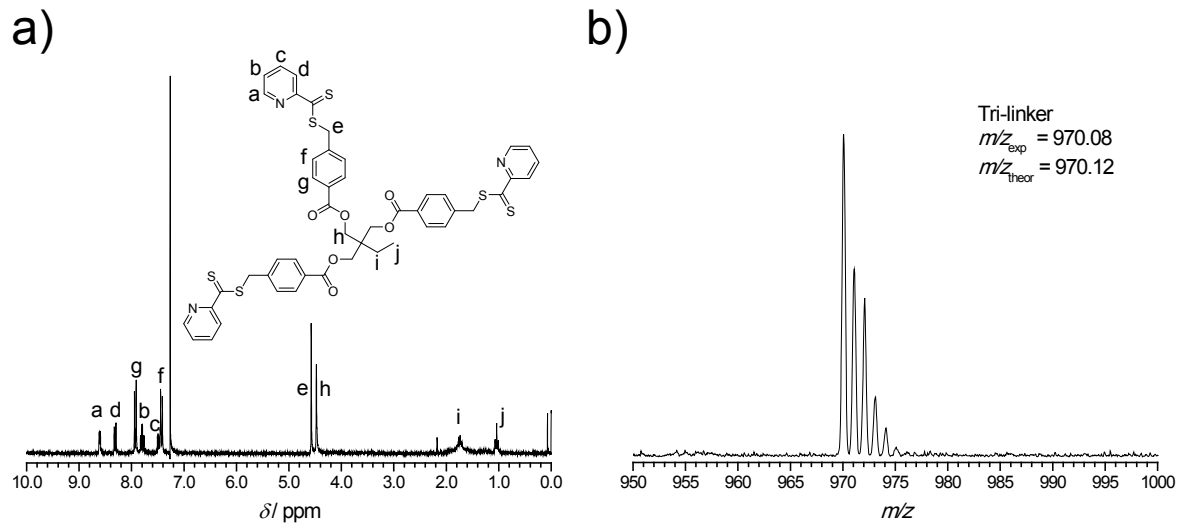

Figure 12.5 ^{1}H NMR spectrum (a) and ESI-MS spectrum (b) of the tri-linker molecule.

In order to generate cross-linked structures under ambient conditions, the tri-linker core was reacted with PMMA-Cp_2 in a 1:1 ratio with respect to functional groups using chloroform as the solvent and TFA as a catalyst. The linkages that are formed via the HDA reaction are depicted in Figure 12.6. Within a maximum time frame of 30 minutes at ambient temperatures, completely cross-linked structures were generated, as indicated by their lack of solubility. When the cross-linking reaction was performed in the solid state, fully cross-linked material was formed within the space of seconds. Therefore, in order to perform an SEC analysis to visualize the changes in molecular weight that occur, the crude reaction mixtures were quickly diluted with THF prior to the gel point ($<$ 10 minutes) and directly analyzed. Figure 12.7 depicts the SEC traces of the starting tri-functional linker and PMMA-Cp_2 having a molecular weight of 990 g·mol^{-1} and 3500 g·mol^{-1} respectively. After a reaction time of 10 minutes, the molecular weight of the system is observed to markedly increase to 12 700 g·mol^{-1}. It is also noted that the *PDI* of the system increases from 1.21 to 2.57. Both of these observations are indicative of the progression of rapid cross-linking reactions.

Aside from the rapid nature of the above cycloadditions, another advantage of the use of the reactive Cp moiety is the reduction in temperature at which the retro-HDA reaction occurs. In previous investigations (Chapter 5), open-chain dienes were utilized, the HDA adducts of which underwent reversion at temperatures exceeding 120 °C. At such temperatures, the liberated dithioesters readily decompose which precludes such systems to be used in a continually reversible fashion. In the present study, the retro or debonding reactions were performed at temperatures between 80 and 100 °C. Referring back to Figure 12.7, it is noted that heating the highly-linked structure for no more than 5 minutes at $>$ 80 °C results in debonding taking place. One can clearly observe not only the reduction in molecular weight of the system (M_n = 3800 g·mol^{-1}), but also an increase in the signal representing the tri-linker molecule, indicating its re-

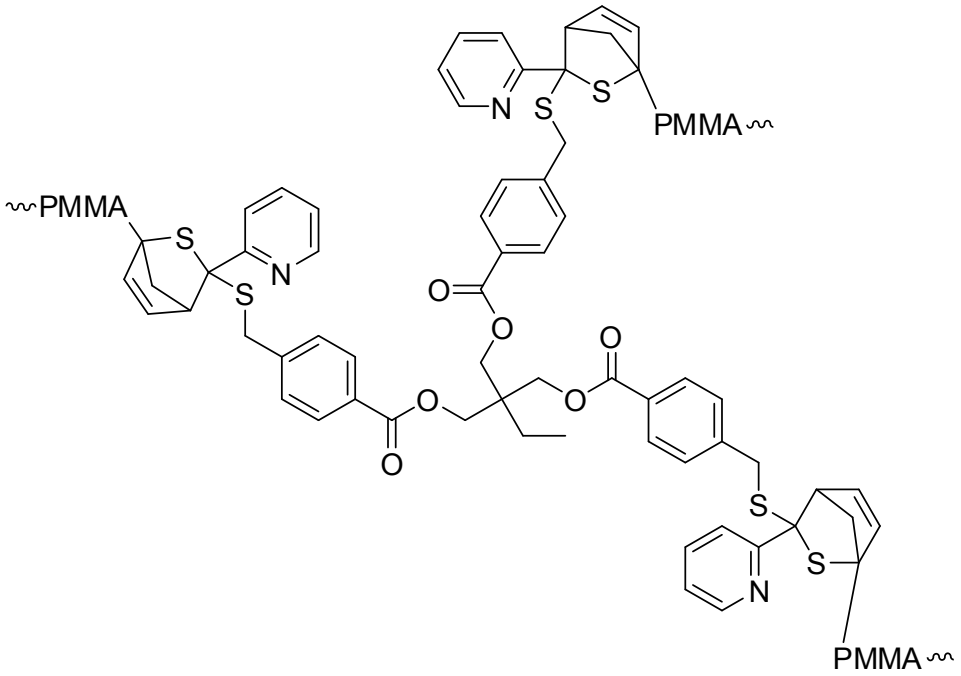

Figure 12.6 Structure of the linkages formed during the HDA reaction. For simplification, not all regio-/stereoisomers are depicted.

lease into solution. The final part of Figure 12.7 depicts an attempt at rebonding the above debonded sample. The debonded polymer/tri-linker mixture was dissolved in fresh chloroform and a catalytic amount of TFA added. Analysis of the reaction mixture via SEC reveals that an increase in molecular weight (10 200 g·mol^{-1}) and *PDI* (2.14) occurred, thus confirming the ability of the system to bond, debond and rebond on demand. Furthermore, the molecular weight data for the above study is included in Table 12.2.

The onset of debonding was also monitored via UV/Vis spectroscopy. In an initial qualitative trial, fully crosslinked material was suspended in toluene. Upon heating with a hand-held heat gun, the material gradually dissolved and the toluene solution turned pink, indicating the release of the starting tri-linker molecule. Performing

Table 12.2 Characterization of the bonded and debonded polymer systems, demonstrating the switching behaviour in both the observed molecular weight and *PDI*.

polymer	$M_{n,\,SEC}$[a] / g·mol^{-1}	*PDI*[b]
PMMA-Cp_2	3500	1.20
Bond	12700	2.57
Debond	3800	1.26
Rebond	10200	2.14

[a]Measured by SEC in THF against linear PMMA standards. [b]Polydispersity index.

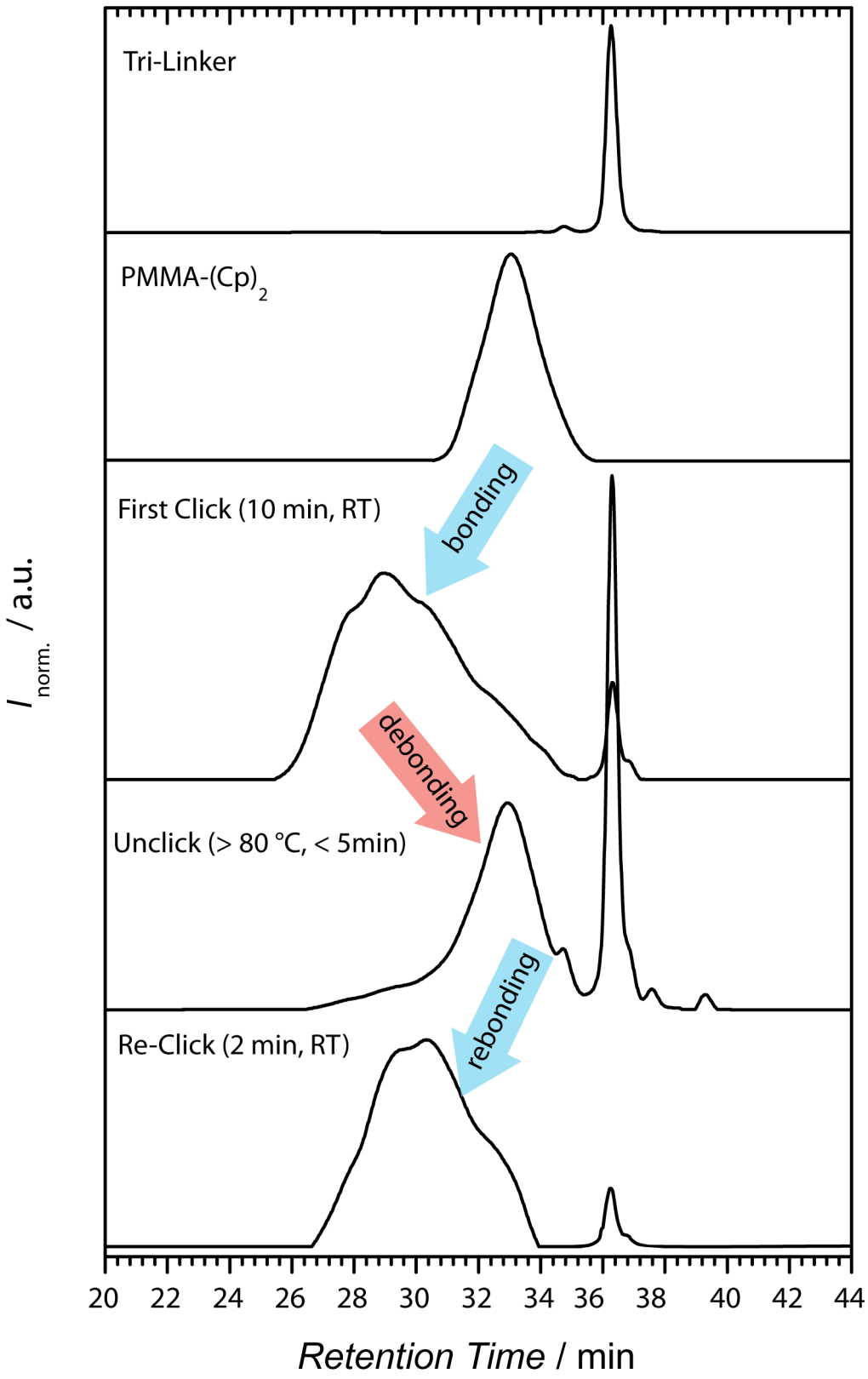

Figure 12.7 Visualizing the changes in molecular weight in the cross-linking system by SEC.

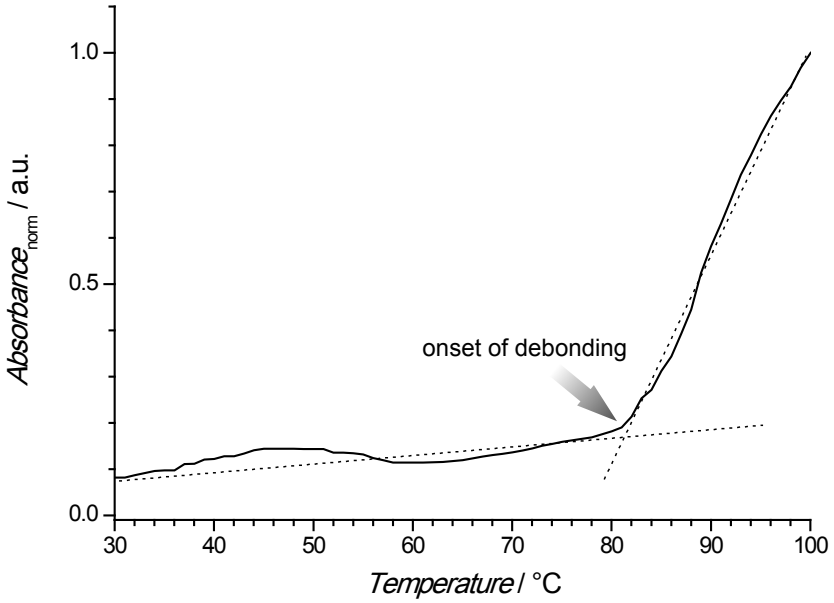

Figure 12.8 UV/Vis spectroscopic monitoring of the onset of debonding (i.e. the reaction solution becomes coloured again). Debonding occurs at close to 80 °C (λ = 522 nm).

the same reaction quantitatively inside a UV/Vis spectrophotometer allowed for the absorbance of the solution to be monitored as a function of temperature. Figure 12.8 depicts the results of such an analysis and it is observed that a sharp increase in the absorbance of the system occurs at around 80 °C (as the solution returns the colour of the dithioester), corresponding to the rapid onset of debonding.

12.4 Conclusion

The reversibility of rapid HDA reactions has been exploited for the generation of a reversibly stimuli-responsive cross-linked polymeric network. The ambient temperature cross-linking of PMMA (bonding) could be reversed upon thermal treatment (debonding) and subsequently reformed (rebonding) again at ambient temperature. Although accessibility to the HDA functionalities are not the same as the widely used maleimide/furan derivatives, the provision and continued development of such systems will ultimately lead to significant advances in such fields as coatings, adhesives and self-healing polymeric materials.

References

[1] Engle, L. P.; Wagener, K. B. *J. Macromol. Sci., Rev. Macromol. Chem. Phys.* **1993**, *C33*, 239–257.

[2] Kloxin, C. J.; Scott, T. F.; Adzima, B. J.; Bowman, C. N. *Macromolecules* **2010**, *43*, 2643–2653.

[3] Furusho, Y.; Oku, T.; Hasegawa, T.; Tsuboi, A.; Kihara, N.; Takata, T. *Chem. Eur. J.* **2003**, *9*, 2895–2903.

[4] Chen, Y.; Chen, K. H. *J. Polym. Sci., Part A: Polym. Chem.* **1997**, *35*, 613–624.

[5] Kamplain, J. W.; Bielawski, C. W. *Chem. Commun.* **2006**, 1727–1729.

[6] Chang, J. Y.; Do, S. K.; Han, M. J. *Polymer* **2001**, *42*, 7589–7594.

[7] Higaki, Y.; Otsuka, H.; Takahara, A. *Macromolecules* **2006**, *39*, 2121–2125.

[8] Reinecke, M.; Ritter, H. *Makromol. Chem.* **1993**, *194*, 2385–2393.

[9] Jones, J. R.; Liotta, C. L.; Collard, D. M.; Schiraldi, D. A. *Macromolecules* **1999**, *32*, 5786–5792.

[10] Imai, Y.; Itoh, H.; Naka, K.; Chujo, Y. *Macromolecules* **2000**, *33*, 4343–4346.

[11] Chen, X. X.; Dam, M. A.; Ono, K.; Mal, A.; Shen, H. B.; Nutt, S. R.; Sheran, K.; Wudl, F. *Science* **2002**, *295*, 1698–1702.

[12] Gheneim, R.; Perez-Berumen, C.; Gandini, A. *Macromolecules* **2002**, *35*, 7246–7253.

[13] Goiti, E.; Heatley, F.; Huglin, M. B.; Rego, J. M. *Eur. Polym. J.* **2004**, *40*, 1451–1460.

[14] Gandini, A.; Silvestre, A. J. D.; Coelho, D. *J. Polym. Sci., Part A: Polym. Chem.* **2010**, *48*, 2053–2056.

[15] Aumsuwan, N.; Urban, M. W. *Polymer* **2009**, *50*, 33–36.

[16] Syrett, J. A.; Mantovani, G.; Barton, W. R. S.; Price, D.; Haddleton, D. M. *Polymer Chemistry* **2010**, *1*, 102–106.

[17] Karanam, S.; Goossens, H.; Klumperman, B.; Lemstra, P. *Macromolecules* **2003**, *36*, 8304–8311.

[18] Abrunhosa, I.; Gulea, M.; Masson, S. *Synthesis* **2004**, 928–934.

13

Well-Defined Star Shaped Polymer-Fullerene Hybrids via Click Chemistry*

13.1 Introduction

The unique structural and chemical properties of C_{60} fullerenes and their various derivatives have led to such structures receiving intense attention in the fields of chemistry and materials science.[1] In the field of polymer chemistry, various approaches have been utilized in the generation of C_{60}-polymer hybrid materials with various physical properties and morphologies.[2–4] Star-shaped polymers and block copolymers bearing a C_{60} core are particularly interesting for their ability to form well-defined microstructures in the solid state.[5, 6] The most frequented method for the synthesis of such C_{60}-based star polymers is the addition of the terminal carbanions of polymers prepared via anionic polymerization directly to C_{60}.[3, 5, 6] While such a technique works rather well, the severe limitation of applicable monomers as well as the stringent reaction conditions required limits the variety of materials that may be synthesized. Recent trends in polymer chemistry demonstrate that *click* chemistry has been an attractive route to prepare well-defined polymer conjugates.[7, 8] To

*In collaboration with the research group of S. Bräse (KIT).

date, the CuAAC has been the main representative reaction of the *click* chemistry philosophy[9] due to its high efficiency, accessibility and orthogonality. Thus far, the CuAAC has been utilized in preparing various C_{60} hexakis adducts[10–12] and C_{60}-polymer conjugates[13] by either equipping the fullerene surface with relatively low molecular weight azide or alkyne functionalities. As of yet, there is no report on the use of the CuAAC for the synthesis of well-defined star polymers bearing a C_{60} core. It is hypothesized that the larger core will lead to higher efficiency conjugations resulting from a reduction in steric hindrance in the system.

If this hypothesis is confirmed, it would aid in the future design of core molecules for the convergent synthesis of highly branched polymeric systems. As such, it is herein reported the first examples of well-defined C_{60}-based star polymers prepared by the CuAAC of alkyne-functional polymers and the recently reported 6-fold azide functionalized hexakis methanofullerene malonate crown-ether **1** (Figure 13.1).[14]

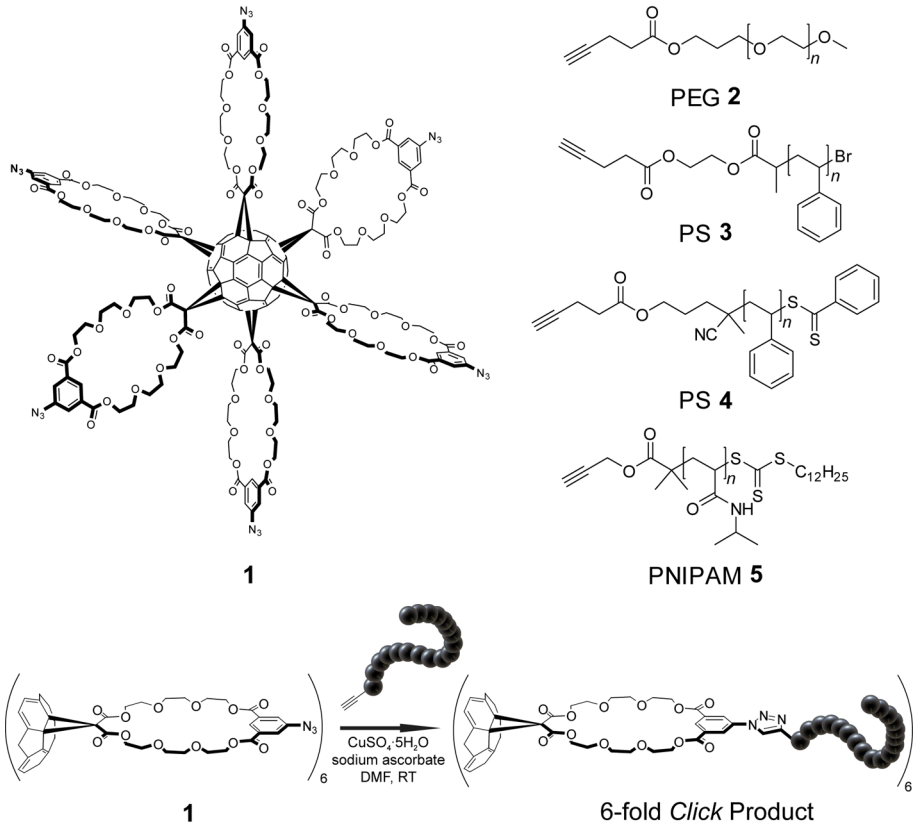

Figure 13.1 Structures of the 6-fold azide functionalized hexakis methanofullerene malonate crown-ether **1** and the various alkyne-functional polymers synthesized for conjugation (top); and the general strategy for the synthesis of 6-arm star polymers via the CuAAC (bottom).

13.2 Experimental Section

The 6-fold azide functionalized fullerene derivative **1** was provided by Philippe Pierrat, Thierry Muller and Stefan Bräse (KIT) and was synthesized according to their published procedure.[14]

2-hydroxyethyl-2′-bromopropionate,[15] 4,4′-azobis(4-cyanopentanol) (ACP),[16] 4-cyano-1-hydroxypent-4-yl dithiobenzoate (RAFT-OH)[17] and *S*-1-dodecyl-*S*′-(*α*, *α*′-dimethyl-*α*″-propargylacetate) (DDPA)[18] were synthesized according to literature procedures.

ATRP of Styrene

Copper (I) bromide was added to a dried Schlenk tube and sealed under nitrogen. Into another Schlenk tube was added styrene and PMDETA. The resulting monomer solution was then deoxygenated by three freeze-pump-thaw cycles and subsequently transferred to the copper (I) bromide via cannula. The tube was sealed under a nitrogen atmosphere and placed in a thermostatic oil bath set to 110 °C. 2-hydroxyethyl-2′-bromopropionate was then added via syringe. The initial ratio of [styrene]:[initiator]:[CuBr]:[PMDETA] was 2100:1:1:1. The polymerization was stopped by cooling the mixture in an ice bath and exposure to oxygen. The mixture was then diluted with the addition of THF and passed through a column of neutral alumina to remove the copper catalyst. Hydroxy-functionalized poly(styrene) PS-OH_{ATRP} was obtained as a white powder after two-fold precipitation in cold methanol. SEC (DMAc): M_n = 12 200 g·mol^{-1}, *PDI* = 1.19.

RAFT Polymerization of Styrene

A mixture of styrene, RAFT-OH and ACP was prepared with ratios of [styrene]:[RAFT-OH]:[ACP] = 440:1:0.17. The mixture was deoxygenated by purging with nitrogen for 40 minutes. The mixture was then placed in a thermostatic oil bath set to 65 °C. After 24 hours, the polymerization was stopped by chilling in an ice bath and exposure to oxygen. Hydroxy-functionalized poly(styrene) PS-OH_{RAFT} was obtained as a pink powder by two-fold precipitation in cold methanol. SEC (DMAc): M_n = 4200 g·mol^{-1}, *PDI* = 1.06.

RAFT Polymerization of N-isopropylacrylamide (5)

A solution of *N*-isopropylacrylamide (NIPAM), DDPA and AIBN in 1,4-dioxane (29 mL) was prepared with the following composition: [NIPAM]:[DDPA]:[AIBN] =

50:1:0.05. The mixture was deoxygenated by purging with nitrogen for 40 minutes and then placed in a thermostatic oil bath set to 70 °C. After 100 minutes, the polymerization was stopped by cooling the mixture in an ice bath and exposure to oxygen. Alkyne-functionalized poly(*N*-isopropylacrylamide) (PNIPAM) **5** was obtained as a yellow powder after two-fold precipitation in cold diethyl ether. SEC (DMAc): M_n = 10 500 g·mol^{-1}, *PDI* = 1.10.

Synthesis of Alkyne Functionalized PEG (2)

Poly(ethylene glycol) monomethyl ether (2.0 g, 1.0 mmol), 4-pentynoic acid (294 mg, 3.0 mmol) and DMAP (24.4 mg, 0.2 mmol) were dissolved in dichloromethane (15 mL). The resulting mixture was cooled to 0 °C and a solution of DCC (619 mg, 3.0 mmol) in dichloromethane (5 mL) was added dropwise. After the addition, the stirred mixture was allowed to warm to room temperature and allowed to continue stirring at this temperature for 20 hours. The formed precipitate was removed by filtration and the polymer was recovered from the filtrate by two-fold precipitation in cold diethyl ether. Yield: 1.91 g, 91 %. SEC (DMAc): M_n = 2010 g·mol^{-1}, *PDI* = 1.04.

Synthesis of Alkyne-Functional PS (3,4)

PS-OH prepared by ATRP or RAFT (0.2 mmol), 4-pentynoic acid (58.8 mg, 0.6 mmol) and DMAP (4.9 mg, 0.04 mmol) were dissolved in dichloromethane (15 mL). The resulting mixture was cooled to 0 °C and a solution of DCC (124 mg, 0.6 mmol) in CH_2Cl_2 (5 mL) was added dropwise. After the addition, the stirred mixture was allowed to warm to room temperature and allowed to continue stirring at this temperature for 20 hours. The formed precipitate was removed by filtration and the polymer was recovered from the filtrate by two-fold precipitation in cold methanol.

Click Reactions (Typical Procedure)

Hexakisazido fullerene derivative **1** (5.0 mg, 1.27 mmol), alkyne-functional polymer (6 equiv.), copper (II) sulfate pentahydrate (18 equiv.) and sodium ascorbate (18 equiv.) were dissolved in DMF (1.0 mL). The resulting mixture was stirred at room temperature for 24 hours before the copper catalyst was removed by passage through a short column of neutral alumina. The solvent was removed under reduced pressure and the residue directly analysed by SEC and ^{1}H NMR spectroscopy.

Aminolysis of PNIPAM$_6$ 9

Under a nitrogen atmosphere, the star-shaped *click* product PNIPAM$_6$ **9** (20 mg, 3.27×10^{-4} mmol) was dissolved in DMF (1.0 mL) in the presence of hexylamine and triphenylphosphine ([PNIPAM$_6$ **9**]:[hexylamine]:[Ph_3P] = 1:10:1). The resulting mixture was allowed to stir at room temperature for 5 hours. Thiol terminated PNIPAM$_6$ **10** was obtained by precipitation in cold diethyl ether and drying under reduced pressure. SEC (DMAc): M_n = 41 700 g·mol^{-1}, *PDI* = 1.11.

13.3 Results and Discussion

13.3.1 Synthesis of Alkyne-Functional Polymers

In order to evaluate the performance of **1** as a core molecule in the convergent synthesis of star polymers, a variety of linear homopolymers bearing quantitative chain-end alkyne functionality were in need of being synthesized. Initially, commerically available poly(ethylene glycol) monomethyl ether (PEG) was equipped with an alkyne moiety via DCC coupling with 4-pentynoic acid (PEG **2** in Figure 13.1). The quantitative functionalization of PEG **2** was confirmed by ^{1}H NMR spectroscopy (Figure 13.2).

Synthesis of further examples of alkyne-functional synthetic polymers using CRP techniques requires the use of initiators/controlling agents that bear the appropriate functionality. In order for both ATRP and RAFT polymerization to be explored within this context, the hydroxyl-functional 2-hydroxyethyl-2′-bromopropionate and 4-cyano-1-hydroxypent-4-yl dithibenzoate (RAFT-OH) were used as an ATRP initiator and RAFT agent for the polymerization of styrene respectively.

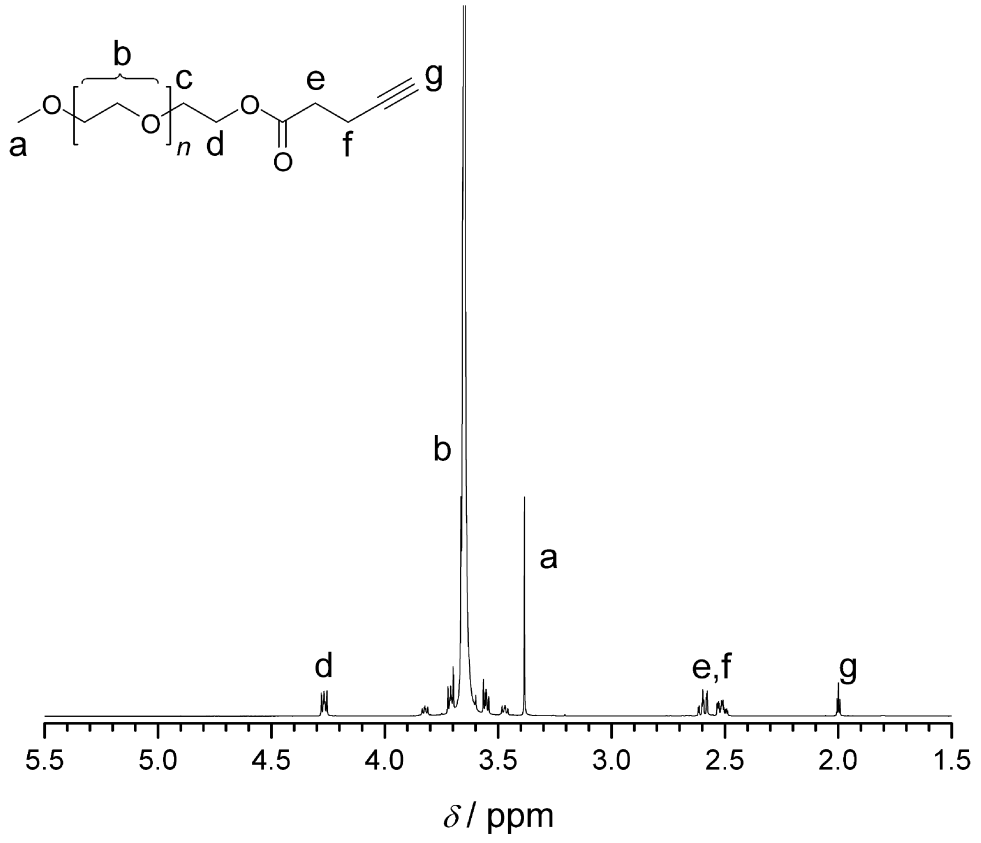

Figure 13.2 ^{1}H NMR spectrum of the alkyne-functional PEG **2**.

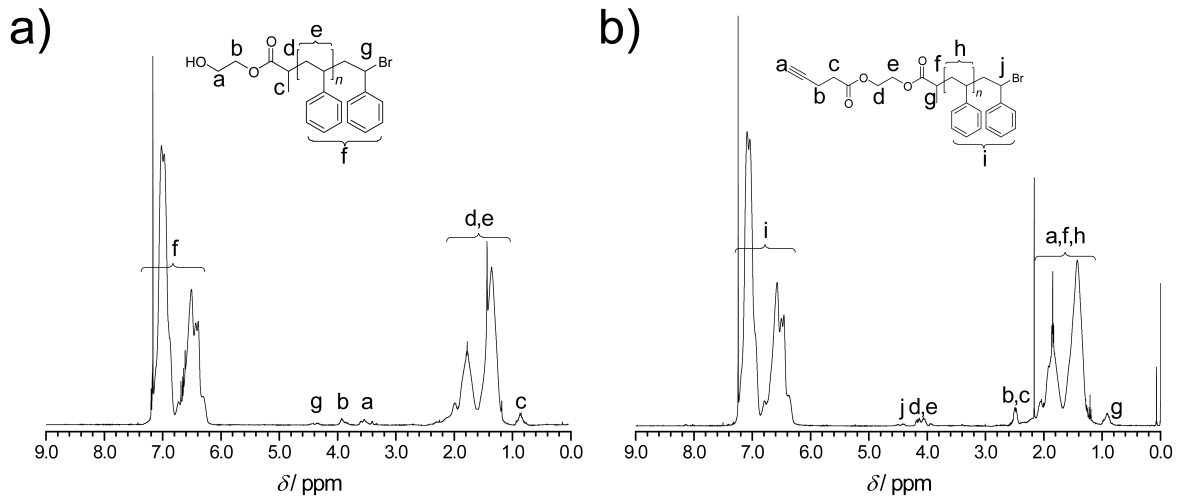

Figure 13.3 ^{1}H NMR spectrum of the hydroxyl-functional PS-OH$_{ATRP}$ (a); and the alkyne-functional PS **3**.

ATRP of styrene with 2-hydroxyethyl-2′-bromopropionate as the initiator yielded quantitatively α-hydoxyl-functional poly(styrene) (PS-OH$_{ATRP}$). Upon inspection of its ^{1}H NMR spectrum (Figure 13.3a), the presence of the α and β protons (with respect to the hydroxyl moiety) are confirmed by characteristic signals appearing between 3.0 and 4.0 ppm. After esterification with 4-pentyonic acid, the appearance of characteristic signals at around 2.5 ppm in the ^{1}H NMR spectrum (Figure 13.3b) confirm the presence of the required alkyne functionality.

Analagously, the use of the hydroxyl-functional controlling agent RAFT-OH in the polymerization of styrene also lead to the formation of quantitatively α-hydoxyl-functional poly(styrene) (PS-OH$_{RAFT}$). In the case of ATRP, all polymer chains are initiated (and grow from) the hydroxyl-functional initiator, meaning that every polymer chain will bear hydroxyl functionality. In the case of RAFT polymerization, a radical initiator is required to initiate the polymerization. In a typical system, the concentration of RAFT agent is much higher than that of the radical initiatior, thus the majority of polymer chains will be actually initiated by the R-fragment of the RAFT agent (cf. Chapter 2). If a reactive functionality (in this case hydroxyl) is introduced to this R-fragment, the majority of the formed polymer chains will bear this functionality. However, there will be a small fraction of polymer chains that have been initiated by the radical initiator and thus, will not be likewise functionalized.

In order to circumvent this problem, a radical initiator bearing a hydroxyl moiety was used such that whether initiated by this species or the hydroxyl-bearing R-fragment of the RAFT agent, all polymer chains will be equipped with the targeted functionality. The ^{1}H NMR spectrum of PS-OH$_{RAFT}$ is depicted in Figure 13.4a.

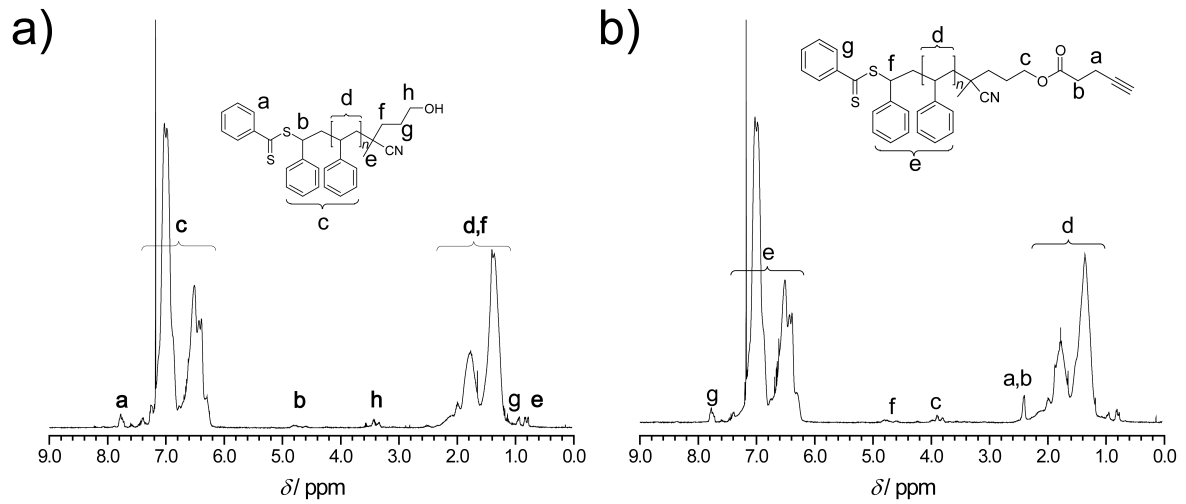

Figure 13.4 ^{1}H NMR spectrum of the hydroxyl-functional PS-OH$_{RAFT}$ (a); and the alkyne-functional PS **4**.

After esterfication of PS-OH$_{RAFT}$ with 4-pentynoic acid, characteristic signals appear at around 2.4 ppm in the ^{1}H NMR spectrum (Figure 13.4b), indicating the presence of the required alkyne functionality.

Recently, Li and co-workers reported the synthesis of C_{60} coupled to thermoresponsive linear diblock copolymers and homopolymers via the CuAAC.[19] Further examples of a similar nature have also been reported.[20, 21] Consequently, the present investigation was extended to include the synthesis of star-shaped PNIPAM. In aqueous media, PNIPAM exhibits a lower critical solution temperature (LCST), implying that a sharp phase transition occurs once a particular temperature is reached. For linear PNIPAM, the LCST is typically 32 °C. Below this temperature, the polymer is water soluble; however upon heating to and above the LCST the chains dehydrate and aggregate which leads to polymer insolubility. This thermoresponsive behaviour of PNIPAM in aqueous media can vary quite substantially with changes in polymer chain end-group,[22, 23] architecture,[23, 24] concentration[25] and molecular weight.[26] Alkyne-functionalized PNIPAM **5** was therefore synthesized by RAFT polymerization, the structure of which is presented in Figure 13.1. In this case, the RAFT agent used was directly equipped with an alkyne moiety prior to polymerization. The resulting polymer was determined to be quantitatively functional upon integration of its ^{1}H NMR spectrum (Figure 13.5).

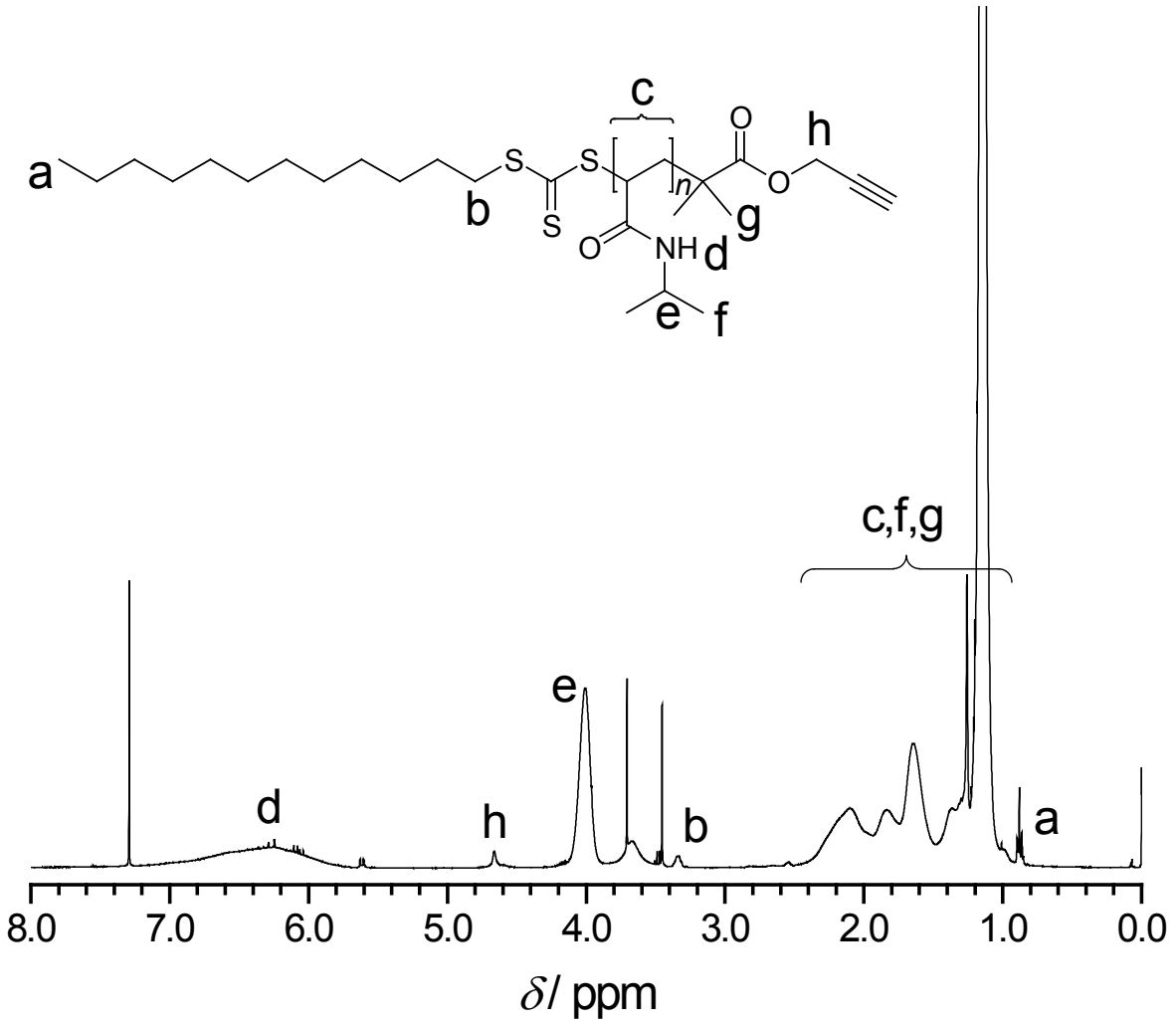

Figure 13.5 ^{1}H NMR spectrum of the alkyne-functional PNIPAM **5**.

13.3.2 Convergent Synthesis of C_{60}-Star Polymers via the CuAAC

The *click* reaction between 6 equiv. of PEG **2** with **1** was performed at ambient temperature in DMF solution in the presence of copper(II) sulfate and sodium ascorbate. After allowing to stir for 18 hours, the reaction mixture was passed though a short column of neutral alumina to remove the copper catalyst. The solvent was removed by evaporation and the product dried under reduced pressure. The series of molecular weight distributions (MWD) labelled **A** in Figure 13.6 are of the starting materials **1**, PEG **2** and the 6-fold *click* product, denoted here as PEG_6 **6**. In comparison to the starting materials, the conjugate shows a clear and complete shift to higher molecular weight. The number average molecular weights, M_n, of the respective components are presented in Table 13.1. It can clearly be observed that the theoretical value of M_n for the six-arm PEG star deviates from the experimentally measured value. This can be explained by the reduced hydrodynamic volume of star-shaped macromolecules in relation to linear analogues of the same molecular weight. However, Radke and co-workers[27] have reported the application of contraction factors that may be used to correct the apparent molecular weight of star polymers (as determined by SEC) to a value that aims to reflect the true molecular weight. The contraction factor for a 6-arm star is reported to be 1.42, thus multiplying this number with the SEC determined value of M_n approximates, reasonably well, the expected molecular weight of the star. Applying this to the M_n for PEG_6 **6** (11 700 g·mol^{-1}) gives a corrected value of $M_{n,corrected}$ = 16 600 g·mol^{-1}. Upon inspection of the data presented in Table 13.1, this value is in excellent agreement with the theoretically expected value of $M_{n,theoretical}$ = 16 400 g·mol^{-1}.

Table 13.1 Polymer characterization.

polymer	$M_{n,\,SEC}$[a] / g·mol^{-1}	*PDI*[b]	$M_{n,\,corrected}$[c] / g·mol^{-1}	$M_{n,\,theor.}$[d] / g·mol^{-1}
1	4300[e]	1.04	-	3943
PEG **2**	2000	1.05	-	-
PEG_6 **6**	11 700	1.05	16 600	15 900
PS **3**	12 200	1.19	-	-
PS_6 **7**	55 400	1.12	78 700	77 140
PS **4**	4200	1.06	-	-
PS_6 **8**	21 900	1.05	31 100	29 143
PNIPAM **5**	10 500[e]	1.10	-	-
$PNIPAM_6$ **9**	43 100[e]	1.08	61 200	66 649

[a]Measured by SEC in *N*, *N*′-dimethylacetamide (DMAc) against linear PS standards. [b]Polydispersity index. [c]Corrected by multiplying the SEC determined M_n values with the 6-arm star contraction factor (1.42) [d]Calculated by the sum of the individual building blocks. [e]Relative to PS.

Furthermore, the success of the conjugation was also confirmed by ^{1}H NMR spectroscopy (Figure 13.7). It can clearly be observed the appearance of a signal at around 8 ppm, which is associated with the proton of the tetrazole ring. These observations, along with the clear disappearance of peaks due to starting materials in the MWD of the 6-fold *click* product, indicates the high efficiency of the CuAAC. Importantly, previous reports on the use of a *click* approach in the synthesis of star-shaped polymers make use of much smaller core molecules bearing the required *clickable* function.[28] It is observed that the efficiency of star formation decreases as the number of branch points on the core increases. Such an occurrence is primarily due to steric crowding of the core molecule. As more and more arms are added to the core, the accessibility of the remaining reactive sites decreases. In the present case, the core molecule is significantly larger, with the reactive sites for conjugation well separated which results in a reduction of the effect of steric crowding and, thus, the efficiency of star formation is enhanced.

Having established the effectiveness of **1** as a core molecule for the covergent synthesis of star-shaped polymers, the use of the alkyne-bearing PS **3** and **4** were subsequently investigated. The *click* reactions were performed under identical conditions to that of the PEG example, resulting in well-defined star-shaped polymers PS_6 **7** and PS_6 **8** (Part **B** and **C** respectively of Figure 13.6). The experimental values of M_n presented in Table 13.1 for both examples are in good agreement with the theoretically expected values. The ^{1}H NMR spectra of both *click* products are presented in Figures 13.8 and 13.9 respectively. In both cases, the signal associated with the formed tetrazole ring can clearly be observed.

The *click* reaction of PNIPAM **5** with **1** again proved to proceed very efficiently, as evidenced by the data in Table 13.1, the MWD presented in Figure 13.6 (part **D**) and its ^{1}H NMR spectrum (Figure 13.10). The resulting $PNIPAM_6$ **9** was not at all water soluble at ambient temperature, which can be explained upon inspection of its structure. $PNIPAM_6$ **9** consists of a highly hydrophobic core with 6 hydrophilic PNIPAM arms radiating outwards. The Z-group of the RAFT agent used in the preparation of PNIPAM **5**, the hydrophobic dodecyl chain, is retained in the final $PNIPAM_6$ **9** as the outer chain termini. The presence of hydrophobic end-groups in highly branched PNIPAM can lower the LCST such that the polymer is insoluble at ambient temperature,[23] thus explaining the present observation.

Interestingly, upon heating a stirred aqueous dispersion of $PNIPAM_6$ **9**, the particles were observed to self-flocculate as shown in Figure 13.11. It has been reported that while aqueous solutions of PNIPAM turn turbid when heated to above its LCST, it can take as long as 24 hours for the chains to fully precipitate.[24] It was discovered that by heating the aqueous dispersion of $PNIPAM_6$ **9** more rigorously (> 50 °C), the onset of particle flocculation could be induced within the space of minutes. Upon cooling, the

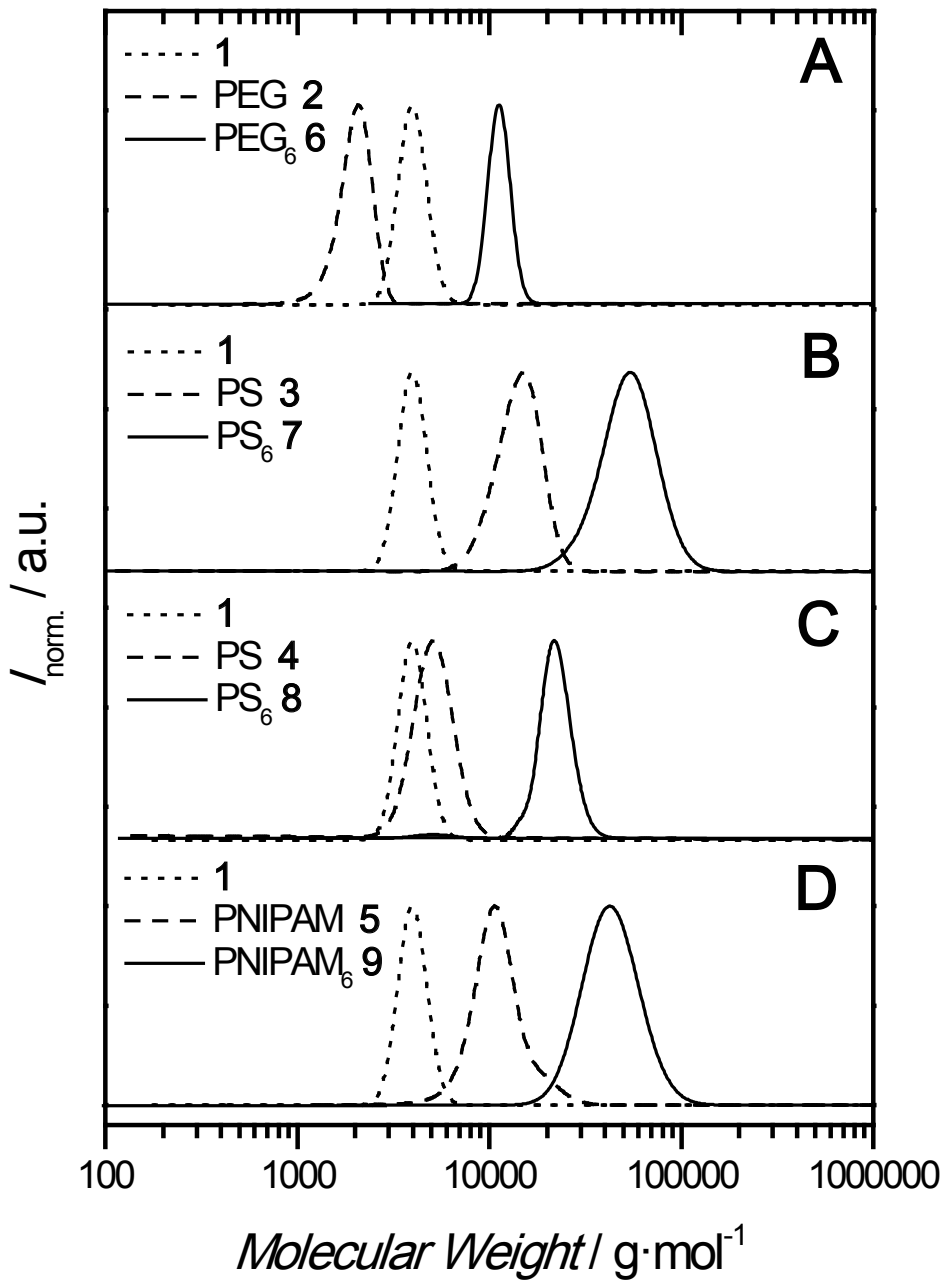

Figure 13.6 Molecular weight distributions of the various *click* products in relation to those of the corresponding precursors.

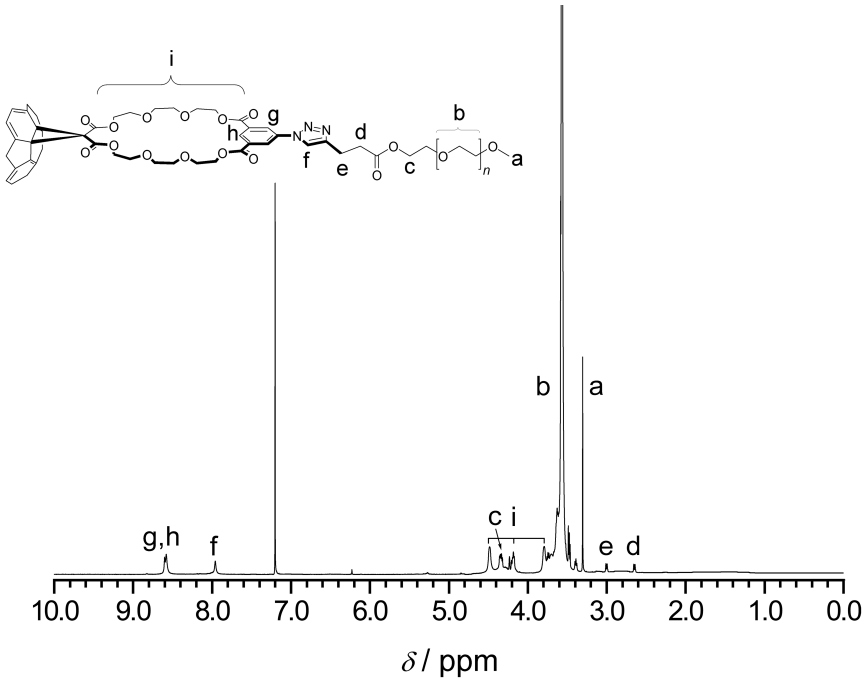

Figure 13.7 ^{1}H NMR spectrum of PEG_6 **6**. The structure depicts a single arm of the 6-arm molecule.

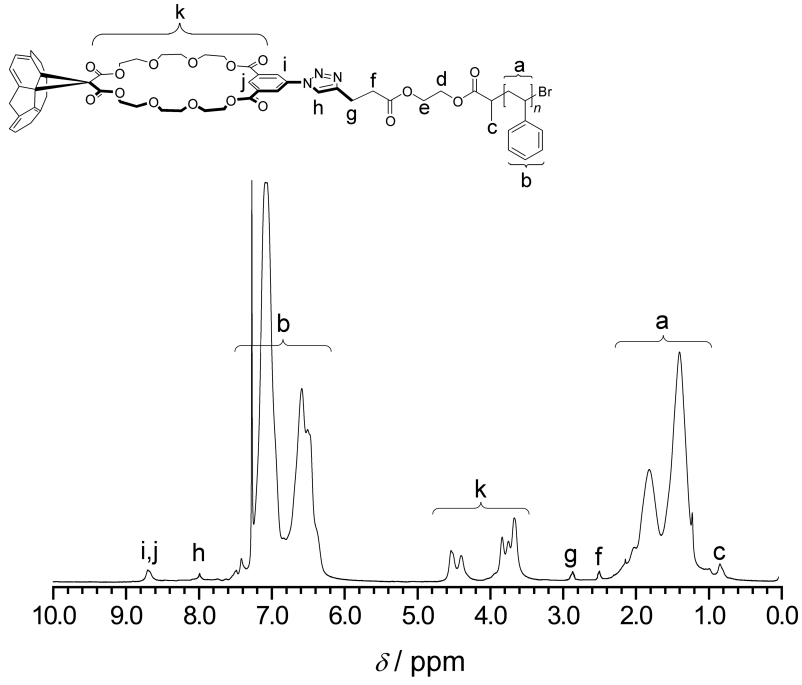

Figure 13.8 ^{1}H NMR spectrum of PS_6 **7**. The structure depicts a single arm of the 6-arm molecule.

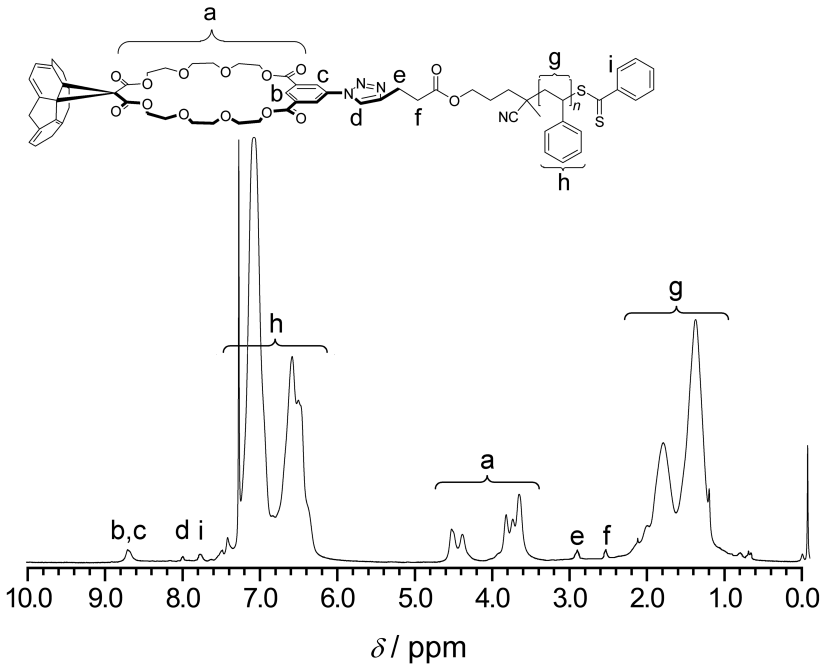

Figure 13.9 ^{1}H NMR spectrum of PS_6 **8**. The structure depicts a single arm of the 6-arm molecule.

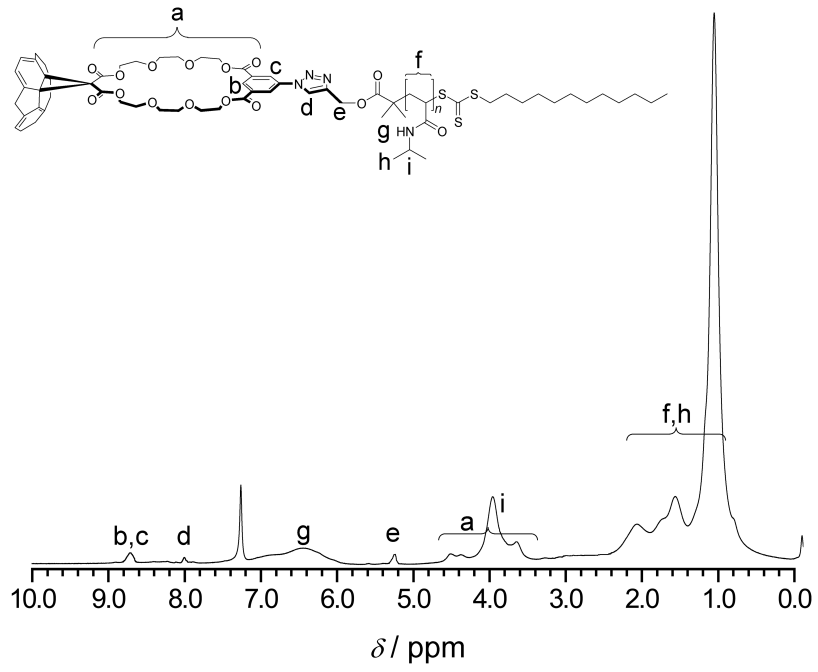

Figure 13.10 ^{1}H NMR spectrum of $PNIPAM_6$ **9**. The structure depicts a single arm of the 6-arm molecule.

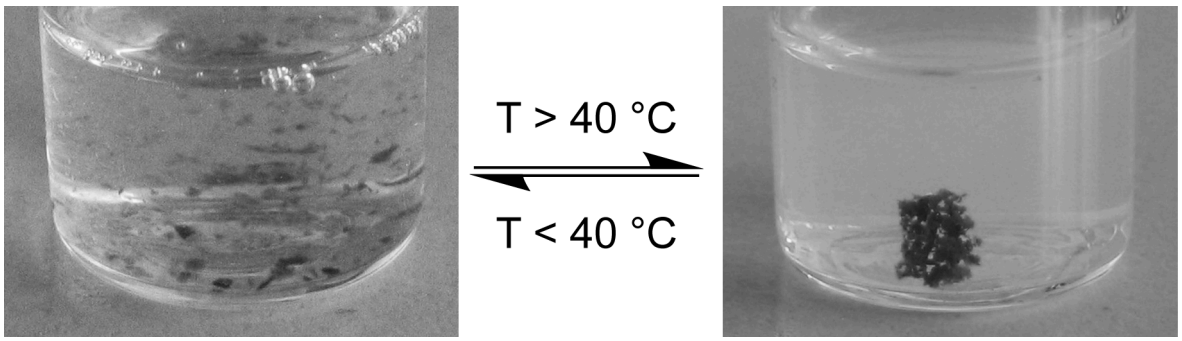

Figure 13.11 Reversible, thermally induced flocculation of PNIPAM$_6$ **9**.

particles re-dispersed and the overall flocculation-dispersion process was found to be reversible.

In an attempt to improve the water solubility of PNIPAM$_6$ **9**, the hydrophobic dodecyl end-groups were removed by aminolysis (Figure 13.12). The success of this transformation was verified by UV/Vis spectroscopy (Figure 13.13a) by monitoring the reduction in absorbance at λ = 310 nm (characteristic of the RAFT agent used). A slight decrease in M_n was also observed, which is consistent with the removal of the dodecyl chain termini (Figure 13.13b). The SEC results also confirm that no disulfide species are formed during the aminolysis, which would lead to polymeric material of higher molecular weight.

Figure 13.14 depicts the optical transmittance of a 3 mg·mL^{-1} aqueous solution of the modified PNIPAM$_6$ **10** at various temperatures, measured at λ = 700 nm. As can be clearly observed, the now water soluble PNIPAM$_6$ **10** retains the LCST behaviour of PNIPAM. At ambient temperature, the aqueous polymer solution exhibits an optical transmittance of ≈ 50 %. Existing reports on the thermoresponsive behaviour of linear PNIPAM-fullerene conjugates describe reduced optical transmittance of aqueous solutions of such structures (≈ 50-70 %) at ambient temperature.[19–21] This has been ascribed to characterisics such as the colour of the solution and the formation of self-assembled aggregates due to the high hydrophobicity of the fullerene component. A

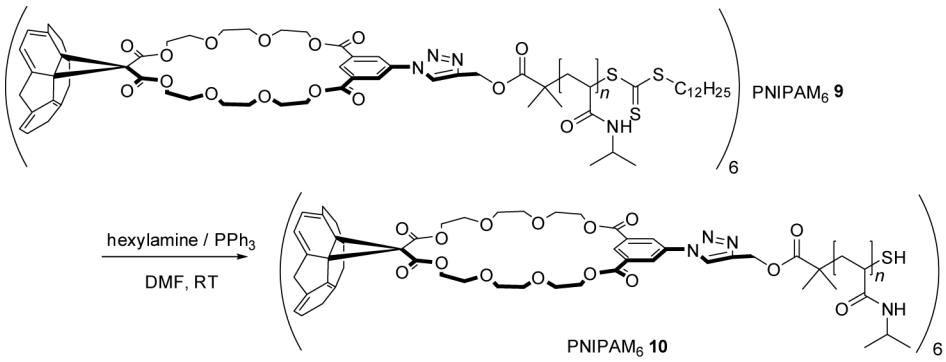

Figure 13.12 Aminolysis of PNIPAM$_6$ **9**.

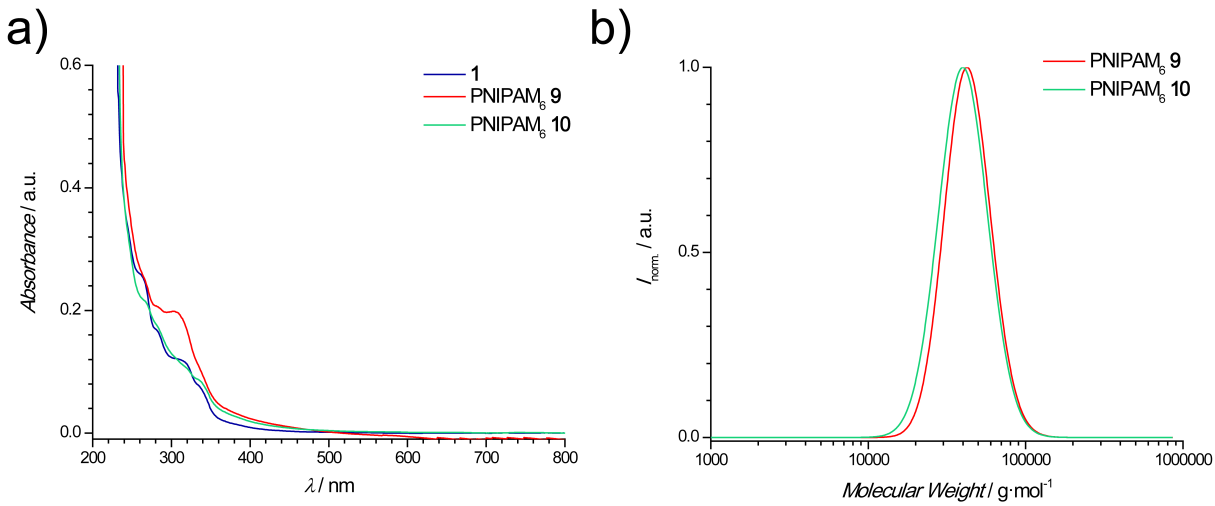

Figure 13.13 a) UV/Vis spectra of PNIPAM$_6$ **9**, the fullerene precursor **1** and the aminolysis product PNIPAM$_6$ **10**; b) MWD of PNIPAM$_6$ **9** in comparison to that of the aminolysis product PNIPAM$_6$ **10**.

similar phenomenon is observed in the case of the presently investigated star conjugates. Figure 13.14 also shows the optical transmittance behaviour of an aqueous solution (3 mg·mL^{-1}) of the precursor PNIPAM **5** under conditions of varying temperature. For comparison, the LCST of the respective solutions was taken to be the temperature at which onset of the phase transition took place. As such, the LCST of the precursor PNIPAM **5** is observed to be 28 °C. This low value with respect to the generally reported 32 °C can be attributed to increased hydrophobic interactions resulting from the presence of the dodecyl end-group. The LCST of the star-shaped PNIPAM$_6$ **10** was determined to be 26.8 °C, an observation which is consistent with previous reports on the reduction in LCST values for branched PNIPAM.[23, 24]

An additional important observation is the broad phase transition behaviour of PNIPAM$_6$ **10** ($\approx$ 10 °C) with respect to the very sharp transition of PNIPAM **5**. Such broadening has been discussed from a theoretical perspective by Zhulina and coworkers[29] for polymer chains attached to surfaces. Schild and colleages[30] have also reported such a phenomenon for highly polydisperse PNIPAM (*PDI* = 2.3-6.9), which can be explained by the fact that the LCST of this polymer in aqueous solution is influenced by the molecular weight of the polymer chains, thus the broadening effect results from the contribution of chains with wide-varying molecular weight. The PNIPAM used in the present investigation, however, is of narrow *PDI*, thus the broadening effect is presumed to be caused by the anchoring of the PNIPAM chains to the highly hydrophobic fullerene core.

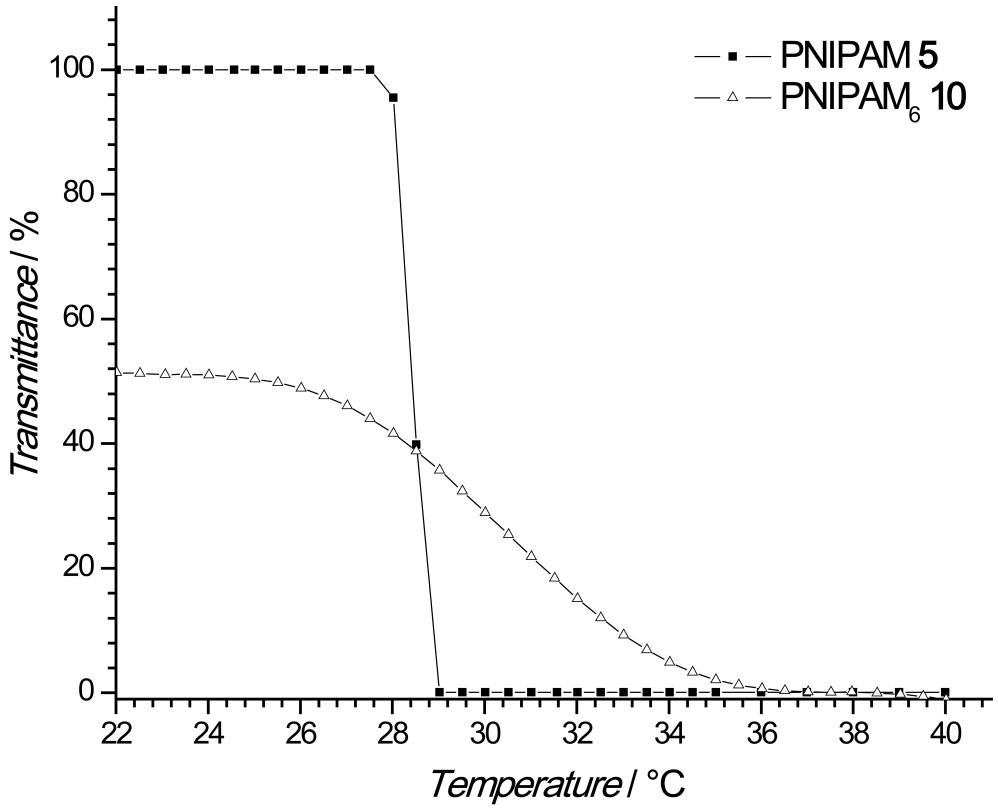

Figure 13.14 Transmittance *vs* temperature for 3 mg·mL^{-1} aqueous solutions of PNIPAM **5** and PNIPAM$_6$ **10** measured at λ = 700 nm.

13.4 Conclusion

The investigation presented herein has, for the first time, shown that hexakisazido fullerene derivatives such as **1** may be efficiently used in the synthesis of well-defined, star-shaped polymers via *click* chemistry. The postulated hypothesis that a larger *click* core would lead to an improved efficiency in the conjugation reactions was confirmed. In addition, novel thermoresponvive star-shaped fullerene derivatives have become easily accessible.

References

[1] Prato, M. *J. Mater. Chem.* **1997**, *7*, 1097–1109.

[2] Zhou, P.; Chen, G. Q.; Hong, H.; Du, F. S.; Li, Z. C.; Li, F. M. *Macromolecules* **2000**, *33*, 1948–1954.

[3] Giacalone, F.; Martin, N. *Chem. Rev.* **2006**, *106*, 5136–5190.

[4] Wakai, H.; Shinno, T.; Yamauchi, T.; Tsubokawa, N. *Polymer* **2007**, *48*, 1972–1980.

[5] Schmaltz, B.; Brinkmann, M.; Mathis, C. *Macromolecules* **2004**, *37*, 9056–9063.

[6] Schmaltz, B.; Mathis, C.; Brinkmann, M. *Polymer* **2009**, *50*, 966–972.

[7] Evans, R. A. *Aust. J. Chem.* **2007**, *60*, 384–395.

[8] Binder, W. H.; Sachsenhofer, R. *Macromol. Rapid Commun.* **2008**, *29*, 952–981.

[9] Barner-Kowollik, C.; Inglis, A. J. *Macromol. Chem. Phys.* **2009**, *210*, 987–992.

[10] Trabolsi, A.; Elhabiri, M.; Urbani, M.; de la Cruz, J. L. D.; Ajamaa, F.; Solladie, N.; Albrecht-Gary, A. M.; Nierengarten, J. F. *Chem. Commun.* **2005**, 5736–5738.

[11] Iehl, J.; de Freitas, R. P.; Delavaux-Nicot, B.; Nierengarten, J. F. *Chem. Commun.* **2008**, 2450–2452.

[12] Iehl, J.; de Freitas, R. P.; Nierengarten, J. F. *Tetrahedron Lett.* **2008**, *49*, 4063–4066.

[13] Zhang, W. B.; Tu, Y.; Ranjan, R.; Van Horn, R. M.; Leng, S.; Wang, J.; Polce, M. J.; Wesdemiotis, C.; Quirk, R. P.; Newkome, G. R.; Cheng, S. Z. D. *Macromolecules* **2008**, *41*, 515–517.

[14] Pierrat, P.; Vanderheiden, S.; Muller, T.; Brase, S. *Chem. Commun.* **2009**, 1748–1750.

[15] Qin, S. H.; Oin, D. Q.; Ford, W. T.; Resasco, D. E.; Herrera, J. E. *J. Am. Chem. Soc.* **2004**, *126*, 170–176.

[16] Clouet, G.; Knipper, M.; Brossas, J. *Polym. Bull.* **1984**, *11*, 171–174.

[17] Thang, S. H.; Chong, Y. K.; Mayadunne, R. T. A.; Moad, G.; Rizzardo, E. *Tetrahedron Lett.* **1999**, *40*, 2435–2438.

[18] Ranjan, R.; Brittain, W. J. *Macromolecules* **2007**, *40*, 6217–6223.

[19] Li, C.; Hu, J.; Yin, J.; Liu, S. *Macromolecules* **2009**, *42*, 5007–5016.

[20] Tamura, A.; Uchida, K.; Yajima, H. *Chem. Lett.* **2006**, *35*, 282–283.

[21] Zhou, G.; Harruna, I.; Zhou, W. L.; Aicher, W. K.; Geckeler, K. E. *Chem. Eur. J.* **2007**, *13*, 569–573.

[22] Xia, Y.; Burke, N. A. D.; Stöver, H. D. H. *Macromolecules* **2006**, *39*, 2275–2283.

[23] Vogt, A. P.; Sumerlin, B. S. *Macromolecules* **2008**, *41*, 7368–7373.

[24] Plummer, R.; Hill, D. J. T.; Whittaker, A. K. *Macromolecules* **2006**, *39*, 8379–8388.

[25] Housni, A.; Narain, R. *Eur. Polym. J.* **2007**, *43*, 4344–4354.

[26] Xia, Y.; Yin, X. C.; Burke, N. A. D.; Stöver, H. D. H. *Macromolecules* **2005**, *38*, 5937–5943.

[27] Radke, W.; Gerber, J.; Wittmann, G. *Polymer* **2003**, *44*, 519–525.

[28] Gao, H. F.; Matyjaszewski, K. *Macromolecules* **2006**, *39*, 4960–4965.

[29] Zhulina, E. B.; Borisov, O. V.; Pryamitsyn, V. A.; Birshtein, T. M. *Macromolecules* **1991**, *24*, 140–149.

[30] Schild, H. G.; Tirrell, D. A. *J. Phys. Chem.* **1990**, *94*, 4352–4356.

14

Materials and Characterization

14.1 Materials

Unless otherwise specified, all chemicals were purchased at their highest available purity.

4,4-azobis(4-cyanopentanol) (ACP),[1] 3-azido-1-propanol,[2] benzyl (diethoxyphosphoryl)dithioformate (BDPDF),[3] benzyl pyridin-2-yldithioformate (BPDF),[4, 5] 1,2-bis(bromoisobutyryloxy)ethane,[6] 4-cyano-1-hydroxypent-4-yl dithiobenzoate (RAFT-OH),[7] 2-hydroxyethyl-2′-bromopropionate[8], 1-phenylethyl(diethoxyphosphoryl)dithioformate[9] and *S*-1-dodecyl-*S′*-(α,α'-dimethyl-α'' propargylacetate)[10] were all synthesized according to literature procedures.

Isobornyl acrylate (technical grade, Aldrich), methyl acrylate (Acros), methyl methacrylate (Acros) and styrene (Merck) were all passed through a short column of basic alumina and stored at -18 °C prior to use. ϵ-Caprolactone (Aldrich) was distilled over calcium hydride and stored over molecular sieves (3 Å, BDH). 2,2′-Azobis(isobutyrlnitrile) (AIBN, Sigma-Aldrich) was recrystallized twice from methanol and stored at - 18 °C prior to use. Copper (I) bromide (Fluka) was purified by sequential washing with sulphurous acid, acetic acid, and ethanol, followed by drying under reduced pressure prior to use. Lipase acrylic resin from *Candida*

antarctica (Sigma) and zinc chloride (Sigma) were stored over phosphorous pentoxide.

Anisole (> 99 %, Fluka), 1,4-bis(bromomethyl)benzene (97 %, Aldrich), 1,3,5-tris(bromomethyl)benzene (97 %, Aldrich), 1,2,4,5-tetrakis(bromomethyl)benzene (95 %, Aldrich), 4-bromomethyl benzoic acid (Acros), 2-bromopropionyl bromide (97 %, Aldrich), 2-chloromethylpyridine hydrochloride (Aldrich), 2,2′-bipyridine (bpy, > 99 %, Aldrich), copper (II) bromide (Fluka), copper (II) sulfate pentahydrate (99.5 %, BDH), 1,8-diazabicyclo[5.4.0]undec-7-ene (DBU, Fluka), *N*, *N*′-dicyclohexylcarbodiimide (DCC, > 99 %, Fluka), 4-dimethylaminopyridine (DMAP,Sigma), elemental sulfur (Aldrich), hexylamine (99 %, Aldrich), methyl 2-bromo-2-methylpropanoate (MBMP, > 99 %, Aldrich), methyl 2-bromopropanoate (MBP, 98 %, Aldrich), sodium cyclopentadienide (2.0 M in THF, Aldrich), nickelocene (99 %, Strem Chemicals), tributylphosphine (95 %, Acros), poly(ethylene glycol) monomethyl ether (2000 MW, Fluka), *N, N, N′, N″, N″*-pentamethyldiethylenetriamine (PMDETA, Merck), 1-phenylethyl bromide (97 %, Aldrich), potassium *tert*-butoxide (Merck), 4-pentynoic acid (95 %, Aldrich), *p*-toluene sulfonyl chloride (Acros), pyridine (extra dry with molecular sieves, water < 50 ppm, Acros), (+)-sodium L-ascorbate (> 98 %, Sigma), sodium hydride (60 % dispersion in mineral oil, Aldrich), sodium iodide (Fluka), sodium phenylsulfinate (Aldrich), *trans*, *trans*-2,4-hexadien-1-ol (Aldrich), triethylamine (TEA, 99 %, Acros), trifluroacetic acid (TFA, Sigma-Aldrich), 1,1,1-tri(hydroxmethyl)propane (Aldrich), and tetrahydrofuran (THF, anhydrous > 99 %, water < 30 ppm, Aldrich) were all used as received.

14.2 Characterization

The work presented in Chapters 3 through 6 was carried out in the laboratories of the Centre for Advanced Macromolecular Design (CAMD) at the University of New South Wales, Sydney. Consequently, descriptions of equipment and characterization techniques used therein are provided and are marked accordingly where they differ from those used at the Karlsruhe Institute of Technology (KIT).

14.2.1 ^{1}H and ^{13}C Nuclear Magnetic Resonance Spectroscopy

The structures of the synthesized compounds were confirmed by ^{1}H and ^{13}C NMR spectroscopy using:

Sydney: a Bruker DPX 300 spectrometer at 300 MHz for hydrogen nuclei and 75 MHz for carbon nuclei or a Bruker DMX 500 spectrometer at 500 MHz for hydrogen nuclei.

Karlsruhe: a Bruker AM250 spectrometer at 250 MHz for hydrogen nuclei, a Bruker AM400 spectrometer at 400 MHz for hydrogen nuclei or a Bruker AM500 spectrometer at 500 MHz for hydrogen nuclei.

All samples were dissolved in either $CDCl_3$ or DMSO d_6 (however specified within each chapter). The δ scale is referenced to tetramethylsilane (δ = 0.00) as an internal standard.

14.2.2 Electrospray Ionization Mass Spectrometry

Electrospray ionization mass spectrometry (ESI-MS) measurements were performed on

Sydney: a LCQ Deca quadrupole ion trap mass spectrometer (Thermo Finnigan) equipped with an atmospheric pressure ionization source operating in the nebulizer assisted electrospray mode which was used in positive ion mode. Polymer samples (0.2 - 0.25 $mg \cdot mL^{-1}$) were dissolved in a THF/methanol (3:2) mixture. Mass calibration was performed using caffeine, Met-Arg-Phe-Ala acetate (MRFA, Sigma-Aldrich) and Ultramark 1621 (Sigma-Aldrich) in the *m/z* range 195-1822. All spectra were acquired over the *m/z* range 150-2000 with a spray voltage of 5 kV and a capillary temperature of 275 °C. Nitrogen was used as a sheath gas (flow: 45 % of maximum) and helium was used as the auxiliary gas (flow: 5 % of maximum). MS-MS investigations (cf. Chapter 3) were performed with parent masses of *m/z*=1680 and 1735 and an isolation width of *m/z* = 1.0 for compounds **6** and **7**, respectively. A normalized collision energy of 25 % at an activation time of 30 ms was used.

Karlsruhe: a LXQ mass spectrometer (ThermoFisher Scientific) equipped with an atmospheric pressure ionization source operating in the nebulizer-assisted electrospray mode. The instrument was calibrated in the *m/z* range 195-1822 using a standard comprising caffeine, Met-Arg-Phe-Ala acetate (MRFA), and a mixture of fluorinated phosphazenes (Ultramark 1621) (all from Aldrich). A constant spray voltage of 4.5 kV and a dimensionless sweep gas flow rate of 2 and a dimensionless sheath gas flow rate of 12 were applied. The capillary voltage, the tube lens offset voltage and the capillary temperature were set to 60 V, 110 V and 275 °C respectively. The LXQ was coupled to a Series 1200 HPLC system (Agilent) that consisted of a solvent degasser (G1322A), a binary pump (G1312A) and a high-performance autosampler (G1367B), followed by a thermostatted column compartment (G1316A). Separation was performed on two mixed bed SEC columns (Polymer Laboratories, Mesopore 250 $\times$ 4.6 mm, particle diameter 3 µm) with pre-column (Mesopore 50 $\times$ 4.6 mm) operating at 30 °C. THF at a flow rate of 0.3 $mL \cdot min^{-1}$ was used as the eluent. The mass spectrometer was coupled

to the column in parallel to an RI detector (G1362A with SS420x A/D) in a setup described in the literature. A 0.27 mL·min^{-1} aliquot of the eluent was directed through the RI detector and 30 µL·min^{-1} infused into the electrospray source after post-column addition of a 0.1 mM solution of sodium iodide in methanol at 20 µL·min^{-1} by a micro flow HPLC syringe pump (Teledyne ISCO, Model 100DM). The polymer solutions (20 µL) with a concentration of $\approx$ 3 mg·mL^{-1} were injected into the HPLC system.

14.2.3 Ultraviolet/Visible Spectroscopy

UV/Vis-spectroscopic measurements were performed on a Cary 300 Bio UV/Vis spectrophotometer (Varian) equipped with a temperature controlled sample holder. The individual experimental set-ups for data acquisition are treated on a case by case basis as they appear in the nominated chapters:

Chapter 5: Absorption was measured in chloroform solution (at 50 °C) from λ = 350 to 850 nm with a resolution of 1 nm in a 10 mm UV cuvette. Experimental details are included within the chapter.
Chapter 8: Absorption was measured in dichloromethane solution from λ = 350 to 850 nm with a resolution of 1 nm in a 10 mm UV cuvette.
Chapter 11: Absorption was measured in toluene solution within the temperature range of 25 - 100 °C with a resolution of 1 nm in a 10 mm UV cuvette. Experimental details are included within the chapter.
Chapter 12: Absorption was measured in toluene solution (3 mg·mL^{-1}) at λ = 522 nm at temperatures ranging from 30 to 100 °C (using a 0.5 °C·min^{-1} heating rate).
Chapter 13: Absorption was measured in dichloromethane solution from λ = 200 nm to 800 nm with a resolution of 1 nm in a 10 mm UV cuvette. Cloud points were measured on the same apparatus. Aqueous solutions of PNIPAM (3 mg·mL^{-1}) were heated at 0.5 °C·min^{-1}. Both the temperature, as determined by the internal temperature probe, and the transmittance of the aqueous solutions were monitored at λ = 700 nm. Further details are included within the chapter.

14.2.4 Size Exclusion Chromatography

SEC measurements were performed on:

Sydney: a Shimadzu modular system comprising an auto-injector, a Polymer Laboratories 5.0 µm bead-size guard column (50 $\times$ 7.5 mm), followed by three linear PL columns (10^5, 10^4 and 10^3 Å) and a differential refractive index detector using THF as the eluent at 40 °C with a flow rate of 1 mL·min^{-1}. The SEC system was calibrated

using linear poly(styrene) standards ranging from 540 to 2 × 10^6 g·mol^{-1}.
Karlsruhe: *THF System* - a Polymer Laboratories (Varian) PL-GPC 50 Plus Integrated System, comprising an autosampler, a PLgel 5 µm bead-size guard column (50 × 7.5 mm), one PLgel 5 µm Mixed E column (300 × 7.5 mm) three PLgel 5 µm Mixed C columns (300 × 7.5 mm) and a differential refractive index detector using THF as the eluent at 35 °C with a flow rate of 1 mL·min^{-1}. The SEC system was calibrated using linear poly(styrene) standards ranging from 160 to 6 × 10^6 g·mol^{-1} and linear poly(methyl methacrylate) standards ranging from 700 to 2 × 10^6 g·mol^{-1}.
DMAc system - a Polymer Laboratories PL-GPC 50 Plus Integrated System, comprising an autosampler, a PLgel 5 µm bead-size guard column (50 × 7.5 mm) followed by three PLgel 5 µm MixedC columns (300 × 7.5 mm) and a differential refractive index detector using *N*,*N*'- dimethylacetamide (DMAc) containing 0.3 wt% LiBr as the eluent at 50 °C with a flow rate of 1.0 mL·min^{-1}. The SEC system was calibrated against linear poly(styrene) standards with molecular weights ranging from 160 to 6 × 10^6 g·mol^{-1}.

14.2.5 SEC Deconvolution

SEC traces were deconvoluted using the Gaussian function of the Peak Fit program (version 4.12 from SeaSolve Software Inc.). The program uses a Gaussian response function with a Fourier deconvolution and filtering algorithm. The algorithm is run iteratively until the correlation coefficient (R^2) of the fitted data is minimized (via the least squares method). It is necessary to use the retention times of the polymer precursors (which have been independently measured) to constrain fitted peaks to the corresponding values. The placed peaks are then iteratively varied in their intensities and area such that the result of their convolution fits to the raw experimental data of the block or star (co)polymer. This procedure was utilized in Chapter 5, 7, and 10.

14.2.6 2D LACCC-SEC

The retention volume (V_R) in a chromatographic process (which is directly related to the retention time via the eluent flow rate) may be expressed by the following equation:

$$\ln \frac{V_R - V_m}{V_m} = \frac{-\Delta H}{RT} + \frac{\Delta S}{R} + \ln \frac{V_s}{V_m} \tag{14.1}$$

where ΔS and ΔH represent the changes in entropy and enthalpy that are associated with the transfer of solute (i.e. polymer) between the mobile and stationary phases in

the chromatographic column respectively. R is the ideal gas constant, T is the temperature and V_s and V_m are the volumes of the stationary and mobile phases respectively. For a chromatographic column with non-compressible porous packing, V_s/V_m is approximately constant.

In an ideal SEC system, the size exclusion mechanism by which the polymer analyte is separated is soley goverened by entropic considerations. These include mixing processes, changes in polymer orientation and changes in the conformation of the swollen polymer coils in solution as they enter and leave the pores of the column packing material. Consequently, a linear relationship between log(M) and V_R is established such that larger polymer chains elute before smaller polymer chains (Figure 14.1).

In reality, however, there is some degree of interaction between the separated polymer chains with the column packing material, with the eluent and between the eluent and the column packing material, all of which provide a change in enthalpy. Such enthalpic considerations introduce a non-linearity in the log(M) vs V_R relationship as illustrated in Figure 14.1.

Conversely, in ideal liquid adsorption chromatography (LAC) the repeat units of the polymer chain (and also the polymer end-groups) can interact with the surface of the column's packing material and thus cause a change in enthalpy. The retention mechansim here provides for an inverse elution pattern to that of SEC in that larger molecules have a stronger interaction with the packing material than smaller molecules. Consequently, larger molecules can more readily adsorb and thus are eluted later (Figure 14.1). LAC is therefore described as an enthalpy dominant or enthalpy driven process.

Through the application of a certain solvent/non-solvent composition at a specified temperature, a situation can be created in which the entropic and enthalpic contributions to the polymer retention mechanism compensate each other. Under these so-called *critical conditions of enthalpic interactions* or, simply *critical conditions*, polymer chains with the same chemical composition (i.e. repeat units and end-groups) will elute at the same elution volume, irrespective of their size. The vertical line in Figure 14.1 illustrates the relationship between log(M) and V_R that is acheived in liquid adsorption chromatography at critical conditions (LACCC).

Consider now a mixture of two chemically distinct polymers **A** and **B**. Chemical distinction may take the form of different repeat units, different end-groups or the presence of a second block as in a block copolymer. Operating under the *critical conditions* of **A**, all such polymer chains will elute at a specific elution volume irrespective of their size. In contrast, the **B** component will either elute under normal size exclusion

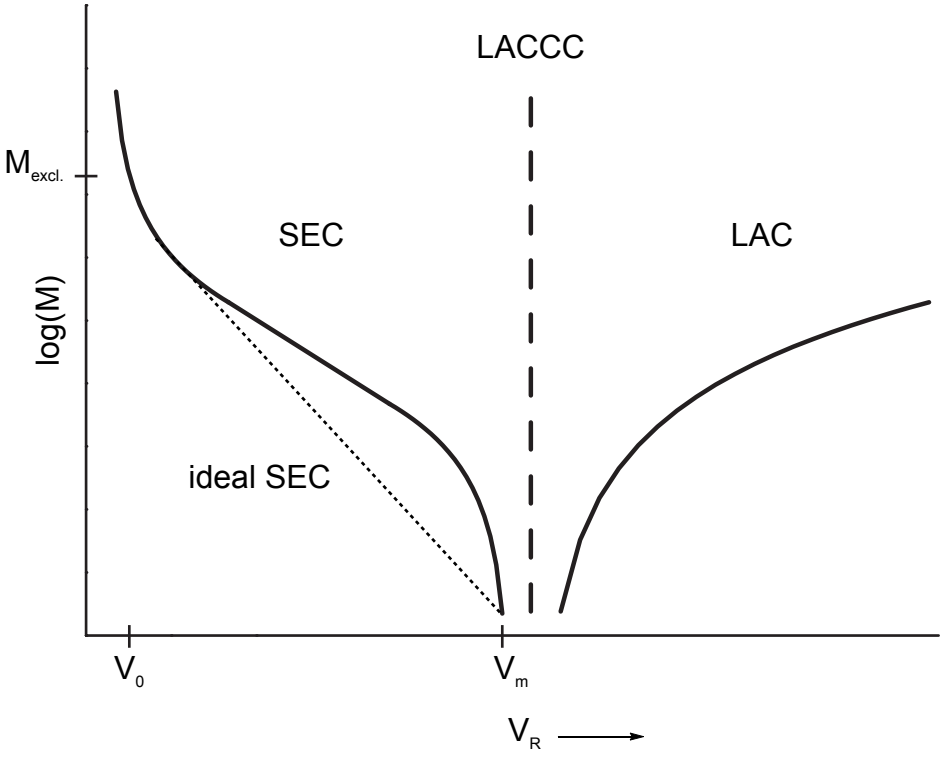

Figure 14.1 log(M) vs. V_R dependencies in the chromatographic analysis of polymers. $M_{excl.}$ is the molecular weight of polymer chains completely excluded from all column packing pores.

mode (left side of Figure 14.1) or adsorption mode (right side of Figure 14.1) depending upon the nature of the chromatographic column and the exact nature of polymers in question. It is in this way that chemically distinct macromolecular species may be separated very efficiently for analytical purposes.

Upon combining LACCC with conventional SEC in a sequential fashion (2D-chromatography), the polymer mixture of **A** and **B** can be separated initally by chemical heterogeneity and then by size. The experimental set-up for performing such an anylsis is depicted in Figure 14.2. Initially, the polymer analyte (**A** + **B**) is injected into the first dimension (LACCC) under the *critical conditions* of **A**. This separates **A** from **B**. Eluates from the first dimension are then transferred to the second dimension (SEC) via a switching valve which injects the eluates into a system which further separates the components according to their size. Upon passing through a detector and subsequent acquistition/processing of data, a contour plot of the separated mixture is obtained (cf. Chapter 10). The details of the equipment used to perform LACCC, SEC and 2D LACCC-SEC are outlined in the following:

LACCC Analysis: The analysis of all samples was performed under the critical conditions of P*i*BoA using an Agilent SECcurity GPC system (1200 series), comprising a binary pump (G1312A), degasser (G1379B) autosampler (G1329A) and a temperature controlling unit (G1316A), which housed two Zorbax Eclipse XDB-C18

columns (4.6 × 150 mm, 5 µm particle size) at 35 °C. SIHS: 13 680. The THF:MeOH (68 %: 32% v/v) eluent was pumped at a flow rate of 0.08 mL·min^{-1}. An evaporative light scattering detector (ELSD 400, SofTA Corporation) operating under an argon pressure of 47.6 psi and a spray chamber temperature of 50 °C was used. ELSD is the most bias-free (mass sensitive) detector when compared to RI or even UV detectors when analyzing block copolymers in terms of detecting both segments of the block with equal weighting. Samples were prepared in the above described eluent at a polymer concentration of 2 mg·mL^{-1} (concentrations were systematically varied to obtain optimal results). Data acquisition and processing was accomplished with the PSS WinGPC Unity software package from Polymer Standards Service (PSS; Mainz, Germany).

2D LACCC-SEC Analysis: The first dimension (LACCC) was operated under the same conditions as detailed above. Sample fractions eluting from the first dimension were transferred to the second dimension (SEC) via an eight-port switch valve system (VICI AG International). The SEC system comprised an isocratic pump (G1310A) delivering a flow rate of pure THF at 3 mL·min^{-1}. SEC separation was achieved via the use of a high-speed column (SDV, linear M, 20 × 50 mm) provided by PSS. Samples were prepared in the above described eluent at a polymer concentration of 2 mg·mL^{-1}. The same ELSD was used for the detection and the data acquisition and processing were performed with the PSS WinGPC Unity software.

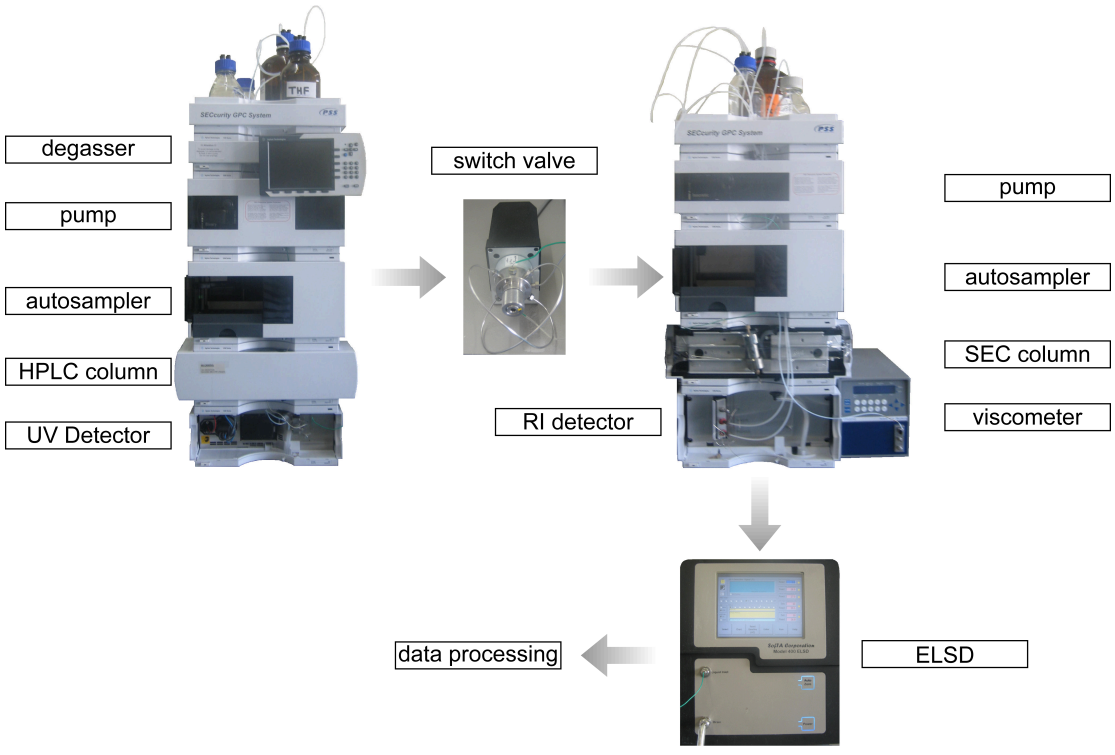

Figure 14.2 Experimental set-up for performing 2D LACCC-SEC.

Theoretical Block Copolymer Composition- Example Calculation (cf Chapter 10).

Taking a basis of 1 mol of PMMA **1** (M_n = 3200 g·mol^{-1}), there will be:

0.97 mol (3104 g) of functional polymer, and

0.03 mol (96 g) of dead polymer

To achieve equimolar stoichiometry, 1.02 mol of P*i*BoA **2** (4600 g·mol^{-1}) is required as it contains:

0.97 mol (4462 g) of functional polymer, and

0.05 mol (236 g) of dead polymer

Therefore, under the assumption of 100 % conjugation efficiency, one can expect:

3104 + 4462 = 7566 g of block copolymer

96 g of remaining dead PMMA **1**, and

236 g of remaining dead P*i*BoA **2**

Thus, the corresponding mass fractions of these components will be:

7566/7898 = 0.958 $\rightarrow$ 95.8 wt% block copolymer

96/7898 = 0.012 $\rightarrow$ 1.2 wt% dead PMMA **1**

236/7898 = 0.03 $\rightarrow$ 3 wt% dead P*i*BoA **2**

References

[1] Clouet, G.; Knipper, M.; Brossas, J. *Polym. Bull.* **1984**, *11*, 171–174.

[2] Quémener, D.; Davis, T. P.; Barner-Kowollik, C.; Stenzel, M. H. *Chem. Commun.* **2006**, 5051–5053.

[3] Laus, M.; Papa, R.; Sparnacci, K.; Alberti, A.; Benaglia, M.; Macciantelli, D. *Macromolecules* **2001**, *34*, 7269–7275.

[4] Abrunhosa, I.; Gulea, M.; Masson, S. *Synthesis* **2004**, 928–934.

[5] Alberti, A.; Benaglia, M.; Guerra, M.; Gulea, M.; Hapiot, P.; Laus, M.; Macciantelli, D.; Masson, S.; Postma, A.; Sparnacci, K. *Macromolecules* **2005**, *38*, 7610–7618.

[6] Karanam, S.; Goossens, H.; Klumperman, B.; Lemstra, P. *Macromolecules* **2003**, *36*, 8304–8311.

[7] Thang, S. H.; Chong, Y. K.; Mayadunne, R. T. A.; Moad, G.; Rizzardo, E. *Tetrahedron Lett.* **1999**, *40*, 2435–2438.

[8] Qin, S. H.; Oin, D. Q.; Ford, W. T.; Resasco, D. E.; Herrera, J. E. *J. Am. Chem. Soc.* **2004**, *126*, 170–176.

[9] Sinnwell, S.; Synatschke, C. V.; Junkers, T.; Stenzel, M. H.; Barner-Kowollik, C. *Macromolecules* **2008**, *41*, 7904–7912.

[10] Ranjan, R.; Brittain, W. J. *Macromolecules* **2007**, *40*, 6217–6223.

15

Concluding Remarks and Outlook

15.1 Concluding Remarks

Diels-Alder chemistry has steadily been growing in popularity in the synthesis of a variety of precision polymeric materials. However, the present body of work has shown the application of such chemistry with unprecedented efficiency, speed and versatility. After initially proving the concept that electron-deficient dithioesters may be sequentially utilized as controlling agents in RAFT polymerization and as a reactive heterodienophile for conjugation chemistry (Chapter 3), the modular synthesis of well-defined complex macromolecular architectures such as block copolymers (Chapter 4) and star-shaped polymers (Chapter 5) were achieved in a manner that was directly comparable to the CuAAC. Typical reaction conditions of 50 °C and 2-24 hour reaction times were required for quantitative conversions.

Within the field of conjugation chemistry (as it is applied to macromolecular species), a highly important characteristic is orthogonality, i.e the conjugation reaction must be tolerant to (and not interfere with) other functionalities that may exist in the system, especially those destined to be used for further and independent transformations. As such, in the modular synthesis of star-shaped block copolymers (Chapter 6) the RAFT-HDA reaction was proven to be applicable in a co-operative fashion with (i.e. orthogonal to) the CuAAC, thus further establishing the concept as a form of *click* chemistry.

In an effort to improve the efficiency and rate of reaction, more reactive diene species were investigated. In Chapter 7, novel cyclopentadienyl end-functional polymers were synthesized and reacted with the same dithioester-functional polymers that were used in the preceding investigations. The ambient temperature conjugation reaction yielded well-defined block copolymers within a reaction time of ten minutes. This work was then extended to include forming block copolymers of higher molecular weights. In doing so, the results presented in Chapter 8 confirm that block copolymers with molecular weights in excess of 100 000 $g \cdot mol^{-1}$ are indeed accessible via a modular pathway.

In Chapter 7, sodium cyclopentadienide was used to perform a nucleophilic substitution reaction on bromide-terminated poly(styrene) and tosylated poly(ethylene glycol). These two polymers did not contain, however, any potentially cross-reactive functionality. When the same procedure was performed on similarly functional poly(acrylate)s and poly(methacrylate)s, the targeted outcome of well-defined Cp-functional materials could not be achieved. In order to resolve this issue, an entirely new strategy was developed involving the use of nickelocene in Chapter 9. This new synthetic pathway has been proven to be very robust and is set to grow in popularity given the current trend of the use of Diels-Alder chemistry within materials chemistry.

Having truly established the ease with which linear polymer chains may be equipped with both electron-deficient dithioester and cyclopentadienyl functionality, an in-depth study into the efficiency of Diels-Alder chemistry in the preparation of block copolymers was conducted (Chapter 10). After using conventional SEC to confirm the success of the coupling reactions, LACCC and 2D-LACCC-SEC were used to quantitatively determined the compositions of the reaction mixtures. In excellent agreement with the preceding findings, a greater than 90 % coupling efficiency (and hence purity) of the synthesized block copolymers was determined. Furthermore, the simple SEC deconvolution procedure that was used in Chapter 5 and Chapter 7 was validated in providing comparably accurate composition data.

In Chapter 5, UV/Vis spectroscopy was used to monitor the progress of the HDA reaction as the coloured dithioester compound transformed into the colourless cycloadduct. In Chapter 11, this colour change behaviour was investigated in a reversible fashion to produce a colour-switchable polymeric material. A cyclopentadienyl functional polymer underwent an ambient temperature HDA cycloaddition with a small-molecule dithioester to yield a colourless material. Upon heating the material (in solution) to 100 °C, the retro HDA reaction could be promoted and, thus, return the colour of the dithioester. Upon cooling, the forward HDA reaction was favoured; returning the material to a colourless state.

Further taking advantage of the reversible nature of RAFT-HDA chemistry, a cross-linked polymeric material was synthesized in a fast, ambient temperature coupling

of macromolecular building blocks (Chapter 12). Upon heating the resulting high-molecular weight and insoluble materials, a dramatic decrease in molecular weight could be obtained within a very short time frame (5 minutes). Upon cooling the now soluble material, the molecular weight increased in a proof-of-concept for a rapid bonding and debonding on demand system. This work has since been patented with Evonik Degussa GmbH, who are continuing to develop this technology.

In a semi-related project, the design and synthesis of novel star-shaped polymers bearing C_{60} as the core was described in Chapter 13. Although providing another route that would grant access to further C_{60} based materials, the important result obtained here was directly related to the convergent and modular synthesis of star-shaped molecules. As observed in Chapter 5, the efficiency of star-formation via a modular pathway decreases with increasing number of arms of the star due to the associated increase in steric crowding of the reactive sites on the core molecule. The C_{60} core molecule used in Chapter 13 is substantially larger than the core molecule used in Chapter 5. Gratifyingly, although not surprising, the efficiency of the formation of the C_{60} star-shaped polymers was observed to be significantly higher.

As it stands, the present body of work has conceptualized, developed and applied RAFT-HDA chemistry as a highly versatile and easy to use tool in materials chemistry. From simple architecture design to the synthesis of more advanced materials, it is anticipated that related and further developments will surely bring not only RAFT-HDA chemistry, but Diels-Alder chemistry in general, to a much broader platform in polymer and materials chemistry.

15.2 Outlook

The *honeymoon* period of *click* chemistry has died down. Although efficient modularity has certainly flourished in polymer science within this burst of activity, it is important to view advances in this field with a grounded perspective. While there are numerous examples in which the philosophy of *click* chemistry has been applied as a solution to certain design problems in previously unattainable materials, there are likewise numerous reports in which the tools of *click* chemistry have transparently been used in place of equally effective (and incumbent) technologies merely to profit from the momentum of a growing research field.

In a field that was (and still is) dominated by the CuAAC, it is refreshing to note that many more highly efficient chemical transformations are increasing in popularity and are finding their way in the development of what many may call the *next generation* of application driven synthetic materials. In terms of the future direction of research

immediately stemming from this work, it would seem prudent to further investigate alternative dienophilic species that may readily be incorporated into a variety of synthetic and biological materials (including surfaces), given the facile synthesis of cyclopentadienyl compounds reported in Chapter 9.

Within the scope of RAFT-HDA chemistry, the major limitation (at this stage) is the non-applicability of all RAFT agents. It appears that the dithioesters used within this investigation (BDPDF and BPDF) offer the optimal balance between dienophilicity and suitability as a controlling agent in a RAFT process. The central feature that governs both of these properties is the Z-group of the dithioester. The best performing RAFT agents bear Z-groups that aren't electron-withdrawing enough to facilitate efficient Diels-Alder chemistry. Although increasing the dienophilicity of RAFT agents will greatly enhance their usefulness in conjugation chemistry via a Diels-Alder pathway, their ability to mediate controlled polymerization in a RAFT process would be significantly hindered. For instance, it has already been demonstrated that highly dienophilic dithioesters (such as those bearing α-sulfonyl functionality) can undergo ill-desired side reactions with such common monomers as styrene and *n*-butyl acrylate (cf. Chapter 2).

A foreseeable challenge is the design of a *universal* RAFT agent that would be able to mediate the RAFT polymerization of a wide variety of different monomers whilst still being a highly efficient dienophile. The concept of *switchable* RAFT agents may be key in meeting such a challenge. It was shown in Chapter 2 that such a RAFT agent has been developed that is able to mediate the RAFT polymerization of both highly active monomers (such as vinyl acetate) when in a deprotonated state, and comparatively less active monomers (such as styrene) when in a protonated state. Furthermore, it was shown in the present investigation that the dienophilicity of BPDF is essentially turned on and off through a similar protonation/deprotonation mechanism.

Another challenge that should be met, ideally in connection with the above proposition, would be to investigate RAFT-HDA chemistry in aqueous solution. As such, water-soluble dithioesters that are able to behave as efficient dienophiles are in need of being developed. Whilst the ability to perform chemical transformations in aqueous solution is highly attractive from an industrial and, specifically, an environmental point of view, an additional advantage lies in the significant increase in efficiency that is observed in Diels-Alder systems in such media.

To go one step further, it would be highly advantageous to have a catalogue of diene/dienophile pairs that may be readily incorporated into a wide range of materials in a universal fashion. Each pair would have a specific *working temperature* range which specifies the conditions required to form a Diels-Alder conjugate, the stability of that conjugate and the conditions under which reversible degradation may be induced.

Being more of a generalistic approach to designing even more elaborate macromolecular architectures would be the use of both reversible and irreversible *click* reactions in a co-operative fashion. Such a strategy would introduce (or revitalize at least) the concept of macromolecular scaffolding and templating to precision materials design. A structure could be imagined to be built up comprising various reversible and irreversible linkages in a very specific fashion. Upon thermal, photolytic or whatever treatment that would effect a reversion of the reversible linkages, the formed materials would degrade in a predicted and targeted fashion. In this way, for example, a compound with a very specific geometry could template the building up of a larger structure and then be removed. Such an innovation would find profound applicability in the design and construction of synthetic materials destined to interface with biological systems in a highly precise manner.

It seems as though one's imagine can run wild and conjure up many different pathways and possibilities to many exciting new synthetic materials. However, in many respects it is far more useful to have, as a guide, a problem in search of a solution rather than a solution in search of a problem. In this way, a far more solid basis for the expression of creativity is provided that should herald the materials technologies of tomorrow.

List of Abbreviations

ACN	acetonitrile
ACP	4,4′-azobis(4-cyanopentanol)
AIBN	2,2′-azobis(2-methylpropionitrile)
ARGET	activators regenerated by electron transfer
ATR-IR	attenuated total reflection - infrared
ATRP	atom transfer radical polymerization
BDPDF	benzyl (diethoxyphosphoryl)dithioformate
BPDF	benzyl pyridin-2-yldithioformate
BPiB	2-bromopropionyl bromide
bpy	2,2′- bipyridine
BSA	bovine serum albumin
C_{60}	60 carbon fullerene
CCL-5	chemokine (C-C motif) ligand 5
CID	collision induced dissociation
Cp	cyclopentadienyl
CRP	controlled radical polymerization
CTA	chain transfer agent
CuAAC	copper (I) catalysed azide-alkyne cycloaddition
DA	Diels-Alder
DBU	1,8-diazabicyclo[5.4.0]undec-7-ene
DCC	dicyclohexylcarbodiimide
DCM	dichloromethane
DDPA	*S*-1-dodecyl-*S*′-(α,α′-dimethyl-α″-propargylacetate)
DMF	dimethylformamide
DIFO	difluorinated cyclooctyne
DMAc	dimethylacetamide
DMAP	4-dimethylaminopyridine
DMPA	2,2-dimethoxy-2-phenylacetophenone
DMPP	dimethylphenylphoshpine
DNA	deoxyribonucleic acid
DPTS	4-(dimethylamino)-pyridinium-4-toluene sulfonate

EBiB	ethyl 2-bromoisobutyrate
ELSD	evaporative light scattering detector
equiv.	equivalents
ESI-MS	electrospray ionization mass spectrometry
EWG	electron withdrawing group
FRP	free radical polymerization
FT-IR	Fourier transform infrared
G2	second generation (dendrimer)
G3	third generation (dendrimer)
G4	fourth generation (dendrimer)
$h\nu$	photon energy
HexAm	hexylamine
HOMO	highest occupied molecular orbital
HPLC	high performace liquid chromatography
*i*BoA	isobornyl acrylate
IUPAC	international union of pure and applied chemistry
IVED-DA	inverse electron-demand Diels-Alder
k_a	rate coefficient of activation
k_{add}	rate coefficient of addition
k_β	rate coefficient of fragmentation
k_d	rate coefficient of dissociation
k_{da}	rate coefficient of deactivation
k_i	rate coefficient of initiation
k_p	rate coefficient of propagation
k_{ri}	rate coefficient of re-initiation
k_t	rate coefficient of termination
k_{tc}	rate coefficient of termination by combination
k_{td}	rate coefficient of termination by disproportionation
λ	wavelength
LAC	liquid adsorption chromatography
LACCC	liquid adsorption chromatography at critical conditions
LC-MS	Liquid Chromatography - Mass Spectrometry
LCST	lower critical solution temperature
LUMO	lowest unoccupied molecular orbital
M_n	number-average molecular weight
MBMP	methyl 2-bromo-2-methylpropanoate
MBP	methyl 2-bromopropionate
MS	mass spectrometry
MS/MS	tandem mass spectrometry
MWD	molecular weight distribution

NaCp	sodium cyclopentadienide
$NiCp_2$	nickelocene
NIPAM	*N*-isopropylacrylamide
NMP	nitroxide mediated polymerization
NMR	nuclear magnetic resonance
PBu_3	tributylphosphine
PCL	poly(ϵ-caprolactone)
PDI	polydispersity index
1-PEBr	1-phenylethyl bromide
PEG	poly(ethylene glycol)
P*i*BoA	poly(isobornyl acrylate)
PLA	poly(lactic acid)
PMDETA	*N, N, N′, N″, N″*-pentamethyldiethylenetriamine
PMMA	poly(methyl methacrylate)
PNIPAM	poly(*N*-isopropylacrylamide)
PS	poly(styrene)
RAFT-OH	4-cyano-1-hydroxypent-4-yl dithiobenzoate
RI	refractive index
ROP	ring opening polymerization
RT	room temperature
SEC	size exclusion chromatography
SET-LRP	single electron transfer - living radical polymerization
SFRP	stable free radical polymerization
TCEP	tris(2-carboxyethyl)phosphine
TEA	triethylamine
TEMPO	2,2,6,6-tetramethylpiperidine-*N*-oxyl
TFA	trifluoroacetic acid
THF	tetrahydrofuran
TMP	1,1,1-tris(hydroxymethyl)propane
Trx	thioredoxin
UV	ultra-violet
UV/Vis	ultra-violet/visible
V_m	volume of the mobile phase
V_R	retention volume
V_s	volume of stationary phase

Curriculum Vitae

Date of Birth:	30 September 1984
Place of Birth:	Sydney, Australia
Nationality:	Australian

Education

2008 - Present	**Doctoral Studies in Chemistry** Under the supervision of Prof. Dr. Christopher Barner-Kowollik Karlsruhe Institute of Technology, Germany
2003-2008	**Bachelor of Engineering** in Industrial Chemistry with Honours Class 1 and The University Medal University of New South Wales, Sydney, Australia *-recipient of a UNSW Co-Op Industrial Scholarship*
2001-2002	**Higher School Certificate** Sydney Technical High School, Bexley, NSW, Australia *University Admission Index: 99.75, Dux of the School*

Employment History

July 2008 - Present	**Institut für Technische Chemie und Polymer Chemie** Karlsruhe Institute of Technology, Karlsruhe, Germany Scientific Co-worker
February 2008 - July 2008	**School of Chemical Sciences and Engineering** Centre for Advanced Macromolecular Design (CAMD) University of New South Wales, Sydney, Australia Scientific Co-worker

August 2006 - December 2006	**The Vaslspar (Australia) Corporation Pty. Ltd** 203 Power St., Glendenning, NSW, Australia Coatings Formulation Chemist/Process Engineer
December 2005 - May 2006	**Siemens Water Technologies** 1 Memtec Parkway, South Windsor, NSW, Australia Research and Development Chemist/ Process Engineer
December 2004 - February 2005	**James Hardie Industries Pty. Ltd.** 10 Colquhoun St., Rosehill, NSW, Australia Process Development Chemist
December 2003 - February 2004	**National Starch & Chemical Pty. Ltd.** 7 Stanton Rd., Seven Hills, NSW, Australia Research and Development Chemist

Further Professional Experiences

February 2003 - June 2008	High School tutor in the subjects of: - Chemistry - Mathematics - Mathematics Extension 1 - Mathematics Extension 2 - Physics
November 2000	**Department of Biomedical Engineering** St. George Hospital, Gray St., Kogarah, NSW, Australia Medical equipment diagnostics and repair
	Department of Nuclear Medicine St. George Hospital, Gray St., Kogarah, NSW, Australia Nuclear Medicine Technologist

List of Publications and Conference Contributions

Refereed Journal Publications

[17] Visualizing the Efficiency of Rapid Modular Block Copolymer Construction
Inglis, A. J.; Barner-Kowollik, C. *Polym. Chem.* **2010**, DOI: 10.1039/C0PY00189A.

[16] Rapid Bonding/Debonding on Demand: Reversible Cross-Linked Functional Polymers via Diels-Alder Chemistry
Inglis, A. J.; Nebhani, L.; Altintas, O.; Schmidt, F.-G.; Barner-Kowollik, C. *Macromolecules*, **2010**, *43*, 5515-5520.

[15] Reversible Diels-Alder Chemistry as a Modular Polymeric Color Switch
Paulöhrl, T.; Inglis, A. J.; Barner-Kowollik, C. *Adv. Mater.*, **2010**, *22*, 2788-2791.

[14] Limitations of Radical Thiol-ene Reactions for Polymer-Polymer Conjugation
Koo, S. P. S.; Stamenovic, M. M.; Arun Prasath, R.; Inglis, A. J.; Du Prez, F. E.; Barner-Kowollik, C.; Van Camp, W.; Junkers, T. *J. Polym. Sci. Part A. Polym. Chem.*, **2010**, *48*, 1699-1713.

[13] Ultra Rapid Approaches to Mild Macromolecular Conjugation
Inglis, A. J.; Barner-Kowollik, C. *Macromol. Rapid Commun.* **2010**, *31*, 1247-1266.

[12] Ambient Temperature Synthesis of a Versatile Macromolecular Building Block: Cyclopentadienyl-Capped Polymers
Inglis, A. J.; Paulöhrl, T.; Barner-Kowollik, C. *Macromolecules*, **2010**, *43*, 33-36.

[11] Well-Defined Polymer-Fullerene Hybrids via Click Chemistry
Inglis, A. J.; Pierrat, P.; Muller, T.; Bräse, S. *Soft Matter*, **2010**, *6*, 82-84.

[10] Ultra-Fast RAFT-HDA Click Conjugation: An Efficient Route to High Molecular Weight Block Copolymers

Inglis, A. J.; Stenzel, M. H.; Barner-Kowollik, C. *Macromol. Rapid Commun.* **2009**, *30*, 1792-1798.

[9] Has Click Chemistry Lead to a Paradigm Shift in Materials Design?
Barner-Kowollik, C.; Inglis, A. J. *Macromol. Chem. Phys.* **2009**, *210*, 987-992.

[8] Ultra-Fast Click Conjugation of Macromolecular Building Blocks at Ambient Temperature
Inglis, A. J.; Sinnwell, S.; Stenzel, M. H.; Barner-Kowollik, C. *Angew. Chem. Int. Ed.* **2009**, *48*, 2411-2414.

[7] Access to 3-Arm Star Block Copolymers by a Consecutive Combination of the Copper (I)-Catalyzed Azide-Alkyne Cycloaddition and the RAFT Hetero Diels-Alder Concept
Sinnwell, S.; Inglis, A. J.; Stenzel, M. H.; Barner-Kowollik, C. *Macromol. Rapid Commun.* **2008**, *29*, 1090-1096.

[6] Efficient Surface Modification of Divinylbenzene Microspheres via a Combination of RAFT and Hetero Diels-Alder Chemistry
Nebhani, L.; Sinnwell, S.; Inglis, A. J.; Stenzel, M. H.; Barner-Kowollik, C.; Barner, L. *Macromol. Rapid Commun.* **2008**, *29*, 1431-1437.

[5] Reversible Addition-Fragmentation Chain Transfer (RAFT) and Hetero Diels-Alder Chemistry as a Convenient Conjugation Tool for Access to Macromolecular Design
Inglis, A. J.; Sinnwell, S.; Davis, T. P.;Barner-Kowollik, C.; Stenzel, M. H. *Macromolecules*, **2008**, *41*, 4120-4126.

[4] An Atom-Efficient Conjugation Approach to Well-Defined Block Copolymers Using RAFT Chemistry and Hetero Diels-Alder Cycloaddition
Sinnwell, S.; Inglis, A. J.; Davis, T. P.; Stenzel, M. H.; Barner-Kowollik, C. *Chem. Commun.* **2008**, 2052-2054.

[3] Synthesis of 4-Arm Star Poly(styrene) by a Combination of RAFT Chemistry and Hetero Diels-Alder Cycloadditions
Inglis, A. J.; Sinnwell, S.; Davis, T. P.;Barner-Kowollik, C.; Stenzel, M. H. *Polymer Preprints*, **2008**, *49*, 210-211.

[2] Well-Defined Block Copolymers Utilizing RAFT Chemistry and Hetero Diels-Alder Cycloaddition
Sinnwell, S.; Inglis, A. J.; Davis, T. P.; Stenzel, M. H.; Barner-Kowollik, C. *Polymer Preprints*, **2008**, *49*, 240-241.

[1] Combining RAFT Chemistry and Pericyclic Reactions for the Construction of Well-Defined Polymer Architectures.
Barner-Kowollik, C.; Sinnwell, S.; Inglis, A. J.; Davis, T. P.; Stenzel, M. H. *Polymer Preprints*, **2008**, *49*, 159-160.

Patents

[2] Funktionsmaterialien mit reversibler Verntetzung
Barner-Kowollik, C.; Inglis, A. J.; Nebhani, L.; Altintas, O.; Schmidt, F.-G.; Fengler, S.; Hilf, S. KIT Erfindungsmeldung IMA Az. EM10309, **2010**.

[1] Improved Monopersulfate Treatment of Membranes
Müller, H.-J.; Wang, D.; Inglis, A. J.; pct int. appl wo2008006173, **2008**

Book Chapters

[2] Ultra-Rapid Approaches to Mild Macromolecular Conjugation
Inglis, A. J.; Barner-Kowollik, C. in *Complex Macromolecular Architectures: Synthesis, Characterization, and Self-Assembly*, Du Prez, F. E.; Hadjichristidis, N.; Tezuka, Y.; Hirao, A.; Eds. Wiley, New York, NY, USA **2010**, *in press*.

[1] Blocks, Stars and Combs: Complex Macromolecular Architecture Polymers via Click Chemistry
Sinnwell, S.; Inglis, A. J.; Stenzel, M. H.; Barner-Kowollik, C. in *Click Chemistry in Biotechnology and Materials Science*, Lahann, J. Ed.; Wiley, New York, NY, USA, **2009**, 89-117.

Conference Contributions

[7] Bonding/Debonding On Demand: Application of Diels-Alder Chemistry to Colour Switch Materials and Reversible Cross-Linking
Inglis, A. J.; Barner-Kowollik, C. *Macro 2010*, Glasgow, United Kingdom, July 11-16, **2010**.

[6] From Ultra-Fast Block Construction to Star Shaped Polymer-Fullerene Hybrids: Advancing Controlled Free radical Polymerization and Click Technologies
Inglis, A. J.; Barner-Kowollik, C. *CRP Meeting 2009*, Houffalize, Belgium, September 17-18, **2009**.

[5] Recent Advances in Macromolecular Engineering by the RAFT-HDA Concept
Inglis, A. J.; Sinnwell, S.; Stenzel, M. H.; Barner-Kowollik, C. *Frontiers in Polymer Science*, Mainz, Germany, June 7-9, **2009**.

[4] Ultra-Fast Click Conjugations for Ambient Temperature Macromolecular Engineering
Inglis, A. J.; Sinnwell, S.; Stenzel, M. H.; Barner-Kowollik, C. *EUPOC 2009*, Gargnano, Italy, May 31- June 4, **2009**.

[3] Combining RAFT Chemistry and Pericyclic Reactions for the Construction of Well-Defined Polymer Architectures
Barner-Kowollik, C.; Sinnwell, S.; Inglis, A. J.; Davis, T. P.; Stenzel, M. H. *235th ACS National Meeting and Exposition*, New Orleans, USA, April 6-10, **2008**.

[2] Well-Defined Block Copolymers Utilizing RAFT Chemistry and Hetero Diels-Alder Cycloaddition
Sinnwell, S.; Inglis, A. J.; Davis, T. P.; Stenzel, M. H.; Barner-Kowollik, C. *235th ACS National Meeting and Exposition*, New Orleans, USA, April 6-10, **2008**.

[1] Synthesis of 4-Arm Star Poly(styrene) by a Combination of RAFT Chemistry and Hetero Diels-Alder Cycloadditions
Inglis, A. J.; Sinnwell, S.; Davis, T. P.; Stenzel, M. H.; Barner-Kowollik, C. *235th ACS National Meeting and Exposition*, New Orleans, USA, April 6-10, **2008**.

Acknowledgements

First, and foremost, I am indebted to Prof. Dr. Christopher Barner-Kowollik for providing me with the freedom to pursue interesting projects in a self-directed manner. Your informal presence, and good humour, is a refreshing quality that does you credit and has made for a highly enjoyable environment in which to work.

Funding from the Karlsruhe Institute of Technology (KIT) within the context of the *Excellence Initiative* for leading German universities, the Deutsche Forschungsgemeinschaft (DFG) and the Ministry of Science and Arts of the state of Baden-Württemberg to my supervisor Prof. Dr. Barner-Kowollik supporting this work is gratefully acknowledged.

In the end, that which is not started can never be finished. Although sounding trite, it nevertheless highlights the importance of those intial steps one must take in completing any task. For this particular task, the person instrumental in helping me to get started was Dr. Sebastian Sinnwell. During the course of the work presented in Chapters 3-7, I have learnt so much from you in the ways of laboratory, experimental design and presentation of data. You have led by example and the impeccable standards by which your work is held has set a benchmark by which I hope to have lived up to.

I would also like to acknowledge and indeed thank Thomas Paulöhrl for being such an outstanding Diploma student. Your ability to learn quickly and to conduct yourself in a self-directed manner is impressive to say the least. This is certainly reflected in your significant contributions to the work presented in Chapters 9 and 11. I have no doubt you will enjoy many a success with your future doctoral studies.

For a highly fruitful industrial collaboration, I wish to thank Georg Friedrich Schmidt, Stephan Fengler, Stefan Hilf, André Hennig and Simon Krause from Evonik Degussa GmbH. It has been a pleasure working with you all and it is, for me, very gratifying to see someone interested in making use of something from this body of work.

Introducing me to the world of fullerenes, I thank Prof. Dr. Stefan Bräse, Dr. Thierry Muller and Dr. Philippe Pierrat for initiating a highly enjoyable and successful collaboration.

Having completed my Honours thesis, and thereafter commencing doctoral studies, at the Centre for Advanced Macromolecular Design (CAMD), I would also like to thank A/Prof. Martina Stenzel as my co-supervisor. To all of those with whom I shared lab and office space in Sydney, I am grateful for the good laughs and friendly company.

Sandy and Leena, we moved together half-way across the world to not only continue our studies, but to set up three (not one) new labs. I thank you for your friendship and those important moments of *togetherness* in those early days when I think we all needed it. I also thank the entire research group of Prof. Dr. Manfred Wilhelm for their warm and inviting friendship.

To Dr. James Blinco, I thank you for keeping the *Aussie* connection strong in Karlsruhe. I have immensely enjoyed our Pub Quiz nights and 'Friday Arvo Drinks' at the Vogelbräu. As way led on to way, the creative ideas borne out of such times certainly proved that inspiration comes from within...a glass of beer (or eight).

Being perhaps the most unique person I know, I must thank Mathias Dietrich for never a dull moment. You truly are a free spirit that cannot be caged. I also wish to express my gratefulness to Michael Kaupp, David Antinori, Thomas Tischer and Mathias Glaßner for generating such a fun and light atmosphere within the group. All I can say is that I hope I have not been a bad influence.

It never ceases to astound me the rate at which the *Arbeitskreis* as grown from a size of six to what it is today. My sincere thanks goes out to all past and present members of *Macroarc* for providing friendly help whenever needed.

It seems as though every conference I go to, I bump in to my Belgian friends. For such far-reaching friendship, I am eternally grateful to Prof. Dr. Filip Du Prez and his research group in Ghent. In particular, I would like to thank Dr. Wim Van Camp, Dr. Pieter Espeel, Dr. Jan Devroede, Leen Billiet and Mieke Lammens...I feel as though I am an honourary member of your group.

For those who took part, the *Click Chemistry* conference of 2009 held in Gargnano, Italy was perhaps the most enjoyable of conferences. Strong friendships were forged there and I am honoured to have taken part. As such, I would like to thank the *Italian Connection*: Claudia Enders, Katharina Hackethal, Haitham Barqawi, Dr. Guillaume Delaittre and, of course Dr. Anja Goldmann. In particular, I am thankful to Anja for promoting the highly enjoyable social aspects of our *Arbeitskreis* and to 'Claudi' for our regular bilingual chats and holiday postcards that never fail to brighten the day.

It has been immensely important for me to be able to escape the lab and leave the world of research behind, even if for only short periods at a time. Being an incomparable source of such escapism, I am forever grateful to Astrid Hirschbiel. Whether

it was simply over coffee or drinks, I wouldn't trade those times for anything else. I would also like to thank Eugenia Tausch for great laughs and great company.

Finally, to my family who have been a tremendous source of strength and support over these past few years, I thank you for all those little things that, seeming trivial in themselves, add up to something so much more.

Which would have advanced the most at the end of a month- the boy who had made his own jackknife from the ore which he had dug and smelted, reading as much as would be necessary for this- or the boy who had attended the lectures on metallurgy at the Institute in the meanwhile, and had received a Rodgers penknife from his father?

Which would be most likely to cut his fingers?

-Adapted from *Walden*-

Henry David Thoreau (1817-1862)

Two roads diverged in a yellow wood,
And sorry I could not travel both
And be one traveler, long I stood
And looked down one as far as I could
To where it bent in the undergrowth.

Then took the other, as just as fair,
And having perhaps the better claim,
Because it was grassy and wanted wear;
Though as for that the passing there
Had worn them really about the same.

And both that morning equally lay
In leaves no step had trodden black.
Oh, I kept the first for another day!
Yet knowing how way leads on to way,
I doubted if I should ever come back.

I shall be telling this with a sigh
Somewhere ages and ages hence:
Two roads diverged in a wood, and I-
I took the one less traveled by,
And that has made all the difference.

Robert Frost (1874-1963)

Ich erkläre hiermit, dass ich die vorliegende Doktorarbeit im Rahmen der Betreuung durch Prof. Dr. Christopher Barner-Kowollik, selbständig verfasst und keine anderen als die angegebenen Quellen und Hilfsmittel verwendet habe.

Karlsruhe, den 31.08.2010